Studies Relating to the Ovarian Monitor

A thesis presented in partial fulfilment of
the requirements for the degree of
Master of Science in Biochemistry
at Massey University.

Delwyn Cooke, B.Sc., Dip.Sc.

December, 1993

Department of Chemistry and Biochemistry
Massey University

Dedication

This thesis is dedicated to

Mervyn George Blackwell

Abstract

Hormonal data contained on the Melbourne Women's Hospital Menstrual Cycle Database and data collected in the Palmerston North Centre of the World Health Organisation trial were analysed and compared. The analysis of the two sets of data showed that the utilisation of a threshold excretion rate for urinary Pregnanediol or Pregnanediol Glucuronide of 7 μmol 24 hr^{-1} was an acceptable marker for the end of the fertile period. The data collected by the women participants in the World Health Organisation Trial also showed that the Ovarian Monitor, a home fertility test, provided the most simple, comprehensive and accurate marker of fertility status available.

Lysozymes from several sources were examined as possible replacements for the hen egg white lysozyme in the Ovarian Monitor as a means of reducing the Estrone Glucuronide assay time. Unfortunately, although they were all found to possess a faster initial rate, the clearing curves were also more biphasic making them unsuitable for use in the current end-point assay. These differences were attributed to the presence of electrostatic fields on both the enzyme and the substrate. However, the human lysozyme obeyed second order kinetics for a significant percentage of the twenty minute clearing curve. Thus, the Estrone Glucuronide assay time could be significantly reduced by adapting the Ovarian Monitor to linearise the human lysoyzme clearing curve with an appropriate algorithm.

Human lysozyme is very expensive thus, it was necessary to optimise conjugation condition for Estrone Glucuronide using the more economical hen egg white lysozyme. Also, chromatographic conditions for conjugate purification had to be established before the human lysozyme could be conjugated and the viability of the above proposal could be tested.

Both the mixed anhydride and active ester conjugation methods were optimised. The most effective purification scheme involved pH 4.3 phosphate buffers using a Mono-S column followed by an Alkyl Superose column.

Acknowledgements

First, and foremost I would like to acknowledge my supervisor Associate Professor Len Blackwell for perseverance in the face of adversity and for the many frank and open discussions we have had during the course of this work.

Secondly, I would like to thank my flatmate Inge Merts, for allowing me to monopolise her computer and convert the lounge into a semi-permanent study for the last unmentionable number of months, not to mention for paying to get the computer fixed during one of its less co-operative phases. I am also equally indebted to Kerry Blackwell for formatting and invaluable assistance in getting this work to press on time.

I would also like to thank Yinqui Wu for synthesising starting material for me and his supervision during my excursion into the world of organic chemistry and Hale Nicholson for his supervision of the molecular biology. I would also like to acknowledge Mr Dick Poll for using my conjugate samples to trial the newly acquired SMART system.

I am also especially grateful to my family for their financial support over my years at Massey and especially this last year. Most notably I am grateful to my mother who always seems to be the initiator of such things.

The receipt of a grant from the Palmerston North Medical Foundation is gratefully acknowledged.

Merry Christmas!!

Table of Contents

List of Figures

Chapter One: Ovarian Physiology and the Ovarian Monitor

List of Tables

List of Schemes

Chapter Three: Kinetic Studies on Lysozymes

Chapter Four: Synthesis of Estrone Glucuronide Conjugates

Abbreviations

α	Smoothing Constant
A_{280}	Absorbance at 280 nm
Abs	Absorbance
BBT	Basal Body Temperature
BIP	Basic Infertility Pattern
bp	Base Pairs
CM	Carboxy-methyl
c type	Chick Type
DCC	Dicyclohexylcarbodiimide
DCU	Dicyclohexylurea
DMF	Dimethylformamide
DMSO	Dimethylsulphoxide
E_o	Total Enzyme Concentration
e	Charge on an electron
E. coli	*Escherichia coli*
E1G	Estrone Glucuronide
E1G-(H)	Estrone Glucuronide (acid form)
E1G-(Na)	Estrone Glucuronide (Na form)
EDTA	Ethylenediamine Tetra-acetic Acid
ESA	Exponentially Smoothed Average
FE	Forecast Error
FPLC	Fast Protein Liquid Chromatography
FSH	Follicle Stimulating Hormone
GEWL	Goose Egg White Lysozyme
GLC	Gas Liquid Chromatography
g type	Goose type
HEWL	Hen Egg White Lysozyme
HuL	Human Lysozyme
Hz	Hertz
IBC	Isobutylchloroformate

I.D.	Internal Diameter
IEP	Iso-electric Point
k	Boltzmann's constant
kb	Kilobase Pairs
LB	Luria-Bertani Broth
LH	Luteinising Hormone
MAD	Mean Absolute Deviation
M. lysodeikticus	*Micrococcus lysodeikticus*
NAG	N-acetylglucosamine
NAM	N-acetylmuramic Acid
NFP	Natural Family Planning
NHS	N-hydroxysuccinimide
NMR	Nuclear Magnetic Resonance
PAGE	Polyacrylaminde Gel Electrophoresis
Pd	Pregnanediol
PdG	Pregnanediol Glucuronide
SD	Standard Deviation
SDS	Sodium Dodecyl Sulphate
SEn	Substrate Molecule with n Number of Lysozyme Molecules Attached
SFE	Smoothed Forecast Error
std. dev.	Standard Deviation
T	Absolute Temperature
T1	Initial Transmittance
T2	Final Transmittance
ΔT	Change in Transmission
T4L	T4 Phage Lysozyme
TAE	Tris-Acetate Buffer containing EDTA
TE	Tris-HCl Buffer containing EDTA or Total Estrogens
TEPDDE	Total Estrogen and Pregnandiol Data Entry
TEWL	Turkey Egg White Lysozyme
TS	Tracking Signal
TLC	Thin Layer Chromatography

TNB	Tri-n-butylamine
WHO	World Health Organisation

CHAPTER ONE

OVARIAN PHYSIOLOGY AND THE OVARIAN MONITOR

1.1 INTRODUCTION

The Ovarian Monitor has been specifically designed as a simple home self test for women who have a need to understand their own fertility (Brown *et al.*, 1989). By the daily measurement of ovarian steroid levels in timed urine samples, information on fertility status is provided as it changes from day to day.

Of all the different states of fertility studied those associated with the cyclical changes in the menstrual cycle are the most familiar and best understood.

1.2 THE MENSTRUAL CYCLE

The menstrual cycle can be defined as the periodic preparation for fertilisation and pregnancy, which occurs as a series of regular cyclic changes unique to women.

The cycle can be divided into two distinct phases, the follicular phase and the luteal phase. These two phases are separated from each other by the events of ovulation and menstruation. A diagramatic overview of these phases and the associated hormone profiles is shown in Figure 1.1.

The follicular phase begins with the stimulation of a group of follicles to further growth by the release of follicle stimulating hormone (FSH) from the pituitary. While the leading (dominant) follicle continues to grow it produces increasingly higher levels of estrogen (mainly estradiol 17ß) which by negative feedback at the level of the hypothalamus depresses the production of FSH. The resulting lower levels of FSH prevent the recruitment of any more follicles, but are sufficient to meet the new lower requirements of the leading follicle (Brown, 1978; Baird, 1987). Thus, while all the

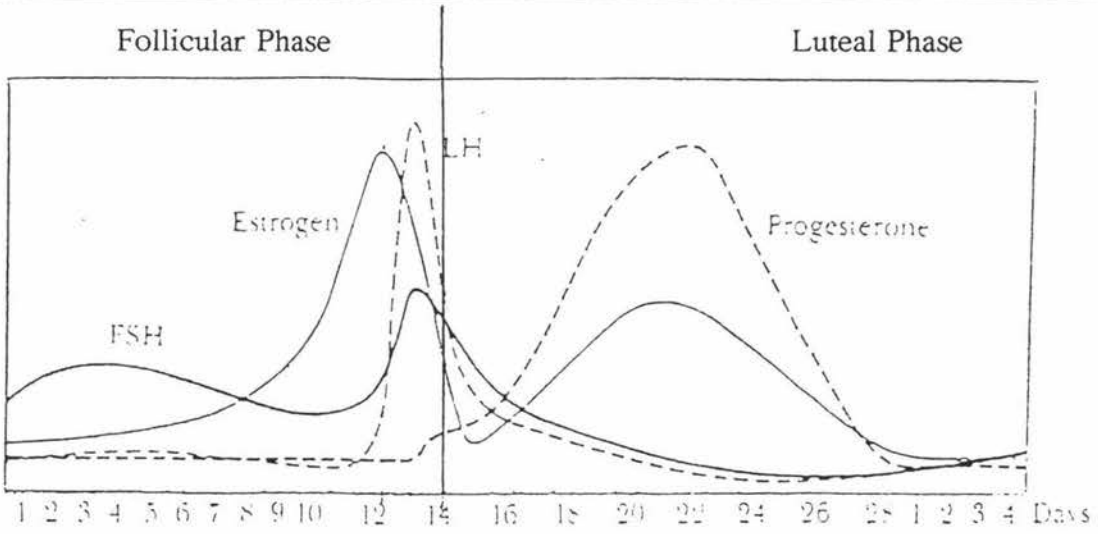

Figure 1.1 *Mean Values for Serum Luteinising Hormone (LH), Follicle Stimulation Hormone (FSH), Estradiol and Progesterone obtained during a Normal 28 Day Human Menstrual Cycle*

other follicles become atretic, the leading or dominant follicle produces increasingly more estrogen. The estrogen produced by the leading follicle is responsible for the thickening of the endometrium (lining of the uterus) and development of its glands and arteries which occurs in the follicular phase (Cormack, 1984). Estrogen also acts on the dominant follicle to stimulate the formation of luteinising hormone (LH) receptors within it in a combined action with FSH (Ireland, 1987), and when the circulating estrogens reach their upper physiological range, the LH surge from the pituitary is induced (Karsch, 1987). The LH surge in turn leads to the final maturation of the follicle, and a rapid drop in plasma estrogen levels with a concomitant increase in progesterone levels (Hoff *et al.*, 1983). Follicular rupture and release of the ovum (ovulation) occurs on average 17 hours after the LH peak (Brown, 1978). The day preceding ovulation is the day of maximum fertility (Austin, 1975), with the day of maximum fertility being defined as the day on which an isolated event of intercourse is most likely to lead to conception. However, although the day of maximum fertility is fairly well defined, the actual length of the follicular phase can be highly variable as the leading follicle may die before it can induce the LH peak, in which case recruitment must start all over again.

The phase following ovulation is known as the luteal phase and is characterised by the

formation of the corpus luteum, an endocrine organ formed under the influence of LH from the remnants of the ovulated follicle. As the corpus luteum develops, its secretion of progesterone and estrogen increases. It is under the influence of these two hormones acting in concert that the endometrial development converts from a growth phase to one of differentiation. The endometrium continues to thicken while the spiral arteries become increasingly prominent and the glands become more extensive in nature and secretory (Cormack, 1984). The combined action of estrogen and progesterone also inhibits the further release of LH and FSH.

Because LH is essential for the maintenance of the corpus luteum, and its release is inhibited by the hormones of the corpus luteum, the activity of the corpus luteum brings about its own regression (with the exception of pregnancy which overrides this mechanism). Thus, towards the end of the luteal phase FSH secretion begins to rise again to initiate another wave of follicular growth for the next cycle. The first day of the next follicular phase is defined as the first day of menstruation and occurs when the steroid hormone secretion from the corpus luteum decreases to a level where the endometrial development can no longer be maintained. The spiral arteries constrict, followed by endometrial necrosis, sloughing off of the functional layer and bleeding (menstruation) (Marshall, 1984).

Unlike the follicular phase the luteal phase is very constant, lasting between 11 to 16 days (Ogino, 1930). Departures from this range are diagnostic of either infertility (<11 days; deficient luteal phase) or pregnancy (>16 days).

1.3 NATURAL FAMILY PLANNING

It is these hormonal changes described in the previous section (Section 1.2) which are responsible for the cyclical changes in the quantity and nature of the cervical mucus, the temperature change observed at mid cycle, changes in the cervix and the timing of menstruation itself; and it is these clinical indicators which are used in natural family planning (NFP) to predict the fertile time. NFP is defined by the World Health Organisation (WHO) as "the voluntary avoidance of intercourse by a couple during the fertile phase of the menstrual cycle to avoid pregnancy," (WHO, 1980).

The relationship between the various sex hormones, fertile mucus and temperature to the

event of ovulation in a normal menstrual cycle is shown in Figure 1.2.

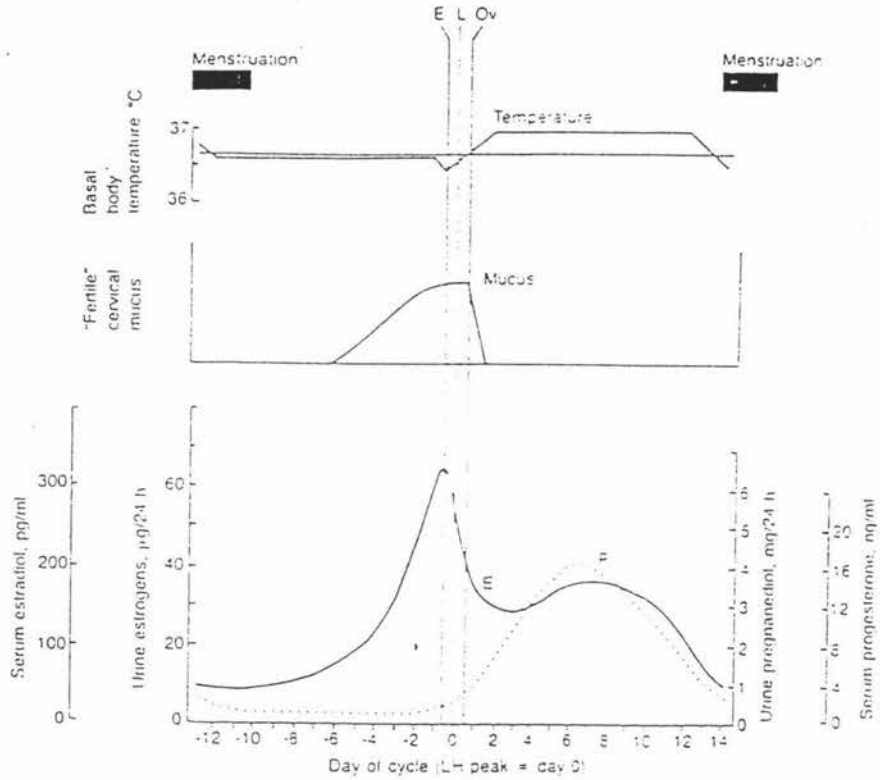

Figure 1.2 Natural Family Planning Markers for Fertility and their Relationship to the Day of the Luteinising Hormone Peak

Mean values for estradiol, progesterone, urinary estrogens, pregnandiol, and basal body temperature, and times of mucus production and menstruation in the normal menstrual cycle are all expressed relative to the luteinising hormone (LH) peak. The vertical lines represent the times of pre-ovulatory estrogen peak (E), LH (L), and ovulation (Ov).

Use of the calender method alone i.e. calculating the fertile phase by the timing of menstruation is the oldest (Ogino, 1930) and most unsatisfactory of all the NFP methods as it relies on the time of ovulation of the previous cycle to predict the time of ovulation for the next cycle i.e. it is retrospective and is dependent on a constant follicular phase.

The utilisation of the change in basal body temperature (BBT) observed at mid cycle as a NFP method was first suggested in 1935 (Parkes, 1971). It is now known that this rise is due to the increasing levels of the thermogenic hormone, progesterone which occurs at this time (Moghissi, 1980). In this method a sustained temperature rise of

0.2°C for three consecutive days is used to delineate the end of the fertile period with reasonable accuracy (Gross, 1989). The method has the disadvantages that the results can be easily invalidated by alcohol, fever and high ambient temperatures (Flynn & Brooks, 1984), and is limited by the fact that it gives no indication as to the beginning of the fertile period.

This disadvantage is overcome in the ovulation (Billings) method where the changes in the cervical mucus throughout the cycle are used to identify both the beginning and the end of the fertile phase. In this method, the early safe days begin with the days directly following menstruation which are characterised by a thick and sticky, pasty yellow or white mucus, if any. Under the influence of increasing estrogen levels the mucus gradually increases in volume and becomes more fluid, clearer, stretchier and lubricative. These days should all be considered as potentially fertile. According to the Billings Method the last day of this mucus, "the peak day" is closely associated with ovulation (Billings *et al.*, 1972) and is the day of maximum fertility.

After ovulation the increasing levels of progesterone cause the mucus to become thick and sticky or dry up altogether. The late safe days are from the morning of the fourth day after the "peak day" until the end of the cycle (Billings *et al.*, 1972; Billings & Westmore, 1980).

The mucus is not only an indicator of fertility, but also helps determine it. The thin, stringy and alkaline nature of the mucus associated with the lead up to ovulation is favourable to sperm transport and survival. In contrast the characteristics of the thick, cellular mucus associated with the infertile phases of the cycle creates a hostile environment for sperm survival while the cellular nature of the mucus blocks sperm transport (Billings & Westmore, 1980; Ganong, 1987).

Although this method does define the entire fertile period it is imprecise, and as a result requires longer periods of abstinence (mean length 17 days; Brown *et al.*, 1989) than the real length of the fertile period would indicate as determined by the gamete survival times (maximum fertile period 7-9 days; Brown & Gronow, 1985). Another disadvantage with this method is that the mucus symptoms can become hidden by infection, semen and the women's own secretions from sexual arousal. It is for these

last two reasons that the method was revised with the addition of the alternate day rule. Using the alternate day rule, intercourse is only recommended every second day during the early safe days. This stops any change in the mucus symptoms from being permanently masked during this time (Billings, 1992).

The observation of changes in the cervix by self palpation is a less popular method of NFP. These changes are also closely related to the circulating levels of estrogen and progesterone. After menstruation the cervix is low and firm and the cervical os (the entrance to the cervix) is closed. As ovulation approaches the os dilates and the cervix softens and rises higher in the vagina. The cervix and os gradually return to their postmenstrual state after ovulation (Gross, 1989).

The most current recommended NFP method is the symptothermal method which uses a combination of the temperature, mucus symptoms and rhythm calculation methods together. This method has the advantage that it has the potential to negate some of the inadequacies that any of the component methods may have had when used in isolation.

Although this method can be quite effective in cycles with very clear symptoms, NFP is still looked upon by the majority of couples as a subjective and ineffective method. This is due to the difficulties, real or imagined, in the interpretation of the symptoms, the high levels of abstinence required, and the apparent relatively high failure rate as a contraceptive method. The surveys show this conspicuously high failure rate has not been brought about by method failure *per se*, but rather by a conscious departure from the rules by those couples who found the long periods of abstinence required too restrictive. For example, the WHO study begun in 1975 on the Billings Method, showed that although the method failure rate was only 2.2%, the user failure rate was 20.1% (Benagiano & Bastianelli, 1989). These findings in conjunction with the fact that the current NFP methods have periods of abstinence which are high because of their failure to precisely define the fertile period shows a requirement for it to be more accurately delineated. This would not only have the effect of making natural family planning methods more precise while increasing the number of days available for intercourse, but would hopefully also decrease the method and user failure rates at the same time.

Because it is the hormone levels themselves which are responsible for the cyclical

symptoms used by natural family planners for the determination of the fertile period (see Figure 1.2), then it follows that any method which measures the hormone levels is going to be a more direct method for the determination of the fertile period than a method dependent on the clinical signs. Also, as discussed previously, the clinical symptoms can sometimes be misleading or masked. Thus, the measurement of hormone levels represents a potentially more reliable method in the determination of the fertile period.

One way of achieving a more precise delineation of the fertile period is to develop methods suitable for home use to measure the levels of the ovarian steroids themselves. This has been a consistent goal of the WHO and Professor Jim Brown in Melbourne since the early 1970's.

1.4 URINE VERSUS BLOOD

When designing a clinical assay, one of the first decisions which has to be made is whether to assay blood or urine for the analyte in question. Blood assays have the advantage that they measure the levels of circulating analyte at the time of sampling, whereas urine samples often have the disadvantage that they can only be used to measure a metabolite of the analyte, and only after its excretion i.e. the appearance of an analyte or its metabolite in the urine is determined by the compounds metabolic clearance rate.

One of the major advantages of urine over blood is that it can be obtained by non-invasive methods. This is particularly important in the area of home testing. An additional factor which must be taken into account when measuring steroids is their episodic mode of secretion. This can cause considerable variation in blood levels throughout the day, making interpretation of blood hormonal data particularly difficult. The use of urine samples avoids this problem because the peaks and troughs are averaged out over the collection time (a minimum of three hours).

The third advantage of urine is that it is easier to measure the steroid levels in urine than in blood because the steroids are present in higher concentrations in the urine, and the urinary patterns of steroid excretion are well documented (Blackwell & Brown, 1992).

It was for these reasons that the Ovarian Monitor was designed to measure ovarian steroid levels in urine.

1.5 BIOSYNTHESIS OF THE ESTROGENS AND PROGESTERONE

Of the three estrogens, estrone, estradiol and estriol, estradiol is by far the most bioactive. Estradiol plays a central role in follicular development and oocyte maturation, stimulates the cervical mucus glands to secrete a fluid favourable to sperm survival and transport, facilitates the mid-cycle surge of LH which precipitates ovulation and is involved in ovum transport and in endometrial proliferation and preparation for implantation (Burger, 1989). Although the ovary only synthesises the estrogens, estrone and estradiol, it still uses the same biosynthetic pathway as other steroidogenic tissues (Figure 1.3).

In the ovary the ability of a follicle to synthesise estrogen is a key step in the maturation process and is dependent upon both LH and FSH stimulation. The aromatisation of androstenedione to estrone, and testosterone to estradiol (Figure 1.3) is mediated by FSH during the follicular phase and by LH during the luteal phase. These aromatisations are irreversible and perform a regulatory role in determining estrogen output from the ovary. Estradiol-17ß and estrone are the principal estrogens produced by the ovary, with estradiol-17ß predominating, being produced in four times the amount as estrone prior to ovulation.

This is in contrast to the extraglandular production of estrone and estradiol, where the aromatisation of adrenal androstenedione to estrone is much greater than the aromatisation of adrenal testosterone to estradiol (Baird *et al.*, 1969; Baird & Fraser, 1974).

The levels of estrone in the blood are further elevated by the hepatic conversion of estradiol-17ß to the less bioactive estrogens, estrone and estriol (Baird, 1977). This is an important control feature of steroid metabolism as the rapid removal of potent estrogens is necessary to ensure the bodies rapid response to changes in the levels of estrogen production from the ovaries e.g. when the ovaries change from producing high

to low amounts of estrogen this ensures that this is rapidly reflected in the circulating blood levels.

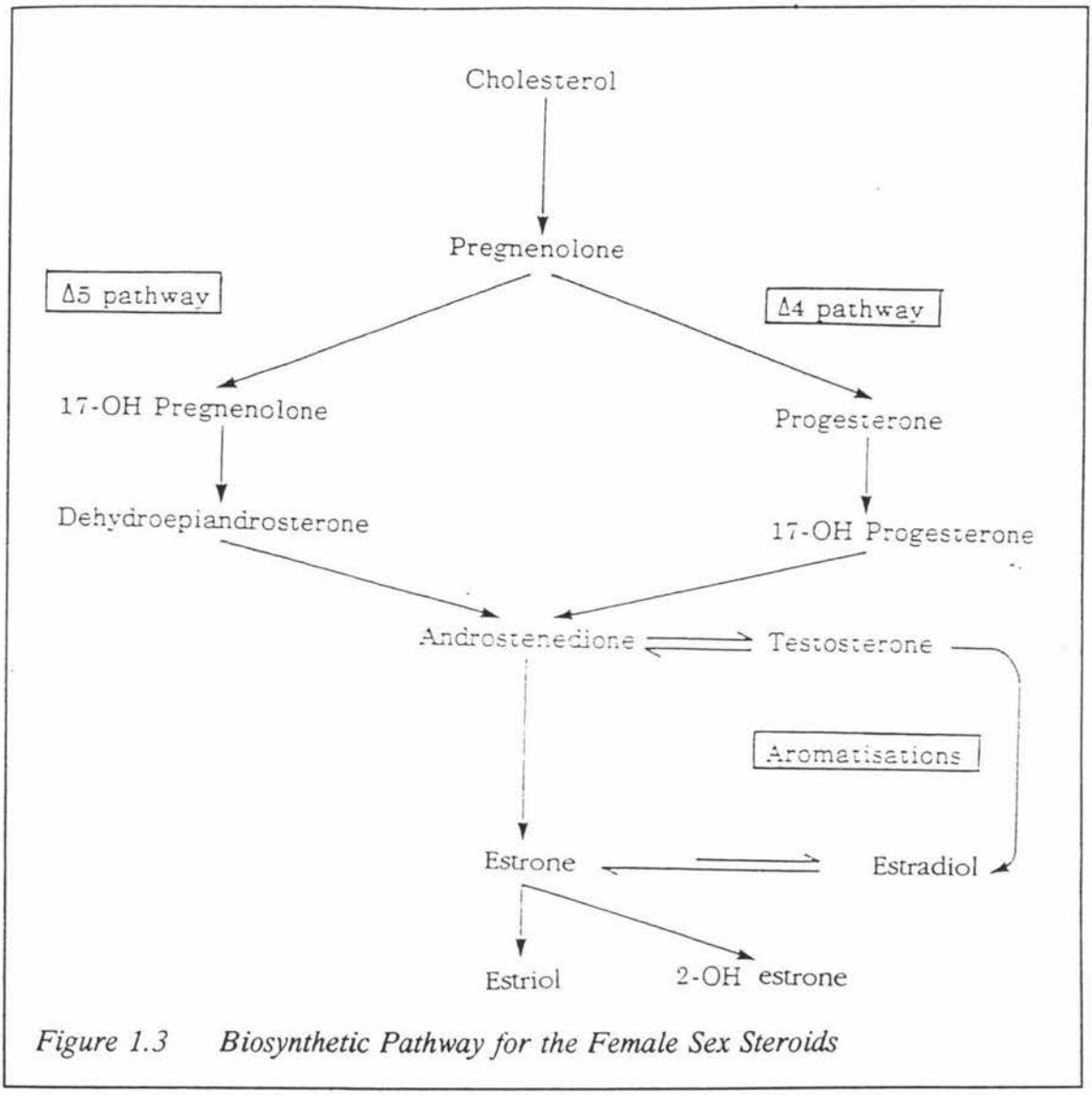

Figure 1.3 Biosynthetic Pathway for the Female Sex Steroids

The synthesis of progesterone in the ovary is dependent upon LH, enhanced by FSH and uses the same biosynthetic pathways as shown in Figure 1.3.

1.6 URINARY EXCRETION OF OVARIAN ESTROGENS

For excretion the lipid soluble steroids must first be made water soluble by conjugation to glucuronic acid, sulphuric acid or both (Bolt, 1979). All three estrogens, estrone, estradiol, and estriol appear in the urine as glucuronide conjugates (see Table 1.1 below).

Table 1.1 The Estrogens and their Principal Urinary Metabolites

Steroid	Conjugate (longhand)	(shorthand)
Estrone (E1)	Estrone-3-glucuronide	E1-3G
	2-Hydroxyestrone-glucuronide	2-OH-E1G
Estradiol (E2)	Estradiol-17ß-3-glucuronide	E2-17ß-3G
Estriol (E3)	Estriol-16-glucuronide	E3-16G
	Estriol-3-glucuronide	E3-3G

There is a large range of values about the mean daily urinary excretion for each of the three estrogens as measured individually by the split estrogen method (the separate measurement of estrone, estradiol and estriol), although the ratios between the various estrogens do tend to be relatively constant throughout the menstrual cycle for a given women (Brown, 1955).

After the decision to assess ovarian activity by the measurement of urinary steroids the next step in the historical development of the Ovarian Monitor was to decide which of the five estrogen conjugates should be used as a marker for ovarian activity. Ideally this conjugate should be excreted rapidly by all fertile women, be present in high concentrations in the urine, and show a large difference between baseline and peak levels. Unfortunately the decision was not easy as none of the conjugates met all of the above criteria.

Although E2-17ß-3G is the first metabolite to be excreted (Hobrick & Nilsen, 1974), and has a steep rise from baseline values (Stanczyk *et al.*, 1980), it is not a major metabolite of estradiol (Musey *et al.*, 1972) and is only present in the urine at low concentrations. In contrast, the sum of the estriol glucuronides, E3-3G and E3-16G is present in large amounts. Unfortunately, their excretion is delayed by approximately 12 hours due to a complex enterohepatic circulation involving bilary excretion and reabsorption (Brown, 1955). For these reasons it was decided to use the estrogen metabolite E1-3G (henceforth referred to as E1G).

Next to E2-17ß-3G, E1G has the highest peak baseline to ratio and is found in the urine at five times the concentration of E2-17ß-3G. As well as being present in the urine in high quantities it is also usually excreted rapidly. Furthermore, increases in estrone glucuronide levels are correlated to increases in circulating levels of estradiol, the most biologically active of the estrogens, due to the enterohepatic conversion of estradiol to estrone (Baird, 1977).

The major disadvantage of measuring E1G is its possible lack of suitability for all women, as not all women excrete estrone as a major conjugate. In these women most of the estradiol and estrone is metabolised into estriol conjugates (Conway, 1986). For this minority of women it would be better to assay for estriol conjugates or the sum of the two.

1.7 URINARY EXCRETION OF OVARIAN PROGESTERONE

Progesterone has more than twenty metabolites, most of which are excreted via the bile and the gastrointestinal tract. The major urinary metabolite in quantitative terms is pregnanediol (5ß-pregnane-3α-20α-diol) (Serra, 1983), most of which is excreted in the urine as a pregnanediol glucuronide (PdG) conjugate. This conjugation of pregnanediol to glucuronic acid occurs in the liver.

The pregnanediol glucuronide in the urine is not solely due to progesterone metabolism, as a significant proportion of pregnenolone from the adrenal gland is also metabolised to pregnanediol (Arcos *et al.*, 1964; Siiteri & MacDonald, 1973). Thus, although there is almost no progesterone produced in the first half of the cycle the urine shows a baseline level of PdG. However, when it comes to the interpretation of PdG data this is not a cause for concern as the rise in PdG levels from baseline due to increased circulating levels of progesterone in the luteal phase is very clear.

Thus, in summary, PdG excretion is a good measure of circulating progesterone levels and E1G is suitable for measurement of circulating estrogen levels by the Ovarian Monitor.

1.8 HOMOGENEOUS ENZYME IMMUNOASSAY

In 1972, Rubenstein published the first "Homogeneous" Enzyme Immunoassay

(Rubenstein *et al.*, 1972), as an alternative to radio-immunoassays and "Heterogeneous" Enzyme Immunoassays. This method was revolutionary as an immunoassay technique as it required no purification, extraction or separation of the antibody bound antigen (i.e. bound fraction) from the unbound antigen (i.e. free fraction) and thus, gave the assay inherent simplicity and potential to be utilised in home assays. This is a role which the other two methods could not realistically fulfil as they both require a separation step for the separation of the bound from the free label, and in the case of the radio-immunoassay there is the unavoidable problem of the use and measurement of radioactive materials, and their disposal in the home.

Rubenstein's work showed that the enzyme activity of a carboxymethylmorphine-lysozyme conjugate could be inhibited up to a maximum of 98% by the addition of morphine antibodies, that this inhibition was inversely proportional to the amount of free morphine in the system and furthermore that this inhibition occured in a stochiometric manner. Thus, he successfully showed, using his system, that the enzyme activity of a mixture of enzyme and antibody can be directly related to the amount of free antigen introduced from a test sample.

In addition, because one molecule of free antigen is capable of freeing up one molecule of enzyme, and one molecule of enzyme is capable of catalysing the conversion of many molecules of substrate to product, this system shows intrinsic amplification.

The conjugate was made by combining lysozyme with carboxymethylmorphine-isobutyl-chloroformate mixed anhydride (Leute *et al.*, 1972), while lysozyme activity was determined by changes in light transmission of a suspension of the substrate *Micrococcus lysodeikticus* (Rubenstein *et al.*, 1972).

This method forms the basis of the assay used in the Ovarian Monitor today (Brown *et al.*, 1989), where the conjugate is a conjugate of hen egg white lysozyme (HEWL) to E1G (or PdG), the unknown or test sample is the urinary E1G (or PdG) content, and the enzyme activity is measured by the change in transmission of a suspension of *Micrococcus lysodeikticus* (*M. lysodeikticus*) over a set time period.

The E1G and PdG used to make the conjugates are either isolated from pregnancy urine or synthetically prepared, while the E1G and PdG conjugates are made using the mixed

anhydride method, as used by Rubenstein (Rubenstein *et al.*, 1972; Leute *et al.*, 1972). After the conjugate has been synthesised it is then purified using column chromatography although no details have yet been published on this procedure.

The E1G and PdG antibodies used in the assay are raised in sheep. This is achieved by inocculating the sheep with synthetic E1G or PdG coupled to a protein carrier. This coupling which again uses the mixed anhydride method, is necessary for the generation of antibodies to the steroid glucuronides. This is because the glucuronides are too small by themselves to be recognised as antigenic by the sheep's immune system. A minimum of three to six months after inocculation is required before antibodies of a high enough affinity and specificity to the steroid glucuronide can be generated. After this period the sheep are bled, and the serum obtained after clotting is of sufficient quality to be used directly in the assay without further purification.

1.9 THE OVARIAN MONITOR ASSAY

The assay described here has been developed and refined for over twenty years by Professor J.B. Brown and co-workers in the Department of Obstetrics and Gynaecology at the University of Melbourne (Brown *et al.*, 1988; Brown *et al.*, 1989).

1.9.1 THE OVARIAN MONITOR

The Ovarian Monitor used for the assay (see Figure 1.4) has three key features. First of all it acts as a miniature spectrophotometer measuring and displaying the transmission values. Secondly, it has an in-built thermostat in the cell holder which is used to keep the assay at a constant 40°C, throughout the enzyme catalysed reaction. Its third feature is an in-built timer. The in-built timer is required to time the three steps (see Section 1.9.4), and is activated by a magnetic switch which is in turn activated by the shutting of the lid. Shutting of the lid is also required for the measurement of transmission as in any other spectrophotometer. The end of timing triggers an alarm; a minute long series of beeps which can be manually over ridden by opening the lid. Visually the end of timing is indicated by the permanent display of two flashing colons which is also terminated by the opening of the lid. Most importantly the end of timing triggers an immediate freezing of the current transmission value on the display which is essential for the calculation of change in transmission.

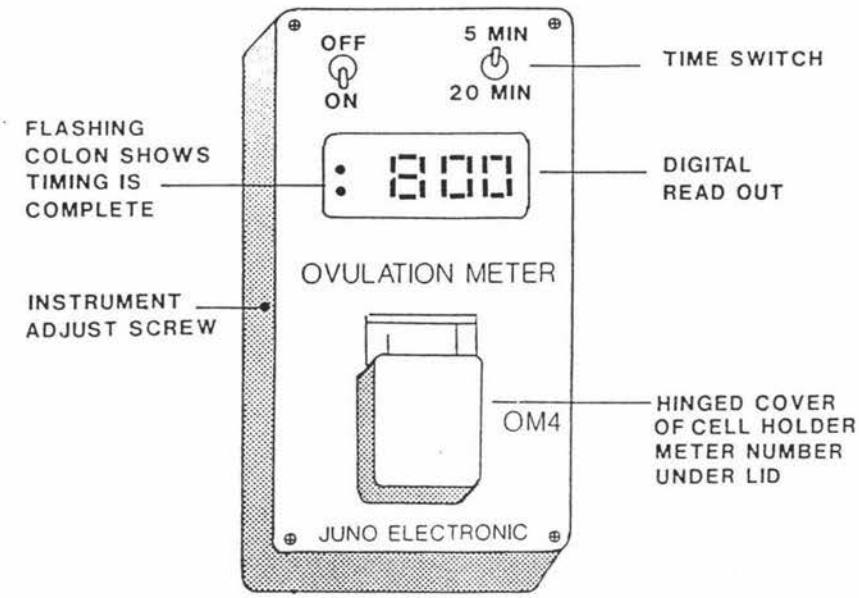

Figure 1.4 A Stylised Diagram of the Ovarian Monitor

1.9.2 THE ASSAY TUBE

Since the assay for E1G and PdG is a homogeneous enzyme immunoassay, all the three

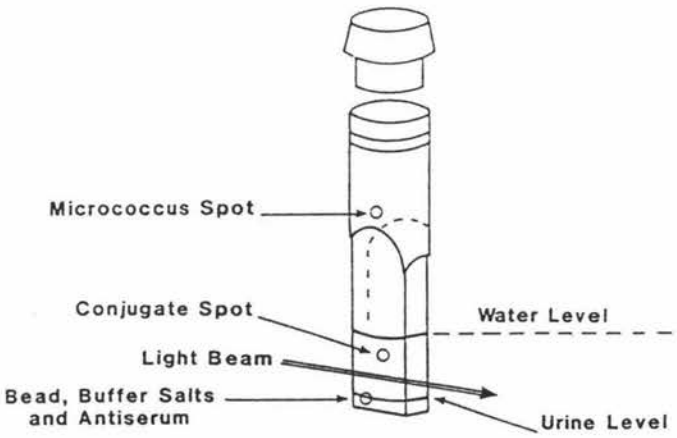

Figure 1.5 A Stylised Diagram of an Ovarian Monitor Assay Tube and its Constituents

steps can be performed in the one assay tube. Separate assay tubes are used for the

E1G and PdG assays.

Each assay tube contains a small glass bead for mixing, buffer salts and a separate antibody, conjugate and *M. lysodeikticus* spot. The E1G assay tubes contain the E1G conjugate and E1G specific antibody, while the PdG assay tubes contain the PdG conjugate and PdG specific antibody. The reactants are all freeze dried at different heights down the length of the tube with the bead, buffer salts and antibody positioned at the bottom, the conjugate spot dried in approximately the middle, and the *M. lysodeikticus* spot dried near the top (Figure 1.5).

1.9.3 THE IMPORTANCE OF TIMED URINE SAMPLES

For the assay it is essential that a timed urine sample is used to correct for the large variations in the rate of urine production which primarily occur due to fluctuations in fluid intake. A minimum collection time of three hours is required so that the overall blood levels of ovarian hormone are not concealed by the pulsatile secretion of the ovarian hormones into the blood (see Section 1.4). A maximum collection time of ten hours is also set so that a more immediate assessment of ovarian activity can be made, without the problems of artificially diluting or concentrating the hormone levels of the moment by the ovarian activity of the past. To collect a timed urine sample a note of the time must be taken at the beginning and end of the collection time to the nearest quarter hour. The collection time begins immediately after the bladder has been completely emptied and the urine from this voiding discarded. At the next urination, all urine is passed directly into a collection jug. If this occurs in less than three hours after the beginning of the collection time, a relatively rare occurence, the urine from the next urination is required to be collected too for the three hour minimum to be reached.

To correct for the fluctuations in urine volume the timed urine sample must be then appropriately diluted in the jug. This is a simple operation as the collection jug is calibrated in hours thus, the urine sample is simply diluted with tap water by eye up to the nearest quarter hour according to the collection time.

The jug is calibrated at 150 ml hr^{-1} which is usually adequate for the range of urine volumes excreted. However, in the rare occurrences where the urine volume is already past its equivalent hour mark, this is simply corrected for by doubling the urine dilution.

For example, if the urine was collected over three hours and was already past the three hour mark on the jug, then the urine is made up to volume by making it up to the six hour mark instead. This is in turn corrected for in the assay by using 100 µl of urine in the test, instead of the usual 50 µl (see Section 1.9.4, step 1).

1.9.4 THE ESTRONE GLUCURONIDE ASSAY

The description below is for the assay procedure used for measuring urinary E1G levels.

Step 1 Antigen-Antibody Reaction

In the first step, 50 µl of the time-diluted urine sample is added by syringe to the bottom of an E1G assay tube which is then placed inside the Ovarian Monitor. The timer on the Ovarian Monitor is then set to five minutes, the lid closed and the E1G tube left to incubate until the timer goes off.

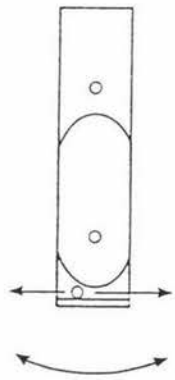

Figure 1.6 Mixing Antibody with the Urine Sample by Shaking Horizontally

This five minute incubation allows time for the bead at the bottom of the tube to free up, and the buffer salts and E1G antibody freeze dried at the bottom of the tube time to dissolve. At the end of the incubation period the tube is shaken horizontally for the count of twenty enabling the urinary E1G to mix freely with the E1G antibody (Figure 1.6). The actual time taken for the antigen-antibody reaction is very short.

(Note: so as not to invalidate the assay, care must be taken while adding the urine sample and during the mixing to ensure the conjugate and *M. lysodeikticus* spots are left dry.

The free E1G in the urine binds irreversibly (within the assay time frame) to the E1G antibody which is present in a slight excess (see Figure 1.7) (Brown *et al.*, 1988). Thus, in the presence of low levels of urinary E1G the majority of the antibody remains free. Conversely, in the presence of high levels of urinary E1G the majority of the antibody

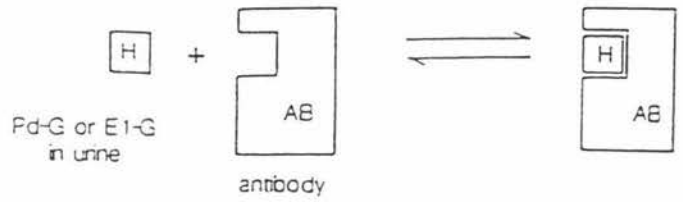

Figure 1.7 Interaction of Antibody with the Estrone Glucuronide in the Urine

is neutralised, while intermediate levels of urinary E1G result in intermediate levels of antibody neutralisation. Thus, the levels of antibody neutralisation are determined by the E1G levels in the urine.

Step 2 Antibody E1G-HEWL Conjugate Reaction

In the second step, the conjugate spot is dissolved by the addition of 300 µl of distilled water by syringe, after which the tube is shaken horizontally again for a count of twenty (see Figure 1.8) and then left to incubate for ten minutes in the Ovarian Monitor. This incubation time is important not just to allow time for the antibody and conjugate to interact, but to allow time for the reaction mix to come to temperature in preparation for the next step. (Note: care must be taken once again throughout the procedure, not to wet the *M. lysodeikticus* spot at the top).

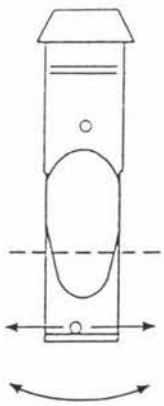

Figure 1.8 Mixing Estrone Glucuronide Conjugate with the Excess Antibody by Shaking Horizontally

Only antibody which was not bound by the E1G in the previous step is able to bind to the E1G-enzyme conjugate (see Figure 1.9). As before, this binding is irreversible within the assay time frame.

If most of the antibody had been neutralised in the previous step, the majority of the

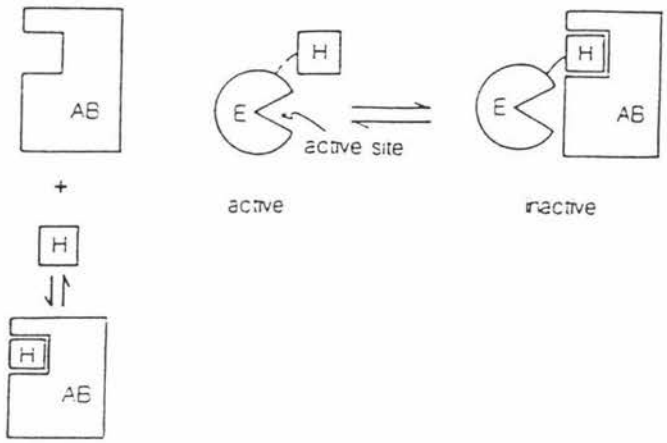

Figure 1.9 *Interaction of the Estrone Glucuronide Conjugate with the Excess Antibody*

conjugate will now remain free. However, if most of the antibody remained free in the previous step then relatively large amounts of antibody would be available to bind to the conjugate. Likewise, intermediate levels of the free antibody lead to intermediate levels of conjugate-antibody binding. Thus, the amount of free conjugate remaining at the end of step 2 is determined by the amount of free antibody left at the end of step 1 which is determined in turn by the E1G levels in the urine.

Step 3 ***Micrococcus lysodeikticus* Reaction**

In the third step, the *M. lysodeikticus* spot is suspended by vigorously shaking the tube up and down for a count of twenty (see Figure 1.10). After ensuring the *M. lysodeikticus* spot has been suspended and thus, enabling the enzyme-conjugate to interact with it, the tube is then placed in the Ovarian Monitor with the timer set to 20 minutes and the first transmission value (T1) is recorded. At the end of twenty minutes the timer goes off and the T2 value, the transmission at 20 minutes,

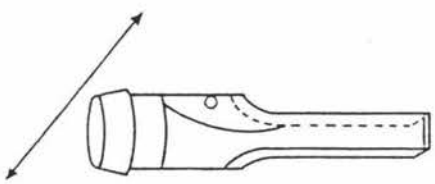

Figure 1.10 *Suspending the Micrococcus lysodeikticus Spot by Shaking Laterally*

is left flashing permanently on the display until the Ovarian Monitor is manually reset. The difference between T2 and T1 is calculated (ΔT (20 min)$^{-1}$) and thus, a measure of the urinary E1G levels is obtained which can then be used to provide information on the current reproductive status.

In this step the conjugate is finally given access to its substrate, *M. lysodeikticus*, but only enzyme-hormone conjugate remaining free after step two is active. As the conjugate proceeds to lyse the *M. lysodeikticus* by breaking the peptidoglycan bonds which form its walls, the initially turbid solution begins to clear as the cell wall collapses (see Figure 1.11). The rate of this reaction is measured by the amount of clearing of the solution over the twenty minute time period.

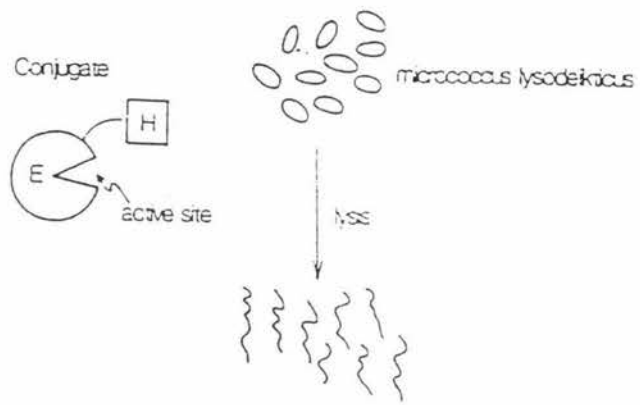

Figure 1.11 Lysis of the Micrococcus lysodeikticus cells by Excess Estrone Glucuronide Conjugate

The rate of clearing is determined by the amount of free conjugate remaining at the end of step 2, with high levels of free conjugate being associated with a fast rate of clearing and thus, a large ΔT value. Conversely low levels of free conjugate are associated with a slow rate of clearing and thus, a low ΔT value.

Thus, in conclusion, a high level of urinary E1G gives rise to a large ΔT (20 min)$^{-1}$, while low levels of urinary E1G only give rise to a small ΔT (20 min)$^{-1}$. This direct relationship between the rate of lysis and the urinary E1G levels is most clearly illustrated by the standard curve (Figure 1.12).

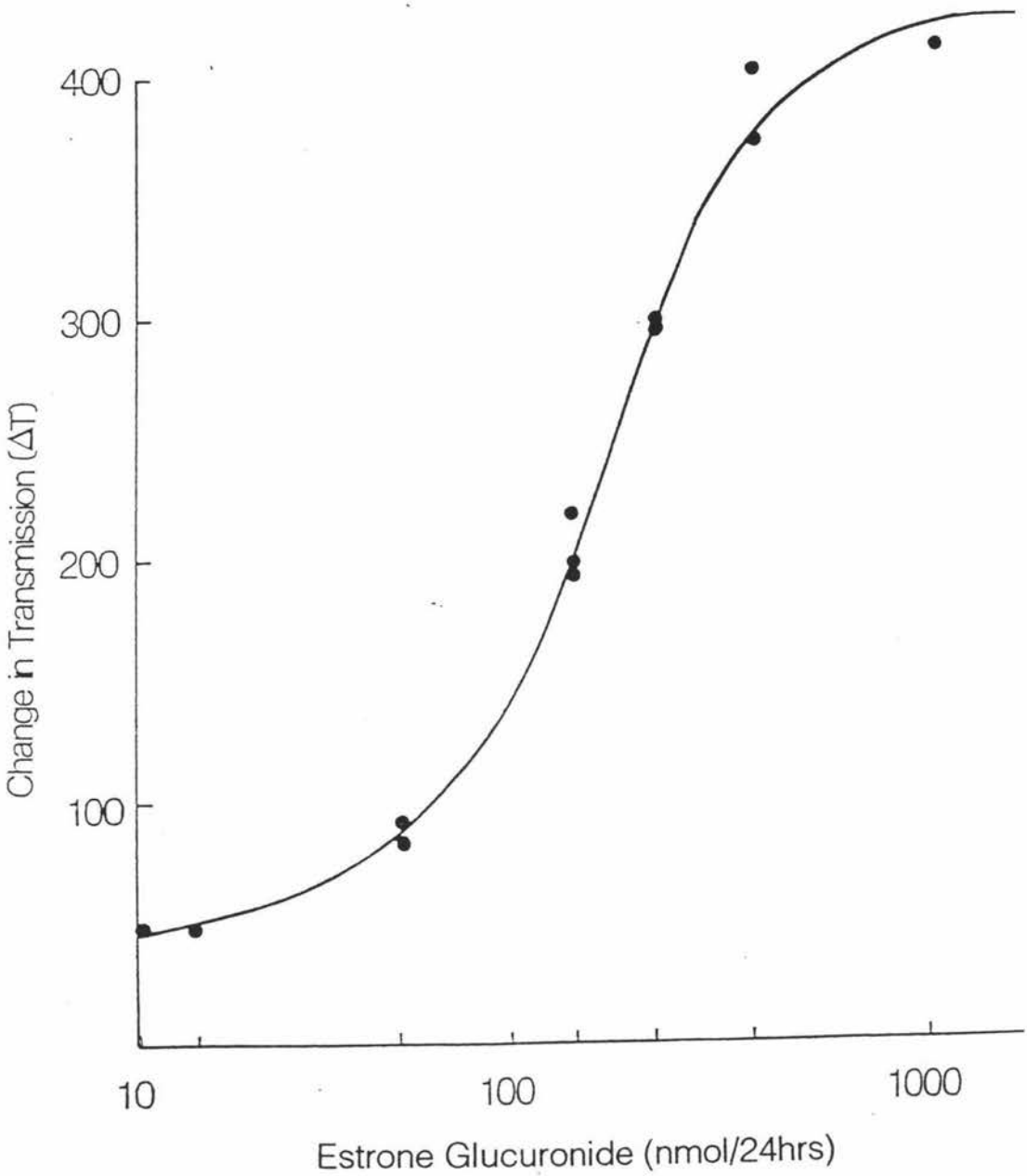

Figure 1.12 The Standard Curve for Estrone Glucuronide

1.9.5 THE PREGNANEDIOL GLUCURONIDE ASSAY

The chemistry of the assay procedure for PdG is essentially the same as that for E1G. However, there are of course a few differences in the reagents and protocol. Most

notably and obviously compared to the E1G assay tubes, the PdG assay tubes contain PdG antibodies and conjugate instead. All the other differences in the PdG assay are

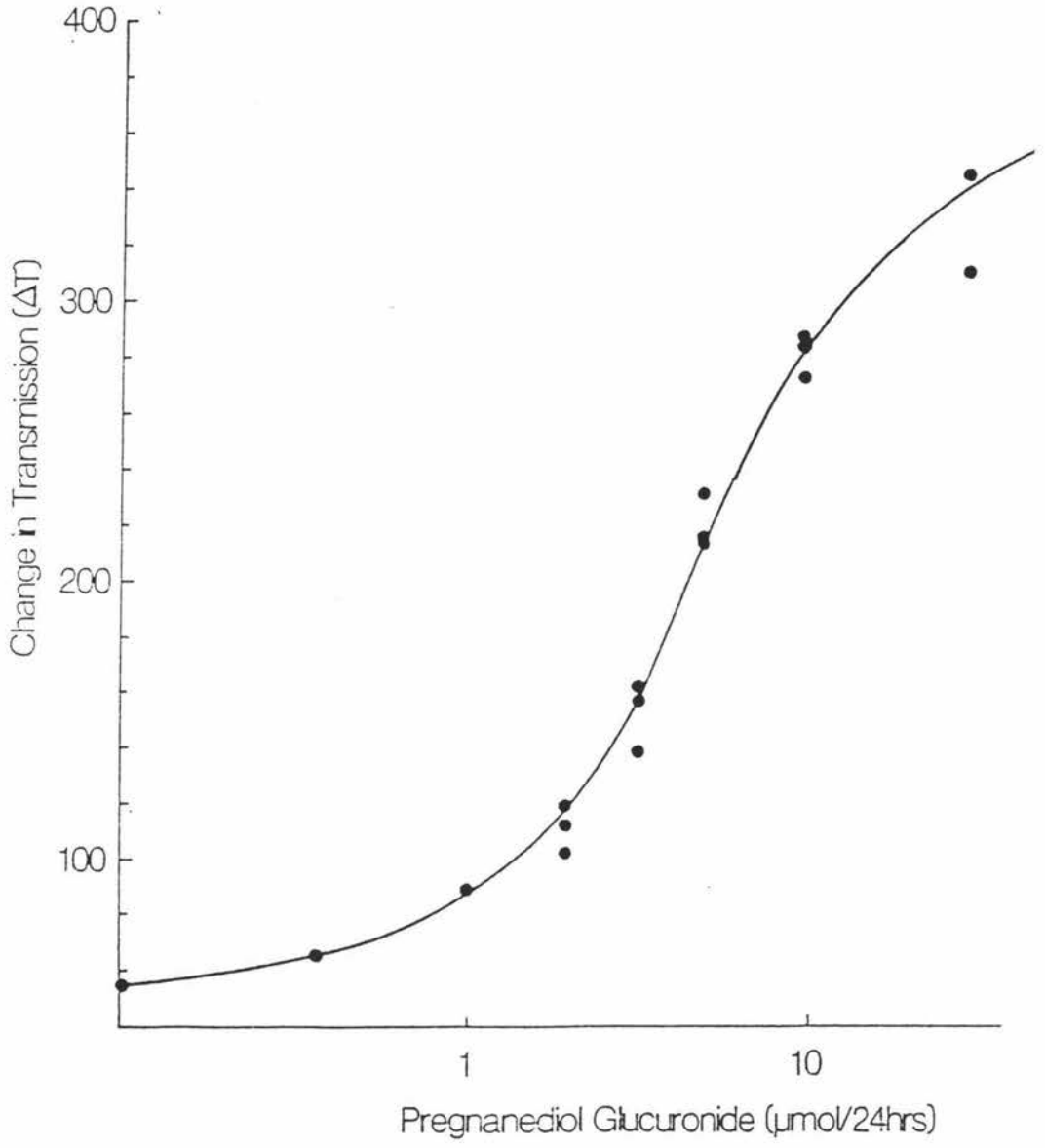

Figure 1.13 The Standard Curve for Pregnanediol Glucuronide

a direct consequence of the ovary producing comparatively much greater amounts of progesterone than estrogen. For example, in the average cycle the maximum E1G value is approximately 300 nmol 24 hr^{-1} and the maximum PdG value is approximately 18,000 nmol 24 hr^{-1} (Brown & Blackwell, 1989) i.e. there is a sixty fold difference

between the maximum E1G and PdG levels. In practical terms this means the assay for PdG is a lot more sensitive and the incubation times and reaction times can be correspondingly shortened. The first incubation step remains the same at five minutes as this time is required for the mixing bead to be freed, but the second incubation is cut from ten minutes to five, and the actual enzymatic reaction time is shortened from twenty minutes down to five as well. Unfortunately the high PdG levels in the urine does mean an additional one in five dilution must be performed on the PdG samples before testing. This is done simply by mixing 200 μl of distilled water up with 50 μl of the already time-diluted urine sample and using 50 μl of this second dilution in the assay instead. Apart from these few changes the protocol is identical to that used for E1G.

A typical PdG standard curve is shown in Figure 1.13.

1.9.6 INTERPRETATION OF OVARIAN MONITOR RESULTS

One of the advantages of the Ovarian Monitor is the standard curve is highly reproducible unlike in radio-immunoassay where a fresh standard curve must be established for each analysis. Thus, it is possible with the Ovarian Monitor to perform daily assays without the necessity of constructing a standard curve. The Ovarian Monitor results as outlined in the previous sections (Section's 1.9.4 & 1.9.5), are recorded as $\Delta T\ (20\ min)^{-1}$ for the E1G test and as $\Delta T\ (5\ min)^{-1}$ for the PdG test. These data are then usually plotted directly against days of the cycle on the X-axis (Figure 1.14), and the standard curve never has to be used unless quantitative data are required. This is because it is the pattern and the changes in the hormone levels which are important for the interpretation. In the case of the PdG assay, a $\Delta T\ (5\ min)^{-1}$ threshold to delineate the end of fertility is also important. This is worked out in the laboratory for each batch of PdG assay tubes before distribution using the standard curve.

One of the major uses of the Ovarian Monitor is to delineate the beginning and end of the fertile period. The fertile period itself is determined by the gamete survival time as for fertilisation to occur, a viable spermatozoon is required to be present in the female genital tract at the same time as a viable ovum. In most couples the maximum

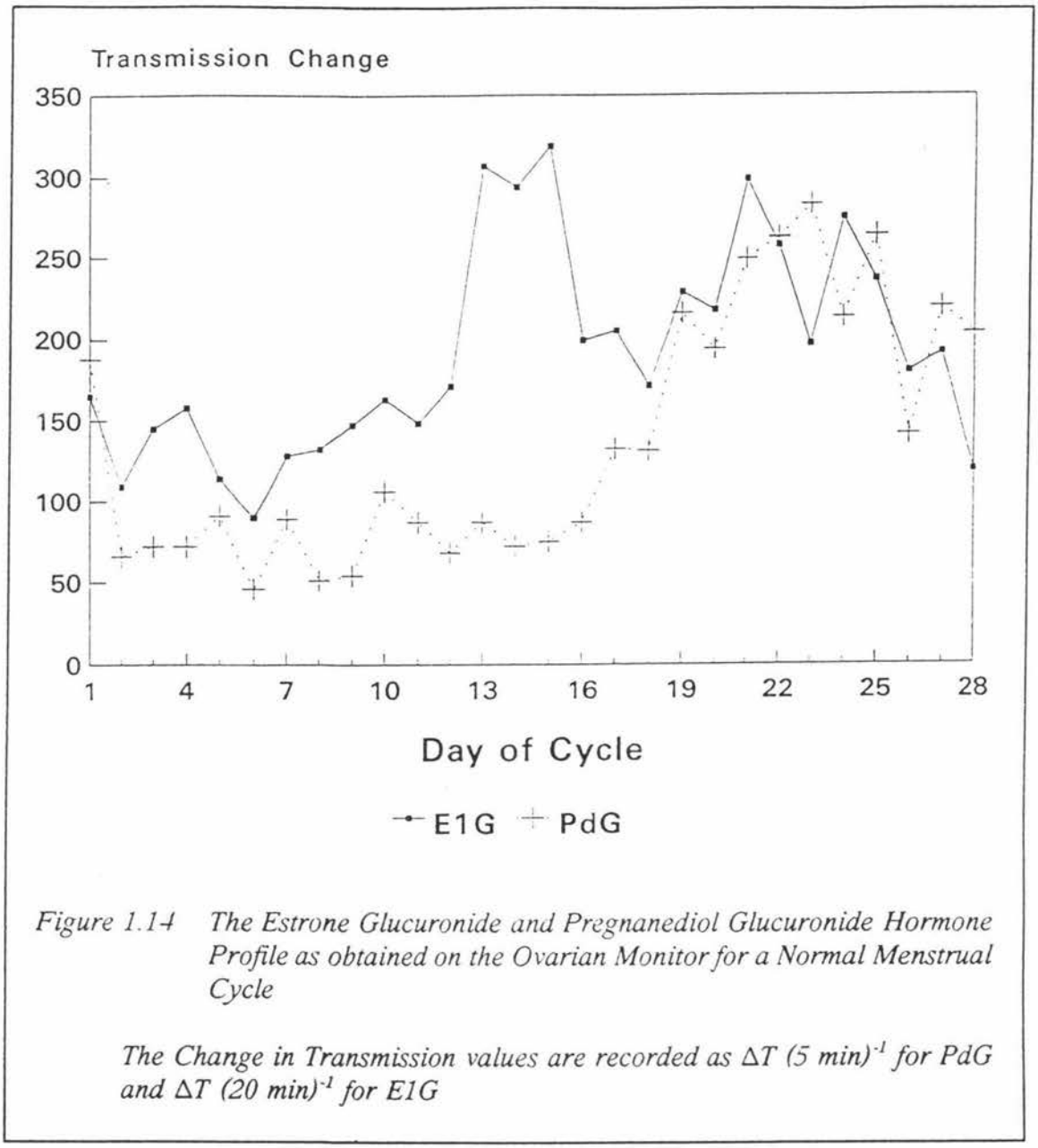

Figure 1.14 The Estrone Glucuronide and Pregnanediol Glucuronide Hormone Profile as obtained on the Ovarian Monitor for a Normal Menstrual Cycle

The Change in Transmission values are recorded as ΔT (5 min)$^{-1}$ for PdG and ΔT (20 min)$^{-1}$ for E1G

fertilisable life of the sperm is three to four days, although it can be up to seven days for very fertile couples. The fertilisable life of the ovum in contrast is very short, being limited to approximately only twelve hours from the time of ovulation (Brown and Gronow, 1985). Thus, the prediction and detection of ovulation is the key to being able to define the fertile period, with the fertile period beginning three to four days before ovulation (for most couples), and ending twelve hours after ovulation (see Figure 1.15).

Using the Ovarian Monitor, ovulation is predicted from the day of the E1G fall. Because LH is responsible for the fall in estrogen levels which preceeds ovulation, and

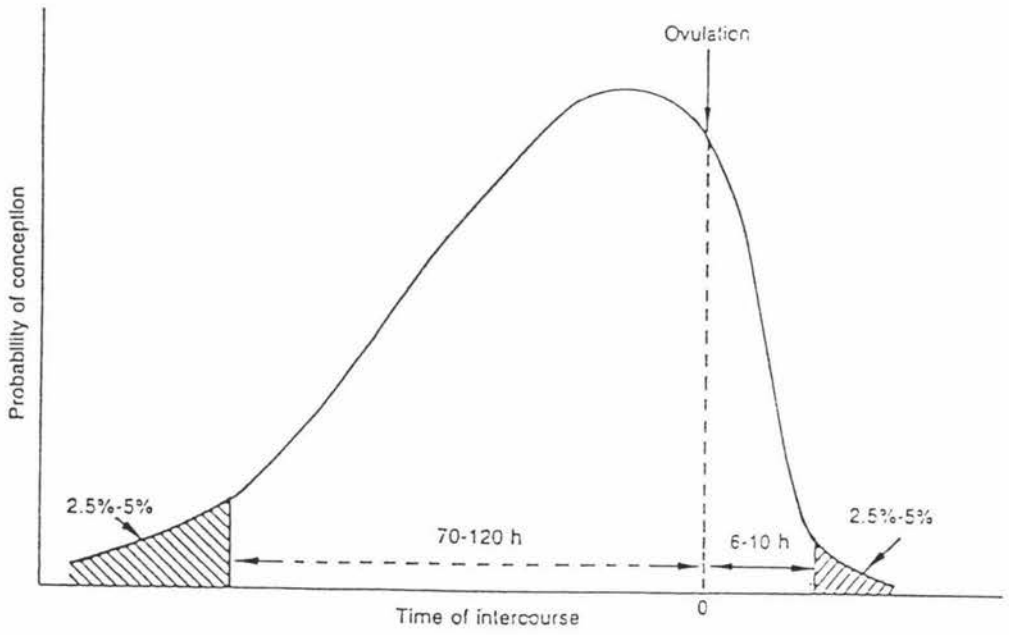

Figure 1.15 *Probability an Isolated Act of Intercourse (expressed in hours relative to the event of ovulation) will lead to Conception in the Human Female*

because it is this LH surge which induces ovulation then a fall in E1G levels can be used as an indicator that ovulation is imminent. The event of ovulation occurs on average 36 hours after the E1G peak (Brown *et al.*, 1989). In contrast to what most people would expect, the day of maximum fertility corresponds more closely to the day of the E1G fall as opposed to the event of ovulation itself. This is because of the lag phase from the time of intercourse to time of sperm capacitation. Capacitation is the process whereby the sperm's acrosomal membrane is dissolved and is a prerequisite for the sperm to be able to penetrate the ovum.

To predict the beginning of fertility, as is required in the avoidance of pregnancy, a marker is needed which can be observed five to six days before ovulation i.e. there must be sufficient warning of ovulation to allow time for the sperm to die before the ovum is released. The Ovarian Monitor uses the first urinary E1G rise after menstruation as the marker for the beginning of the potentially fertile days as this occurs on average six days before ovulation (Blackwell & Brown, 1992). Even for women whose cycles do

not give this much warning, the first E1G rise is still believed to be a valid marker for the beginning of fertility. This is because the cervical mucus produced in the absence of estrogen creates an environment in the vagina which is unfavourable to sperm survival. It is only when estrogen levels rise above baseline that the mucus begins to take on the fertile characteristics essential for sperm survival. This combined with the average fertilisable lifespan of the sperm of three days makes pregnancy an unlikely event for these women (Brown & Blackwell, 1989).

The marker used to delineate the end of fertility is a threshold level of urinary PdG as an increase in progesterone production from baseline levels is completely dependent upon ovulation. This is in contrast to the drop in estrogen levels which always preceeds ovulation, as a drop in estrogen levels can also occur when the leading follicle becomes atretic. Thus, a drop in E1G levels is not always associated with ovulation, and for this reason cannot be used as a universal marker from which the end of the fertile period can be calculated.

A threshold level of 6.3 μmol 24 hr^{-1} is used with the equivalent ΔT (5 $min)^{-1}$ being calculated for each separate batch of tubes (see above). The validation of this threshold value is discussed in detail in Section 2.3.1.2.

Thus, in summary, when using the Ovarian Monitor, all days from the first rise in E1G levels following menstruation, to the day before the threshold level of 6.3 μmol 24 hr^{-1} for PdG is reached, should be considered as potentially fertile. When using the Ovarian Monitor the day of the E1G peak and the day following should be considered as the days of maximum fertility.

1.10 POTENTIAL OF THE OVARIAN MONITOR

As discussed in Section 1.9.6, the Ovarian Monitor was specifically designed to delineate the fertile period and the days of maximum fertility so it could be used as a natural aid in both the achievement and avoidance of pregnancy.

Studies show that the chance of conception is on average only 25% per cycle (Royston, 1982), while other studies show that when the days of maximum fertility are used for intercourse the pregnancy rate increases to 70%. Thus, attempts to define the days of

maximum fertility and the use of these days for intercourse should always be the first step taken in the treatment of infertility. Because the Ovarian Monitor delineates this period of maximum fertility so precisely, its value in the early stages of infertility treatment is considerable. A major benefit of the Ovarian Monitor, is that the tests can be done by the women themselves in their own homes and thus, minimises stress which can also be a contributing factor in infertility (Thornton *et al.*, 1990).

Even in the cases where infertility is still a problem, it can provide information on what the next step in the treatment of infertility should be. For example, if the hormone patterns and levels are all well within the expected range, and the days of maximum fertility are easily depicted, then one possibility is that the infertility is a consequence of blocked fallopian tubes. However, if the hormone levels are abnormally low then this could indicate gonadotrophin treatment as the next appropriate action.

The Ovarian Monitor can also be used to advantage in *in vitro* fertilisation programmes, gonadotrophin releasing hormone therapy, gonadotrophin ovulation induction and the treatment of breast cancer.

Studies examining the relationship between the phase of the menstrual cycle during surgery for breast cancer and the long term survival rate, show a negative correlation between unopposed estrogen stimulation and the survival rate compared to other phases of the cycle (Badwe *et al.*, 1991). Thus, by the restriction of surgery for breast cancer to the luteal or menstrual phases of the cycle the chances for long term survival for these women could be improved. The most effective timing for surgery could easily be assured by issuing the women pre-operatively with Ovarian Monitors.

The big advantage with the Ovarian Monitor in the monitoring of infertility compared to the alternative laboratory assays e.g. radio-immunoassays and the total estrogen method, is that it is a lot cheaper in terms of labour, time and equipment, and in fact a lot of the time required can be provided by the women themselves in their own homes.

1.11 AIMS OF THE PRESENT STUDY

The Ovarian Monitor is a valuable aid for modern couples in determining their fertility and provides laboratory quality data to assist in decision making. Data from the Ovarian

Monitor is accumulating rapidly and analysis of information being provided is important to guide future directions of the research. Also, further development of the procedure is required in an attempt to provide users with a system which is in tune with their needs and perceptions of those needs.

This thesis is presented in three sections:

i) analysis of clinical data with a view to providing a rational basis for the PdG threshold used to mark the end of fertility with the Ovarian Monitor and to assess the value and quality of the data currently being obtained;

ii) a study of the kinetic properties of lysozymes from different sources aimed at finding a more active enzyme and thus, reducing the assay time for the measurement of estrone glucuronide;

iii) establishment of synthetic and chromatographic procedures for production of lysozyme estrone glucuronide conjugates for use in homogenous enzyme immumoassays utilised by the Ovarian Monitor.

CHAPTER TWO

CLINICAL STUDIES

2.1 INTRODUCTION

An objective method for the detection of the end of fertility has been sought by researchers for a number of years, and a consensus as to which method if any is the most appropriate has yet to be reached.

A study conducted by the World Health Organisation (WHO) Task Force on Methods for the Determination of the Fertile Period (Adlercreutz *et al.*, 1982) examined the value of using a PdG threshold as a marker for the end of fertility. Threshold values of both 10 μmol l^{-1} and 12 μmol l^{-1} of urine were tested for their ability to mark the end of fertility where the first day of infertility was defined as the day these thresholds were first equalled or exceeded. The value of utilising the first significant rise in urinary PdG levels from baseline to mark the end of fertility was also investigated. Two different methods for defining the first significant rise were tested for their ability to correctly mark the end of the fertile period. The first method defined the infertile period as beginning on the day when the urinary PdG values first increased 50% above the mean of the three immediately preceding values. For the second method, the infertile period was defined as beginning on the day when the PdG values first exhibited a rise 100% above the mean PdG value for the follicular phase.

In this study, the LH peak was used as the definitive marker of ovulation and the fertile period was defined as occurring between days -3 to +2 relative to the LH peak, with day +2 being the first day of infertility. Using the above definition of the fertile period, all the methods examined by Adlercreutz *et al.* (1982) were shown to be associated with the generation of a significant number of cycles in which the end of fertility was predicted as having occurred before the event of ovulation. Furthermore, all methods

were also associated with the generation of a significant number of cycles in which there was a delayed confirmation of the end of fertility compared to the reference definition. This led the authors to conclude that the use of a threshold level of urinary PdG, and the use of the first rise in urinary PdG levels above baseline, were both unsuitable methods for the reliable delineation of the end of fertility. However, examination of the results obtained using an E1G/PdG ratio as a marker for the end of fertility was found to be more promising, and led to their recommendation of the E1G/PdG ratio as the preferred end of fertility marker.

A similar study was conducted by Cekan *et al.* (1986) in which a variety of different urinary hormonal methods were examined for their ability to successfully delineate the end of fertility. From their results, it was again concluded that both the use of a threshold level of urinary PdG, and the use of the first sustained rise in urinary PdG levels above baseline, were unsatisfactory as methods for determining the end of fertility. This, in conjunction with their other findings, led them to conclude that the markers for the end of fertility which had the most potential were the E1G/creatinine (day of peak +4 days) and PdG/creatinine ratios.

The conclusions from these two studies are in marked contrast to the practice of Brown's group in Melbourne (Brown *et al.* 1991), which used a threshold value for urinary PdG as an acceptable marker for the end of fertility, based on their experience over a number of years. These conflicting experiences can probably be explained by the failure of some of the researchers to recognise the importance of time diluted urine samples (see Section 1.9.3) for the assessment of physiological processes by the analysis of metabolites in the urine.

The studies performed on behalf of the WHO (Adlercreutz *et al.*, 1982) and by Cekan *et al.* (1986) had no correction for urine volume. That is, in these groups the hormones and metabolites in the urine were all measured as concentrations as opposed to excretion rates. However, because the rate of production of urine can vary markedly throughout the day, due to differences in fluid intake and respiratory and sweat losses, the hormone concentrations in the urine will not necessarily directly correlate with the hormone excretion rates. Since these differences were not taken into account by Cekan *et al.* (1986) and Adlercreutz *et al.* (1982) when examining the use of threshold levels of PdG

and the rise in PdG levels above baseline, their experimental results and thus, their conclusions were affected.

Because creatinine is excreted into the urine at a constant rate from the body, when a PdG or E1G to creatinine ratio is used in the determination of the end of the fertile period, the variations in the rate of urine production are accounted for. This explains why for Cekan *et al.* (1986) the best results obtained were those where a creatinine ratio was used. The best results obtained by the WHO trial also used a ratio (E1G/PdG) and thus, they too involved a correction for changes in the rate of urine production.

Two of the reasons why these two research groups neglected to use timed urine samples were because they considered there would be too much opposition against it from the women and that the samples would prove to be too difficult to collect. However, it has been the experience of Brown's group in Melbourne, which utilises a simple collection jug calibrated in hours specifically for this purpose (see Section 1.9.3), that the collection of timed urine samples has never been a problem.

Thus, in conclusion it can be said that the potential use of a threshold level of urinary PdG or increase in urinary PdG levels from baseline as markers for the end of fertility cannot be dismissed based only upon the published work of Adlercreutz *et al.* (1982) and Cekan *et al.* (1986). Consequently, the use of these methods in the delineation of the end of the fertile period warrants further study.

This chapter describes a detailed analysis of the clinical data obtained from the Royal Women's Hospital menstrual cycle database, Melbourne, and home data obtained with the Ovarian Monitor from the Palmerston North centre in an independent controlled study currently being conducted by the World Health Organisation (WHO). Both these data sets were compiled from results which have been expressed in terms of hormone excretion rates as opposed to urine concentrations, and thus, are not subject to errors caused by variations in urine volume. Thus, they provide an ideally suited body of data for the assessment of the success of urinary Pd or PdG levels as markers for the end of fertility. To date, no critical, objective mathematical analysis of this type has been reported in the literature despite the fact that a threshold value has been used for some years in Melbourne. The WHO data also allows the first assessment of the quality and usefulness of the hormone results obtained in the home under controlled conditions.

2.2 METHODS

2.2.1 THE ROYAL WOMEN'S HOSPITAL DATABASE

The Royal Women's Hospital in Melbourne has compiled a large number of largely complete menstrual cycle records of urinary steroid data and collected them together to form a hormonal database on the normal menstrual cycle. This unique database serves as a valuable reference set.

2.2.1.1 The Women

The majority of the women contributing to the database were under 44 years of age, of good health and had a history of regular menstrual cycles. It included no cycles from women who were currently on, or had been recently using, oral contraceptives. At the time of the examination of the data for this thesis, the total number of menstrual cycles in this database was 259, although not all the cycles were from different women.

2.2.1.2 Urine Collection and Analysis

All urine collections were timed 24 hour urine specimens, and were checked for volume and specific gravity to ensure no major errors in collection had occurred. If a specimen was lost during a 24 hour collection, the subject recorded the approximate time interval of the loss and the 24 hour value was corrected accordingly.

Total urinary estrogens (TE) were measured in Melbourne by the highly specific and accurate Kober Ittrich procedure (Brown *et al.*, 1968) after removal of the glucuronide group by hydrolysis and the subsequent extraction of the steroid. This procedure was used to measure the major urinary metabolites of estradiol (estrone-3-glucuronide, estriol-3-glucuronide and estriol-16-glucuronide). Urinary pregnanediol was measured by gas-liquid chromatography also after hydrolysis and extraction (Barrett & Brown, 1970).

2.2.1.3 Data Analysis

i) *A Statistically Defined Increase in Pregnanediol Levels from Baseline Values*

In this thesis, the Royal Women's Hospital database was used to analyse normal

menstrual cycles using a new algorithm developed by Associate Professor L.F. Blackwell and Mr A. Rowsall. A computer program (TEPDDE - total estrogen and pregnanediol data entry) has been written which allows the Melbourne data to be read in cycle by cycle. The program calculates the first significant rise in Pd above baseline using Trigg's tracking signal (see Section 2.2.3.3) at the 95% and 99% confidence intervals. Thus, for each cycle, the day of the first statistically significant rise of Pd was recorded at two confidence intervals with this day representing the first calculated day of infertility. Only cycles for which the database records were sufficiently complete for analysis by Trigg's tracking signal were examined in this study, with 173 cycles being analysed in total. All data were expressed relative to the day of the total estrogen peak (see Section 2.2.1.2) where the total estrogen peak day was designated day zero.

ii) *The Pregnanediol Glucuronide Threshold*

Because the most accurate set of urinary hormonal data currently available on the menstrual cycle is the Melbourne database, the urinary pregnanediol data from this database were used to assess the most appropriate threshold value for the Ovarian Monitor. Therefore, pregnanediol values were used to evaluate the suitability of three different threshold values as markers for the end of fertility and the chosen threshold value was then converted into the equivalent pregnanediol glucuronide value (i.e. equivalent Ovarian Monitor hormone concentrations) by using relative molar masses.

The most appropriate Pd threshold value was defined as the value which allowed the minimal, but sufficient time (99% confidence interval) for the ovum to die. The three Pd levels examined were 1.2, 1.4 and 1.6 mg Pd 24 hr^{-1} with the day these thresholds were first equalled or exceeded representing the first predicted day of infertility. Only cycles for which the database records were complete for all three Pd levels were included in the analysis. A total of 184 cycles were analysed.

To enable the Pd levels to be compared they must be expressed relative to a mid-cycle marker. Thus, all Pd levels were again expressed relative to the total estrogen peak day (day 0), where day -1 is the day directly preceding the total estrogen peak day, and day +1 is the day immediately following it. Thus, for each cycle, the days relative to the total estrogen peak day where each of the three hormone excretion rates were equalled

or exceeded, were recorded and the totals tallied.

2.2.2 THE WORLD HEALTH ORGANISATION STUDY

Currently the WHO Task Force on Methods for the Natural Regulation of Fertility is conducting a three centre multi-national study on the Ovarian Monitor for which Palmerston North is one of the centres. This study has been designed to analyse the suitability of the Ovarian Monitor as a home monitoring system for the hormonal definition of the fertile days of the cycle in natural family planning. The WHO study was conducted in three different centres, excluding Melbourne, in order to test if other centres around the world could duplicate Melbourne's success and results with the Ovarian Monitor.

To assess the feasibility of the Ovarian Monitor as a natural family planning aid a comprehensive set of objectives were drawn up by the WHO steering committee.

2.2.2.1 Study Objectives

The official objectives of the study were as follows:

1) To establish in a population of regularly menstruating women with ovulatory cycles (as judged from natural family planning records), the relationship in time between:

   a) the early basic infertile pattern (B.I.P) of mucus secretion and the baseline values of E1G during the initial part of the follicular phase;

   b) the first mucus change from the B.I.P. and the first rise in E1G levels;

   c) the peak mucus symptom and the pre-ovulatory peak day for E1G;

   d) the onset of the post-ovulatory infertile phase (determined from the peak mucus symptom and/or BBT shift) and the rise of PdG levels above the threshold value.

2) To compare the various phases of the cycle (early infertile days, fertile period

and late infertile days) as determined from the clinical symptoms with those determined on the basis of the hormonal data.

3) To assess if use of the Ovarian Monitor would reduce the recommended number of days of abstinence required for pregnancy avoidance.

4) To make a qualitative assessment of the Ovarian Monitor and its potential through focus group discussions with the participants in the study.

2.2.2.2 Subject Recruitment

To ensure the study methodology would be valid, a number of strict selection criteria had to be met by the participating women.

Among these criteria were included most notably the following:

- the woman must have successfully used a natural family planning method for the last twelve months for the avoidance of pregnancy;
- be living in a stable sexual relationship;
- have regular menstrual cycles of 25-40 days duration;
- have evidence that the last three cycles prior to entry into the study were ovulatory as judged from the corresponding natural family planning charts;
- must be willing to continue using their current natural family planning method with the intention of avoiding pregnancy for the duration of the project, i.e. six consecutive cycles;
- be willing to record daily all clinical signs and symptoms used in the current natural family planning method, and all acts of intercourse including barrier contraceptives if applicable;
- be willing to perform and record the daily measurements of E1G and PdG levels as obtained using the Ovarian Monitor;
- be willing to record their interpretation of the first and last day of fertility

according to their clinical signs as well as on their assay results.

2.2.2.3 Urine Collection and Analysis

For this study urines were collected daily by the women as outlined in Section 1.9.3. An aliquot of each time diluted urine sample was stored frozen in the 5 ml plastic specimen tubes supplied for the follow up laboratory assays which were performed at Massey University as part of this study. Although the women collected a urine sample daily for six complete cycles, daily E1G and PdG measurements for the complete cycle were performed by the women for the first two cycles only. Confirmation of the hormone assay results obtained by the women of these two cycles was carried out by repeating the assays in the laboratory. The laboratory repeats were performed using tubes provided from Melbourne and using the protocol outlined in Sections 1.9.4 and 1.9.5. Unlike for the home assays where each test was performed daily, a specially designed heating block set at 40°C was used to incubate the assay tubes. This enabled the assays to be performed in runs of forty and fifteen tubes for E1G and PdG respectively with the aid of a stopwatch. Transmission values were measured on the Ovarian Monitor as in the home assays.

All cycles were also assayed for LH to identify the pre-ovulatory surge which was used as the mid-cycle marker in the WHO study. In the Palmerston North centre this was performed by the Palmerston North Hospital Biochemistry Laboratory using a Boehringer-Mannheim enzyme immunoassay.

2.2.2.4 Data Analysis

Three different analyses were performed on the data collected from the Palmerston North centre of the WHO trial in this study. Only data collected from the first two cycles by the women themselves were analysed, not the laboratory repeats, as it was the viability of the assay as a home test which was being assessed.

i) *Markers of Fertility*

As part of the WHO study, the participants of the trial were required to fill in diary sheets of not only the daily hormone values they obtained using the Ovarian Monitor, but also of all the daily clinical signs and symptoms of fertility they used in their normal

method of natural family planning. In addition, using the hormone data they obtained with the Ovarian Monitor, the women's own personal interpretations of the days marking the beginning and end of fertile period as well as the day of the E1G peak, were recorded for each cycle. This assessment was made independently of the information provided by the other markers of fertility. An interpretation by the women of their changing fertility status from their own clinical signs usually used as their natural family planning method was also made for each cycle. This assessment was made independently of the information provided by the hormonal data and included the women's estimates of the day marking the beginning of fertility, the day marking the first day of infertility as well as the day of the peak mucus symptom.

For the purposes of this study, after measurement of the LH peak, the day of the LH peak and the information provided by the diary sheets was summarised for each woman. Using the resulting summary sheets, a total of 119 cycles from the Palmerston North centre were analysed. This involved a comparison of the apparent beginning, end and total length of the fertile period using the different fertility markers, and also the markers of ovulation i.e. the peak mucus symptom and the day of the E1G peak.

For a reliable comparison to be made of the different fertility markers, the cycle days were numbered relative to the LH peak as day zero. Using the LH peak day as a reference, day -1 was defined as the day directly preceding the LH peak, and day +1 as the day immediately following it. Thus, for each individual cycle, the day any given fertility marker was reached relative to the LH peak day was established. The total number of cycles which reached a certain fertility marker on any given day relative to the LH peak day was calculated thus, allowing a statistical comparison of the different fertility markers to be made. These results were all expressed as percentages of the total number of cycles.

The lengths of the total fertile periods for the mucus method, hormones and the symptothermal method were analysed by comparing the corresponding means and standard deviations. In the symptothermal method, the end of fertility is defined according to the indicator (mucus or BBT) which gives the most conservative (i.e. latest) estimate.

ii) *An Increase in Pregnanediol Glucuronide Levels from Baseline*

The daily data for the first forty cycles for which the women had complete records of their E1G and PdG measurements obtained with the Ovarian Monitor, were manually entered into an ASCII file as ΔT $(20\ min)^{-1}$ and $(5\ min)^{-1}$ respectively. The day of the first significant increase in PdG levels above baseline as defined by the Trigg's tracking signal (see Section 2.2.3) was then calculated by the TEPDDE program at both the 95% and 99% confidence intervals. The day of the first significant increase in PdG levels above baseline was used as the tracking signal's predicted day of the first day of infertility. The distribution of first rises for all cycles was expressed relative to the E1G peak in each case.

This set of data was then compared to the equivalent set of data obtained by a similar computer analysis of the cycles from the Royal Women's Hospital database with Trigg's tracking signal.

iii) *Reproducibility of the Women's Hormonal Data*

Using the laboratory repeats carried out at Massey University for each woman's first two cycles, the reproducibility of the test was evaluated and the ability of the women to correctly perform the test was assessed.

2.2.3 TRIGG'S TRACKING SIGNAL

Chronological data i.e. data consisting of a series of values which are made sequentially in time, may be statistically analysed by time series analysis. This method of statistical analysis, also known as trend analysis, has been specifically designed for data where the time order of the observations is important, and the values are not completely independent of each other. By analysing such a data set by time series analysis, the prediction of values further along in the series can be made. Because the hormonal data of menstrual cycles is chronological and serially dependent, it is ideally suited for trend analysis.

There are several different methods by which data can be analysed by trend analysis. The method chosen in this study, and incorporated into the TEPDDE program, by which the changes in hormone levels throughout the cycles were analysed, was based on a

method refined by Trigg (1964). This method has since been renamed Trigg's tracking signal.

2.2.3.1 Calculation of Trigg's Tracking Signal

For any continuous series of relatively unchanging values

$$x(1), x(2), x(3), x(4), ..., x(n)$$

an exponentially smoothed average (ESA) can be calculated for the data. Exponential smoothing involves taking the geometrically weighted sums of the past values such that the greatest weight is placed on the most recent values. Thus, the observations are weighted in order of their decreasing age. It is called exponential smoothing because it reduces (smooths) the noise from the data before analysis, and the equation the ESA is calculated from is in the form of an exponential series.

$$ESA_{(n)} = \alpha.x_n + \alpha(1 - \alpha).x_{n-1} + \alpha(1 - \alpha)^2.x_{n-2} + ... \qquad \text{Eqn. 2.1}$$

where x_n is the latest value, and α is an adjustable parameter called the smoothing constant with a range of 0-1.

The above expression can be simplified to:

$$ESA_{(n)} = \alpha.x_n + (1 - \alpha).ESA_{(n-1)} \qquad \text{Eqn. 2.2}$$

For a comprehensive description of the derivation see Cembrowski *et al.* (1975).

The smoothing constant can be calculated from the number of baseline observations (N) in the equivalent moving average by the following formula. In this formula, the equivalent moving average is an average of the most recent observations.

$$\alpha = 2/(N + 1) \qquad \text{Eqn. 2.3}$$

Thus, the smoothing constant is inversely proportional to the number of baseline observations used to calculate the equivalent moving average. For example, when N = 1, α = 1, and when N = 39, α = 0.05. The closer α approaches 1, the more weighting is given to the more recent values in the calculation of $ESA_{(n)}$ due to the αx_n term, and the less weighting is given to the previous values due to the $(1 - \alpha).ESA_{(n-1)}$ term i.e. the previously calculated ESA. Thus, when N = 1, and consequently α as well, all

weighting is given to the last data point and none to any of the earlier ones. In contrast, when α approaches zero as is the case when N is very large, most of the weighting is given to the previous $ESA_{(n-1)}$ value, and very little to the latest data point.

Alternatively, the value for the smoothing constant does not have to be calculated according to its formula, but can be arbitrarily assigned instead, according to the balance of weighting desired.

The value selected for the smoothing constant is of critical importance. When a small value for α is used, the estimate behaves like the averages of the past data. Thus, an α value which is set too low, results in the tracking signal being very insensitive to change i.e. compared to a more moderate α value, much larger departures from the mean would be required before the changes were considered statistically significant. Alternatively, if a large α value is used, the estimate responds rapidly to any changes in the data series pattern. However, if the value for α is set too high, the resultant tracking signal would become too sensitive to change, and thus, more prone to the generation of false positives than a more conservative estimate of α would indicate.

Statistically significant changes in the series of data points cannot be detected by the values generated from the ESA of the raw data. Rather, the ESA smooths the raw data in preparation for the detection of a significant change in a later analysis as described below.

The exponentially smoothed average is used as a predictor (forecast) of the next observation. The difference between this value predicted (or forecasted) by $ESA_{(n-1)}$, and the actual experimental value $x_{(n)}$ is called the forecast error (FE).

$$FE_{(n)} = x_n - ESA_{(n-1)} \qquad \text{Eqn. 2.4}$$

If the values remain constant, the forecasted and averaged measurements should be approximately the same, and the resultant forecast errors should fluctuate around zero. However, a systematic change in the raw data in either direction will cause $ESA_{(n-1)}$ to differ from the actual data with the result that $FE_{(n)}$ becomes consistently positive or negative. The significance of this departure from the established pattern is calculated using the exponentially smoothed forecast error (SFE).

$$SFE_{(n)} = \alpha.FE_{(n)} + (1 - \alpha).SFE_{(n-1)} \qquad \text{Eqn. 2.5}$$

Only non-random changes in the data will result in the steadily increasing or decreasing smoothed forecast errors indicative of significant increases or decreases in the mean. The statistical measurement of the significance of these changes from the mean is based on the ratio known as Trigg's tracking signal. Trigg's tracking signal is the normalised smoothed forecast error and is calculated by dividing the smoothed forecast error by the mean absolute deviation (MAD).

$$TS_{(n)} = SFE_{(n)}/MAD_{(n)} \qquad \text{Eqn. 2.6}$$

The mean absolute deviation, which corresponds for the normal distribution to 80% of the value of the standard deviation (Lewis, 1971), is a measure of the amount of noise or random variation present in the set of raw data. It is obtained by the exponential smoothing of the absolute forecasting errors (Trigg, 1964).

$$MAD(n) = \alpha.|SFE_{(n)}| + (1 - \alpha).MAD_{(n-1)} \qquad \text{Eqn. 2.7}$$

2.2.3.2 Interpretation of the Tracking Signal

The tracking signal has a theoretical minimum value of -1 and maximum of +1, with the magnitude of the tracking signal being directly related to the probability that a change in the data is significant. When the values of the raw data are relatively constant, the expected and observed values will be similar, and both the forecast error and the tracking signal will fluctuate around zero. Fluctuations around zero for the forecast error and the tracking signal will also occur with random variations in the raw data. However, when the raw data consistently changes in one direction, the smoothed forecast error will become increasingly negative (data values becoming smaller) or positive (data values becoming larger), and the tracking signal will approach the theoretical minimum (-1) or maximum (+1) respectively. A value of +1 for the tracking signal is associated with a 100% certainty that there has been a significant increase in the values being measured. Conversely, a value of -1 for the tracking signal is associated with a 100% certainty that there has been a significant decrease in the values being measured. With tracking signals between the two extremes, the degree of significance is a function of the smoothing constant.

For a small smoothing constant two assumptions can be made. Firstly, it can be assumed that the local estimate of MAD is relatively constant and approximates the true MAD. The second assumption is that the smoothed forecast error is normally distributed with a mean of zero and a variance which can be calculated. The formula from which the variance for a small smoothing constant is calculated, and its derivation is described in full by Batty (1969). If the above two assumptions are made, then it can also be assumed that the tracking signal is normally distributed with a mean of zero and a calculable variance. The calculation of variance for Trigg's tracking signal is also reviewed by Batty (1969). This calculation of variance for Trigg's tracking signal was used by Cembrowski *et al.* (1975) for the formulation of tables of the tracking signal limits and the confidence levels that these limits were normally exceeded.

For larger values of the smoothing constant i.e. greater than 0.1, where the local estimate of the MAD is not constant, these tables are inaccurate, and simulation tables should be used instead (Cembrowski *et al.*, 1975). Simulation tables for Trigg's tracking signal over a range of confidence levels for α values of 0.1, 0.2, 0.3, 0.4 and 0.5 are provided by Batty (1969). These tables include values for both single and double exponential smoothing, with single exponential smoothing being the method used to calculate the tracking signal before refinement of the method by Trigg (1964).

2.2.3.3 Application of Trigg's Tracking Signal to Menstrual Cycle Data

Trigg's tracking signal was utilised in this study to analyse menstrual cycle data for the determination of the first significant rise in Pd or PdG levels from the follicular phase baseline. It was used in the analysis of data from both the Melbourne database and the Palmerston North centre of the WHO study.

To enable the tracking signal to be utilised for the analysis of menstrual cycle hormonal data, appropriate values must be set for α and the initial values of $ESA_{(0)}$, $FE_{(0)}$, $SFE_{(0)}$, and $MAD_{(0)}$. $ESA_{(0)}$ was calculated by taking the geometric average (i.e. log mean) of the first six baseline values. When the PdG levels were still falling from the previous cycle, the first six days following stabilisation of the baseline, were used. The initial values for $FE_{(0)}$ and $SFE_{(0)}$ were set equal to zero, and the initial estimate for $MAD_{(0)}$ was calculated from the standard deviation of the baseline data for that cycle with

$MAD_{(0)}$ being equal to 0.798σ (Blackwell & Brown, 1992). The standard deviation of the baseline data itself was calculated according to the following equation where x is the antilogarithm of the geometric mean and λ is the standard deviation of the logarithms.

$$\lambda^2 = 0.4343 \log_{10} (1 + \sigma^2/x^2) \qquad \text{Eqn. 2.8}$$

The necessity for this equation and a description of its derivation is given by Gaddum (1945).

Because the mean of the baseline was based on six values, and $\alpha = 2/(N+1)$ where N is the number of baseline observations, α was set at 0.286. The tracking signal limits corresponding to the confidence levels of 95% and 99% were obtained by extrapolation between appropriate values of the simulated probability tables in Batty (1969). This gave the tracking signal limits to be 0.632 and 0.745 for the 95% and 99% confidence intervals respectively. Thus, tracking signal values at or above 0.632, are associated with a 95% certainty that the increase in the tracking signal and thus, the data is significant and not due just to random variation in the data. Likewise for tracking signal values at or above 0.745 there is a 99% probability that the increase in the tracking signal has been brought about by a significant rise in the data.

2.3 RESULTS AND DISCUSSION

2.3.1 THE ROYAL WOMEN'S HOSPITAL DATABASE

2.3.1.1 The First Statistically Significant Pregnanediol Rise

Figure 2.1 shows the daily total estrogen and Pd levels over a complete cycle as recorded for a typical menstrual cycle from the Melbourne database.

In Figure 2.1 the beginning of ovarian activity characteristic of a new cycle is clearly indicated by the rise in urinary estrogens from the follicular phase baseline on day -5. Selection of a dominant follicle and its subsequent rapid growth brings about a transition in estrogen production from the slow increases observed between days -5 and -2 to the logarithmic growth observed between days -2 and 0. The estrogen peak occurred on the

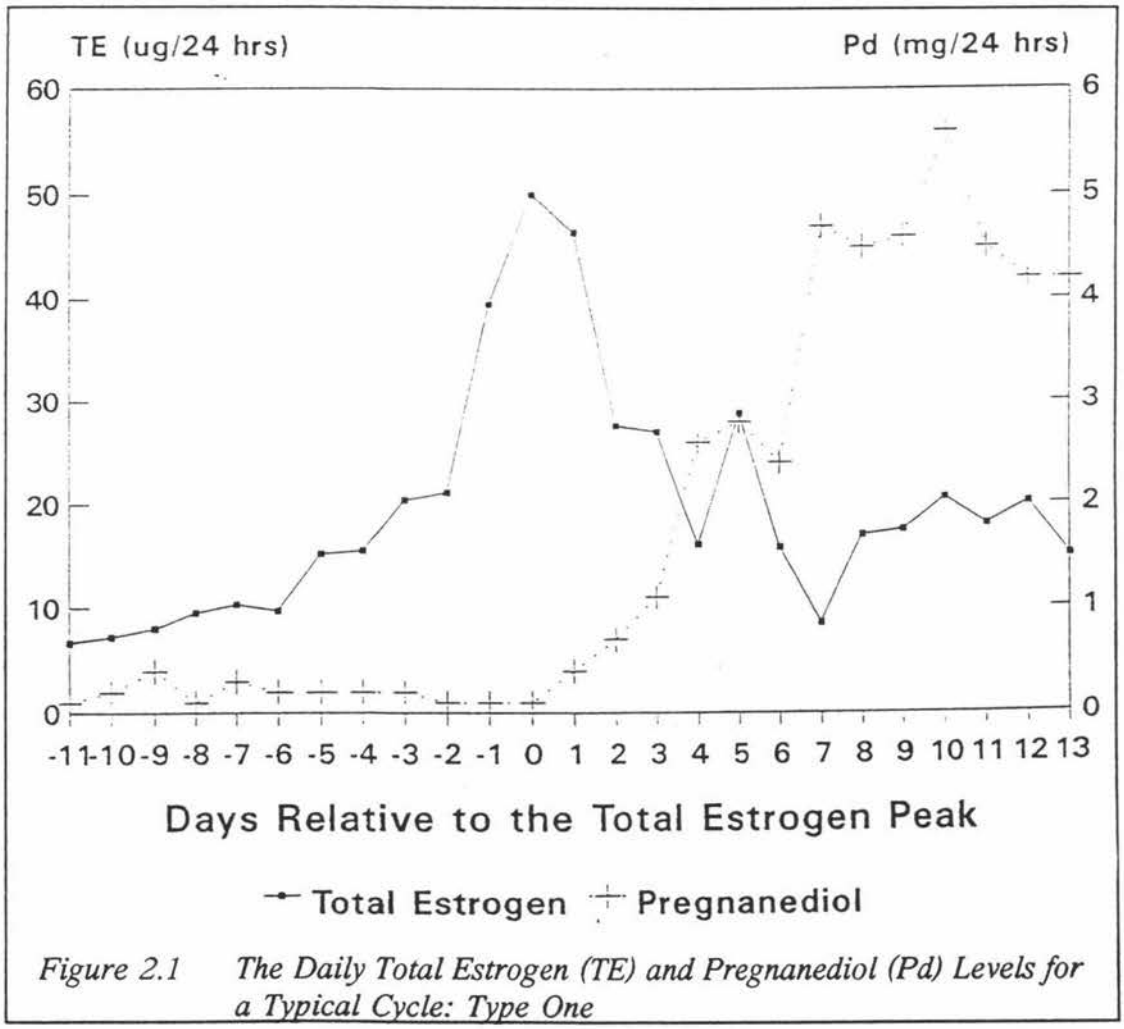

Figure 2.1 The Daily Total Estrogen (TE) and Pregnanediol (Pd) Levels for a Typical Cycle: Type One

same day as the LH peak and was followed by the sharp drop in estrogen values which

is characteristic of normal menstrual cycles. There is usually, but not always, a second rise in estrogen levels in the luteal phase. Figure 2.1 shows this cycle to be one of the exceptions.

The Pd profile of Figure 2.1 shows the Pd levels at the beginning of the cycle to be more or less constant stabilising at a minimum level between day -2 and day 0 relative to the total estrogen peak day. Day 0 to the end of the cycle was characterised by a Pd peak which was preceded by a slow rise over days 1 to 3. The Pd peak reached its maximum value on day 10.

The statistical significance of these changes as measured by Trigg's tracking signal is shown graphically in Figure 2.2. The tracking signal fluctuates around 0 (-0.2 to +0.4) for the first nine days of the cycle, which is consistent with a steady baseline. This was followed by a sharp decline in the tracking signal which reached a minimum value of -0.787 on day 0, the day of the total estrogen peak. Thus, at day 0, the tracking signal recorded a decrease in the mean Pd levels which was significant at the 99% confidence

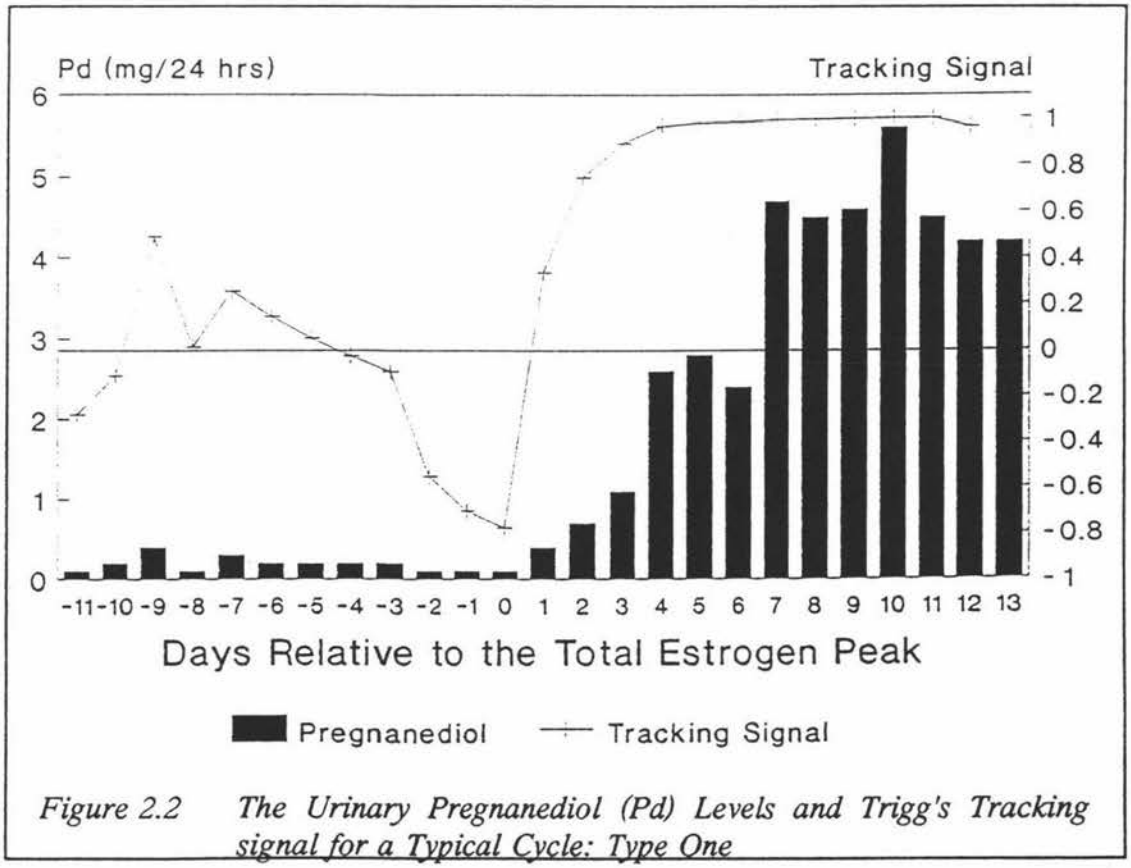

Figure 2.2 *The Urinary Pregnanediol (Pd) Levels and Trigg's Tracking signal for a Typical Cycle: Type One*

interval. The physiological significance of this slow decline is unknown, but it was a

feature of approximately 30-40% of the cycles. From this minimum value the tracking signal then proceeded to increase for the rest of the cycle to reach a value of 0.773 on day +2 of the cycle, relative to the total estrogen peak, when the Pd excretion rate had reached a level of 0.7 mg 24 hr^{-1}. A tracking signal of 0.745 is associated with a greater than 99% certainty that there has been a positive increase in the data. Thus, with a tracking signal of 0.773 there is less than one chance in a hundred that the observed pregnanediol rise is derived from random fluctuations in the data.

Figure 2.3 shows the Pd values and tracking signal from another type of typical cycle from the database. Again, in this cycle the Pd levels remained relatively constant throughout the first phase of the cycle. However, unlike in the previous cycle (see Figure 2.2) there was no visible decrease in Pd levels before they began to rise again.

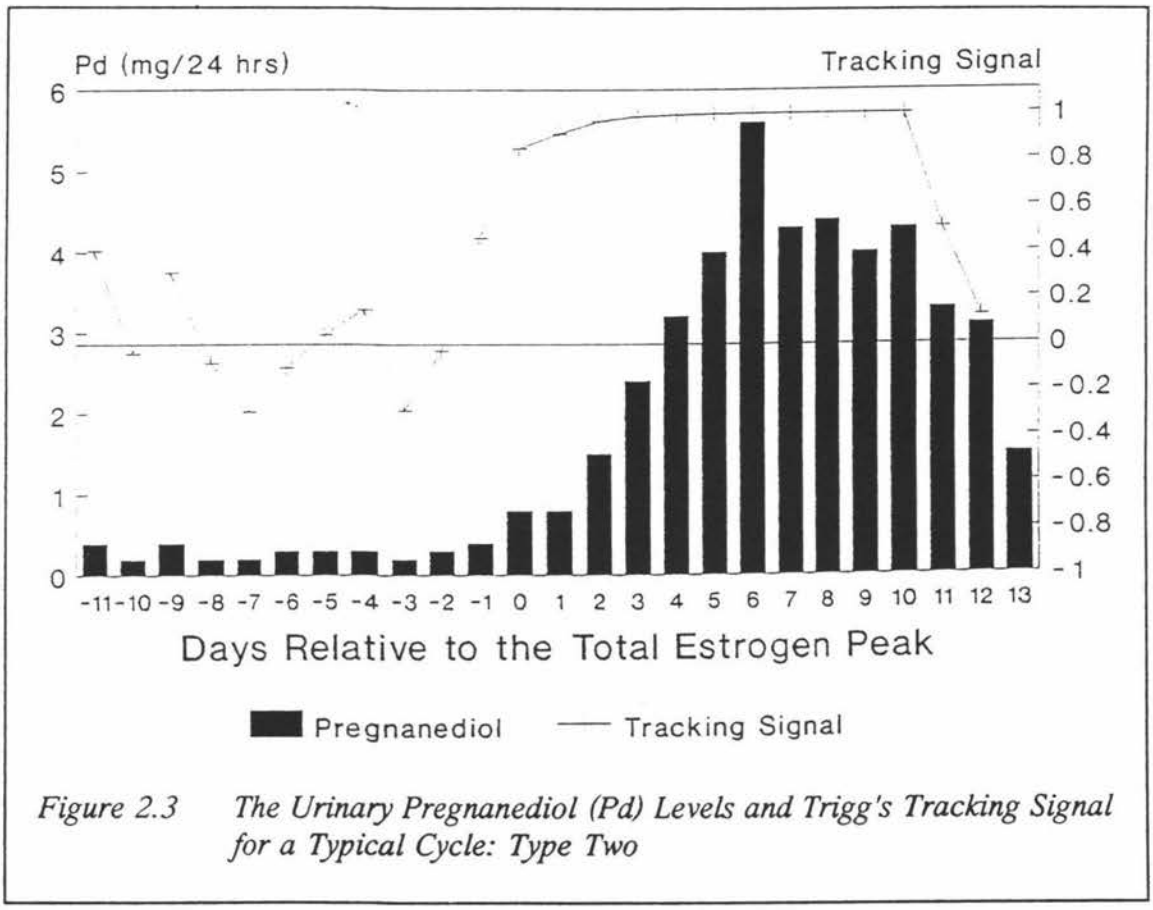

Figure 2.3 *The Urinary Pregnanediol (Pd) Levels and Trigg's Tracking Signal for a Typical Cycle: Type Two*

More importantly, the rise in Pd levels as measured by the tracking signal was considered to be significant (greater than 99% confidence interval) on the day of the total estrogen peak when the Pd value was 0.7 mg 24 hr^{-1}.

All the cycles in the database for which the tracking signal could be calculated were segregated into these two different groups; those that showed a significant increase in Pd levels as measured by the tracking signal on a day following the total estrogen peak (as in the cycle of Figure 2.2), and those in which the first significant rise was recorded as having occurred on, or preceding, the day of the total estrogen peak (as in the cycle shown in Figure 2.3).

At the 95% confidence level, 67% of the cycles fell into the first category, i.e. it can be said with 95% confidence that 67% of the cycles examined had a significant rise in Pd levels which was not attributable to random fluctuations in the data on a day after the total estrogen peak day, while the remaining 33% had their first significant rise in Pd levels before, or on, the day of the total estrogen peak (Figure 2.4).

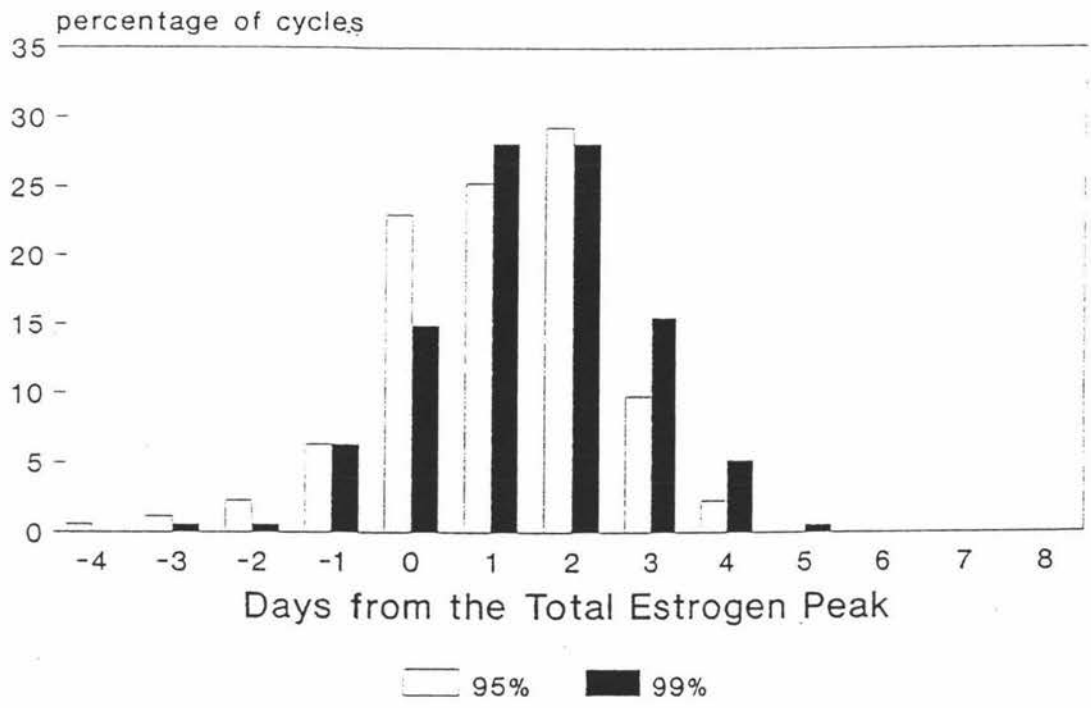

Figure 2.4 *The First Significant Pregnanediol Rise using Trigg's Tracking Signal at 95% and 99% Confidence Intervals*

Even when the level of confidence was increased to 99%, 22% of the cycles still exhibited a rise in the Pd levels on the day of the total estrogen peak or before (Figure 2.4). Thus, if the assumption that ovulation cannot occur on the day of the total

estrogen peak or before holds true, then the use of the first rise in Pd levels is unacceptable as a marker for the first day of infertility in nearly one quarter of the cycles.

This assumption is based on the findings that the beginning of the fall in serum estradiol which defines the peak, and the beginning of the LH surge, occur simultaneously (Hoff, *et al.*, 1983). Since it is the LH surge which induces ovulation, and the previously described peak of serum estradiol which is the major precursor of the urinary estrogens which form the total urinary estrogen peak, it is physiologically impossible for the fertile period to be finished before the total urinary estrogen peak occurs.

The details of the mid-cycle dynamics of circulating hormone levels were clearly elucidated by Hoff *et al.*, (1983) by the measurement of hormone levels every two hours over the peri-ovulatory period. This study showed that the large post-ovulatory peak of progesterone was preceded by a less commonly known, much smaller, pre-ovulatory rise. This small pre-ovulatory increase in progesterone levels began twelve hours before and continued until twelve hours after the onset of the LH surge. One possible physiological function of this early rise, which has since been demonstrated experimentally, is to augment estrogen action in the initiation of the LH surge (Liu & Yen, 1983).

Thus, the pattern of progesterone production observed in the normal menstrual cycle is the result of the production of progesterone from three different sources. The baseline level of progesterone which characterises most of the follicular phase is mainly due to the constant production of progesterone precursors from the adrenal glands. The small rise in progesterone levels which occurs just prior to ovulation is probably produced by the pre-ovulatory follicle, while the large peak of progesterone which characterises the luteal phase is produced by the corpus luteum.

It was this small pre-ovulatory rise in progesterone levels which Trigg's tracking signal was detecting at the 99% confidence interval in the 22% (see Figure 2.4) of the cycles which exhibited a rise in urinary Pd levels on the day of the total estrogen peak or before (mean ± SD; 0.71 ± 0.25 mg Pd 24 hr^{-1}, n = 38, range 0.3-1.2 mg Pd 24 hr^{-1}). For the remaining 78% of the cycles, the first statistically significant rise in urinary Pd

levels was detected by the Trigg's tracking signal after the total estrogen peak day and the data had a mean Pd value of 1.13 mg Pd 24 hr^{-1} with a standard deviation of 0.59 and a range of 0.3 to 3.4 mg Pd 24 hr^{-1} (n = 133).

Because the first rise in Pd levels, i.e. the pre-ovulatory rise, occurs before ovulation, any method which detects this rise as opposed to the main luteal phase peak, at least some of the time, cannot be used to measure the end of fertility. Thus, for physiological reasons Trigg's tracking signal is not a suitable method for the determination of the end of fertility and neither would be any other method which depends on an algorithm to detect the first rise in progesterone levels. This accounts for the consistently high number of false positives generated in the determination of the end of fertility when methods such as the Cusum procedure (Schiphorst *et al.*, 1985) have been implemented. A false positive is defined as a cycle where the end of fertility is signalled as having occurred before the event of ovulation.

From the above discussion, it becomes obvious that in order for the small pre-ovulatory rise in Pd not to be confused with the much larger luteal phase Pd peak in the determination of the end of fertility, a Pd level must be set which exceeds that obtained by the pre-ovulatory rise. A 99% probability that the Pd level exceeds that obtained in the pre-ovulatory Pd rise would appear to be a reasonable lower limit to set as a marker for the first day of infertility. This is equivalent to the mean of the first significant value of the small pre-ovulatory rise of Pd as determined by the Trigg's tracking signal + 2 standard deviations i.e. approximately 1.2 mg Pd 24 hr^{-1} or greater.

2.3.1.2 The Threshold Level for Pregnanediol

Three threshold values were chosen to evaluate the suitability of the use of a single threshold level of Pd as a reliable measure of the first day of infertility. The lowest Pd threshold level tested was 1.2 mg Pd 24 hr^{-1}, and was set for the reasons outlined at the end of the previous section (Section 2.3.1.1).

Figure 2.5 shows the percentage of cycles from the Melbourne database which reached the threshold value on each day relative to the day of the total estrogen peak for each of the three selected Pd threshold values. This graph shows that at 1.2 mg Pd 24 hr^{-1}, three cycles reached the threshold on, or before, the day of the total estrogen peak, but

at the two higher threshold values, 1.4 mg Pd 24 hr^{-1}, and 1.6 mg Pd 24 hr^{-1}, no cycle reached the threshold before the day of the total estrogen peak +1.

Because the use of a threshold value of 1.2 mg Pd 24 hr^{-1} resulted in two cases where the first day of infertility was predicted on the day of the total estrogen peak and one on the day before, it is clearly not appropriate for the threshold value to be set this low for all women. This is consistent with the previous conclusion that the pre-ovulatory Pd rise will sometimes encompass this value.

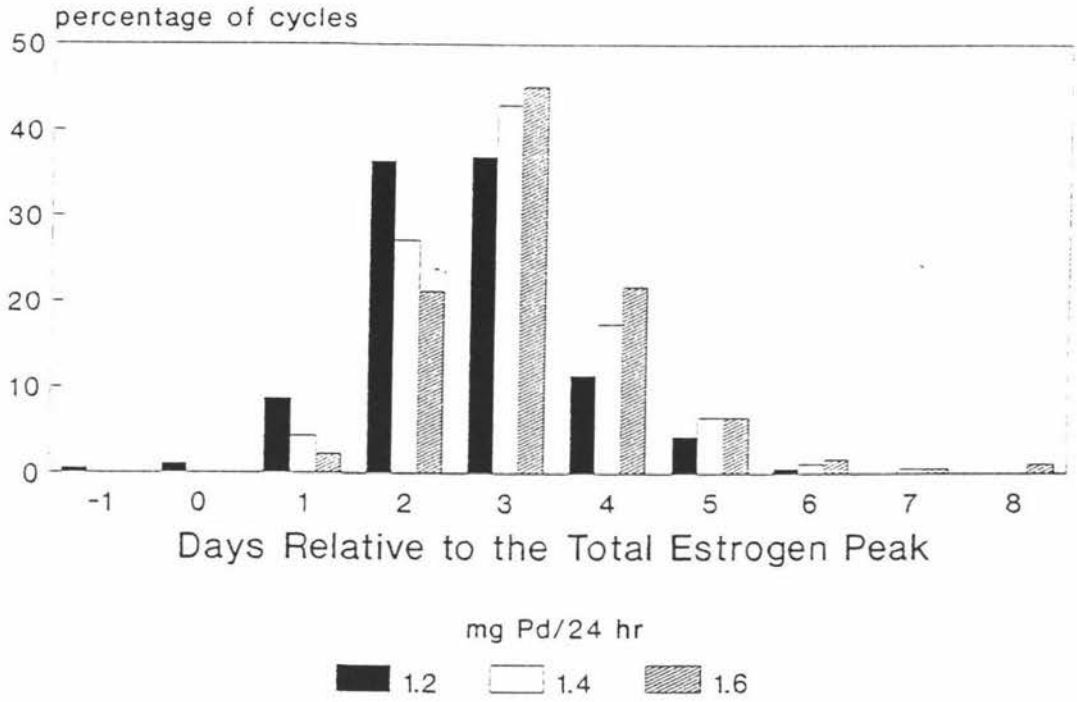

Figure 2.5 *The Pregnanediol (Pd) Threshold using Three Different Threshold Values*

Although the threshold value of 1.4 mg Pd 24 hr^{-1} did not underestimate the first day of infertility, the threshold value of 1.6 mg Pd 24 hr^{-1} did give an unnecessarily conservative estimate producing twice as many estimates for the first day of the infertile period for days +6, +7 and +8 relative to the total estrogen peak, compared to that obtained using the threshold value of 1.4 mg 24 hr^{-1} (see Figure 2.5). Thus, of the three different threshold values examined, a statistical analysis of the data indicated the use of the threshold value 1.4 mg Pd 24 hr^{-1} as being the most suitable and hence, justifies

the Melbourne practice.

By visual examination of each individual cycle in the database, it was evident that once the Pd levels reached the higher value of 1.4 mg Pd 24 hr^{-1}, no cycle had a subsequent ovulation (defined as having a menstrual bleed more than sixteen days after the threshold; this assumes a normal luteal phase has a maximum length of sixteen days). Thus, this value can be used with confidence even in the absence of estrogen peak data. That is once a measurement of 1.4 mg Pd 24 hr^{-1} is obtained, infertility can be assumed even if the previous menstrual cycle data is unavailable.

Although the threshold value of 1.4 mg Pd 24 hr^{-1} is sometimes reached within 24-36 hours after the total estrogen peak or less (Hoff, *et al.*, 1983), it is still considered to be a suitable marker for the first day of infertility as other studies have shown that a Pd level in this range is associated with infertility in any case. Because a urinary Pd value of this level is reflective of a high level of circulating progesterone, it may be that the infertility associated with a high urinary Pd level could be due to the progesterone exerting a contraceptive effect similar to the progestogenic effect of the progesterone derivative contained in the combination oral contraceptive pill (Brown *et al.*, 1991).

This proposal of high Pd levels during the follicular phase leading to infertility has been supported by the findings of Brown & Gronow (1985). It has been their experience that when a woman's level of urinary Pd is raised above 1 mg 24 hr^{-1} there is a failure to conceive, but at half these levels, Pd forms no barrier to conception. Similarly, in another unpublished study by Brown, a woman experiencing ovulatory infertile cycles which were also exhibiting high follicular phase Pd levels (range 1.2-1.7 mg Pd 24 hr^{-1}), conceived in her first subsequent cycle where her Pd levels in the follicular phase were reduced to normal with cortisone treatment. Furthermore, the conception cycles encountered with spontaneous abortions within the first trimester in Brown's study were all cycles which exhibited elevated Pd levels in the follicular phase.

Thus, it can be concluded that a pregnancy leading to term is extremely unlikely in cycles where the Pd values in the follicular phase are elevated above normal baseline levels. Therefore the use of a threshold level for Pd of 1.4 mg Pd 24 hr^{-1} is justified even for the cycles where these levels for Pd are achieved close to the presumed time

of ovulation i.e. the day following the total estrogen peak day.

However, further testing with a larger population sample where the day of the Pd threshold is also used for intercourse is required for a more complete appraisal of the use of the Pd threshold as a marker for the first day of infertility. This information is currently being provided by the home use of the Ovarian Monitor by natural family planners. To date, the charts show no pregnancy has occurred from an act of intercourse on a day for which the PdG level (which are equivalent to the Pd levels) equals or exceeds the threshold level of 1.4 mg Pd 24 hr^{-1}.

The Melbourne database consists of many complete menstrual cycle data sets on estrone, estradiol, estriol, total estrogens and pregnanediol levels as measured using methods of the highest accuracy from timed urine samples. Thus, this database represents the largest, most accurate and detailed source of information currently available for urinary hormonal data on the menstrual cycle. It also provides a source of reference information with which any home method which relies on urinary estrogens or progesterone or metabolites thereof, for the determination of the fertile period can be compared. Of more relevance to the current discussion is the use of the database as a reference in the assessment of the Ovarian Monitor. By using the first rise in total estrogen levels and the Pd threshold of the cycles in the database as references for the beginning and end of fertility, the Ovarian Monitor's ability to correctly delineate the fertile period using the first rise in urinary E1G levels and the PdG threshold can be evaluated.

When the length of the fertile period was determined for all the cycles of the Melbourne database using the first total estrogen rise (Blackwell & Brown, 1992) and a Pd threshold of 1.4 mg Pd 24 hr^{-1}, the fertile period was calculated to have a mean length of 7.08 ± 1.5 days with a range of 4-10 days (n = 130). Because these values are calculated from the most reliable urinary hormonal data currently available on the menstrual cycle, any method which deviates markedly from this in its delineation of the fertile period must be regarded as inaccurate and in need of futher refinement.

2.3.2 ANALYSIS OF THE WORLD HEALTH ORGANISATION DATA

2.3.2.1 The First Significant Pregnanediol Glucuronide Rise

As for the cycles of the Melbourne database, the tracking signal was calculated for the first forty cycles (see Section 2.2.2.4) and the results used to sort the cycles of the WHO trial into two groups. The cycles were sorted according to the day the tracking signal first recorded a significant increase in PdG levels relative to the day of the E1G peak. As before, these cycles were sorted into two groups i.e. a group for cycles in which the first significant increase in PdG levels was recorded on, or before, the day of the E1G peak and a second group for cycles in which this increase occurred after the day of the E1G peak.

At the 95% confidence level, 10% of the cycles fell into the first category, i.e. it can be said with 95% confidence that 10% of the cycles examined had a significant rise in PdG levels, on, or before, the day of the E1G peak, which was not attributable to random

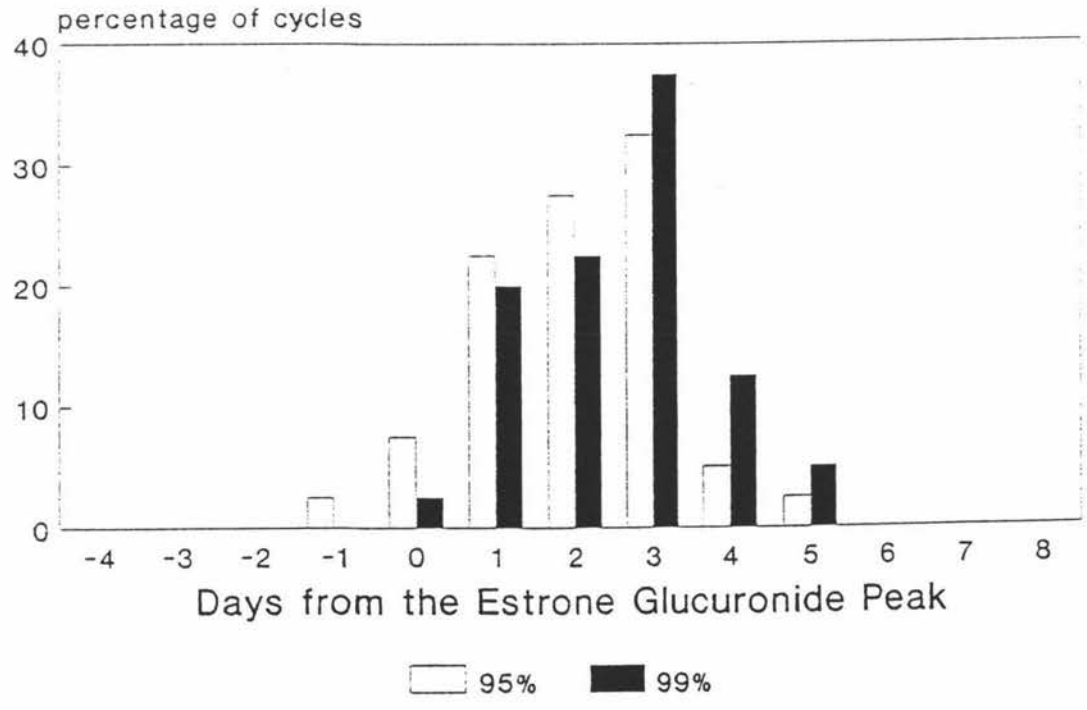

Figure 2.6 *The First Significant Pregnanediol Glucuronide Rise using Trigg's Tracking Signal at 95% and 99% Confidence Intervals*

fluctuations in the data. For the remaining 90% their first significant rise in PdG levels

was recorded after the day of the E1G peak (Figure 2.6). When the level of confidence was increased to 99%, the number of cycles which still exhibited a rise in the PdG levels on the day of the E1G peak, or before, was further reduced to 2.5%.

These values were significantly lower than the value of 33% obtained for the 95% confidence interval and the value of 22% obtained for the 99% confidence interval using the Melbourne database (see Figure 2.7 for a comparison of the first significant Pd and PdG rise at the 99% confidence interval). Thus, the application of the tracking signal to the Ovarian Monitor results shows more promise than when it was applied to the more accurate data of the Melbourne database.

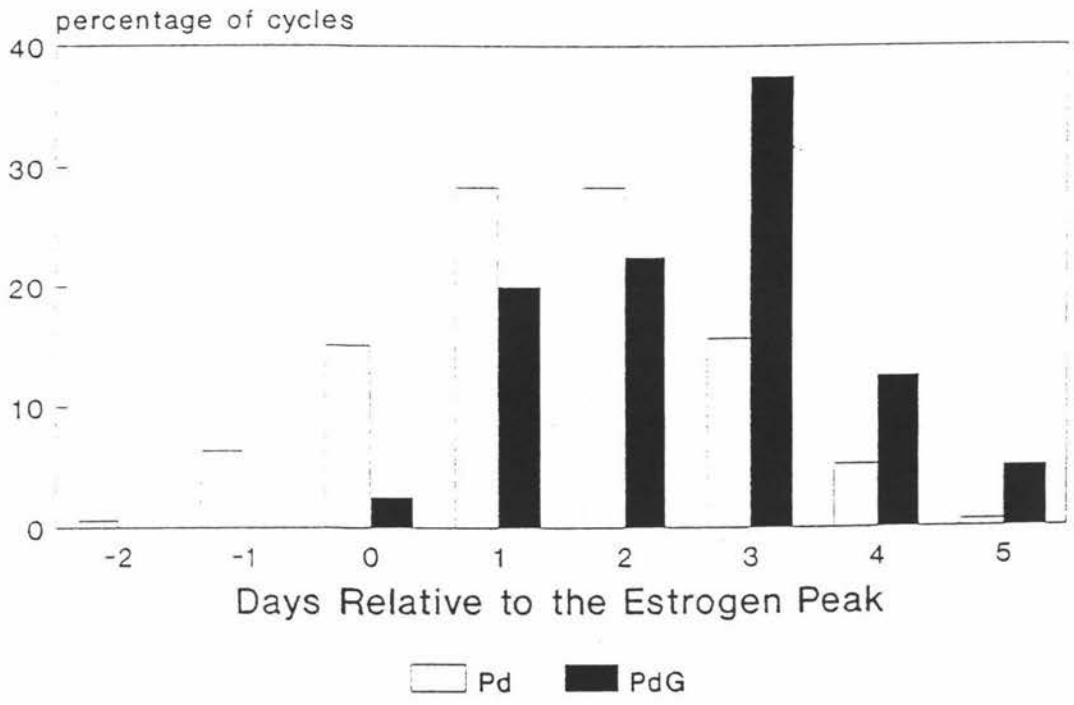

Figure 2.7 *The First Significant Pregnanediol (Pd) and Pregnanediol Glucuronide (PdG) Rise at the 99% Confidence Interval*

This difference in first significant rises, according to the tracking signal, between the Melbourne data and the data obtained from the WHO trial is due to the variation in the baseline PdG values obtained with the Ovarian Monitor (WHO trial). Since the Ovarian Monitor data had much more variability in its baseline values than the Pd data obtained by the more accurate method of gas liquid chromatography (GLC) used in the

construction of the Melbourne database thus, it also had a much greater Mean Absolute Standard Deviation (MAD).

Because the MAD is related to Trigg's tracking signal by the formula:

$$TS_{(n)} = SFE_{(n)}/MAD_{(n)}$$

a set of data with a large MAD (e.g. the Ovarian Monitor data) will generate a smaller tracking signal at any given level of confidence compared to a data set with a smaller MAD (e.g. the Melbourne data). Because a larger MAD is associated with a smaller tracking signal it will require larger changes from baseline values before the first rise is considered statistically significant. Thus, the tracking signal recorded a much greater percentage of cycles, using the Ovarian Monitor, where the first rise in progesterone metabolites was detected after the day of the estrogen peak than for the cycles of the Melbourne database at both the 95% and 99% confidence intervals.

However, when the first significant rise in PdG levels as determined by the tracking signal was used as a marker for the first day of infertility, it still resulted in 2.5% of the cycles from the WHO trial being recorded as having the infertile period beginning on or before the day of the E1G peak. This, in conjunction with the generally accepted view that ovulation cannot occur on the day of the E1G peak or before, suggests the use of algorithms to detect the first rise in PdG levels, would still not provide an acceptable marker for the first day of infertility. However, somewhat paradoxically, this is still a considerable improvement on the results obtained using the tracking signal on the more accurate GLC derived data (i.e. from the Melbourne database).

2.3.2.2 Markers of Fertility

One of the main uses of the Ovarian Monitor is in the complete hormonal definition of the menstrual cycle. The following analysis was carried out to examine the effectiveness of the hormonal markers, and to compare them with the clinical signs and symptoms.

i) *The Beginning of Fertility*

The most difficult aspect of NFP is being able to correctly define the beginning of

fertility such that the opportunities for intercourse are maximised without increasing the risk of pregnancy. Figure 2.8 shows the first day of fertility relative to the LH peak as perceived by the women in the WHO trial and expressed as a percentage for two different fertility markers. For the Ovarian Monitor, the marker for the first day of fertility was defined as the day of the first E1G rise as determined by the woman's visual inspection of her data. For the mucus it was defined according to the woman's normal rules in the interpretation of her mucus symptoms (see Section 1.3).

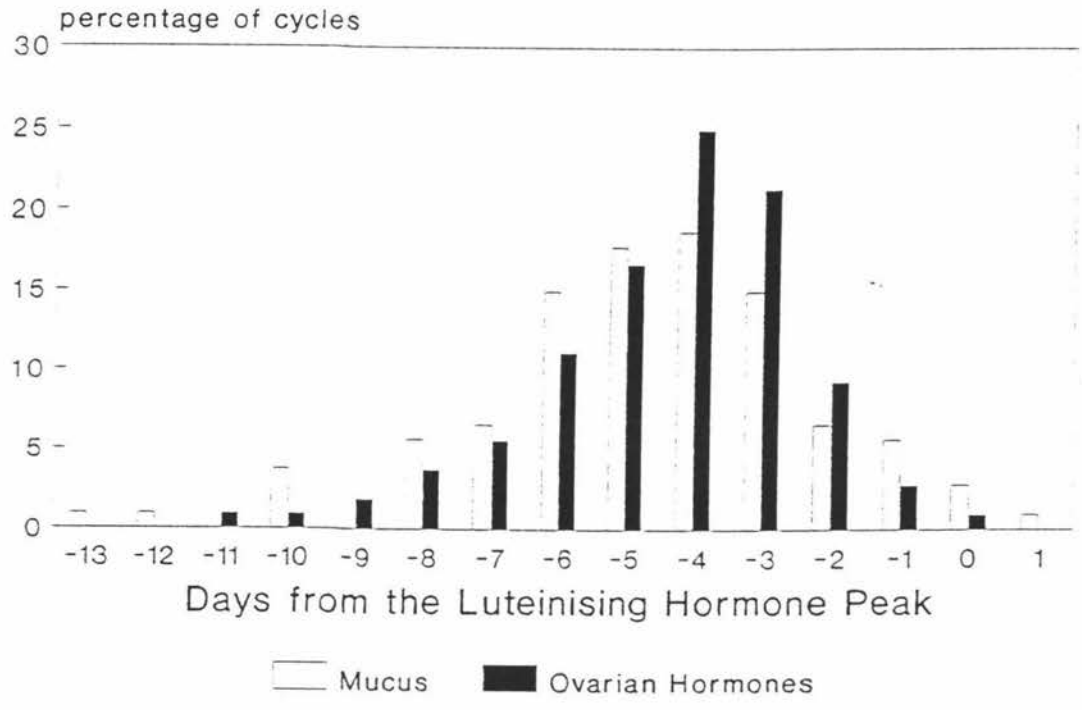

Figure 2.8 *The Beginning of the Fertile Period by Mucus and Ovarian Hormones*

From Figure 2.8 it can be seen that the general shape of the distribution curves for the first day of fertility for the two markers relative to the LH peak are very similar and thus, supports the Billings claim that the first day of fertile mucus and the hormone profile are closely correlated (Billings *et al.*, 1972). However, there was a significantly broader range of values for the first day of fertility as defined by the mucus symptoms (day -13 to day +1) compared to the day of the first E1G rise (day -11 to day 0). A statistical analysis of the data is given in Table 2.1.

Table 2.1 *The First Day of the Fertile Period*

Method	No. of Cycles	mean*	std. dev.*
Mucus (Billings)	107	-4.67	2.48
Ovarian Monitor	108	-4.40	1.95

* days relative to the LH peak

Although the means estimated by the two markers for the first day of fertility were very similar, the data obtained using the mucus symptoms were more variable. This is in accordance with other studies which suggest that the day of the first E1G rise is a more precise marker for the first day of the fertile period than the Billings Ovulation Method.

The ideal marker should be able to predict the start of fertility six days before ovulation. Because the maximum fertilisable life-span of the sperm is only three to four days in the average fertile couple (Austin, 1975), this should generally provide ample warning for the beginning of the fertile phase and impending ovulation. Any marker which results in the fertile period being predicted as having started more than six days before the LH peak (which occurs 17 ± 12 hours before ovulation) is obviously associated with more abstinence than is required for the avoidance of pregnancy. The figures for the two different markers where the fertile period was predicted to have started more than six days before the LH peak were slightly worse for the mucus method (17%) than for the first E1G rise (13%). However, these figures for both the mucus method and the Ovarian Monitor may include some cycles where the advanced warnings are in fact accurate and are due to an extended follicular phase resulting from atrophy of the leading follicle. In these cycles the increase in the length of the follicular phase would be equal to the time it takes for another follicle to be recruited and develop to the same stage the previous leading follicle had reached. These cycles should not be included with the figures for cycles with overly conservative estimates of the beginning of the fertile period as they would probably have been fertile over at least some of this period of time if the first leading follicle had not died.

Although it is desirable for the period of abstinence to be kept to a minimum i.e. that

the warning for the impending ovulation is not excessive, it is of even more critical importance that the beginning of the fertile period is not observed too late. Because in very fertile couples, sperm can sometimes remain viable up to six days in the female genital tract, for the risk of pregnancy to be minimal in these couples it is imperative, that the beginning of the fertile period is not predicted with less than six days warning of ovulation.

The mean warning for ovulation from the day of the first E1G increase can be calculated. Since the day of the first E1G rise is day one of the fertile period, the mean number of days from the day of the first E1G rise up to and including the day of the LH peak for the trial data was 5.4 days (see Table 2.1). The mean number of hours from the LH peak to the event of ovulation itself is 16.5 hours (0.7 days) (Brown & Gronow, 1985). Thus, the event of ovulation occurs on average 6.1 days (5.4 days + 0.7 days) after the day of the first rise in E1G levels. This data is in good agreement with the distribution of first total estrogen rise days calculated from the Melbourne database by the Trigg's tracking signal (Blackwell & Brown, 1992). In that study the event of ovulation occurred with a mean of 6.5 ± 1.4 days and had a range of 10 days before to 3.5 days before the presumed day of ovulation. Thus, the Ovarian Monitor is producing data in the hands of the women which is as good as that obtained from the Melbourne reference database.

Hence, for a menstrual cycle with the mean warning of ovulation, the use of the day of the first E1G rise would be successful in defining the first day of the fertile period except in cases of exceptionally long sperm survival times. This is an impressive achievement, although the pregnancy rates for intercourse on the last E1G baseline day used as the marker for the beginning of the fertile phase remain to be determined.

The mean warning for ovulation from the first day of fertility as indicated by the mucus symptoms can also be calculated. For the trial data the mean number of days from the day of the start of fertility as indicated by the mucus symptoms up to and including the day of the LH peak was 5.7 days (Table 2.1). Because the mean number of days from the LH peak to ovulation is 0.7 days, then the mean total number of days from the beginning of fertility as indicated by the mucus symptoms to the event of ovulation itself is 6.4 days.

Thus, for a menstrual cycle with the mean warning of ovulation, the use of the mucus symptoms would also be successful method for the determination of the first day of fertility. This agrees with other studies on the Billings Ovulation Method and the Symptothermal Methods (France, 1982). However, the larger standard deviation of the data for the mucus symptoms makes it less reliable in a number of cases, being either too conservative, or too late, which when coupled with the subjective nature of the clinical signs accounts for the lack of widespread acceptance of the method.

Unfortunately, for a substantial percentage of cycles neither of the Billings Ovulation Method or the first E1G rise would give the recommended six days warning of ovulation. However, cycles with short warnings of ovulation using the day of the first E1G rise are often the same cycles in which the mucus symptoms give a short warning of ovulation as well. Because the nature of the mucus is an important determinant of fertility (see Section 1.3), if the mucus gives a short warning of ovulation then it is also likely that the length of the fertile period is similarly reduced. Thus, it appears that these cycles with late warnings of ovulation by both the mucus symptoms and the first day of the E1G rise will not be fertile for all of the six days preceding ovulation and that the beginning of the fertile period as predicted by the mucus and the day of the first rise in E1G levels is correct. This proposal is supported by the low pregnancy rates encountered using the Billings Ovulation Method when intercourse was restricted to the non-fertile days as indicated by the mucus symptoms.

ii) *Ovulation and Mid-cycle Markers*

The day of ovulation and the peak mucus symptom (i.e. last day of fertile mucus, see Section 1.3), and the day of ovulation and the day of the first E1G peak are known to be closely related in time. In all previous studies (Brown *et al.*, 1989) for 80% of cycles, the peak mucus symptom occurs within ± 1 day of the day of ovulation, with the event of ovulation occurring on average 36 hours after the E1G peak (Brown *et al.*, 1989).

A comparison of the day of the peak mucus symptom and the day of the E1G peak as markers for ovulation, in the WHO trial is shown in Figure 2.9. Because the only absolute marker for the exact timing of the event of ovulation is ultrasound and this

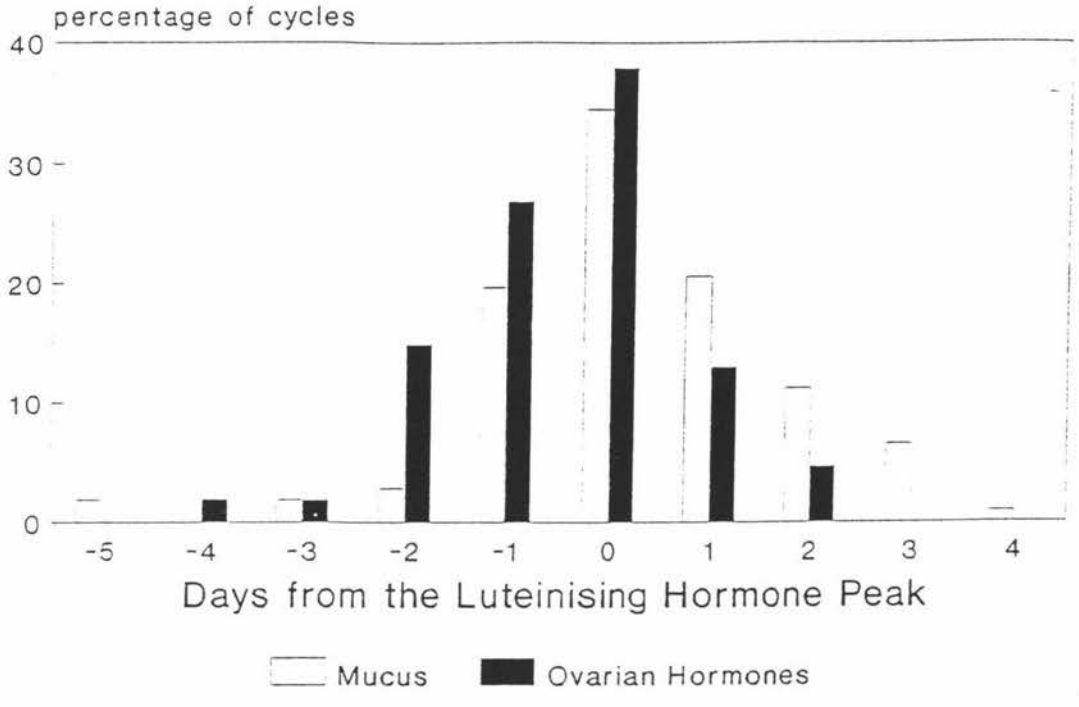

Figure 2.9 The Prediction of Ovulation by Mucus and Ovarian Hormones

method is not feasible for a home study, the LH peak was used as the reference marker for ovulation instead (which occurs 17 ± 12 hours after the LH peak). Figure 2.9 shows again that the peak mucus symptom gives a much broader range and distribution of values compared to the data provided by the daily E1G levels. While the day of the peak mucus symptom gave a range for the presumed day of ovulation between days -5 to +4 relative to the LH peak, the E1G peak day gave the more limited range of -4 to +2 days. As consistent with the smaller range, these latter data had a significantly smaller standard deviation.

The mean of the E1G peak day was further removed in time from the LH peak than the peak mucus symptom and thus, was even further removed from the time of ovulation. However, although the E1G peak day is further removed in time from the event of ovulation, because it has a much smaller standard deviation it is a more accurate predictor of ovulation. The mean number of days from the E1G peak day and the mucus peak day to the LH peak and their associated standard deviations is shown in Table 2.2.

Table 2.2 *Mid-cycle Markers*

Method	No. of Cycles	mean*	std. dev.*
Mucus (Billings's)	107	0.26	1.51
Ovarian Monitor	108	-0.43	1.14

* days relative to the LH peak

From Table 2.2 it can be calculated that the mean E1G peak day occurs 27 hours (1.13 days i.e. 0.43 + 0.7 days) before ovulation compared to only 11 hours (0.44 days i.e. 0.7 - 0.26 days) from the mean day of the peak mucus symptom. These results are consistent with ovarian physiology since it is rising progesterone levels which cause the peak mucus symptom and this event can only occur following the E1G peak. Thus, it appears that the pre-ovulatory progesterone rise is of a sufficient amplitude to change the characteristics of the mucus and hence, the mean day for the "peak" symptom. This makes the peak mucus symptom very closely related to the actual event of ovulation, although the spread of the data was significantly larger than that obtained for the day of the PdG threshold.

Although the E1G peak day is further removed from the event of ovulation than the peak mucus symptom, it is in fact a more important marker because the day of the E1G fall corresponds to the day of peak fertility where the day of peak fertility is defined as the day an isolated act of intercourse is most likely to lead to conception. This makes the day of the E1G fall a particularly important marker as although the day of the E1G peak can only be identified retrospectively, the day of the E1G fall can be identified on the day. This day of peak fertility occurs not on the day of ovulation as is commonly thought, but the day before to allow time for sperm capacitation, a necessary prerequisite for fertilisation.

The spread of the data around the LH peak for the E1G data is broader for the predicted day of ovulation than the E1G peak data from previous studies. This is the result of an oversight in the protocol where the women were directed to stop measuring for E1G once the day of the first E1G fall was reached and to start assaying for PdG.

Unfortunately this method fails to take into account the possibility of double E1G peaks which are quite common (Blackwell & Brown, 1992). For some of these cycles it may have been more correct to predict the day of ovulation from the second peak. However, when the protocol was followed this second peak was not always detected forcing the prediction of the day of ovulation for these cycles to be out by up to a couple of days. This explanation is supported by the uncharacteristically late PdG rises observed in some of the cycles relative to the women's estimated E1G peak day.

Furthermore, the data for both the E1G and the mucus have more potential for variation in this study because of the age distribution of the women in the trial. A woman's cycle is maximally fertile and regular between the ages of 20 and 35 years (Collins, 1989). It is this sub-group of women whose mucus symptoms and hormonal data is the most consistent, fits best into the patterns of the normally fertile cycle and is the easiest to interpret. The mean age of the women in the WHO trial, corrected for the number of cycles contributed, was 34.9 ± 4.8 years. Expressed as percentages this breaks down into only 40% of the cycles being contributed by women under the age of 35 years, 24% at age 35 years, and 36% by women who were over 35 years of age. This aging distribution for women in the trial, is probably a result of one of the trials selection criteria. The criterion that for selection a woman could not be planning to conceive within the next six months, would have introduced a bias into the sample population of the study towards older women who were not planning to extend their families. This older sample population for the study was probably a significant contributing factor to the relatively high frequency of outliers in many of the variables examined. This probably goes a long way towards explaining many of the better results obtained in similar trials for both mucus symptoms and hormone assays where a younger sample population was recruited.

iii) *The End of Fertility Marker*

The Billings Ovulation Method (i.e. mucus method), the Ovarian Monitor and the symptothermal methods were all tested and compared for their ability and consistency to delineate the end of the fertile period. Figure 2.10 shows the first day of infertility relative to the LH peak as perceived by the women in the WHO trial and expressed as a percentage of total cycles for the three different end of fertility markers. For the

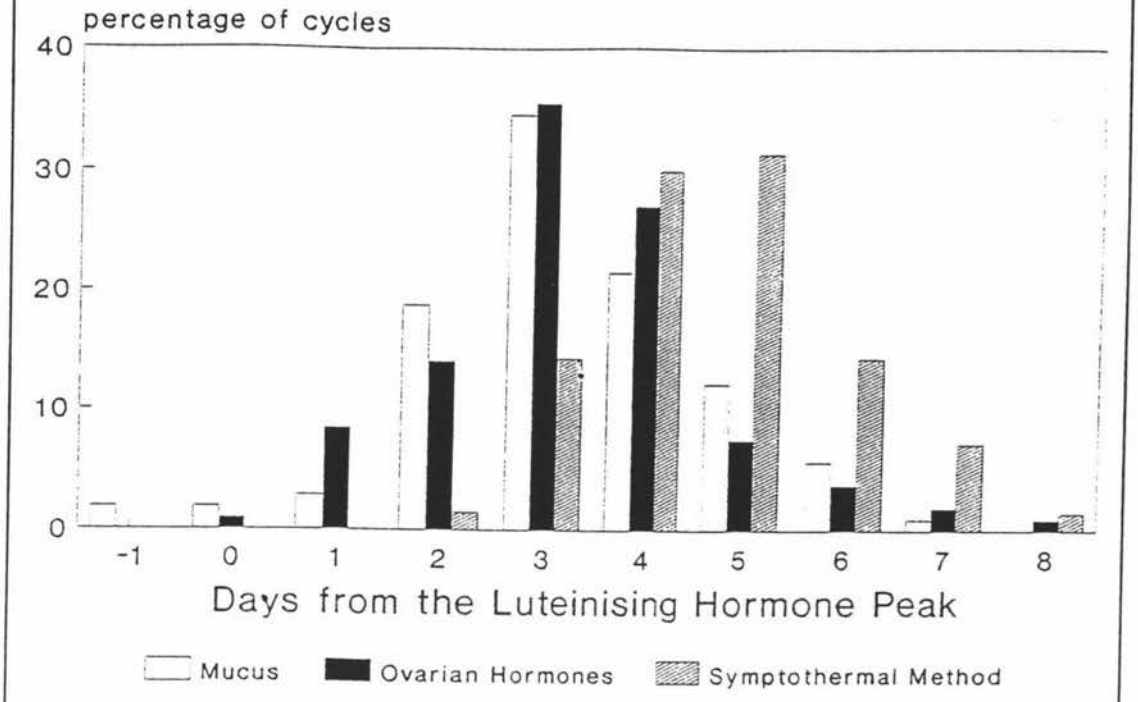

Figure 2.10 *The End of the Fertile Period by Mucus, Ovarian Hormones and the Symptothermal Method*

Billings Ovulation Method this first day of infertility is defined according to the woman's normal rules in the interpretation of her mucus symptoms (see Section 1.3). The symptothermal method defines the first day of infertility according to either the first rise in BBT +2 days (see Section 1.3) or the mucus symptoms, depending upon the method which predicts the latest end for the fertile period. For the Ovarian Monitor, the marker for the first day of infertility was defined in this study as the first day for which the PdG excretion exceeded or equalled the rate of 7 μmol PdG 24 hr^{-1}. These results are summarised in Table 2.3.

Table 2.3 *The First Day of the Infertile Period*

Method	No. of Cycles	mean*	std. dev.*
Mucus (Billings's)	107	4.27	1.50
Ovarian Monitor	107	3.32	1.38
Symptothermal	70	4.70	1.22
BBT	70	3.73	1.21

* days relative to the LH peak

Once again the use of the Billings Ovulation Method is seen to generate a greater range and a larger standard deviation than the data generated using the Ovarian Monitor. The Billings Ovulation Method gave a range of days for the first day of infertility of -1 to +8 relative to the LH peak compared to the PdG threshold day obtained with the Ovarian Monitor which had the slightly smaller range of 0 to +8 days. More importantly, the Ovarian Monitor predicted the fertile period to end on average one day earlier than the Billings Ovulation Method and so reduced the period of abstinence required.

Figure 2.10 also shows the date predicted for the first day of the infertile period using the mucus method to be a lot less reliable than that supplied by the Ovarian Monitor. The mucus method resulted in two cycles (n = 107, 1.9%) where the first day of infertility was predicted as having occurred before the day of the LH peak. Because it is the LH peak which initiates the event of ovulation itself, it is therefore theoretically impossible for the fertile period to be ended before the LH peak has occurred as discussed in Section 2.3.1.1. Thus, the Billings Ovulation Method failed completely to correctly delineate the end of the fertile period for these two cycles and in fact predicted the first day of infertility at what was probably one of the most fertile days of the cycle. Furthermore, although the Ovarian Monitor did predict for one cycle (n = 107) the first day of the infertile period as beginning on the day of the LH peak, because high levels of circulating progesterone are associated with infertility (see Section 2.3.1.2) this prediction of infertility as early as the day of the LH peak using the PdG threshold could well be correct.

Compared to the Ovarian Monitor, the Billings Ovulation Method also resulted in substantially more cycles where the end of the fertile period was predicted considerably after the maximal limits of ovum survival had been exceeded. Four days after the LH peak is well in excess of the time required to ensure that the ovum is dead and the fertile period over for that cycle considering ovulation usually occurs within a day of the LH peak and the ovum has an average lifespan of approximately only twelve hours. For the Billings Ovulation Method, the first day of the infertile period was delineated in 40% of the cycles as beginning between five and eight days after the LH peak compared to only 14% for the Ovarian Monitor.

This figure of 14% for the Ovarian Monitor can be further reduced by applying rules such as the 2/3 rule to the cycle data. This rule states that in cycles with a clear cut E1G peak, the first day of infertility can be redefined as beginning on the day the PdG levels first reach 2/3 of the threshold value of 7 μmol PdG 24 hr^{-1} i.e. the PdG threshold value can be reduced to 4.7 μmol PdG 24 hr^{-1} (Brown & Blackwell, 1989).

This rule benefits the subset of women with slow PdG rises. In these women the usual PdG threshold value is reached a lot later than the E1G peak day and thus, later than the predicted day of ovulation would indicate. Thus, for these women when the usual threshold value is used, the first day of infertility is predicted long after the period of maximal ovum survival time has elapsed. The application of the 2/3 rule by this sub-population of women enables them to predict the first day of infertility using a method which is not associated with an excessive period of abstinence but which still allows sufficient time for the ovum to die.

A further advantage of the Ovarian Monitor over the Billings Ovulation Method in the determination of the end of fertility is that the Ovarian Monitor directly predicts the first day of infertility from a current marker i.e. a threshold level of PdG, while the Billings Ovulation Method relies on a presumptive method i.e. the peak mucus symptom +4 days. Thus, this could be a possible explanation as to why the Ovarian Monitor consistently gave better results in the prediction of the beginning of the infertile period compared to the Billings Ovulation Method.

However, although the prediction of the first day of the infertile period by the Ovarian Monitor was considerably more reliable than the Billings Ovulation Method, the results obtained by the Ovarian Monitor were not as good as they have been in previous studies. Although the older average age for the women of the trial compared to previous studies was probably a factor, the most major contributing factor is believed to be a change in the value used for the PdG threshold. Previously a threshold value of 6.3 μmol PdG 24 hr^{-1} was used, while for the trial this threshold value was increased to 7 μmol PdG 24 hr^{-1} and increased the period of abstinence required by the method. This higher threshold value of 7 μmol PdG 24 hr^{-1} is equivalent to the value of 1.56 mg Pd 24 hr^{-1} which is in turn, very close to the value of 1.6 mg Pd 24 hr^{-1} used in Section 2.3.1.2. This value of 1.6 mg Pd 24 hr^{-1} was identified as being unnecessarily

conservative when the best threshold level of PdG was evaluated using the Melbourne database. Thus, it is hardly surprising that the current study found that the mean for the end of the fertile period was significantly later than in previous studies.

The Billings Ovulation Method was also compared with the symptothermal method as a marker for the first day of infertility. This comparison showed the symptothermal method to have the more limited range of +2 to +8 days (n = 70 cycles) relative to the LH peak, in contrast to the range of -1 to +8 (n = 107 cycles) for the Billings Ovulation Method. Thus, the symptothermal method was the better marker for the first day of the infertility as it never predicted the fertile period to end prematurely when referenced to the LH peak. Analysis of the data also showed the symptothermal method to have a higher mean and smaller standard deviation than the data generated using the Billings Ovulation Method (see Table 2.3). These conclusions agree with current perceptions of the relative merits of the two methods.

The higher mean and the later range of values (relative to the LH peak) for the first day of infertility found in the symptothermal method relative to the Billings Ovulation Method is to be expected. This is because in the symptothermal method, the first day of infertility is calculated according to which of the methods out of the BBT rise +2 days or the peak mucus symptom +4 days (i.e. the Billings Ovulation Method), has the latest estimate for the beginning of the infertile period. Furthermore, because the symptothermal method is dependent upon the BBT in its prediction of the first day of the infertile period it is also more likely to be correct than the Billings Ovulation Method. This is because it is high progesterone levels which determine the beginning of the infertile period, and the BBT is a direct consequence of this increase. Thus, the symptothermal method is more likely to be accurate in its estimate of the first day of the infertile period than the Billings Ovulation Method.

When the symptothermal method and the BBT only method were compared (Figure 2.11), the BBT method was found to have a lower mean number of days relative to the LH peak for the estimation of the first day of infertility than the symptothermal method (see Table 2.3) similar to the Ovarian Monitor data. Once again, this is to be expected from the nature of the symptothermal method since when the peak mucus symptom is later than the temperature rise it must take precedence although it is less directly related

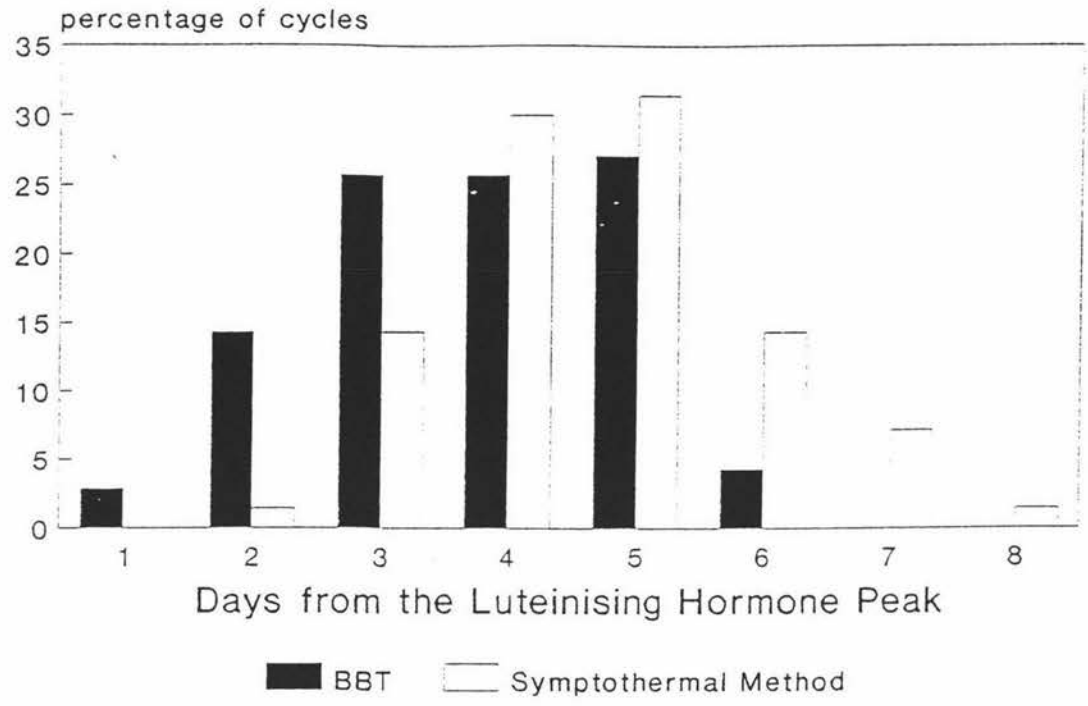

Figure 2.11 The End of the Fertile Period by the Basal Body Temperature (BBT) and Symptothermal Methods

to the rise in serum progesterone.

Thus, in summary, of the three different symptom oriented (non-hormonal) methods for marking the infertile period, the BBT method is the best because, as discussed above, it is dependent solely upon the production of progesterone. This method is based on the premise that a rise in progesterone sufficient to cause the temperature shift indicates that the corpus luteum has reached a stage of development sufficiently removed from the time of ovulation to be used as proof that the ovum is no longer viable. On the other hand the other two methods both rely solely, or in part, on an estimate of the most fertile day based on the peak mucus symptom to predict the infertile period. However, because the peak mucus symptom is defined as the last day of fertile mucus, and the first day of infertile mucus which defines the peak is due to the early increase in progesterone levels, then the peak mucus symptom can also be related to changes in circulating progesterone levels. Even so, it is still a prospective method which relies on what is expected to occur without the definite confirmation as with the other two methods and is clearly not as closely related to the progesterone levels.

Because it is the circulating progesterone levels which determine the beginning of infertility, the use of the PdG threshold is potentially a better marker than the BBT method. Although the results for the two methods are very similar (see Figure 2.12) with the means only ten hours apart, they do have quite different modes. The BBT method has a mode of five days while the PdG threshold has a mode of only three days relative to the LH peak. Part of this difference is due to the different distributions of the two sets of data; the PdG threshold data is skewed towards the LH peak day and the BBT data is skewed away from it.

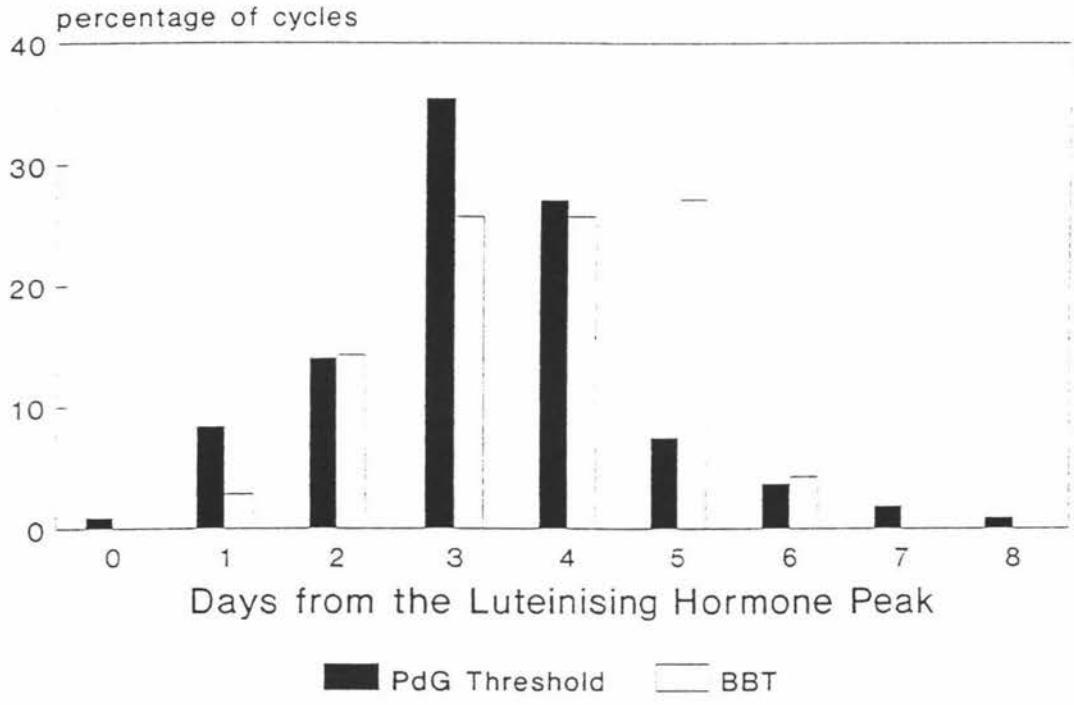

Figure 2.12 The End of the Fertile Period using the Pregnanediol Glucuronide (PdG) Threshold and Basal Body Temperature (BBT) Method

Another way of examining the data is to express the two estimations of the end of the fertile period relative to each other. This was achieved by subtracting the estimated number of days till the end of fertility for the PdG data from the corresponding BBT data. If for a given cycle, the above calculation gave a negative answer for the difference in days, then the PdG method gave a more conservative estimate for the end of fertilty compared to the BBT method. On the other hand, if the above calculation resulted in a positive answer, then the BBT method gave the more conservative estimate

for the end of the fertile period.

When all the cycles from the Palmerston North centre of the WHO trial were analysed by this procedure it resulted in the distribution seen in Figure 2.13. In this figure the predicted end of fertility by the BBT method is expressed relative to the predicted end of fertility by the PdG threshold. Figure 2.13 also shows that for only 23% of the cycles, the two methods predicted the same day for the end of the fertile period. Furthermore, it shows that while the BBT method predicted the end of fertility ahead of the PdG threshold in only 27% of the cycles, the PdG method predicted the fertile period ending ahead of the BBT method in 50% of the cycles examined. This general

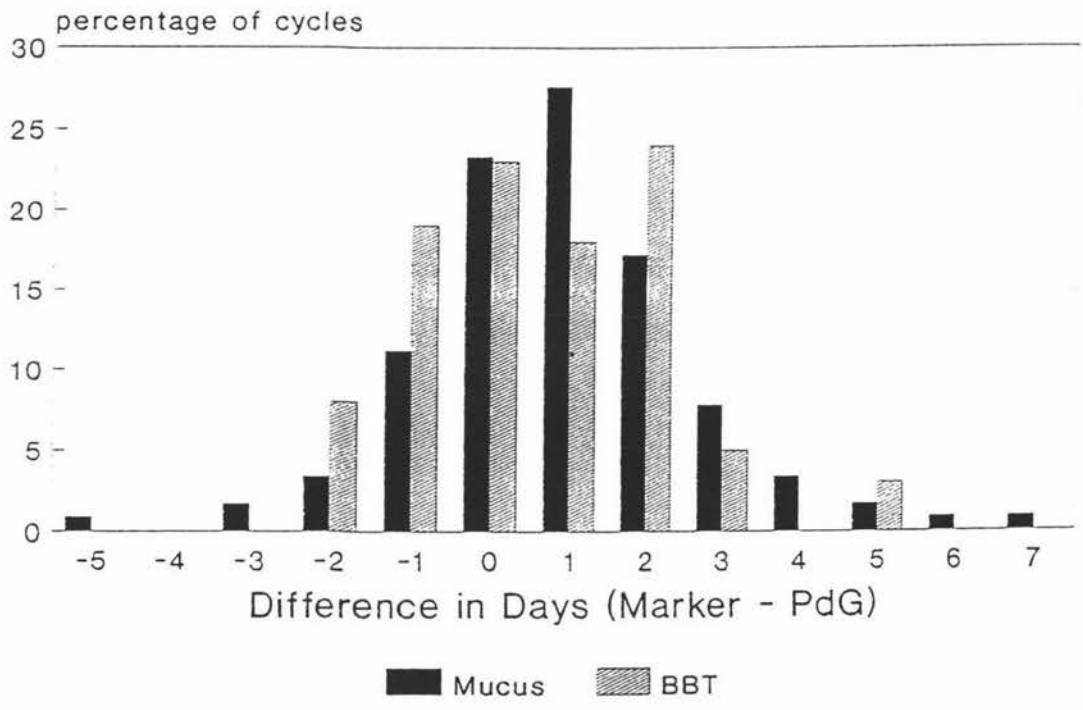

Figure 2.13 *The End of Fertility as Predicted by the Basal Body Temperature Method and the Mucus Method Expressed Relative to the Predicted End of Fertility by the Pregnanediol Glucuronide Threshold*

pattern where the BBT method is shown to be more conservative overall in its estimation of the end of the fertile period is further evidenced by the distribution of days where there are large discrepancies between the BBT and the PdG threshold data for the predicted end of the fertile period. There was a difference of three or more days for 16% of the cycles where the PdG method predicted the fertile period to end in advance

of the day predicted by the BBT method. In contrast there were no equivalent cases where the BBT method predicted the fertile period ending three or more days ahead of the day indicated by the PdG threshold. Thus, it appears that for a significant percentage of the cycles the BBT method over-estimated the end of the fertile period relative to the PdG threshold. In conclusion, on the basis of these findings it appears that of the four different methods investigated as markers for the beginning of the post-ovulatory infertility, the PdG threshold was the most accurate. Thus, even if no other widespread use was found for the Ovarian Monitor it still represents a considerable advance over other methods being cheap as well as easy to apply.

Furthermore, while the measurement of the BBT is theoretically simple and quick relative to the measurement of PdG levels, this is not the case in practice where the charts often prove to be difficult to interpret. Another advantage of the Ovarian Monitor over the BBT method in the prediction of the end of the fertile period is that although the test takes longer to perform it does not have to be repeated on every day leading up to first day of infertility from the mid-cycle marker. This is because it makes use of a threshold where it is possible for a single measurement to give the required information. as opposed to a change like the BBT method where a baseline must first be established.

2.3.2.3 The Length of the Fertile Period

For the determination of the length of the fertile period by the BBT method, the beginning of the fertile period was defined according to the Billings Ovulation Method (i.e. the mucus symptoms) and the first day of infertile period was defined by the first increase in BBT +2 days.

When determining the best method for the delineation of the fertile period two factors must be taken into account. Obviously, the method must successfully detect all the potentially fertile days. Secondly, taking this first factor into account, the best method is then the one which predicts the shortest fertile period and is thus, associated with the shortest period of abstinence.

When the LH peak is used as a reference marker for the fertile period, the fertile period is defined as beginning three days before and ending two days after the LH peak where day +2 is the first day of infertility (Collins, 1989).

The mean length of the fertile periods calculated in this analysis of the WHO study data and their associated standard deviations obtained using the four different methods are tabulated in Table 2.4.

Table 2.4 *The Length of the Fertile Period*

Method	No. of Cycles	mean*	std. dev.*
Mucus (Billings's)	118	8.76	2.63
Ovarian Monitor	118	7.58	1.95
Symptothermal	75	9.39	2.39
BBT	75	8.47	2.27

* days relative to the LH peak

Table 2.4 clearly shows that of the four different methods, the shortest mean length and standard deviation for the fertile period was obtained using the Ovarian Monitor. This method was also associated with the smallest number of cycles where the fertile period was underestimated. This is because all the other methods tested were dependent on the mucus symptoms for the determination of the beginning of fertility and there were several cycles for which the beginning of fertility was estimated as having begun after, or on, the day of the LH peak. The mean length of the fertile phase as measured in the home by the Ovarian Monitor compares favourably with the mean 7.08 ± 1.5 days determined by the Melbourne data base (see Section 2.3.1.2). Thus, the WHO data shows the Ovarian Monitor to give an accurate delineation of the fertile period in the hands of the women and should significantly reduce the periods of abstinence when rules and guidelines for its use are established.

Thus, in summary it can be concluded that for the determination of the fertile period in the home for the avoidance of pregnancy the use of the Ovarian Monitor is the safest and most precise method currently available. Although the use of the Ovarian Monitor for the avoidance of pregnancy would significantly reduce the number of days of abstinence required, the pregnancy rate associated with the use of the Ovarian Monitor

in pregnancy avoidance is yet to be established.

2.3.2.4 Reproducibility of the Women's Home Data

One of the key criticisms of home data is that it is inherently unreliable. Thus, it is important to demonstrate that untrained operators (i.e. the women) can produce reliable hormonal data in the home independent of the laboratory.

Repeated experience has shown that the most reliable data obtained using the Ovarian Monitor is that obtained using fresh urine samples. This is presumed to be because over

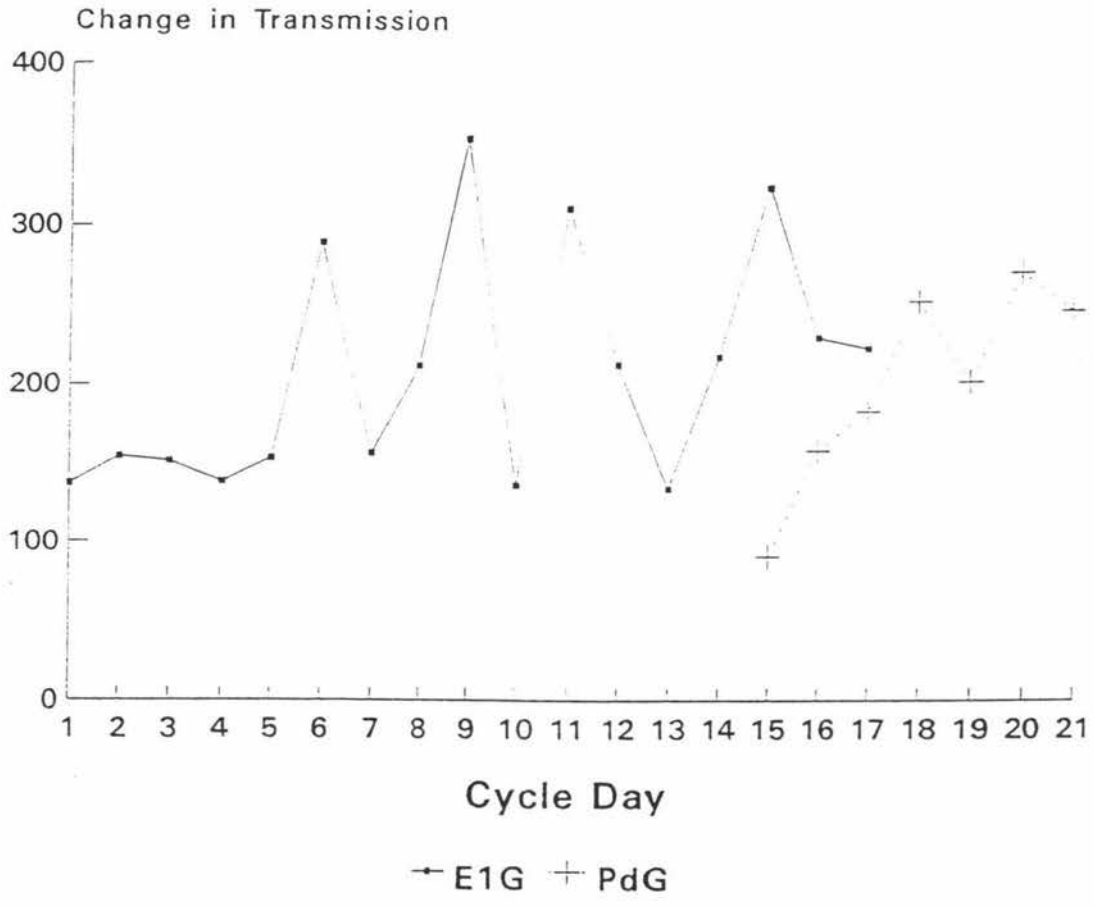

Figure 2.14 The Effect of a Urinary Infection on the Estrone Glucuronide Profile

The Change in Transmission values are recorded as ΔT (5 min)$^{-1}$ for PdG and ΔT (20 min)$^{-1}$ for E1G

time, bacterial growth can sometimes produce an endogenous source of lysozyme or ß-

glucuronidase in the urine sample.

In the case of a urine sample with endogenous supplies of lysozyme, the change in transmission values on the Ovarian Monitor will become artificially inflated by the extra lysozyme. The hormonal profile of a cycle analysed by the Ovarian Monitor in which some urines are so affected then becomes characterised by isolated spikes. This effect of extra lysozyme in the urine sample on the hormone profile is most clearly demonstrated in cases of urinary infections when the lysozyme concentrations in the urine become unavoidably high. As a result, the hormonal profiles for these cycles become a series of spikes making interpretation difficult. Figure 2.14 shows part of the E1G and PdG profile of the only cycle in the study which was associated with a urinary infection. However, because human lysozyme is less thermally stable than hen egg white lysozyme, it is possible to denature the urinary lysozyme by using heat treatment. Alternatively, the lysozyme could be removed by adsorption onto glass fibres. Thus, with proper provisions the extra lysozyme present in cases of a urinary infection does not have to be left to interfere with the assay. These extra precautions need not be used routinely as the user would be only too aware as to whether they are presently in the throes of a urinary infection.

In contrast to the effect of extra lysozyme, the effect of ß-glucuronidase on the assay is to reduce the change in transmission. ß-Glucuronidase activity hydrolyses glucuronide linkages to give estrone which is only poorly recognised by the antibody in the kit. This leaves more antibody free to bind to the E1G-Lysozyme conjugate. Thus, the amount of free conjugate able to participate in the lysis of *M. lysodeikticus* is reduced, resulting in an overall decrease in transmission change compared to the fresh urine.

Thus, in conclusion it can be said that the change in transmission values obtained by the women on the Ovarian Monitor are more liable to be correct than the repeats on the same urine specimens performed in the laboratory several months after collection.

i) *Estrone Glucuronide*

Figure 2.15 shows the reproducibility of an E1G profile for a complete cycle on the Ovarian Monitor expressed relative to the day of the first E1G peak. Both the results obtained by the woman at home and the laboratory repeats carried out for this study are

shown. Figure 2.15 shows a good agreement in the general pattern for the two sets of E1G values. However, a closer analysis of the data shows the day of first rise from the E1G baseline (i.e. the first day of fertility) to vary between the two sets of results. The

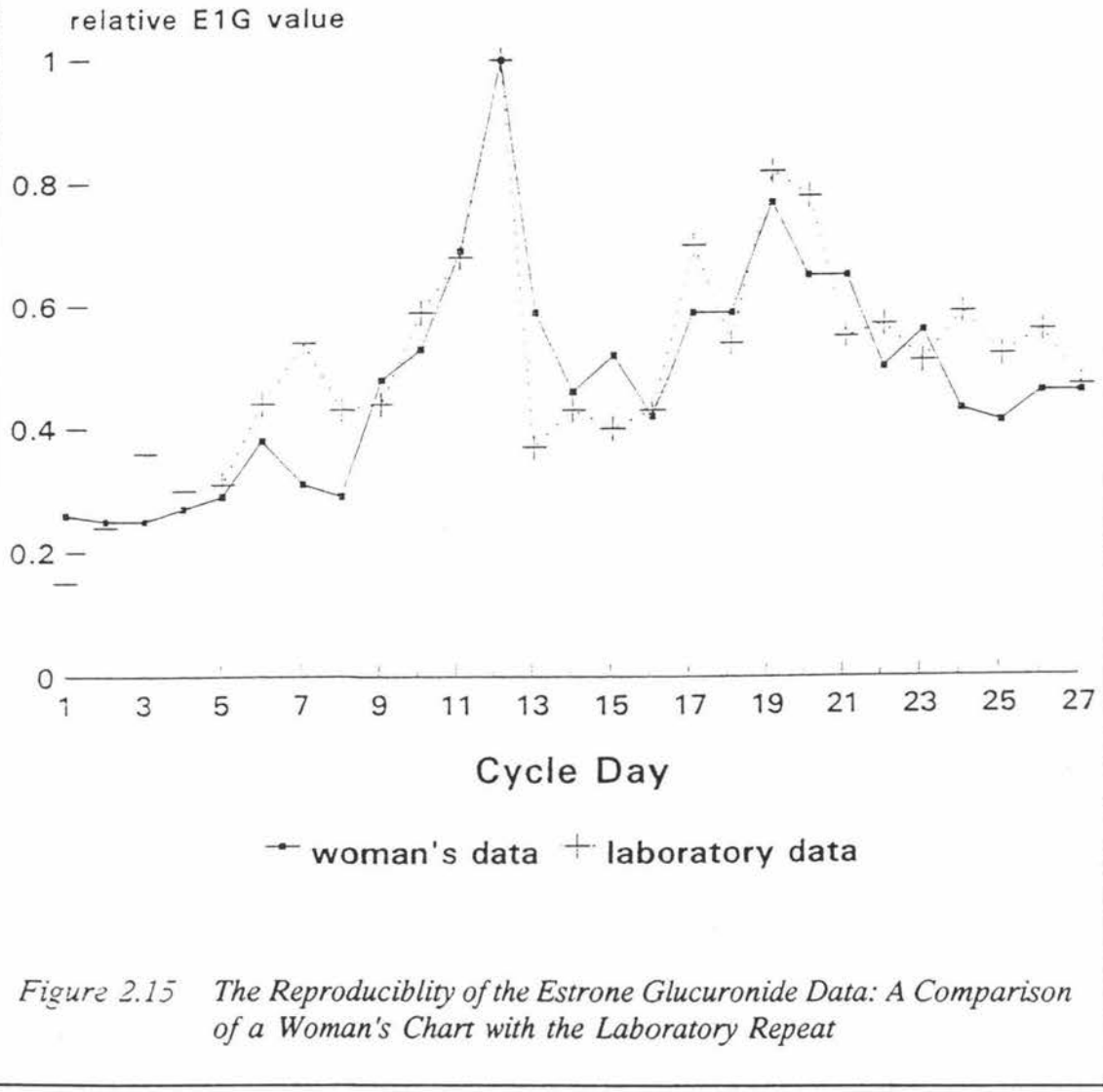

Figure 2.15 *The Reproduciblity of the Estrone Glucuronide Data: A Comparison of a Woman's Chart with the Laboratory Repeat*

woman detected the first rise on day nine of the cycle and the laboratory repeat detected it on day ten. Assuming the day of ovulation is the day of the fall in E1G levels from the peak, then the woman's data would give five days warning of ovulation and the laboratory repeat only four. Thus, although the data from the laboratory repeat is acceptable for the prediction of the beginning of the fertile period it is not as good as the woman's home data.

Furthermore, the woman's home data did not pick up any spikes in the baseline unlike

the laboratory repeat at day seven. As described earlier this spike is possibly the result of lysozyme produced from bacteria which have grown over the months of storage and so presumably would only be characteristic of urines which have not been immediately analysed. Because these spikes are generally isolated events, when the hormone profile of the cycle is examined as a whole as is the case in the laboratory repeats, the fertile period can still usually be easily identified. Furthermore, when the E1G values are revealed one day at a time as is the case when it is being used as a natural family planning aid, it is still unlikely that there will ever be confusion in the delineation of the fertile phase due to the spikes. This is because there is not sufficient time for bacteria to grow in the fresh urine sample.

Although the laboratory repeat for the E1G data is marred by the spike at day seven, the day of the E1G peak i.e. the day of m ximum fertility is still detected by both the woman's data and the laboratory repeat on the same day (day twelve of the cycle). Thus, the quality of this woman's data appears to be high (as was the case for the other forty cycles examined).

ii) *Pregnanediol Glucuronide*

Figure 2.16 shows the reproducibility of the PdG hormone profile for a complete cycle on the Ovarian Monitor using the same cycle used to illustrate the reproducibility of the E1G data in Figure 2.15. Because the woman's data and the laboratory repeats were done on different batches of PdG tubes, the PdG threshold of 7 μmol PdG 24 hr^{-1} was reached at different change in transmission thresholds for the two data sets. Thus, the PdG levels of the cycle have been expressed relative to the change in transmission threshold (i.e. equivalent PdG thresholds).

Figure 2.16 also shows the PdG data to be more reproducible than the E1G data; a trend which all the WHO trial cycles generally followed. The higher reproducibility of the PdG data compared to the E1G data is because the metabolite PdG is excreted at much higher rates than E1G thus, making the assay for PdG comparatively much more accurate (see Section 1.9.5).

Both the woman's data and the laboratory repeats showed a stable baseline during the follicular phase of the cycle followed by a luteal phase dominated by the PdG peak.

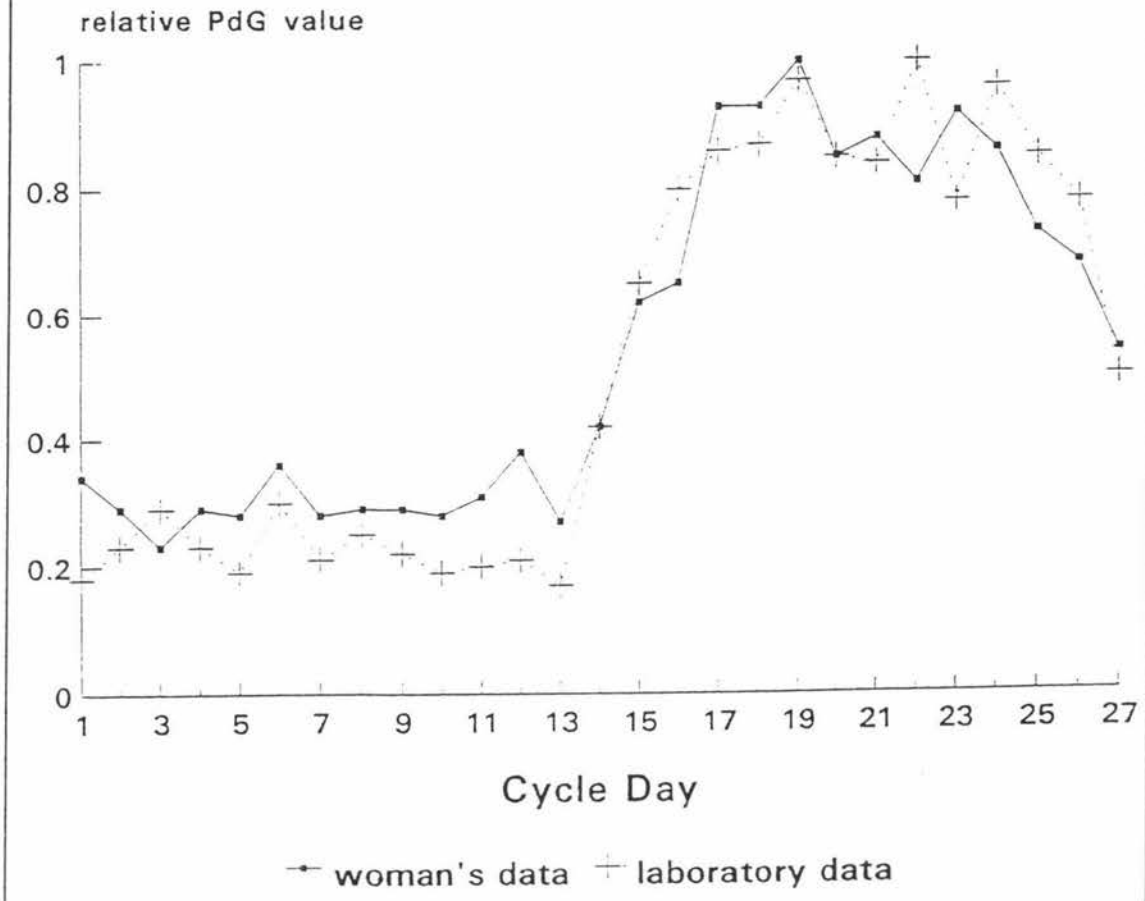

Figure 2.16 *The Reproducibility of the Pregnanediol Glucuronide Data: A Comparison of a Woman's Chart with the Laboratory Repeat*

More importantly both the woman's data and the laboratory repeat showed a clear increase from baseline PdG levels on the same day of the cycle (day fourteen) and thus, indicated the infertile period to have begun on the same day.

Thus, when the cyclical pattern of the hormonal data obtained by the women at home was compared with the laboratory repeats, it was found to be extremely reproducible. This good correlation between the two sets of data was also observed with practically all the cycles examined indicating that the women's home data is not only of a high quality but that the women can produce accurate, reliable hormonal data of value for themselves. This observation was further verified in the follow-up sessions at the completion of the data collection phase where no subject indicated any difficulty in performing the tests.

2.4 CONCLUSION

In conclusion, the results of this chapter show that the best objective urinary marker for the detection of the end of fertility in the home, was the utilisation of a PdG threshold and not an increase in PdG levels as argued by some researchers. The use of a PdG threshold is superior as a marker for the end of fertility for several reasons. Firstly, by selecting the right threshold value, the small pre-ovulatory rise in PdG levels cannot be mistaken for the major luteal phase peak unlike with the use of an increase from a baseline. However, somewhat ironically the use of an increase from baseline (as detected by Trigg's Tracking Signal) was a better marker for the less accurate Ovarian Monitor derived data than that obtained from the Melbourne database which had a much more stable baseline and thus, was more liable to detect the first rise. The second advantage is related to the fact that high circulating levels of progesterone inhibit implantation. It is relatively easy to select a threshold level of PdG which exceeds the level of progesterone necessary to ensure its inhibitory effect. However, it is technically much more difficult to select a deviation from baseline which would ensure this inhibitory effect, as it would be dependent upon the PdG level at which the baseline was stabilised. In addition, a threshold marker does not require daily PdG readings to be taken to establish the baseline. The final advantage of the use of a threshold level of PdG as a marker for the end of fertility, is that a threshold marker does not require an algorithm to calculate when the infertile period begins and thus, it has more value as a home test than a method based on increases from baseline.

The most appropriate threshold PdG level for the Ovarian Monitor was evaluated by using the cycles in the Melbourne database to compare the positions of the predicted first day of infertility relative to the total estrogen peak for three different Pd thresholds. The value of 1.4 mg Pd 24 hr^{-1} served as a compromise between the lower threshold value of 1.2 mg Pd 24 hr^{-1} which resulted in a significant proportion of the cycles having their fertile period predicted as ending before the presumed time of ovum viability had passed, and the higher threshold value of 1.6 mg Pd 24 hr^{-1} which appeared to result in a more conservative estimate of the period of abstinence than was strictly necessary for the avoidance of pregnancy.

A comparison of the Ovarian Monitor results obtained by women in the home, with those previously obtained in Melbourne in the laboratory, as well as with those obtained by the women using their normal non-hormonal markers was carried out. The markers assessed were the following; the first day of fertility, the day of ovulation, the most fertile day, and the first day of infertility. For all these markers the LH peak was used as a reference with the fertile period delineated as occurring between days -3 to day +2 (Collins, 1989) and ovulation defined as occurring 17 hours after the onset of the LH peak.

The day of the first E1G rise was easily defined by visual inspection of the data, and was compared with the day of the first fertile mucus for the ability of the two markers to predict the beginning of the fertile phase. Both the markers examined were associated with a similar number of cycles for which less than the recommended six days warning of ovulation was given. However, studies with the Ovarian Monitor and the Billings Ovulation Method have shown that acts of intercourse on days when there is no indication that the fertile phase of the cycle has begun, even though retrospectively these days were shown to be less than six days from the event of ovulation, were associated with very low pregnancy rates. This supports the theory that the production of fertile mucus is dependent upon high circulating levels of estrogens, and is required for sperm survival. Thus, it appears the use of the first rise in E1G levels as well as the presence of fertile mucus can be used successfully to mark the beginning of fertility even when these markers do not occur six days in advance of the day of ovulation.

The peak mucus symptom i.e. the last day of fertile mucus, and the day of the E1G peak were examined for their value as mid-cycle markers. This analysis showed the peak mucus symptom to be more closely related in time to the event of ovulation than the E1G peak. However, consistent with its physiological basis, the day of the fall of the E1G peak was a better marker for the potentially more important day, the day of peak fertility. This marker also had the advantage that it was not a retrospective marker unlike the day of the peak mucus symptom.

Four markers were compared for their ability to predict the first day of infertility. These were the Billings Ovulation Method (peak mucus day +4 days), the BBT method (day of BBT rise + 2 days), the symptothermal method (mucus or BBT marker which gives

the latest estimate for the beginning of the infertile period) and the Ovarian Monitor (the day the PdG threshold is first equalled or exceeded).

Of these four markers, the BBT method and the PdG threshold were the most reliable indicators for the end of the fertile phase. In comparison with the Billings Ovulation Method, these two markers resulted in less cycles where the fertile period was predicted as having ended in advance of the LH peak day +2, as well as less cycles in which the predicted end of the fertile period appeared to be overly conservative relative to the LH peak. This relatively poor marking for the end of the fertile phase by the Billings Ovulation Method is a reflection of its dependence on a mid-cycle marker to predict the end of the fertile period. This is in contrast to the other two methods, which are both dependent upon high levels of circulating progesterone i.e. a luteal phase marker, to delineate the end of the fertile period.

Overall the daily use of the Ovarian Monitor gave the best results as a fertility marker. However, the best practical method is to use it in conjunction with the mucus symptoms and thus, reduce the total number of assay days required. Although the Ovarian Monitor did come out best in this study, the data generated from it is not as good as previous studies would lead one to expect. This is thought to be due to a combination of factors. Firstly, a woman's cycle is maximally fertile and regular between the years of 20 to 35. However, the subjects of the WHO trial formed an aging population with 60% of the cycles being contributed by women aged 35 years or above. Secondly, the results of the first day of infertility and the length of the fertile period were effected by an increase in the PdG threshold level employed, leading to an overly conservative period of abstinence for the avoidance of pregnancy. Finally, the study was adversely affected by a decrease in quality control of the assay tubes over a critical period of the trial due to the relocation of the Melbourne laboratory which prepared them.

However, clearly women can perform the Ovarian Monitor assays correctly with a minimum of training and derive benefits from the results. More specifically, the Ovarian Monitor defines the fertile period with more objectivity and precision than the current symptoms can provide and is a major advance in fertility control in that it places the information and control normally provided by clinical laboratories directly in the hands of the users. Thus, it is vitally important that the knowledge required to produce

the Ovarian Monitor System is secured outside of Melbourne to ensure survival of the home kit. Furthermore, further development and refinement of the Ovarian Monitor is important so it can be made available cheaply and in sufficient numbers to the public. Some of these aspects are addressed in the next two chapters.

CHAPTER THREE

KINETIC STUDIES ON LYSOZYMES

3.1 INTRODUCTION

Feedback from home users of the Ovarian Monitor and from the focus group discussions with participants in the World Health Organisation study indicated that a reduction in the time required for the estrone glucuronide (E1G) assay was one of the leading requirements for the long term improvement of the Ovarian Monitor. At present, the assay for pregnanediol glucuronide (PdG) takes only five minutes for the final enzyme reaction and fifteen minutes for the total assay (including incubation steps). This is considerably shorter than the time required to perform the E1G test, which needs twenty minutes for the final enzyme reaction and a total of thirty-five minutes for the entire assay when the incubation periods are included. Thus, a major aim of this project is to explore means for modifying the E1G test so that the assay can be completed in a shorter time period without sacrificing precision or accuracy. This means that the same ΔT value (see Section 1.9.4) must be obtained over a shorter time interval. To achieve this, there are several possible strategies which could be investigated.

1. The present hen egg white lysozyme (HEWL) in the Ovarian Monitor could be replaced with a more active lysozyme from a different source.

2. An electronic chip programmed with an algorithm for linearising the transmission data relative to time could be introduced into the Ovarian Monitor thus, shortening the assay time by carrying out an intitial rate determination as opposed to the present end-point assay.

3. Introduce another estrogen conjugate and antibody into the test so that two steroids are measured together as opposed to one. This method would result in two different enzyme reactions occuring simultaneously and thus, the observed

rate would be the sum of the two and the assay time halved.

4. Use a strain of *Micrococcus lysodeikticus* (*M. lysodeikticus*) which is more sensitive to lysozyme or sensitise the commercial strains by utilising additives in the assay, for example the addition of a lactoferrin peptide (S.V. Rumball) or bovine serum albumin (Morsky, 1983).

In this project only the first two options have been examined in detail and will be discussed in this chapter.

3.1.1 THE HISTORY OF LYSOZYME

In 1922 Alexander Fleming performed an experiment when, while suffering the effects of a cold, he allowed a few drops of his nasal mucus to fall onto a culture plate containing bacteria, only to discover some time later that a zone of clearing had developed around the sites of the mucal contamination. Fleming then went on to prove that this anti-bacterial action was enzymatic in origin. Hence, he named the newly discovered lytic enzyme, lysozyme - *lyso* because of its ability to lyse bacteria and *zyme* because it was an enzyme.

Not only did Fleming discover lysozyme, he also discovered a small round bacterium which was particularly susceptible to lysis by the enzyme. Because of this bacterium's exceptional sensitivity to lysis by lysozyme he subsequently named it *Micrococcus lysodeikticus* - with the species name *lysodeikticus* being derived from the word lysis and the word deikticos which means able to show (Stryer, 1981).

After Fleming's initial discovery of lysozyme in nasal mucus, he then proceeded to examine other potential sources of lysozyme in the human body. These studies revealed lysozyme to be widely distributed throughout the human body in both tissues and secretions including tears, saliva, breast milk and the skin, with the richest source of lysozyme being found in tears. Subsequent studies on other species showed lysozyme to be as widely distributed throughout the rest of the animal and plant kingdom as in the human body (Jolles & Jolles, 1984). Most notably the best overall source of lysozyme was found to be hen egg white where it is found at a concentration one hundred times higher than that found in human tears. Ever since this discovery of a readily available

source of lysozyme, hen egg white lysozyme (HEWL) has become the preferred choice for studies on this enzyme. This has lead to it becoming freely available commercially in a purified form reasonably cheaply, as well as being one of the most intensely studied enzymes with respect to its structure and mechanism.

3.1.2 GENERAL STRUCTURAL AND KINETIC CHARACTERISTICS OF LYSOZYME

3.1.2.1 The Three Dimensional Structure of Hen Egg White Lysozyme

The three dimensional structure of HEWL was first determined in 1965 by David Phillips (Phillips, 1966) using a high electron density map which made it the first enzyme molecule to have its tertiary structure determined by x-ray crystallography. HEWL is a compact relatively small enzyme, roughly ellipsoidal in shape with dimensions 45 x 30 x 30 Å and a well defined cleft on one side which divides the enzyme into two lobes (Figure 3.1). HEWL has a molecular weight of 14.6 kilodaltons and consists of 129 amino acid residues linked together into a single polypeptide chain which is cross-linked by four internal disulphide bridges. These disulphide bridges confer a high degree of stability to the enzyme (Stryer, 1981).

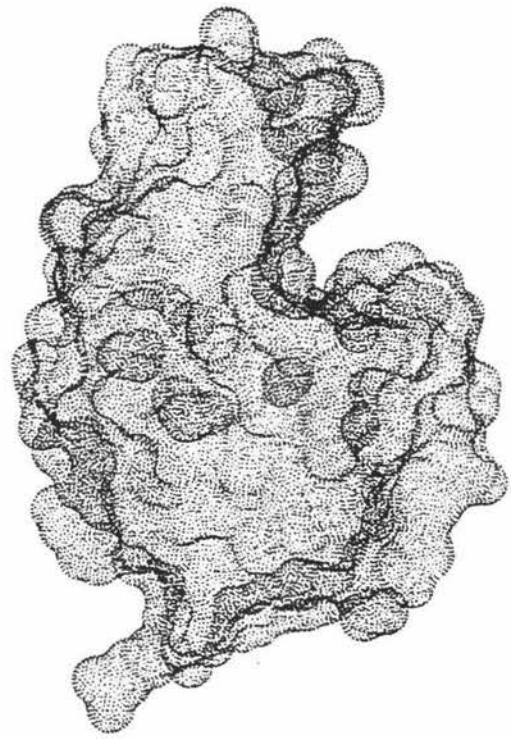

Figure 3.1 *Connolly Surface Model of Hen Egg White Lysozyme*

The enzyme cleft can be seen at the top right hand side of the molecule.

3.1.2.2 The Substrate

The natural substrate for HEWL is the polysaccharide component of the bacterial cell wall. The cell wall polysaccharide is made up of alternating N-acetyl glucosamine (NAG) and N-acetylmuramic acid (NAM) residues joined together by ß(1→4) glycosidic

linkages (see Figure 3.2). The different polysaccharide chains themselves, are cross-linked through amide bonds to the lactic acid side chains of the muramic acid residues

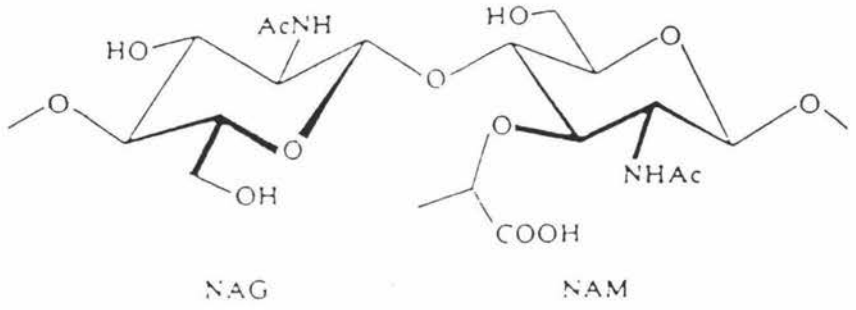

Figure 3.2 *Structure of the Polysaccharide Component of the Cell Wall of the Bacterium Micrococcus lysodeikticus*

by short polypeptide bridges. Lysozyme specifically hydrolyses the glycosidic bond between C-1 of NAM and C-4 of NAG residues but fails to cleave the glycosidic bond between C-1 of NAG and C-4 of NAM (Stryer, 1981). When a bacterial cell wall has been cleaved a specific, but unknown number of times by lysozyme the cell collapses. The collective lysis by lysozyme of many cell walls gives rise to the well known clearing phenomenon (see Section 3.1.4).

HEWL and all other c (chick) type lysozymes as well as the g (goose) type lysozymes (see Section 3.1.3) are equally active towards peptide substituted and non-peptide substituted peptidoglycan. Chitin, a polysaccharide consisting only of NAG residues joined by ß(1→4) glycosidic links, found in the shell of crustaceans, is also a substrate for c type lysozymes, but not for g type lysozymes. Phage lysozymes are even more specific, and will only cleave glycosidic residues next to peptide substituted N-acetylmuramic acid residues, while plant lysozymes in contrast to the other lysozymes only exhibit a high specificity towards chitin (Jolles & Jolles, 1984).

3.1.2.3 Binding of Substrate to Hen Egg White Lysozyme

The binding site of HEWL was successfully mapped due to crystallographic studies performed with the aid of substrate analogs and model building. These studies showed the active site cleft of the HEWL molecule to contain an extended binding site consisting of six subsites in series capable of accomodating a linear linked

hexasaccharide. For practical purposes, these subsites and the sugar residues they contain have been labelled A to F, with F representing the sugar residue and sub-binding site closest to the reducing end of the polysaccharide chain. The polysaccharide chain binds in the HEWL cleft such that the order of binding to the subsites is NAG-NAM-NAG-NAM-NAG-NAM from binding sites A to F. Hydrolysis by HEWL occurs between sugars D and E (i.e. NAM and NAG) on the NAM side of the glycosidic oxygen (see Scheme 3.1).

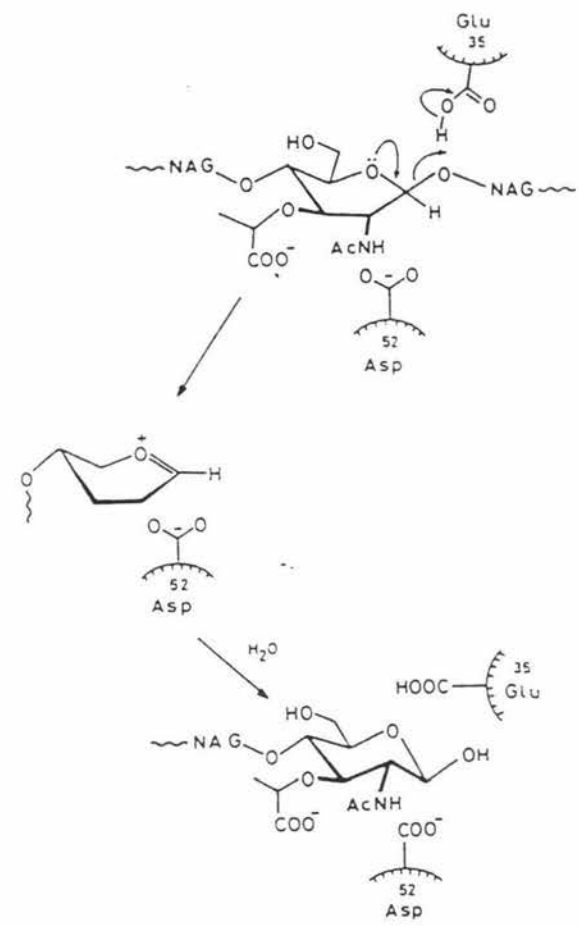

Scheme 3.1 *The Catalytic Mechanism of Hen Egg White Lysozyme*

Lysozyme specifically hydrolyses the glycosidic bond between C-1 of NAM and C-4 of NAG residues on the NAM side of the Glycosidic Oxygen

Of particular significance is the finding that to achieve satisfactory binding of the sugar residues E and F with their respective binding sites without serious nonbonded interactions with the CH_2OH group of residue D occurring, the distortion of residue D from its normal ground state chair conformation into a half chair conformation is required. Because this is not a ground state conformation for a pyranose, sugar residues on both sides of residue D must be bound before this conformation is favoured (Kirby, 1987).

3.1.2.4 The Mechanism of Catalysis for Hen Egg White Lysozyme

Analysis of the structural data has lead to the proposal of the following catalytic

mechanism for HEWL (see Scheme 3.1).

1. The carboxyl group of the glutamic acid residue 35 donates a proton to the bond between the C-1 of the D sugar residue and the glycosidic oxygen resulting in the cleavage of this bond.

2. This creates a positive charge on C-1 of the D ring and thus, converts it into a carbocation.

3. Residues E and F (NAG-NAM) diffuse away from the catalytic site.

4. The carbocation intermediate reacts with a hydroxyl group of a solvent water molecule, releasing the sugar residues A, B, C, and D (NAG-NAM-NAG-NAM).

5. The glutamic acid residue 35 is reprotonated ready for another round of catalysis.

The enzymatic reaction is driven in a forward direction by the stabilisation of the carbocation intermediate. This stabilisation of the intermediate is the result of both electrostatic and geometric forces (Stryer, 1981).

Electrostatically, the intermediate is stabilised by the attraction between the negatively charged carboxyl group on the aspartic acid residue 52 and the positive charge on C-1 on the carbocation intermediate which are separated by a distance of 3 Å.

Geometrically, the carbocation is stabilised by the geometric constraints of the binding site which forces the distortion of the D sugar residue into the half chair conformation. This distortion of the D sugar residue enhances catalysis because the half chair conformation markedly promotes formation of the carbocation. It does this because in the half chair form the planarity of the carbon atoms 1, 2 and 5 and the ring oxygen atom enables the positive charge to be shared between C-1 and the ring oxygen atom. Thus, in the process of the substrate binding to lysozyme, the enzyme forces the substrate to assume the geometry of the carbocation i.e. the transition state.

This proposed mechanism for catalysis by HEWL has been supported by studies where the Glu-35 and Asp-52 residues were chemically modified and the catalytic activity was shown to be destroyed (Stryer, 1981). Similarly, when HEWL's amino acid residues Asp-52 and Glu-35 were replaced by site directed mutagenesis with their corresponding

amides i.e. asparagine and glutamine respectively, the enzyme's catalytic activity was also destroyed (Malcom *et al.*, 1989).

3.1.2.5 Measurement of Lysozyme Activity

The standard kinetic method for measuring lysozyme activity is to determine the initial rate of absorbance change in a turbid suspension of *M. lysodeikticus* at a wavelength of 450 nm (Shugar, 1952), although there are many variations on this procedure (Jolles, 1962; Gorin *et al.*, 1971). Not only does the assay for lysozyme activity vary, but so can the results using any given assay depending on the source of substrate. In 1971, Gorin *et al.*, reported the relative rate of clearing by HEWL of five different substrate suspensions which included two suspensions prepared from lyophilised *M. lysodeikticus* pellets. They observed that a suspension of *M. lysodeikticus* cells prepared from bacterial pellets distributed by Calbiochem was cleared by HEWL at a rate which was a factor of 1.7 times faster than a suspension of *M. lysodeikticus* which was prepared using an identical procedure from *M. lysodeikticus* pellets distributed by Sigma. However, when the two substrates were compared in Melbourne (unpublished results) the opposite effect was observed. Since this experiment was repeated by Brown's group some years after the paper by Gorin *et al.*, was published and Brown's group has also observed that the relative rate of clearing has increased with each subsequent batch of *M. lysodeikticus* supplied by Sigma, this contrasting finding may be due to Sigma developing a strain of *M. lysodeikticus* in the intervening years which was of an increased sensitivity to lysozyme relative to the *M. lysodeikticus* supplied by Calbiochem at the time. Furthermore, these findings also suggest that the proposal for decreasing the urinary hormone assay time by utilising more sensitive bacteria in the Ovarian Monitor may become a feasible method in the future.

The apparent change in absorbance observed upon the addition of lysozyme to a *M. lysodeikticus* suspension is due to the light scattering effects of the bacterial cells and thus, is only indirectly related to the lysozyme activity and the mechanism shown in Scheme 3.1. This indirect effect has been best demonstrated by Colobert and Lenoir (1957) where they showed that in spite of a successful chemical attack by lysozyme upon the bacterial cell wall the enzyme activity proceeded without lysis to the cells and thus, no resultant change in absorbance could be observed. The advantage of measuring

lysozyme activity by changes in the turbidity of a *M. lysodeikticus* suspension is that it is associated with a very large amplification factor, and thus, it can under the right reaction conditions, be easily and precisely measured. However, although the use of changes in turbidity as measured by the rate of change in absorbance can be very precise, this method does have the disadvantage that it is dependent upon the choice of spectrophotometer being used to measure the change. This is because the light scattering is to some degree determined by the geometric optics of the measuring instrument and thus, the results obtained in one laboratory on one machine may not necessarily be reproducible in another (Gorin *et al.*, 1971). Thus, the optics of the spectrophotometer used to obtain a series of results must be taken into consideration when discussing the kinetic properties of lysozyme.

3.1.3 LYSOZYMES FROM OTHER SOURCES

Although the lysozyme purified from hen egg white is the most extensively studied and best understood of the lysozymes, studies with lysozymes from other sources have also been made.

Lysozyme is widely distributed throughout nature in many different forms which can be grouped into several distinct families based on their structural and catalytic similarities. All the avian egg white lysozymes so far examined can be simply divided into two major categories; those which are structurally analogous to HEWL (chicken type, c type) including turkey, and those which resemble the lysozyme characteristic of goose egg white (g type) (Jolles & Jolles, 1984). All the mammalian lysozymes, including human, so far examined belong to the type c class of lysozyme, while the distribution of the type g class of lysozyme seems to be restricted to avian families only. T4 lysozyme belongs to a family of lysozymes distinct from the two avian types so far discovered.

An important characteristic of lysozyme is the observation that its rate of clearing of a turbid suspension of *M. lysodeikticus* decreases over time with the decreasing substrate concentration (Figure 3.4). Thus, the rate of clearing is not zero order. Because the rate of absorbance change decays with time, lysozyme activity is usually measured in terms of initial rates.

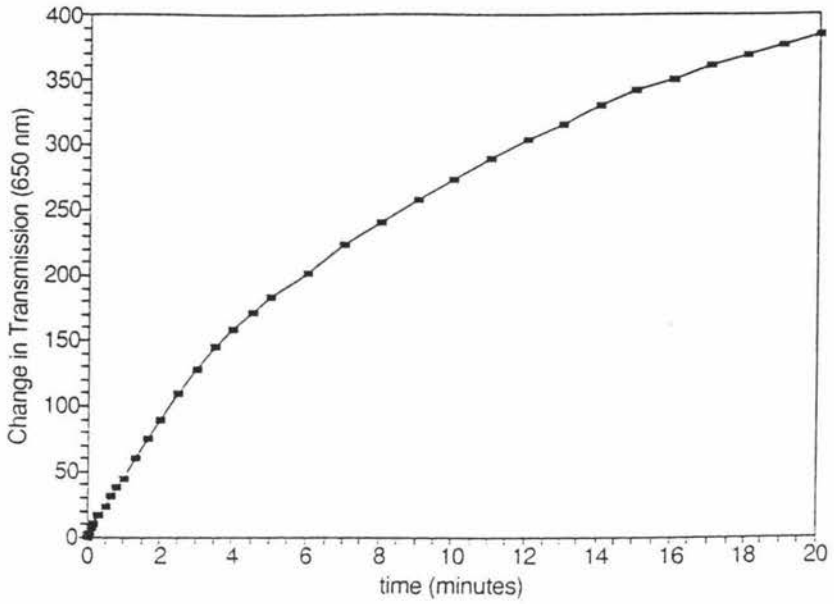

Figure 3.3 *A Typical Ovarian Monitor Clearing Curve of a Micrococcus lysodeikticus Suspension by Hen Egg White Lysozyme*

The above twenty minute clearing curve was obtained using a substrate concentration of 214 mg L^{-1} and an enzyme concentration of 24 nM in a total reaction mixture volume of 350 µl.

Table 3.1 shows a comparison of the lysozymes examined in this thesis.

Table 3.1 *Structural and Kinetic Characteristics of a Variety of Lysozymes*

Lysozyme	M.W*	Residues	Rel.I.R.¶	Cat.§ Acid	Cat.§ Base
HEWL[a]	14.6	129	1.0	Glu 35	Asp 52
HuL[b]	14.6	129	4.4	Glu 35	Asp 53
GEWL[c]	20.4	185	3.0	Glu 73	Asp 86
TEWL[d]	14.6	129	1.5	Glu 35	Asp 52
T4L[e]	18.7	162	6.3	Glu 11	Asp 20

[a] hen egg white lysozyme, [b] human lysozyme, [c] goose egg white lysozyme, [d] turkey egg white lysozyme, [e] T4 lysozyme; * molecular weight (Kdal), ¶ initial rate relative to HEWL at standard conditions; § catalytic residue. Relative initial rates: HuL, Morsky (1983); GEWL, Canfield & McMurray (1967); T4L, Tsugita *et al.* (1968); TEWL, La Rue & Speck (1970). Amino Acid residues: HEWL, HuL, GEWL, TEWL, Jolles & Jolles (1984); T4L, Rossman & Argos (1976). Catalytic acid and base residues: HEWL, HuL & T4L, Dao-pin *et al.* (1989); GEWL & TEWL, Jolles & Jolles (1984).

Table 3.1 records the relative initial rate of T4 lysozyme to be only 6.3 times faster than HEWL using *M. lysodeikticus* as a substrate. However, when *Escherichia coli* (*E. coli*) is used as a substrate this rate increases to a factor of 250 relative to HEWL (Tsugita *et al.*, 1968).

Furthermore, studies on the various lysozymes in Table 3.1 indicate that they all catalyse the lysis of bacteria through the same general mechanism as HEWL (see Section 3.1.2.4). Although the position of the catalytic groups in the amino acid chain does vary in some cases, the catalytic acid and base residues are the same i.e. always a glu or an asp residue respectively. Furthermore, because the initial rates for enzyme activity do vary between lysozymes from different sources, other factors in addition to the positioning of these catalytic residues must be involved in the determination of the initial rates (see Section 3.3.5 for further discussion).

3.1.4 THE OVARIAN MONITOR

In order to make the Ovarian Monitor readily available for home use, it is essential that the costs of the Ovarian Monitor itself and the associated assay be kept to a minimum. As a result of this requirement, the Ovarian Monitor assay differs from the standard lysozyme assays reported above. In the interests of cost effectiveness, the assay is performed in transmission as opposed to absorbance and at a wavelength of 650 nm as opposed to a more standard wavelength of 450 nm. Furthermore, it utilises an end-point assay as opposed to the initial rate assay more commonly implemented. An end-point assay is defined as an assay which measures rate by calculating the change in magnitude of the chosen variable over a pre-determined period of time. Because the Ovarian Monitor assays for lysozyme activity in transmission using an end-point assay the shape of the clearing curve, the initial transmission value at time zero and the assay run time become critical factors.

Over the years several attempts have been made to explain the shape of the lysozyme clearing curve in terms of the underlying catalytic mechanism. This is a particularly difficult task as the clearing phenomenon is a highly complex process.

With most enzymes the absorbance changes observed by the measuring instrument during the catalysed reaction are the direct result of differences in the chemical

absorption of light between the enzyme's substrate and product molecule. In contrast, in the enzymatic reaction between lysozyme and the intact *M. lysodeikticus* cell, the observed absorbance is not due to the absorbance of the light by the substrate i.e. the *M. lysodeikticus* cells, but rather due to their physical obstruction of the light path. Thus, although the *M. lysodeikticus* cells do not absorb the light they do cause an apparent absorbance by scattering some of the light waves and thus, preventing them reaching the detector. As the enzymatic reaction between lysozyme and its substrate proceeds, the observed absorbance decreases as the cell walls of the numerous *M. lysodeikticus* cells collapse, with the collapse of each cell being the product of many catalytically distinct events. Because the cell remnants do not provide an obstruction to the light path, the observed absorbance decreases in proportion with the number of cells lysed. However, although the changes in absorbance are directly related to the rate of cell lysis they are not, unlike most other enzymes, so closely related to the rate of enzyme catalysis.

A very good, but extreme example of this indirect relationship between the observed absorbance and lysozyme activity was demonstrated by Colobert and Lenoir (1957). Their research showed that under very specific conditions, lysozyme can be made to successfully attack the polysaccharide residues of the cell wall without bringing about the disruption of the cell itself. Because it is the disruption of this cell wall which is responsible for any apparent changes in absorbance it was thus illustrated that lysozyme's catalytic activity on a suspension of *M. lysodeikticus* cells is not necessarily coupled with a decrease in the observed absorbance.

This experiment and any other experiment which requires the direct measurement of lysozyme's catalytic activity (i.e. the hydrolysis of glycosidic bonds) does so by quantifying the production of reducing groups. When the two processes, i.e. increases in the level of available reducing groups and the observed absorbance changes, were compared it was clearly shown that the two processes do not proceed in parallel. While the clearing curve was found to reach a plateau (i.e. the absorbance value stabilised), for the same time frame the hydrolytic reaction was found to continue to proceed at the initial rate (Gorin *et al.*, 1971). A possible explanation for this phenomenon is that although the clearing curve would stabilise when all the cells were lysed, the cell

fragments remaining still contain many polysaccharide chains available for hydrolysis.

As already implied, lysozyme generates a very large change in observed absorbance for a given enzyme concentration. However, when its rate of production of reducing groups (i.e. its true catalytic activity) is compared with the catalytic activity of other enzymes, lysozyme scores relatively poorly having a catalytic activity three orders of magnitude less than enzymes such as catalase, urease and aldehyde dehydrogenase (Gorin *et al.*, 1971). This means that compared to lysozyme's true catalytic rate the observed change in absorbance is very large relative to that observed for other enzymes. This large amplification factor whereby only a small amount of enzyme catalysed reaction generates a much larger easily measured physical change is one of the key features of lysozyme which make it so valuable for the Ovarian Monitor assay.

In summary, because of the unusual nature of lysozyme's substrate, the relationship between lysozyme and its substrate, and the associated clearing curve has many unique features. A list of these features which must be taken into account in any hypothesis put forward to explain the underlying kinetic mechanism of the clearing curve is given below.

- The observed absorbance of a reaction mixture of lysozyme and its substrate is the result of light scattering by the substrate as opposed to a true absorbance of light by the substrate or product;
- A change in absorbance is not directly brought about by lysozyme activity, and lysozyme activity doesn't have to be associated with a change in absorbance;
- One discrete change in absorbance requires many catalytically distinct events as opposed to only one on a single molecule of substrate as is required for most other enzyme mechanisms.
- There are many enzyme molecules per discrete substrate assembly, and the average number of enzyme molecules which can bind to a discrete assembly of substrate depends on the relative enzyme and substrate concentrations;
- The spectrophotometric measurement of lysozyme activity is associated with a very large amplification factor.

For a lysozyme catalysed reaction the observed changes in absorbance i.e. the clearing curve, is not the simple sum of a series of discrete catalytic events as is the case with most enzyme catalysed reactions which are followed by changes in absorbance. On the basis of this premise it would be naive to assume for lysozyme that the observed rate of clearing would follow a simple kinetic order as is observed with other simple chemical reactions. However, in spite of the complexity of the kinetics of the clearing curve it has been observed by several lysozyme research groups that for the first part of the HEWL catalysed reaction the second order rate equation provides a reasonable approximation to the true curve (Bernath & Vieth, 1972, Gorin *et al.*, 1971; McKenzie & White, 1986). Although these groups have managed to fit the clearing curve with a reasonable degree of success, no convincing explanation has yet been reported in the literature as to the underlying kinetic mechanism which causes the clearing curve to have the shape it does.

Although the initial rates of GEWL, TEWL, T4L and HuL have all been previously recorded in the literature as being faster than HEWL (see Table 3.1), very little information on the clearing curves of these enzymes has been published to date. Thus, for the suitability of one of these enzymes in a simple substitution for HEWL in the Ovarian Monitor to be assessed, it was necessary for the clearing curves of these enzymes to be examined. This chapter therefore describes details of the preparations of the afore mentioned lysozymes and their associated kinetic characteristics.

3.2 METHODS

3.2.1 ENZYME ASSAYS

3.2.1.1 The Tris Maleate Stock Buffer

1 M stock tris maleate buffer (pH 8.0) was made up according to the following recipe:

Maleic Acid	7.25 g
Tris	19.80 g
NaCl	12.75 g
Tween 80	20.0 mls (1/100 dilution with Milli-Q water)
HCl (conc.)	2.8 mls

Milli-Q water was added to make to a final volume of 375 mls and the pH was adjusted to 7.0 with HCl (conc.).

The 40 mM and 75 mM tris maleate buffers were prepared using appropriate dilutions of the 1 M stock buffer with Milli-Q water.

3.2.1.2 The Bacterial Suspension

The *M. lysodeikticus* suspension was prepared fresh each day. Lyophilised *M. lysodeikticus* (15 mg) (Sigma) was triturated with two mls of 75 mM tris maleate buffer (pH 8.0) in a manual two piece glass homogenator. When a uniform suspension was obtained (approximately two minutes), the suspension was then transferred to a small glass vial and sonicated using a Bandelin Sonorex RK100 for five minutes to ensure homogeneity. The sonicated suspension was kept on ice and resonicated approximately every hour.

3.2.1.3 The Assay Protocol

The enzyme reaction mixture was made up as follows:

M. lysodeikticus suspension	10 µl
enzyme solution	10 - 100 µl
40 mM tris maleate buffer (pH 8.0)	x µl

The reaction mixture was made up to a total volume of 350 µl with 40 mM tris maleate

buffer (pH 8.0) and the assay was performed in an Ovarian Monitor cuvette. The enzyme solution and buffer were pre-incubated to a temperature of 40°C using the Ovarian Monitor for a single assay or a heating block if there were more than one; this incubation period took approximately five minutes. The assay was initiated with the addition of the *M. lysodeikticus* suspension using a 10 µl stepping syringe. This was followed by a quick vortex (2-3 seconds) before placing the cuvette in the Ovarian Monitor. The first transmission value was recorded upon shutting the lid, followed by the second transmission value five minutes or twenty minutes later, depending on the assay, and the rate was measured as ΔT (5 min^{-1}) or ΔT (20 min^{-1}) respectively.

When more than one assay was performed at a time the assays were carried out in series using a stopwatch, and a heating block to incubate the assay mixtures between readings.

Initial rate assays were also performed using the above reaction mixture by measuring the transmission value every five, ten or fifteen seconds for the first few minutes of the assay and then measuring the tangent to the resulting clearing curve.

3.2.2 PURIFICATION OF GOOSE EGG WHITE LYSOZYME

GEWL was purified by two different methods. These were as follows:

3.2.2.1 Goose Egg White Lysozyme Purification Method One

Freeze dried goose egg white (10 g) was mixed with approximately 250 mls of 50 mM ammonium acetate buffer (pH 8.0) and left to dissolve over 48 hours at 4°C. The solution was then centrifuged at 15,000 G for fifteen minutes and the supernatant decanted. The pH of the supernatant was adjusted back to pH 8.0 with 1 M HCl and the ionic strength adjusted with Milli-Q water to below the ionic strength of the buffer. The column (10 x 2 cm I.D.) was packed with the ionic exchange resin, Carboxy-methyl Sepharose, equilibrated with 50 mM ammonium acetate buffer (pH 8.0) and the column outlet connected to an ultraviolet monitor. The column was loaded overnight using a peristaltic pump before the GEWL was eluted from the column as a sharp band using 50 mM ammonium acetate buffer containing 1 M NaCl (pH 8.0). The GEWL fraction was then dialysed against 10 litres of 50 mM ammonium acetate buffer (pH 8.0) over sixteen hours with three dialysis changes. After dialysis the GEWL preparation was

ready for further purification and analysis by Fast Protein Liquid Chromatography (FPLC).

A 2 ml aliquot of the first supernatant, the column breakthrough, and of the eluant before and after dialysis, were taken for enzyme assays. All enzyme assays were performed in duplicate or triplicate.

3.2.2.2 Goose Egg White Lysozyme Purification Method Two

Carboxy-methyl Sepharose (20-40 g wet weight) was equilibrated with 50 mM ammonium acetate buffer (pH 8.0) overnight. Freeze dried goose egg white (10 g) was mixed with approximately 500 mls of 50 mM ammonium acetate buffer (pH 8.0). After leaving the GEWL to dissolve overnight at 4°C, the solution was then centrifuged at 15,000 G for fifteen minutes and the supernatant decanted. The pH of the supernatant was adjusted back to pH 8.0 with 1 M HCl and the ionic strength checked before being added to the pre-equilibrated resin. The resin and the supernatant were then mixed at room temperature for 3½-4 hours using an automatic stirrer. The non-binding fraction was removed by transferring the resin to a buchner funnel and rinsing with 50 mM ammomium acetate buffer (pH 8.0). The washed resin was then packed into a glass column (10 x 2 cm I.D.) using the same buffer and the column outlet connected to an ultraviolet monitor. The GEWL was eluted from the column using a single step gradient with 50 mM ammonium acetate buffer (pH 8.0) containing 1 M NaCl to give one peak which was eluted immediately and followed by a later peak containing GEWL. The GEWL peak was then dialysed against 10 litres of 50 mM ammonium acetate buffer (pH 8.0) for sixteen hours with two buffer changes. This GEWL dialysate was ready for further purification and analysis by FPLC.

Enzyme assays to identify the main lysozyme containing fraction were performed in triplicate throughout the steps of the purification.

3.2.2.3 Goose Egg White Lysozyme Purification by Fast Protein Liquid Chromatography

GEWL was further purified on a Pharmacia FPLC system by ion-exchange chromatography using a Carboxy-methyl Superose column (20 x 2.6 cm I.D). All

buffers used on the FPLC system were first filtered through 0.2 μm filters (Millipore) and all samples prepared for FPLC analysis were filtered through 0.2 μm Gilman ACRO™ TC 13 filters before loading.

Buffer A: 50 mM ammonium acetate buffer
Buffer B: 50 mM ammonium acetate + 1 M NaCl

Buffers at three different pH values were investigated; pH 7.0, 8.0 and 9.0. The column was pre-equilibrated with buffer A before loading. Sample volumes of 2 mls or less were injected manually while samples between 10 mls and 25 mls were loaded using a peristaltic pump and the sensitivity of the detector adjusted according to the loading. Two different gradients were used in the determination of the best elution conditions for GEWL.

Gradient One:	0% buffer B for 20 minutes
	0-100% buffer B in 40 minutes
	(total running time 60 minutes)
Gradient Two:	0% buffer B for 20 minutes
	15-35% buffer B in 60 minutes
	35-100% buffer B in 15 minutes
	100% buffer B for 10 minutes
	(total running time 105 minutes)

The flow rate was 2.0 ml min^{-1} for each gradient. All the peaks were collected and then tested for enzyme activity as described in Section 3.2.1.

Checks for purity throughout the GEWL purifications were performed on a Pharmacia Phast gel electrophoresis system using silver nitrate to stain the protein bands.

3.2.3 T4 LYSOZYME EXPRESSION AND PURIFICATION

3.2.3.1 Reconstruction of the T4 Lysozyme Gene in an Expression System

All glassware, plasticware and solutions required for the isolation and manipulation of the DNA were autoclaved prior to use. All methods utilised in the isolation and

manipulation of the DNA were carried out using asceptic techniques.

All restriction digests, phenol choroform extractions, ethanol precipitations, ligations, electroporation techniques, rapid boil mini-preparations, agarose gel electrophoresis of DNA and preparation of Luria-Bertani (LB) broth were carried out using standard methodology (Sambrook *et al.*, 1989). Restriction endonuclease digestion of DNA samples was in accordance with suppliers instructions. All enzymes and buffers for the plasmid digests and ligations were supplied by Bethesda Research Laboratories (BRL). All agarose gels were prepared and run in tris acetate ethylene-diamine tetra-acetic acid (TAE) buffer (Tris acetate 0.04 M, ethylene-diamine tetra-acetic acid (EDTA) 0.2 mM, pH 8.5), and had an agarose component of 1% (1 g agarose (100 ml)$^{-1}$ TAE buffer). Agarose used for gels was either Sigma Low EEO or ultrapure grade. All samples for gel electrophoresis were run in conjunction with a 1 kb (kilobase pairs) DNA ladder (GIBCO, BRL). TE buffer (100 mM Tris-HCl, 1 mM EDTA, pH 8.0) was used for resuspension of the ethanol precipitated DNA pellet. Electroporation was carried out according to the methodology outlined in Sambrook *et al.*, (1989) and under the following conditions: voltage, 2.5 volts; resistance, 600 ohms; and capacitance, 25 farads.

The plasmid pHS1401e (5 μg) containing the bacteriophage T4 lysozyme (T4L) gene was digested with restriction enzymes *Bam* HI (10 units), *Hind* III (10 units) and *Pvu* I (12.5 units) while the plasmid expression vector pHN1403 (Poteete *et al.*, 1991) (5 μg) was digested with restriction enzymes *Bam* HI (10 units), *Hind* III (10 units) and *Sal* I (10 units). The DNA from each digest was then extracted by two successive phenol chloroform extractions using a 1:1 sample:phenol/chloroform ratio before being precipitated with a mixture of 2.5 volumes of ethanol (95%) and a 1/10 volume of sodium acetate (3 M). The resulting pellet was then washed with 1 ml of ethanol (70%) and evaporated to dryness followed by re-suspension in a small volume of TE buffer (15 μl) in preparation for ligation by ligase. Ligation mixtures with three different molar ratios of 1403:1410e were tested; these were 1:4.4, 1:36, and 1:0.88. A mixture of 1403 digest and ligase, and a mixture of 1401e digest and ligase were also prepared as controls. After ligation the buffer salts were removed by pipetting the samples onto a fragment of dialysis membrane (pore size 0.025 μm) floating on the surface of a 10%

glycerol solution and leaving them to dialyse for 30 minutes with mild stirring. *Escherichia coli* (*E. coli*) cells, strain RR1, were transformed by electroporation with the above ligation mixtures. Immediately after the termination of the current discharge, SOC medium (Sambrook *et al.*, 1989) (250 μl) was added to the cells to aid their recovery. The cells were incubated at 37°C for twenty minutes before plating on LB plates supplemented with ampicillin at 100 μg ml^{-1}, which were then incubated overnight at 37°C. Ampicillin resistant colonies from the 1:0.88 1403:1410e LB plate were used to inocculate twelve culture tubes containing LB broth (5 mls) also supplemented with ampicillin (100 μg ml^{-1}). The inocculated culture tubes were then incubated in a shaker bath for six hours, before storing at 4°C overnight. Transformants possessing the T4L gene were identified by subjecting a sample of DNA from each rapid boil mini-preparation (5 μl) to digestion by a cocktail of B*am* HI, H*in*d III, and P*st* I followed by agarose gel electrophoresis. Thus, transformants bearing the T4L gene were identified. A sample of the culture containing one of the successful transformants was then used to produce a clone of *E. coli* cells containing the pHN1403e plasmid by streaking a sample onto an ampicillin plate. This was used to select a single colony for liquid culture using LB broth supplemented with ampicillin (100 μg ml^{-1}). A permanent stock of the clone was then prepared by mixing a sample of the resulting liquid culture with an equal volume of glycerol and storing at -80°C.

3.2.3.2 Purification of T4 Lysozyme

E. coli cells, strain RR1, bearing the T4L plasmid were removed from frozen culture and used to inocculate LB broth (10 g of tryptone, 5 g of yeast extract, 5 g of NaCl, and 1 ml of 1 M NaOH per litre) (100 mls) supplemented with ampicillin (100 μg ml^{-1}). The starter culture was then aerated in a shaker bath at 37°C overnight before diluting into 2.5 litres of LB broth (12 g of tryptone, 5 g of yeast extract, 10 g of NaCl, and 1 g of glucose per litre). The 2.5 litre cultures were incubated at 37°C in a shaker bath until an optical density of 1.1 (Abs_{595}) was obtained at which point the temperature was reduced to 28.5°C and 0.7-0.8 g of isopropylthiogalactoside (IPTG) added to induce protein production. After sixteen hours further incubation a clear solution was indicative of successful expression of the T4L gene (by showing that cell lysis had occurred). The lysates were centrifuged for 10 minutes at 5,000 G, and the supernatant decanted off and

recentrifuged for 80 minutes at 39,000 G to remove cellular debris. The supernatants were then combined, diluted with water to give a conductivity of less than 4 mmho and then run using hydrostatic pressure through a CM Sepharose column (2.5 x 10 cm I.D.) pre-equilibrated with 50 mM Tris-HCl, pH 7.25, and 1 mM sodium EDTA. Elution was undertaken using a linear gradient of 50-300 mM NaCl in the same buffer, and eighty 8 ml fractions collected. The peak fractions were identified by measurement of the absorbance at 280 nm on a Shimadzu 160A UV-Visible recording spectrophotometer. The protein fractions were tested for activity using initial rate assays as described in Section 3.2.1.3.

3.2.4 KINETICS OF CELL LYSIS

As discussed in Section 3.1.2.5, for the majority of studies performed on lysozyme, the enzyme activity has usually been determined by measuring the initial change in absorbance of a *M. lysodeikticus* suspension containing the lysozyme sample. In contrast, McKenzie's group (McKenzie & White, 1986) is one of the few research teams which have examined the actual kinetics of the clearing curve of lysozyme itself and attempted to fit it to a mathematical equation. For this work the method described by McKenzie for the determination of the kinetic order of the lytic reaction for various lysozymes in different buffer systems at 450 nm has been applied to our transmission data collected on the Ovarian Monitor at 650 nm. It has also been used for the examination of the kinetic order of data obtained at both 450 nm and 650 nm on commercial instruments; i.e. Cary and Cecil spectrophotometers. By using the following parameters the different kinetic orders can be defined. If S is the concentration of cells in the reaction mixture at zero time and if x is the concentration of cells lysed by time t, the concentration of cells remaining at time t can be defined as S-x. Because under the reaction conditions examined by McKenzie and White (1986) it was demonstrated experimentally that the absorbance at 450 nm (A_{450}) is linearly related to the *M. lysodeikticus* concentration then all of the above can be redefined in terms of absorbance at 450 nm. If the concentration of bacterial cells at zero time is proportional to the absorbance at zero time (A^0_{450}), and the concentration of cells remaining at time t is proportional to the absorbance at time t (A'_{450}), then the concentration of cells lysed at time t can also be redefined as the change in absorbance over a time period of t

(ΔA^{t}_{450}). For any enzyme concentration (E) and initial *M. lysodeikticus* concentration, if the kinetics of the reaction are zero order, a plot of x (or ΔA_{450}) versus t will be linear with a y intercept of zero and a slope equal to k'_0, where k'_0 is the zero order velocity constant. If the kinetics of the reaction are first order, a linear plot with a y intercept of zero and a slope equal to k'_1 (the first order velocity constant) will be obtained if $\ln(S/(S-x))$ (or $\ln(A^0_{450}/A^t_{450})$), is plotted against time. If the reaction is second order, a linear plot with a y intercept of one and a slope of k'_2S (or $k'A^0_{450}$) where k'_2 is the second order velocity constant, will be obtained if $S/(S-x)$ (or A^0_{450}/A^t_{450}) is plotted against time. The velocity constants of an enzyme with zero order, first order and second order kinetics are related to the half life of the reaction by the equations $A^0_{450}/2k_0$, $0.693/k'_1$ and $1/A^0_{450}k'_2$ respectively.

When the enzyme concentration is varied the apparent rate constants obtained from the various fits will also vary. For each kinetic order a new rate constant k'cat may be defined as:

$$k'cat = \frac{k'_n}{[E]} \qquad \text{Eqn. 3.1}$$

where k'_n is the zero, first or second rate constant respectively. The k'cat value (or turnover number) is the effective kcat value at the substrate concentration of the assay. For the *M. lysodeikticus* reaction the k'cat value will also depend on the substrate concentration as shown in Equation 3.2 if Michaelis Menten kinetics are obeyed.

$$k'cat = \frac{kcat \times [S]}{K_m + [S]} \qquad \text{Eqn. 3.2}$$

where K_m is the apparent Michaelis constant for the *M. lysodeikticus* clearing reaction.

A comparsion of the rates of clearing of two lysozymes can be made from the k'cat values but it must be borne in mind that the true result may depend on the substrate concentration at which the clearing curve was determined if the apparent K_m values for the two enzymes are different. Nevertheless, screening of the various lysozymes may be achieved by comparison of rates of clearing on a single instrument at a single subsrate concentration simce the factor $[S]/(K_m+[S])$ is unlikely to vary by more than

two for published values of K_m (Locquet *et al.*, 1968).

For this thesis, the zero, first and second order rate equations have been applied to data collected from clearing curves obtained with various spectrophotometers including the Ovarian Monitor. This involved entering the raw data into a spreadsheet programme (QUATTRO-PRO), converting them into absorbance as necessary and then applying the appropriate rate equations to the absorbance data. A plot of the rate equation expression versus time was then drawn, and the duration for which the resulting curve remained linear was estimated by visual inspection. A linear regression was then performed on the linear region using the regression option on the QUATTRO-PRO programme. The regression option calculated the goodness of fit (r^2) of this linear part of the curve, and also the parameters pertaining to the equation of the line y=mx+c, where m equals the slope, x equals the time (in seconds), c equals the y intercept, and y equals the y co-ordinate at time x.

The absorbance value at any time interval over the duration of the clearing curve which would have been obtained if the *M. lysodeikticus* suspension had cleared at a rate predicted by the simple kinetic order of interest, could then be calculated. The first step involved entering the m and c values calculated by regression into the formula y=mx+c on the spreadsheet. Thus, the theoretical y value (i.e. absorbance value) which would have been obtained if the reaction obeyed the simple rate equation, could then be calculated for each time co-ordinate. The y values were then converted into theoretical absorbance values using the absorbance rate expression corresponding to the kinetic order of interest (see above). A plot of this theoretical absorbance against time gave the clearing curve which would have been obtained if it had obeyed the simple kinetic order for the whole of the clearing curve. Thus, the degree of fit of a set of data to the kinetic order of interest was immediately apparent by a visual comparison of the experimental data with the theoretical clearing curve.

An alternative measure of the degree to which a given clearing curve fits zero, first or second order kinetics can be made in terms of the number of half lives for which the order of reaction fits the data. Although the number of half lives for which an enzyme reaction follows simple kinetic order varies with the enzyme, in all cases the reaction rate will eventually diverge from a simple kinetic order.

3.2.5 CONVERSION BETWEEN TRANSMISSION AND ABSORBANCE VALUES

Two different equations were used to convert the transmission data into absorbance values. Transmission data collected on the Ovarian Monitor were converted into absorbance units by the following equation:

$$Abs_{650} = \log\left(\frac{T_{buffer,650}}{T_{sample,650}}\right) \qquad \text{Eqn. 3.3}$$

where $T_{buffer,\ 650\ nm}$ is the transmission value when the cuvette contains buffer only.

Transmission data collected on the commercial spectrophotometers were converted into absorbance where necessary by using the following equation:

$$Abs_{650} = 2 - \log(\%T_{650}) \qquad \text{Eqn. 3.4}$$

3.2.6 MICHAELIS MENTEN PARAMETERS

The apparent Michaelis Menten constant (K_m) was measured for HEWL, TEWL, HuL and T4L on the Cary spectrophotometer at a wavelength of 450 nm. The initial rate data with which the K_m's of TEWL, HuL and T4L were obtained using a concentration of enzyme in the reaction mixture of 35 nM, 7 nM and 7 nM respectively, while the K_m for HEWL was measured using four different enzyme concentrations; these were 7 nM, 35 nM, 70 nM and 105 nM. Unfortunately the K_m value could not be measured for GEWL because the activity of the previously purified GEWL was zero after the months of storage and the time and effort required to repurify some from the stock of freeze-dried goose egg white was not deemed to be worthwhile. The substrate concentrations from which the initial rates were calculated ranged from 6.3 to 200 mg L^{-1} of reaction mixture. All enzyme assays were performed in triplicate, and in cases where the triplicate assays showed large discrepancies with each other the assay was repeated until a clear consensus as to the correct value could be ascertained. This poor replication of results was found to be particularly a problem at the lowest HEWL concentration (7 nM) where the rates were very low. The apparent K_m values for each enzyme were

calculated by entering the average initial rate (v) with the corresponding substrate concentration into the computer programme ENZFITTER. ENZFITTER is a computer programme which draws a plot of rate against substrate concentration and then fits the resulting data points to a hyperbola utilising the Michaelis Menten equation (see Equation 3.5) and thus, calculating the parameters K_m and V_{max}.

$$v = \frac{V_{max} \times [S]}{K_m + [S]} \qquad \text{Eqn. 3.5}$$

3.2.7 CALCULATION OF ELECTROSTATIC FIELDS FOR LYSOZYMES

The electrostatic fields for HEWL, TEWL, HuL and T4L were calculated by the Klapper algorithm (Dao-pin *et al.,* 1989) at 298 K on a 65 x 65 x 65 three-dimensional grid. The software package, Del Phi, was used for the computations. Co-ordinates for the various lysozymes were obtained from the Protein Data Bank (entry set 2lzt, 2lz2, 1lz1 and 3lzm for HEWL, TEWL, HuL and T4L respectively). Since in HEWL, TEWL and HuL the uncharged state is considered as the catalytically active form for Glu-35, Glu-35 was assumed to be electrically neutral for all three lysozyme molecules. Similarly for T4L the catalytic residue Glu-11 was assumed to be electrically neutral. All other appropriate side chains of the four different lysozyme molecules including histidine and the N and C termini were assumed to be fully charged. The di-electric constant (ε) of the protein and the water region was set to two and eighty respectively, while the ionic strength of the solvent was assumed to be 0.15 M. The Coulombic approximation was applied to the boundary condition. Iterations were terminated when the maximum change in potential in the final iteration was $<10^{-5}$ kT/e.

The graphics of the electrostatic potential maps were displayed using the software package Insight II (Biosym Technologies).

3.3 RESULTS AND DISCUSSION

3.3.1 GOOSE EGG WHITE LYSOZYME PURIFICATION

The first attempt at purification of GEWL from goose egg white involved loading a solution of goose egg white supernatant directly onto a CM Sepharose column (see Method One, Section 3.2.2.1). However, the rate of loading slowed down drastically with time due to the goose egg white albumin forming a visual plug at the bottom of the column. This effect was such that at eighteen hours after the beginning of loading the supernatant was still being pumped onto the column. Thus, the column was unpacked, most of the albumin plug removed before repacking the column, and the rest of the goose egg white supernatant was successfully loaded at a much faster flow rate. GEWL was then eluted from the column as a sharp band with 50 mM ammonium acetate buffer (pH 8.0) containing 1 M NaCl using a step gradient and the resulting 112 ml fraction dialysed against 50 mM ammonium acetate for 16 hours (3 changes x 10 litres).

The GEW supernatant (550 mls), column breakthrough (515 mls), eluent (112 mls) and dialysed eluent (116 mls) were all tested for lysozyme activity using standard assay procedures (see Section 3.2.1.3) where one unit of activity was defined as 100 ΔT units (5 min^{-1}). A summary of the results calculated from these enzyme assays is given in Table 3.2.

Table 3.2 *Goose Egg White Lysozyme Activity for Various Fractions generated using Method One*

Fraction	Units of Total Activity
GEW Supernatant	85,000
Breakthrough	520
Eluent	16,500
Dialysed Eluent	15,800

These results showed that a considerable amount of lysozyme activity was lost during the purification. This was presumably through a failure for the enzyme to be completely eluted from the ion exchange column with the 1 M NaCl step gradient. However, the amount of GEWL lost in the breakthrough volume during chromatography was negligible, as was the amount lost during dialysis.

Because of the problems experienced with flow rate using the first method, the procedure was modified for the next attempt at purification of lysozyme from goose egg white (see Method Two, Section 3.2.2.2.). In Method Two the CM Sepharose resin was mixed directly with the GEW supernatant, washed by filtration to remove the albumin fraction (935 mls) and then packed into a column with the GEWL already bound. Elution was then undertaken as for Method One i.e. by using a 1 M NaCl step gradient. As before, this procedure resulted in the elution of two absorbance peaks from the column, first a small breakthrough peak (103 mls) and then a second much larger peak (92 mls) which contained the bulk of the GEWL activity. Thus, the amount of activity recovered was on a similar scale to that obtained in the first method, but without the problems of flow rate. The total activities of the resulting fractions from this second purification scheme are given in Table 3.3.

Table 3.3 *Goose Egg White Lysozyme Activity for Various Fractions generated using Method Two*

Fraction	Units of Total Activity
Filtrate	20
Breakthrough	130
Main Peak	27,500

Thus, once again the bulk of the GEWL activity was found associated with the main A_{280} peak.

After this initial purification step, all further purification was performed on an FPLC system (see Section 3.2.2.3). Of the two different gradients tested, Gradient Two which

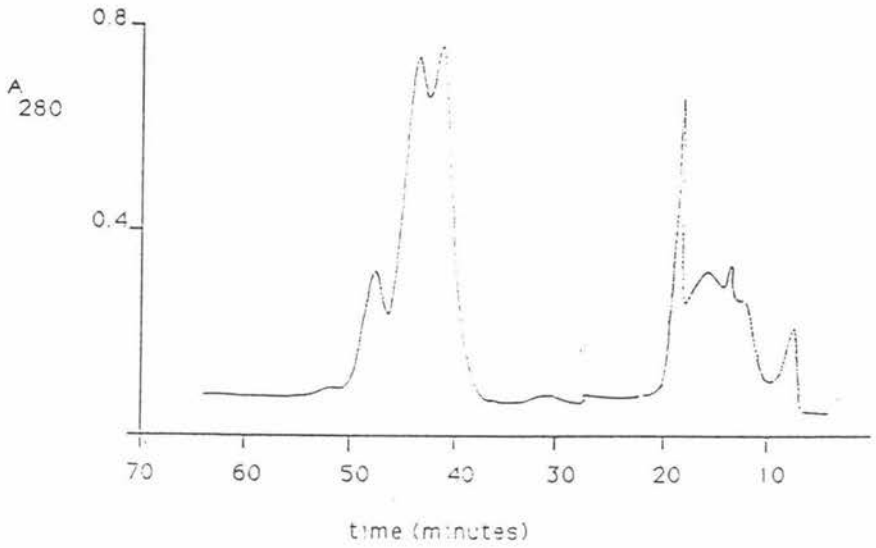

Figure 3.4 *Elution Profile of a Goose Egg White Lysozyme Purification by Ionic Exchange on a Carboxy-methyl Superose Column using Gradient One*
Conditions: See Section 3.2.2.3; manual load - 12 mls; flow rate - 2.0 ml min^{-1}

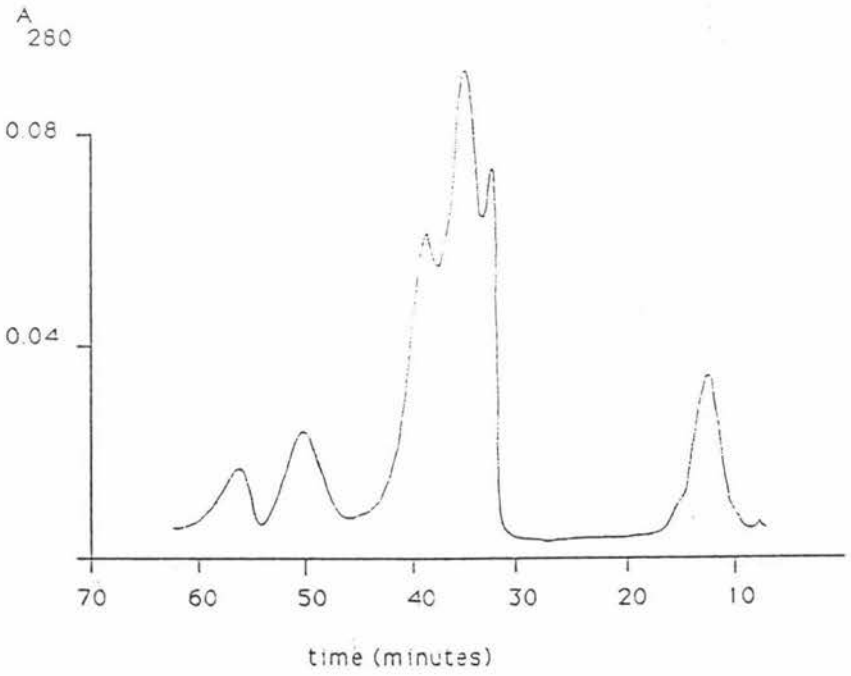

Figure 3.5 *Elution Profile of a Goose Egg White Lysozyme Purification by Ionic Exchange on a Carboxy-methyl Superose Column using Gradient Two*

Conditions: See Section 3.2.2.3; manual load - 2 mls; flow rate - 2.0 ml min^{-1}

contained the shallower salt gradient of 0-0.35 M NaCl as opposed to 0-1 M NaCl was

found to be the more successful resulting in a better resolution of the different peaks. Figures 3.4 and 3.5 show the different elution profiles obtained at pH 9.0 with Gradient One and Two respectively. Lysozyme activity was found predominately in the later peaks with both gradients as shown in Table 3.4.

Table 3.4 Goose Egg White Lysozyme Activity for Various Fractions generated using Gradient One and Two on a Carboxy-methyl Superose Column

Peak Number	Gradient One Units of Total Activity	Gradient Two Units of Total Activity
1	300	0
2	700	0
3	9,800	2,900
4		172,000
5		200

Thus, while the first gradient resulted in the elution of several peaks which all contained small amounts of lysozyme activity, the second gradient showed more discrimination, with the fourth peak, which was clearly resolved from the other peaks, containing the bulk of the lysozyme activity. Buffers at pH 7.0 and pH 8.0 were also tested using the two different gradients, but the combination of pH 9.0 buffers used in conjunction with the shallow gradient was found to give the best results.

The best fractions from each run (as determined by total activities) were combined and the pooled fractions were dialysed for sixteen hours against 50 mM ammonium acetate + 0.1 M NaCl (pH 9.0) (10 litres x 3 changes). This pooled fraction (150 mls) was further purified by re-chromatography on the CM Superose column using the second gradient in conjunction with the pH 9.0 buffers (see Figure 3.6). The peaks resulting from this FPLC run were then assayed for enzyme activity (see Section 3.2.1.3). The results of these assays are summarised in Table 3.5.

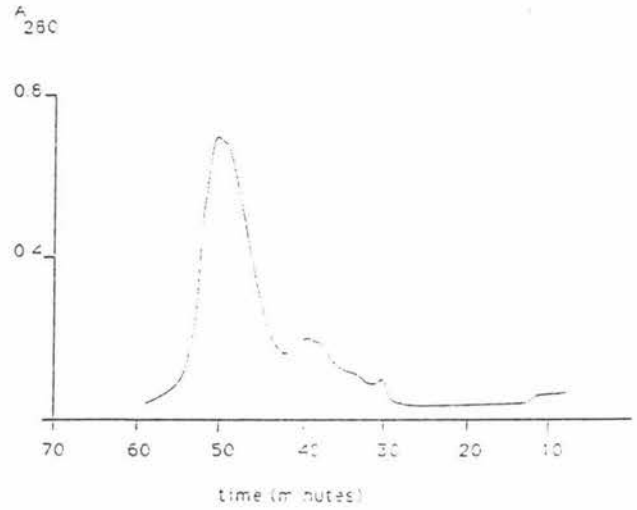

Figure 3.6 *Elution Profile of Combined Best Goose Egg White Lysozyme Fractions after Ionic Exchange Chromatography on a Carboxy-methyl Superose Column using Gradient Two*

Conditions: See Section 3.2.2.3; manual load - 135 mls; flow rate - 2.0 ml min^{-1}

Table 3.5 *Goose Egg White Lysozyme Activity for the Two Fractions resulting from Re-chromatography of the Best Goose Egg White Lysozyme Fractions on a Carboxy-methyl Superose Column*

Peak Number	Best Fraction Units of Total Activity
1	700
2	7,000

On the basis of these results the main peak (i.e. peak 2) was dialysed against Milli-Q water and a sample (1 ml) saved for analysis by gel electrophoresis followed by silver nitrate staining. Gel electrophoresis showed this fraction to contain a very slight contamination (see Figure 3.7). However, due to the well known sensitivity of the silver nitrate stain to protein this sample was considered sufficiently pure for the kinetic studies envisaged and no attempts at further purification of this fraction were made.

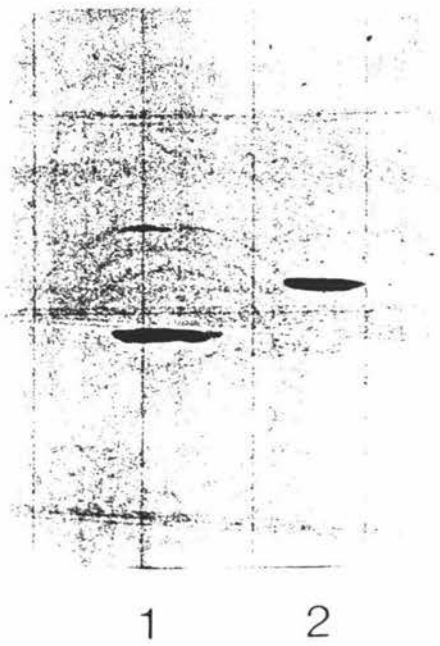

Figure 3.7 *Gel obtained from Goose Egg White Lysozyme (GEWL) after Purification and Hen Egg White Lysozyme (HEWL), after Sodium Dodecyl Sulphate Polyacrylamide Gel Electrophoresis (SDS-PAGE)*

Obtained on the Pharmacia PHAST system using 20% SDS buffer strips and stained with Silver Nitrate. Lane 1: HEWL (Sigma), Lane 2: GEWL after purification on a Carboxymethyl Superose Column

All characterisation of the kinetics and clearing curve of the GEWL was done on the GEWL purified from this step.

3.3.2 T4 LYSOZYME EXPRESSION AND PURIFICATION

3.3.2.1 Reconstruction of the T4 Lysozyme Gene in an Expression System

The general strategy for transferring the T4L gene from the pHS1401e plasmid to the expression vector, pHN1403, is summarised in Figure 3.8. Briefly, it involved cleaving both plasmids at the restriction enzyme B*am* HI and H*ind* III sites to produce cohesive ends, and then ligating the 630 bp fragment containing the T4L gene which was flanked by a B*am* HI and H*ind* III site, into the pHN1403 plasmid.

Because the difficulty in constructing a viable plasmid increases in a non-linear fashion with the number of fragments involved, the most probable construct is the one formed from the smallest number of fragments. Thus, in order to select for the desired construct, an attempt was made to further cleave the DNA fragments which were not part of the target plasmid (i.e. the pHN1403e plasmid) into smaller fragments. Thus, the 30 bp fragment of the pHN1403 plasmid resulting from the cleavage at the B*am* HI and H*ind* III sites was further cleaved with the restriction enzyme S*al* I. Cleaving with

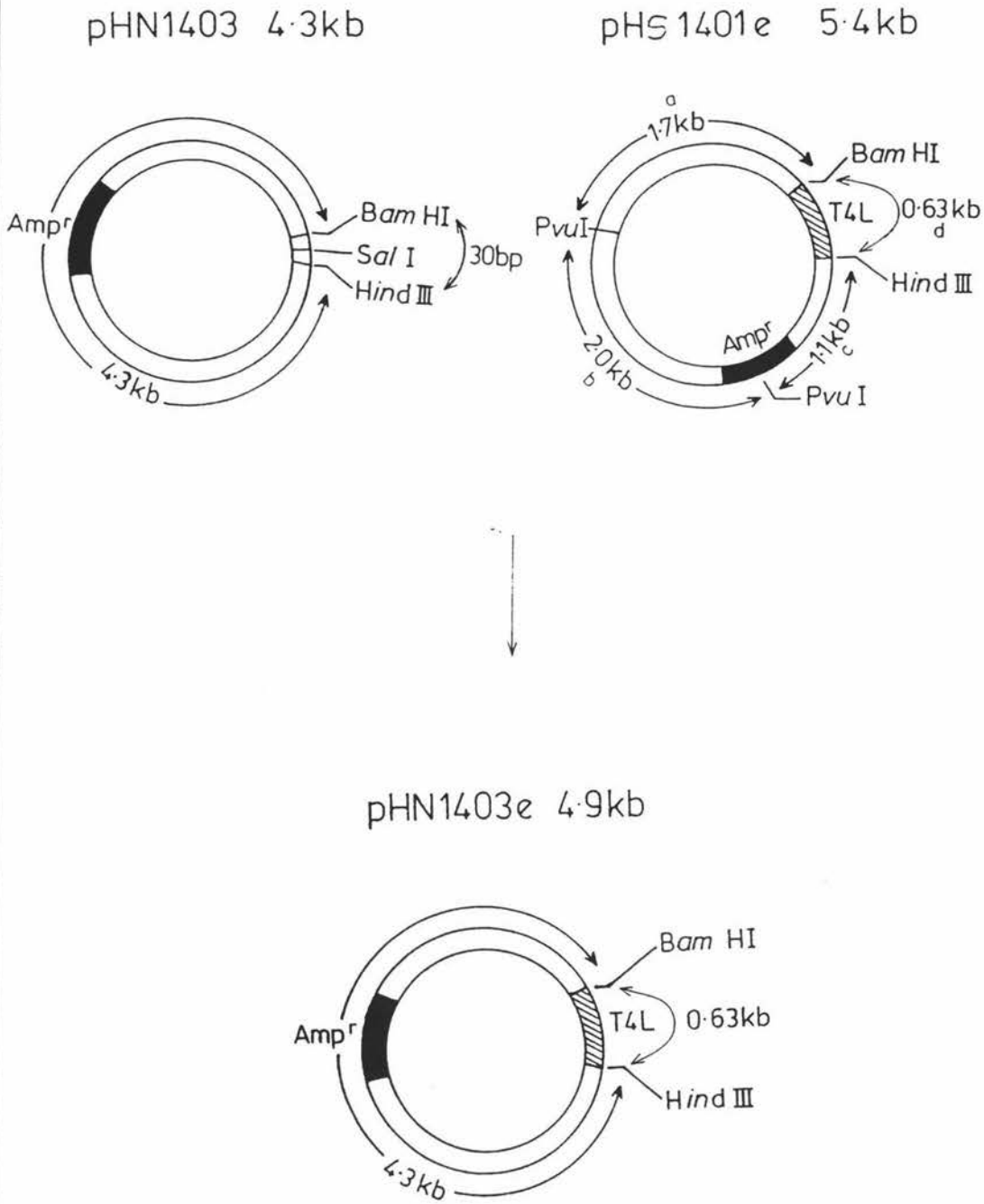

Figure 3.8 *Schematic Diagram of the Transfer of the T4 Lysozyme Gene from pHS1401e into pHN1403 for Expression*

the restriction enzyme *Sal* I also had the added advantage that it produces blunt ends and hence its use further reduced the likelihood of the two fragments re-annealing with each other. Likewise the 4.8 kb fragment from the pHS1401e plasmid was further cleaved with the restriction enzyme *Pvu* I for which the DNA fragment contains two cleavage sites. Because one of these *Pvu* I sites is within the gene which codes for ampicillin resistance the use of this restriction enzyme has the added advantage that after the transformation of the *E. coli* cells with the ligation mixture, many of the possible constructs would be selected against due to a failure of their host cells to grow on ampicillin plates. Conversely, the ampicillin resistance gene from the pHS1403 plasmid should remain intact and thus, *E. coli* cells successfully transformed with constructs made from this DNA fragment should remain viable upon plating on ampicillin medium. Thus, *E. coli* cells containing the pHN1403e plasmid (i.e. the pHN1403 plasmid containing the T4L gene) would be selected for.

Figure 3.9 *Ethidium Bromide Gel of pHN1403 and pHS1401e Digests*

Lane 1: pHN1403 after digestion with Bam HI, Hind III and Sal I

Lane 2: pHS1401e after digestion with Bam HI, Hind III and Pvu I

Lane 3: pHS1401e after digestion with Bam HI, and Hind III

Lane 4: Ladder

Figure 3.9 shows the electrophoresis profile obtained for the digests of the two different plasmids. The interpretation of the migration distance of the bands is given in Figure 3.10. Thus, it appears that the digestion of the pHS1401e plasmid by the

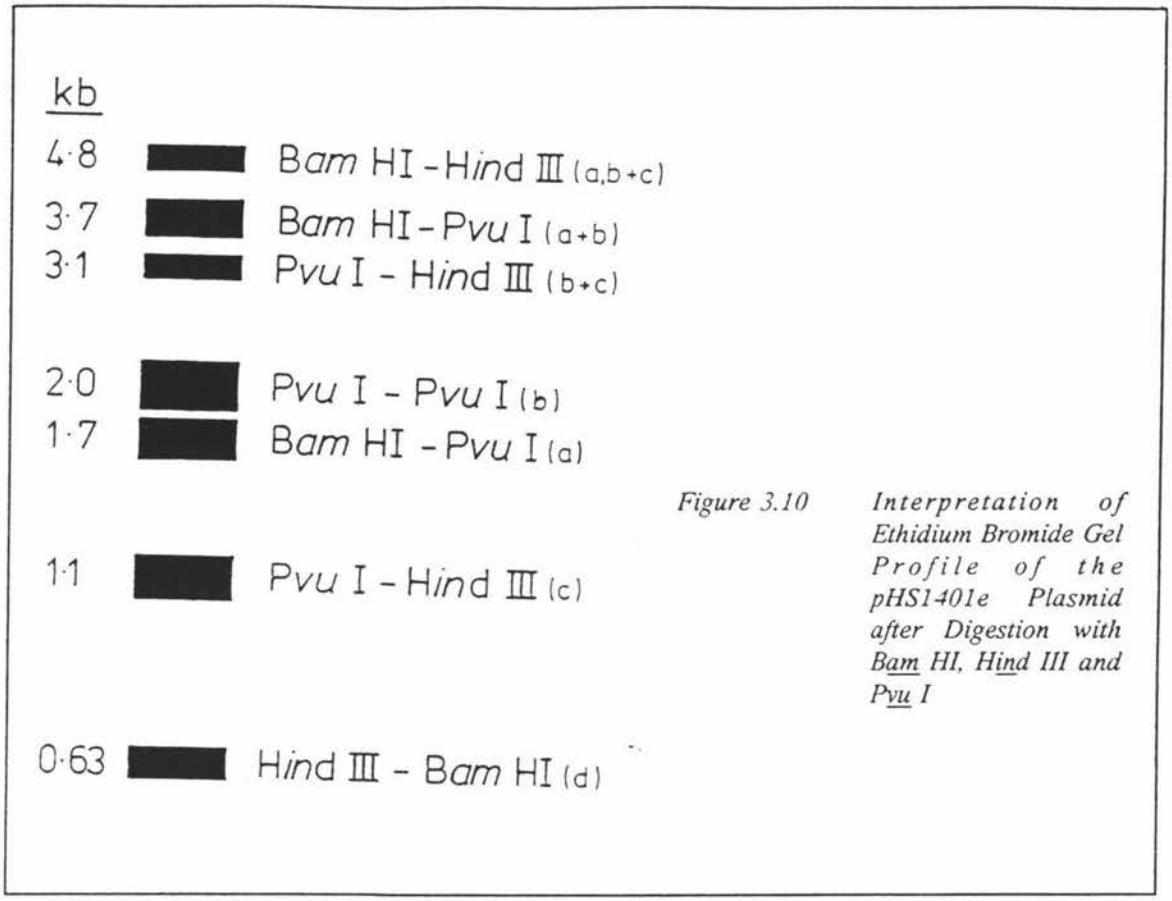

Figure 3.10 *Interpretation of Ethidium Bromide Gel Profile of the pHS1401e Plasmid after Digestion with Bam HI, Hind III and Pvu I*

restriction enzyme P*vu* I was only partially successful. Although the 30 bp fragment from the pHN1403 plasmid is too small to be visible with the ethidium bromide staining, the cleavage of the plasmid with the three restriction enzymes must have been at least partially successful to result in only one UV band upon staining with ethidium bromide (no band for supercoiled or nicked DNA present).

As discussed above only *E. coli* cells, strain RR1, which have been successfully transformed with a plasmid containing a complete copy of an ampicillin gene will grow on the LB ampicillin plates. Low counts were obtained on both the pHN1403 and pHS1401e controls. This growth on the pHN1403 control plate suggests that the digestion by the restriction enzymes might not have been complete allowing the pHN1403 vector to religate into its original form upon the addition of the DNA ligase. Likewise the growth on the pHS1401e plate suggests that either some of the original pHS1401e plasmid was never cleaved, or alternatively it was only partly cleaved allowing its constituent fragments to religate back into their original form upon the addition of the DNA ligase. It is also possible that some of this growth is derived from

the pHS1401e plasmid which although completely digested religated back into its original form. However, this would probably be a very rare occurrence as it would require a four fragment ligation.

Of the three pHN1403:pHS1401e transformation plates, the 1:0.88 (mg of DNA, 80 µl plated) plate was found to have been associated with the most growth. Thus, twelve colonies from this plate were selected for the isolation of ampicillin resistant transformants. Ten of the twelve transformants were successfully cultured in LB broth, of which nine were found by restriction digest analysis to contain the T4L gene. Thus, the strategy implemented for the transfer of the T4L gene from the pHS1401e plasmid into the pHN1403 vector for expression proved to be very effective and was associated with the generation of a high yield of transformants containing the T4L gene.

3.3.2.2 Purification of T4 Lysozyme

All T4L was prepared from a clone of one of the nine successful transformants which was stored in glycerol at -80°C. T4L was successfully purified as described in Section 3.2.3.2. The advantage of purifying T4L from *E. coli* compared to the purification of other enzymes from a host cell is that the expression of T4L is easily visualised by the clearing of the bacterial suspension due to T4L attacking the "hosts" cell wall. This enzyme activity is also associated with the additional benefit that it simplifies the purification procedure for T4L from *E. coli* by eliminating the need for lysis buffers normally required for the purification of other enzymes expressed intracellularly. Thus, after the expression of the T4L gene, the T4L was simply separated from the resulting cellular debris by centrifugation.

One pass through the CM Sepharose column resulted in a single protein peak. Additionally, because this closely mapped the activity profile obtained (see Figure 3.11) no further purification of the protein was deemed necessary. All kinetic studies performed on T4L were performed on fraction 37, the peak fraction which was shown to be pure upon gel electrophoresis by yielding a single band when stained with silver nitrate.

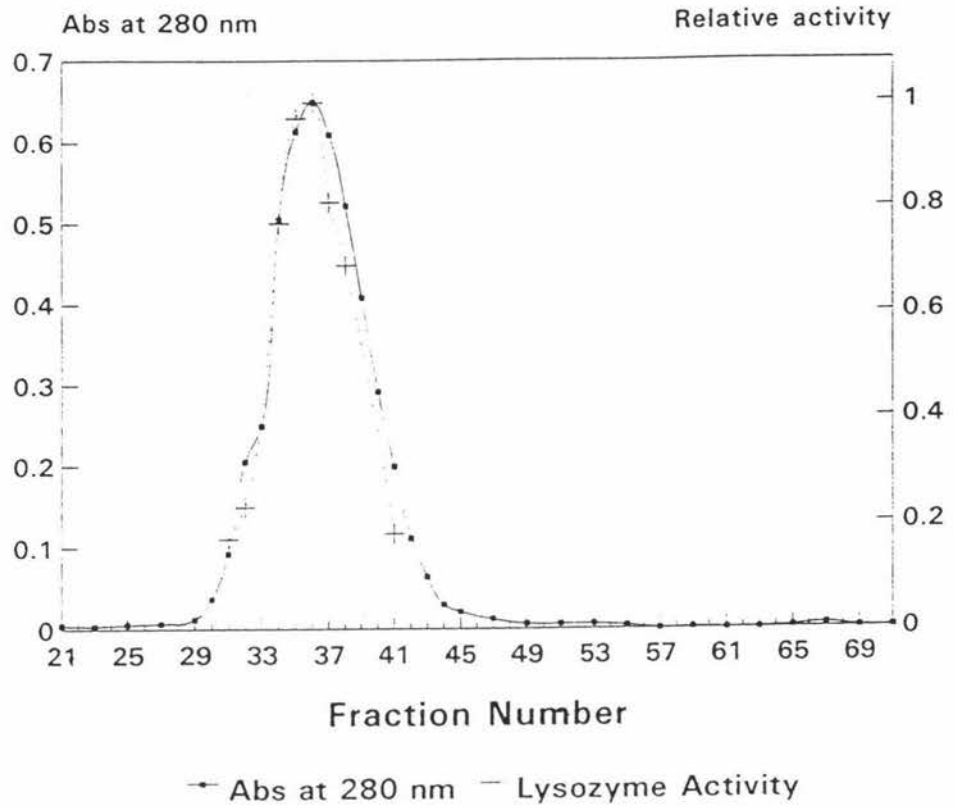

Figure 3.11 *Absorbance (280 nm) and Lysozyme Activity Profile of Escherichia coli lysates after One Pass Through a Carboxy-methyl Sepharose Column*

Column Conditions: Buffer A - 50 mM Tris-HCl + 1 mM sodium EDTA (pH 7.25), Buffer B - 50 mM Tris-HCl + 1 mM sodium EDTA + 300 mM NaCl (pH 7.25); gradient - 16.66%-100% buffer B; fraction volume - 8 ml.

3.3.3 LYSOZYME CLEARING CURVES

In this section the lysozymes obtained from goose egg white (GEWL), turkey egg white (TEWL), human milk (HuL) and phage T4 lysates (T4L) were screened for their potential use in the Ovarian Monitor. For the replacement of HEWL in the Ovarian Monitor with one of the above lysozymes to be viable it would have to generate a rate of clearing of the *M. lysodeikticus* suspension which is at least two to three times greater than that of a HEWL control under the same assay conditions i.e. obtained with the same enzyme and substrate concentration on the same spectrophotometer. The simplest method of reducing the E1G assay time would be by replacing the HEWL with another lysozyme which was capable of generating the same change in transmission in a shorter time period i.e. a shorter end-point assay. However, a less ideal but possibly more

realistic method of reducing the E1G assay time would be by the application of algorithms to the clearing curve (e.g. initial rates) although the more complex the algorithm required the less practical the alternative becomes.

During the course of this work it was necessary to obtain the kinetic data on several different spectrophotometers which resulted in the use of non-standard conditions. In each case a concentration of *M. lysodeikticus* was chosen to give an absorbance in the region of the greatest photometric accurarcy (i.e. 0.3-0.8) at the chosen wavelength (450 or 650 nm). Hence, the substrate concentration was not always the same as used in the Ovarian Monitor. However, it has been assumed that any lysozyme showing a rate enhancement of two or greater could provide a possible means of improvement for the Ovarian Monitor and also that the kinetic parameters defining the shapes of the clearing curves are valid generally. Of course, the ultimate test regarding the potential use of a lysozyme with a given assay procedure as an alternative to the current Ovarian Monitor assay must be made on the Ovarian Monitor itself.

3.3.3.1 Hen Egg White Lysozyme

Since HEWL represents the control in any new method of assaying for E1G, the general features of the HEWL clearing curves obtained with the Ovarian Monitor were examined first. Figure 3.3 shows a typical clearing curve obtained over twenty minutes in the Ovarian Monitor with native HEWL (i.e. unconjugated) and its substrate *M. lysodeikticus*. This clearing curve was obtained using a concentration of enzyme (24 nM) similar to that of the free E1G-HEWL conjugate (i.e. conjugate not bound to antibody) which is encountered in the E1G assay at high levels of urinary E1G (see Step 2, Section 1.9.4). The concentration of *M. lysodeikticus* (214 mg l^{-1}) was the same as that used in the home assay. From Figure 3.3 it is apparent that under these conditions the HEWL clearing curve, in transmission at 650 nm, is not linear, but gently curved.

As discussed in Chapter One, in the current Ovarian Monitor end-point assay system for E1G, the change in transmission, ΔT (20 min) is defined as the difference between the transmission value recorded by the Monitor at time zero, T_0, and the transmission value recorded by the Monitor at twenty minutes, $T_{20\ min}$. For HEWL, this difference (ΔT) is

a linear function of the free lysozyme concentration up to a concentration of 60 nM as encountered during measurement of urinary PdG levels $\Delta T\ (5\ min)^{-1}$ (or urinary E1G $\Delta T\ (20\ min)^{-1}$) with the Ovarian Monitor (see Figure 3.12). This relationship between the change in transmission and enzyme concentration implies that despite the curvature of the clearing curve all points on it are linearly related to the HEWL concentration. Thus,

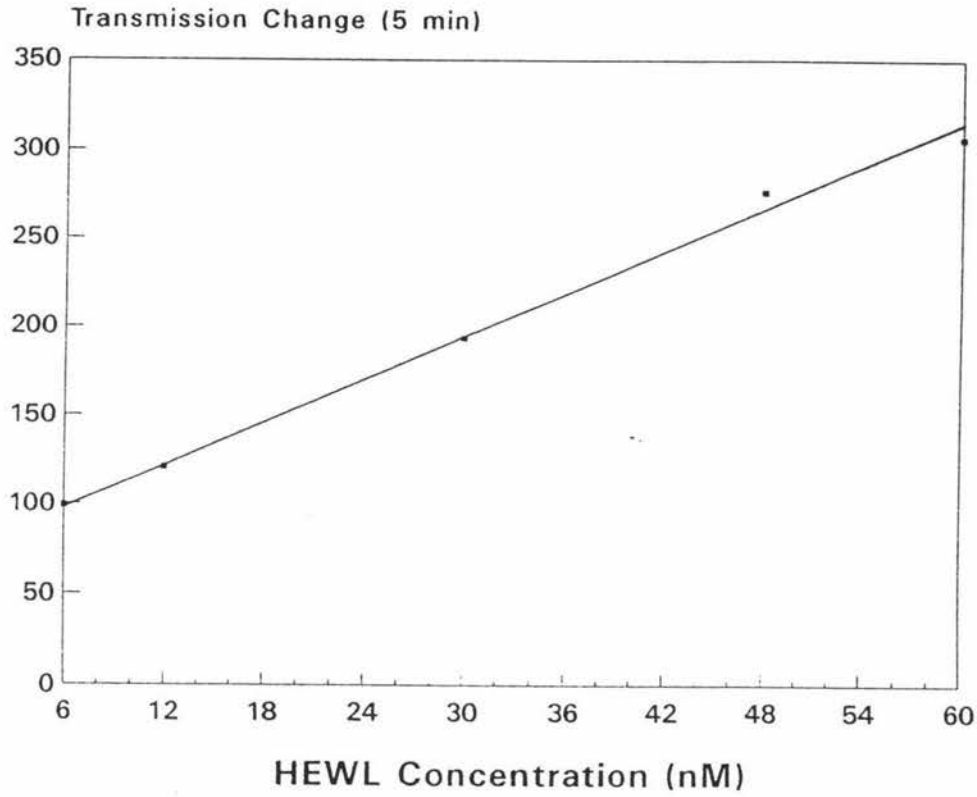

Figure 3.12 *Dependence of Transmission Change in Five Minutes on Hen Egg White Lysozyme Concentration*

The data in the above graph were obtained on the Ovarian Monitor using a concentration of Micrococcus lysodeikticus of 214 mg L^{-1} and a total reaction mixture volume of 350 µl.

the measurement of change in transmission over five (or twenty minutes) gives an accurate measurement of the free enzyme concentration. In the Ovarian Monitor this is related to the concentration of PdG and E1G respectively via a standard curve (see Figures 1.12 and 1.13). However, this does assume that the clearing curves for the native HEWL and the HEWL conjugates are similar.

For studies pertaining to the Ovarian Monitor the starting substrate concentration was chosen so that the initial transmission value was between 200-250, while the maximum

enzyme concentration was chosen so that the maximum ΔT value obtained was always between 300-400 over the time period of interest. Thus, the final transmission value never exceeded a value of 650. This is important as experience with the Ovarian Monitor shows that when the transmission value is less than 200 or exceeds 650 the relationship between transmission change and enzyme concentration becomes uncertain i.e. for the greatest photometric accuracy all recorded transmission values must fall within the range of 200-650 units.

For a lysozyme from a different source, e.g. an egg white lysozyme from a different species of bird, to be effective in reducing the time of the E1G assay by a direct substitution for HEWL, it must generate a clearing curve which is either linear, or gently curved as is the case with HEWL.

The remainder of this section on HEWL considers the ability of different mathematical methods for linearising the HEWL clearing curve. Thus, the same set of data which was used in Figure 3.3 was also used to determine the kinetic order for the rate of clearing by HEWL of a turbid suspension of *M. lysodeikticus*. The second order rate equation found by McKenzie and White (1986) to fit the clearing curve for HEWL with *M. lysodeikticus* in a tris maleate buffer system at 450 nm can not be assumed to apply to data collected at a different wavelength under different conditions. Thus, because the Ovarian Monitor operates at a wavelength of 650 nm, instead of 450 nm, the kinetic order of the clearing reaction at 650 nm in the Ovarian Monitor was verified.

An attempt was made to fit the HEWL clearing curve to zero, first and second order rate equations as described in Section 3.2.4. However, because the rate equations are expressed in terms of absorbance, the transmission data had to first be converted into the corresponding absorbance values (see Equation 3.3, Section 3.2.5).

The fit of the HEWL clearing curve data to a zero order rate equation was particularly poor (see Figure 3.13), fitting for only 0.47 $t_{½}$ lives i.e. 100 seconds ($t_{½}$ = 214 seconds). Thus, under the Ovarian Monitor assay conditions HEWL does not display zero order kinetics for any significant length of time i.e. the rate of clearing is not constant with respect to time. However, it is sufficiently constant to allow an initial rate to be calculated from the data.

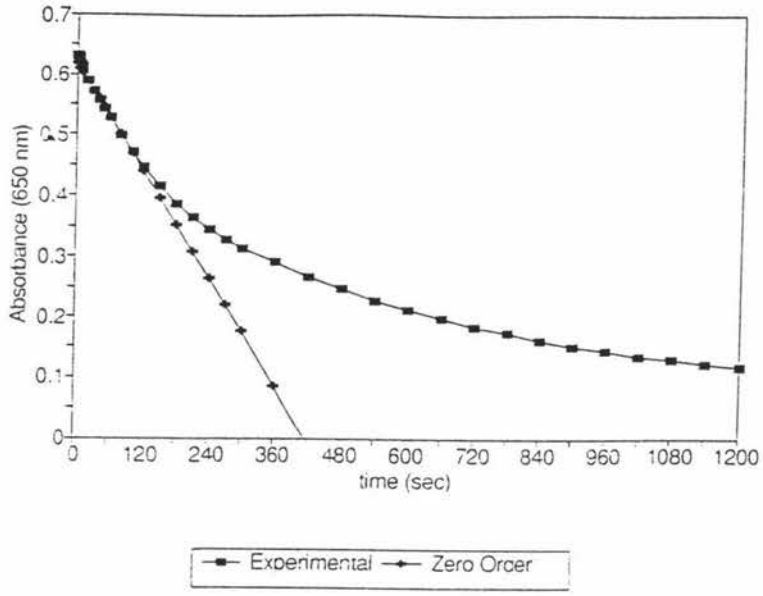

Figure 3.13 *A Twenty Minute Ovarian Monitor Clearing Curve of a Micrococcus lysodeikticus Suspension by Hen Egg White Lysozyme and its Fit to a Zero Order Rate Equation*

The above clearing curve was obtained using a substrate concentration of 214 mg L^{-1} and an enzyme concentration of 24 nM in a total reaction mixture volume of 350 µl.

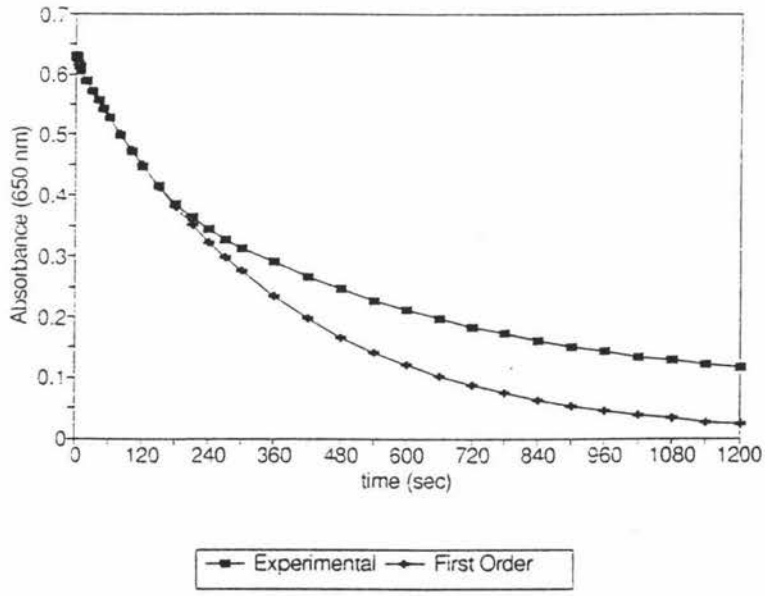

Figure 3.14 *A Twenty Minute Ovarian Monitor Clearing Curve of a Micrococcus lysodeikticus Suspension by Hen Egg White Lysozyme and its Fit to a First Order Rate Equation*

The above clearing curve was obtained using a substrate concentration of 214 mg L^{-1} and an enzyme concentration of 24 nM in a total reaction mixture volume of 350 µl.

Figure 3.14 shows a graph of the change in absorbance obtained with the Ovarian

Monitor along with the theoretical absorbance change calculated for a first order reaction both plotted against time. The experimentally obtained clearing curve resembled first order kinetics for 150 seconds i.e. 0.59 half lives ($t_{½}$ = 253 sec). Although this was significantly longer than its fit to a zero order rate equation, 150 seconds still represents only 12.5% of the twenty minute clearing curve. Thus, the incorporation of a first order kinetic algorithm into the Ovarian Monitor is not a practical means of reducing the enzyme assay time for E1G.

However, in agreement with the findings of McKenzie and White (1986) and Bernath and Vieth (1972) when second order kinetics were used to fit the absorbance clearing curve (see Figure 3.15) the two curves were shown to closely parallel each other. The

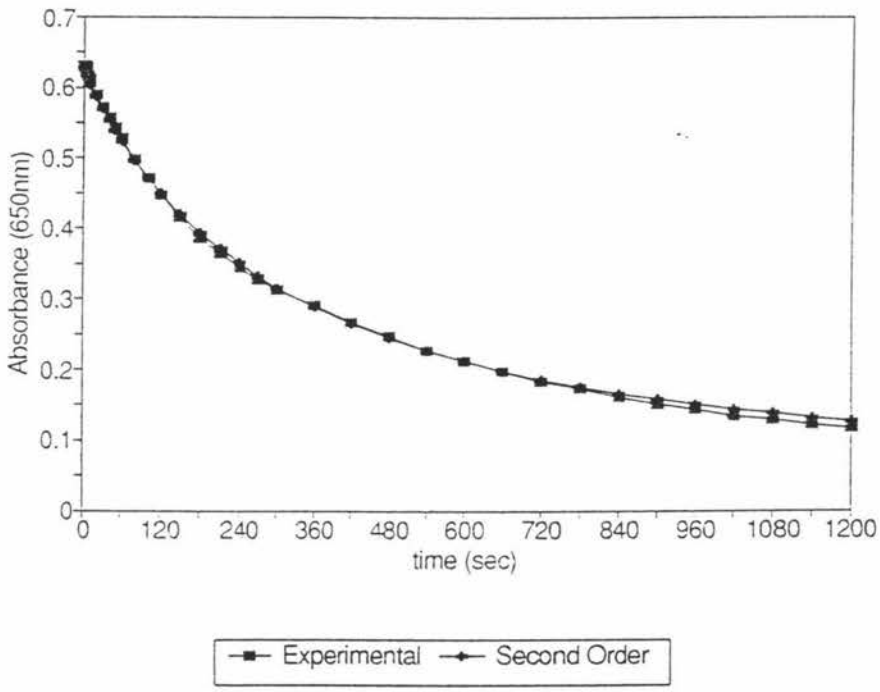

Figure 3.15 *A Twenty Minute Ovarian Monitor Clearing Curve of a Micrococcus lysodeikticus Suspension by Hen Egg White Lysozyme and its Fit to a Second Order Rate Equation*

The above clearing curve was obtained using a substrate concentration of 214 mg L^{-1} and an enzyme concentration of 24 nM in a total reaction mixture volume of 350 µl.

experimentally derived data followed second order kinetics for 720 seconds i.e. 2.4 half lives ($t_{½}$ = 253 sec), with the deviations from second order kinetics beginning only after twelve minutes of the twenty minute clearing curve. Furthermore, at the end of the twenty minutes this deviation was only 0.01 absorbance units from the true second order

clearing curve. Because the HEWL clearing curve so closely obeyed second order kinetics (see Figure 3.15), the initial slope of the second order plot (i.e. A^0_{650}/A^t_{650} versus time) changed linearly with HEWL concentration (see Section 3.3.3.3). Thus, since the observed second order rate constant k'_2, is obtained by dividing the initial slope of the second order fitting by the initial absorbance value (McKenzie & White, 1986), a graph of k'_2 versus HEWL concentration was also linear as predicted by Equation 3.1 (Section 3.2.4). This linearity provided a potential method for reducing the Ovarian Monitor assay time for E1G. This could be achieved by introducing an electronic chip into the Ovarian Monitor which would be capable of linearising the transmission data by first converting it into absorbance values, and then calculating the associated k'_2 values. Because k'_2 and the enzyme concentration are linearly related, a digital display of k'_2 could then be related to the amount of free HEWL-E1G conjugate and thus, form a measure of the amount of urinary E1G in the assay.

3.3.3.2 Goose Egg White Lysozyme

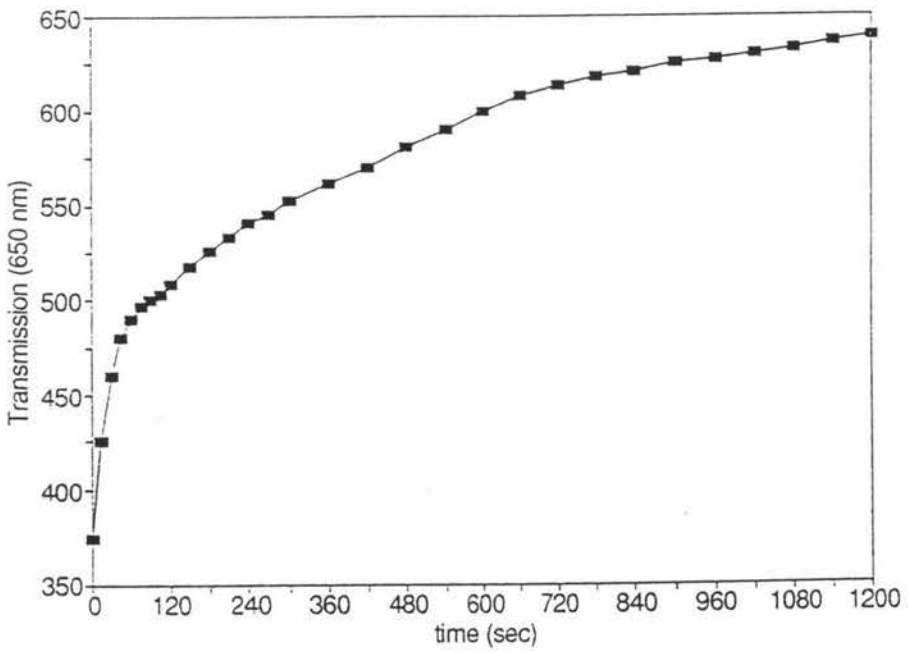

Figure 3.16 *A Twenty Minute Ovarian Monitor Clearing Curve of a Micrococcus lysodeikticus Suspension by Goose Egg White Lysozyme*

The above clearing curve was obtained using a substrate concentration of 21.4 mg L^{-1} and an enzyme concentration of 34.6 nM in a total reaction mixture volume of 350 µl.

Figure 3.16 shows a twenty minute clearing curve obtained on the Ovarian Monitor for

GEWL. This clearing curve was obtained using a concentration of GEWL in the reaction mixture of 34.6 nM which was substantially higher than the concentration of 24 nM of HEWL used to give an acceptable clearing rate in twenty minutes (ΔT=384). However, despite the higher concentration of GEWL relative to the standard concentration of HEWL, the GEWL only managed to generate a change in transmission over twenty minutes of 265 units. Even when the concentration of GEWL in the reaction mixture was doubled to a concentration of 69.1 nM which was approximately three times the standard concentration of HEWL, GEWL only produced a change in transmission in twenty minutes of 292 units. This rather surprising result from an enzyme which is reported in the literature as having an initial rate three times faster than HEWL (Canfield & McMurray, 1967) is the result of the extremely biphasic nature of the GEWL clearing curve. When the $\Delta T(20\ min)^{-1}$ reached approximately 200, the initial fast rate of clearing was replaced by a second phase which had a much slower clearing rate (see Figure 3.16). The same behaviour was observed at different GEWL concentrations with the initial fast rate finishing at roughly the same ΔT value irrespective of the enzyme concentration. This effect was most apparent at enzyme concentrations greater than 3.5 nM because it was only at these concentrations that the twenty minute assay allowed sufficient time for a change in transmission of 150-200 units to be reached early enough for the slow phase to be observed on the twenty minute clearing curve. Thus, at the higher enzyme concentrations when the clearing curve entered the slow phase before twenty minutes had elapsed, the differences in ΔT for the different enzyme concentrations began to decrease. This effect of increasing enzyme concentrations in illustrated clearly in Figure 3.17 which shows a plot of the $\Delta T(20\ min)^{-1}$ over a range of GEWL concentrations. At low concentrations of GEWL the $\Delta T(20\ min)^{-1}$ value increased linearly with increasing enzyme concentrations as required and the clearing rate (as measured by $\Delta T(20\ min)^{-1}$ was indeed greater (14 times from a comparison of the slopes) than for an equivalent amount of HEWL. This rate enhancement was greater than that reported in the literature. However, at the higher enzyme concentrations the clearing curve rapidly entered the slow second phase and further increases in the $\Delta T_{20\ min}$ only occurred very slowly with respect to increasing enzyme concentration. Thus, over the range of high GEWL concentrations there was a levelling out of the plot of $\Delta T(20\ min)^{-1}$ versus enzyme concentration so that it became

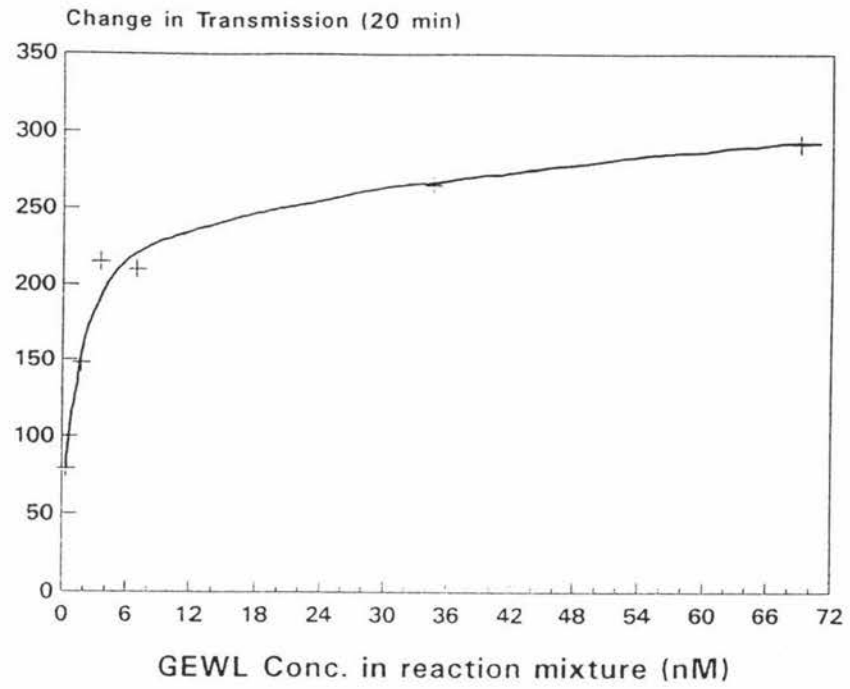

Figure 3.17 *Dependence of Transmission Change in Twenty Minutes on Goose Egg White Lysozyme Concentration*

The data in the above graph was obtained on the Ovarian Monitor using a concentration of Micrococcus lysodeikticus of 214 mg L^{-1} and a total reaction mixture volume of 350 µl.

inferior to the $\Delta T(20\ min)^{-1}$ value for the same concentration of HEWL.

It is this levelling effect that renders GEWL unsatisfactory in an end-point assay in the Ovarian Monitor. Firstly, for the replacement of HEWL by GEWL in the Ovariam Monitor to be viable it must produce a maximum change in transmission of approximately 350 in less than the present twenty minutes. This criterion for a maximum ΔT of 350 or greater is required to maintain assay sensitivity and discrimination between different hormone concentrations. Similarly, for the assay to remain sensitive it is also critical that the concentration of GEWL in the assay is not higher than the level of HEWL currently utilised in the E1G assay. Thus, because it was found that GEWL was clearly incapable of generating a ΔT of greater than 350 in less than twenty minutes with the same level of lysozyme, or less than is, currently utilised in the E1G assay, it was concluded that GEWL could not be utilised as a substitute for HEWL in the E1G end-point assay. Furthermore, as shown in Figure 3.17 the ΔT values experienced at high concentrations of GEWL were not directly

proportional to the enzyme concentration. This factor would also result in a decrease in assay discrimination because the differences in the $\Delta T(20\ min)^{-1}$ are reduced at high concentrations of GEWL. In the E1G assay this would translate into a reduction in ΔT values at high E1G concentrations which would reduce the definition of the E1G peak during a menstrual cycle.

Although GEWL is unsatisfactory as a substitute for E1G using an end-point assay, the GEWL clearing curve was examined further to determine if the E1G assay time could nevertheless be shortened by the application of algorithms to fit the initial part of the GEWL clearing curve. The clearing curve of GEWL, i.e. the decrease in absorbance with respect to time, under Ovarian Monitor conditions was never linear (see Figure 3.18) and thus, as for HEWL could not be fitted to a zero order rate equation, although

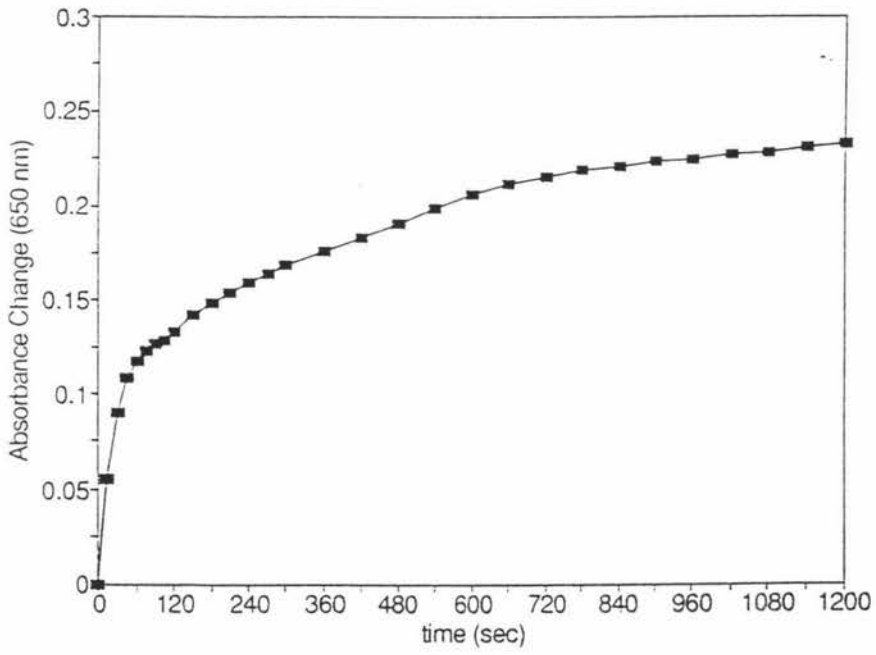

Figure 3.18 *Change in Absorbance over Twenty Minutes of a Suspension of a Micrcoccus lysodeikticus by Goose Egg White Lysozyme*

The data in the above graph were collected in transmission on the Ovarian Monitor and converted into absorbance values using Equation 3.3. It was obtained using a substrate concentration of 214 mg L^{-1} and an enzyme concentration of 34.6 nM in a total reaction mixture volume of 350 µL.

an approximation could be made to yield an initial slope. A similar pattern was also revealed when an attempt was made to fit the clearing curve to a first order rate

equation. Thus, GEWL did not obey first order kinetics either i.e. the decrease in absorbance was not directly proportional to the remaining concentration of substrate. The fitting of the GEWL clearing curve to a second order rate equation was more successful (see Figure 3.19). Although GEWL did obey second order kinetics, the enzyme only followed it for a very short portion of the total clearing curve, with the first phase of the GEWL clearing curve fitting second order kinetics for only 0.47 $t_{½}$ lives i.e. 30 seconds ($t_{½}$ = 64 seconds). However, in spite of the first phase only representing approximately 30 seconds of the twenty minute clearing curve, the change in absorbance experienced over this short initial phase was very large corresponding to 45% on the initial absorbance.

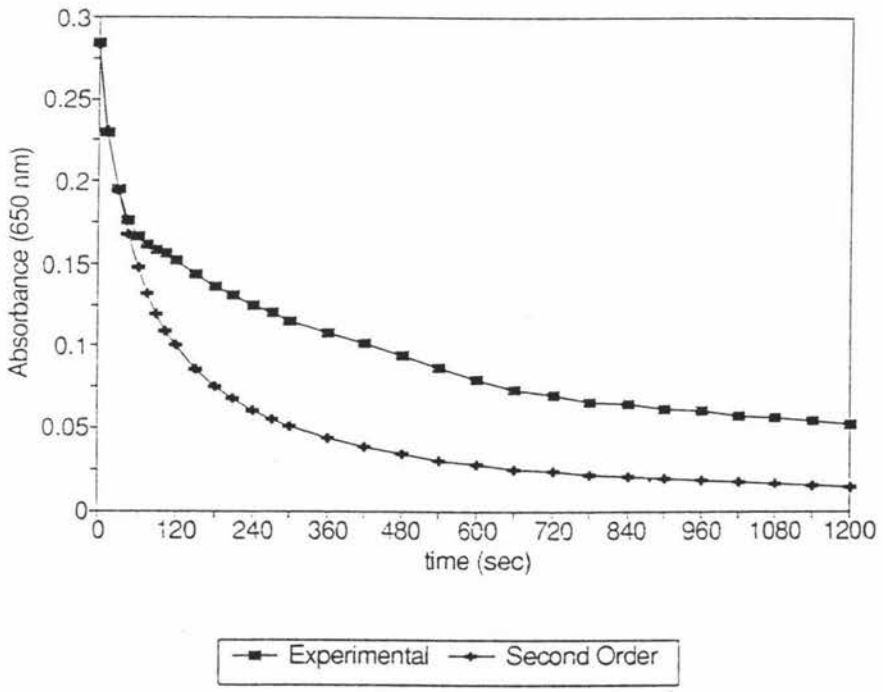

Figure 3.19 *A Twenty Minute Ovarian Monitor Clearing Curve of a Micrococcus lysodeikticus Suspension by Goose Egg White Lysozyme and its Fit to a Second Order Rate Equation*

The data in the above graph were collected in transmission on the Ovarian Monitor and converted into absorbance values using Equation 3.3. It was obtained using a substrate concentration of 214 mg L^{-1} and an enzyme concentration of 34.6 nM in a total reaction mixture volume of 350 µl.

The most successful method for fitting the GEWL clearing curve to a kinetic order appeared to be by fitting both phases of the clearing curve to a second order rate

equation. As can be seen in Figure 3.20 when the GEWL clearing curve was regarded as two second order processes almost all of the curve was successfully fitted. The second phase of the GEWL clearing curve fitted from 45 seconds to the end of the full twenty minute clearing curve and had a $t_{1/2}$ of 294 seconds.

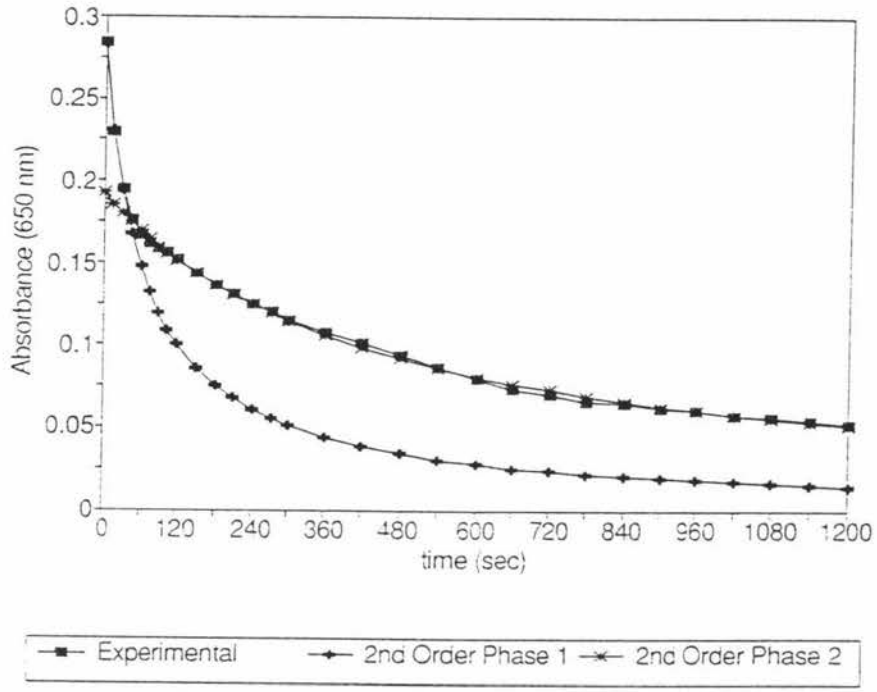

Figure 3.20 *A Twenty Minute Ovarian Monitor Clearing Curve of a Micrococcus lysodeikticus Suspension by Goose Egg White Lysozyme and its Fit to Two Second Order Rate Equations*

The data in the above graph were collected in transmission on the Ovarian Monitor and converted into absorbance values using Equation 3.3. It was obtained using a substrate concentration of 214 mg L^{-1} and an enzyme concentration of 34.6 nM in a total reaction mixture volume of 350 µl.

However, it was not clear whether the clearing process is better represented by two parallel second order processes or two consecutive second order processes. If the former situation was true then the observed second order rate constants for the first phase of clearing should be corrected by subtraction of the contribution of the second phase. This would decrease the values of k'_2 reported but the overall conclusions would remain unchanged. The fact that the plots of k'_2 versus enzyme concentration were linear suggests that the curve may consist rather of two consecutive second order phases in which case no correction is necessary.

As can be seen from Figure 3.20 the two second order processes varied greatly in their rates of clearing. These differences in rates for the two different phases were quantified by comparing the magnitudes of their respective second order rate constants (k'_2) as a function of the enzyme concentration. This relationship was linear over the enzyme concentration range of 0.35-34.57 nM (see Figure 3.21) with the *k*'cat value (slope of the plot) for the first phase having a magnitude 4.8 times the *k*'cat for the second phase.

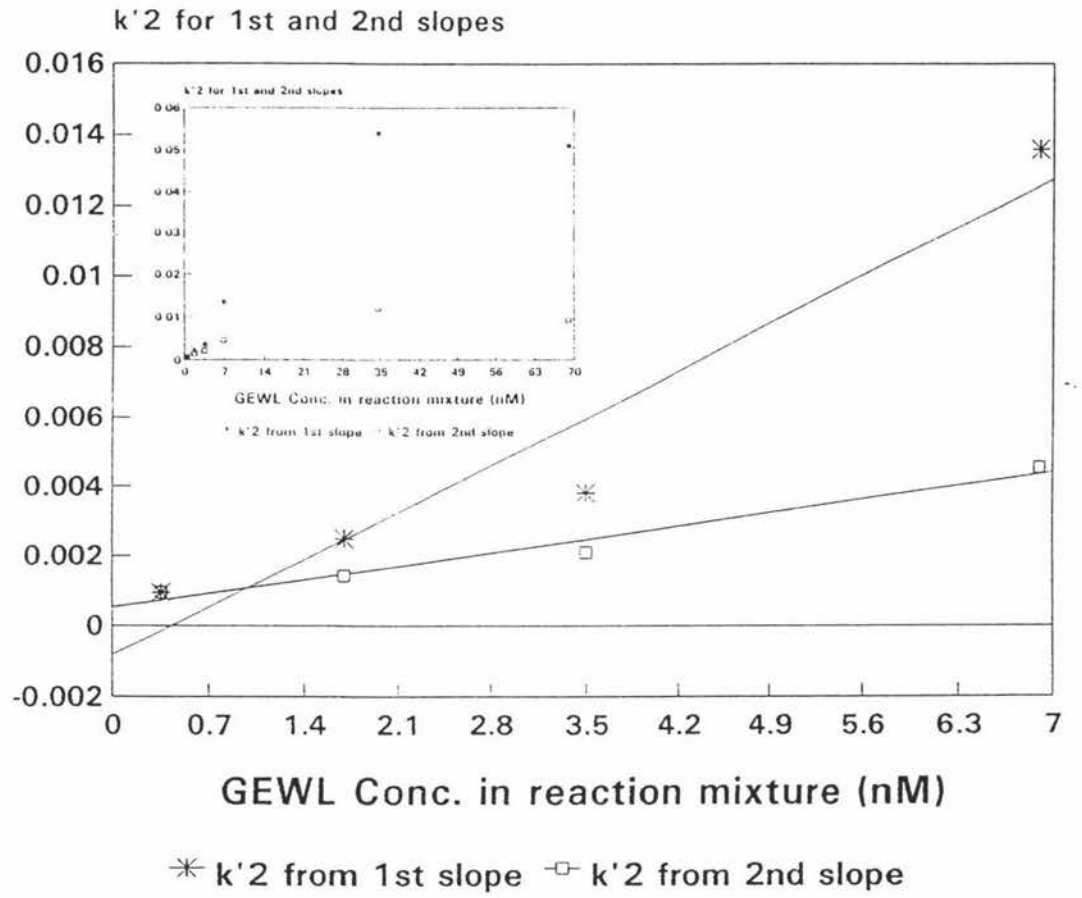

Figure 3.21 *The Dependence of the Observed Second Order Rate Constant for the First and Second Phases of the Goose Egg White Lysozyme Clearing Curve on Enzyme Concentration*

The data in the above graph were collected in transmission on the Ovarian Monitor and converted into absorbance values using Equation 3.3. I Micrococcus lysodeikticus concentration equaled 214 mg L^{-1}, enzyme concentrations equaled 0.35-7 nM and the total reaction mixture volume was 350 µl. The inset shows the same data for enzyme concentrations up to 69 nM.

The reason for the difference in the slopes of the two phases (*k*'cat values) is not clear but will be discussed further in Section 3.3.5. However, because the rates of both

phases were concentration dependent it is theoretically possible to obtain a measure of the amount of GEWL in an enzyme assay by fitting the associated clearing curve to two second order processes. This method as well as being complicated also has the disadvantage that the concentration of GEWL which may be used in the assay is limited. When the concentration of GEWL was increased to 69.1 nM the rate constant for the second phase began to deviate from the line through the other points (see Figure 3.21 inset) and thus, the ratio of the first and second order rate constants began to decrease.

Hence, in conclusion, in spite of the faster initial rate of clearing of GEWL relative to HEWL, the characteristics of its clearing curve make GEWL an unsuitable choice as a replacement for HEWL in the Ovarian Monitor. GEWL could not be utilised in an end-point assay because of the highly biphasic nature of its clearing curve which also made it difficult to fit to a simple kinetic order, while the fitting of its clearing curve to two second order processes although successful, mathematically was considered to be too complicated to be utilised in an algorithm. Furthermore, because of the poor structural similarity between the HEWL and GEWL type lysozymes (Grutter, *et al.*, 1983) the conjugation conditions and purification procedures (Chapter Four) optimised for the conjugation of HEWL (or HEWL-like lysozymes) to E1G do not necessarily apply to GEWL. Similarly, due to the structural variations between the two different families of lysozyme, no attempt could be made to predict the effect the introduction of a GEWL conjugate would have on the standard curve. Thus, neither a conjugation of GEWL to E1G, nor the generation of a GEWL-E1G standard curve was considered profitable because of the unsuitable shape of the GEWL clearing curve.

3.3.3.3 Turkey Egg White Lysozyme

Turkey Egg White Lysozyme (TEWL) was also investigated as a potential lysozyme to replace HEWL in the Ovarian Monitor. However, for convenience most of these assays were performed on a Cecil spectrophotometer, as opposed to the Ovarian Monitor, making the conversion of transmission data into absorbance values for fitting the clearing curves unnecessary. Clearing curves on the Cecil were performed at two different wavelengths; 650 nm, the wavelength used in the Ovarian Monitor, and 450 nm, the wavelength most often reported in the literature as used for studies on lysozyme. Because of the observed absorbance of a suspension of *M. lysodeikticus* cells is not an absorption phenomenon at all, but rather a reflection on the scattering of

incident light by the bacterial cells, the apparent absorbance is very much dependent on wavelength and the geometry of the optics of the spectrophotometer. Due to the different optics of the Cecil at 450 nm compared to the Ovarian Monitor at 650 nm, the initial absorbance of the reaction mixture observed with the Ovarian Monitor was substantially lower than that observed by the Cecil at 450 nm for the same concentration of *M. lysodeikticus*. This difference arises because the *M. lysodeikticus* cell walls scatter light with a short wavelength to a greater extent compared to light with a long wavelength and hence the shorter wavelengths are associated with a higher initial apparent absorbance. In order for the absorbance range experienced for the duration of the clearing curve to remain similar between the different machines (i.e. between 0.3-0.8 absorbance units for greatest photometric accuracy) the concentration of *M. lysodeikticus* in the reaction mixture had to be decreased. Thus, while the concentration of *M. lysodeikticus* of 214 mg L^{-1} in the reaction mixture was standard for use in the Ovarian Monitor this was reduced to a concentration of 113 mg L^{-1} for the work performed on the Cecil. This highlights one of the difficulties in working with lysozyme since even when the clearing curves obtained on the different machines were fitted and a similar value for the initial absorbance was entered into the rate equations the k'_2 values were not strictly comparable since the substrate concentration was different in the two cases. Also, there is the effect of the $[S]/(K_m+[S])$ factor to be considered. However, as discussed in Section 3.3.3 a preliminary screening of the lysozymes can be carried out on different machines using the criteria of i) the shape of clearing curves and ii) the ratio of initial rates measured by ΔT, initial slopes or observed k'_2 values.

For convenience, the concentration of HEWL in the reaction mixture was increased from the 24 nM used in the Ovarian Monitor to 63 nM to enable a similar absorbance change to be obtained on the Cecil in five minutes instead of in the normal E1G assay time of twenty minutes. Thus, at the higher HEWL concentration an absorbance change of approximately 0.38 units in five minutes was obtained on the Cecil spectrophotometer compared with a change in transmission of between 350-400 units on the Ovarian Monitor. The general shape of the clearing curves obtained on the Cecil and the Ovarian Monitor under these two sets of conditions were similar (see Figure 3.22) which justified the different conditions under which the HEWL and TEWL clearing curves were compared.

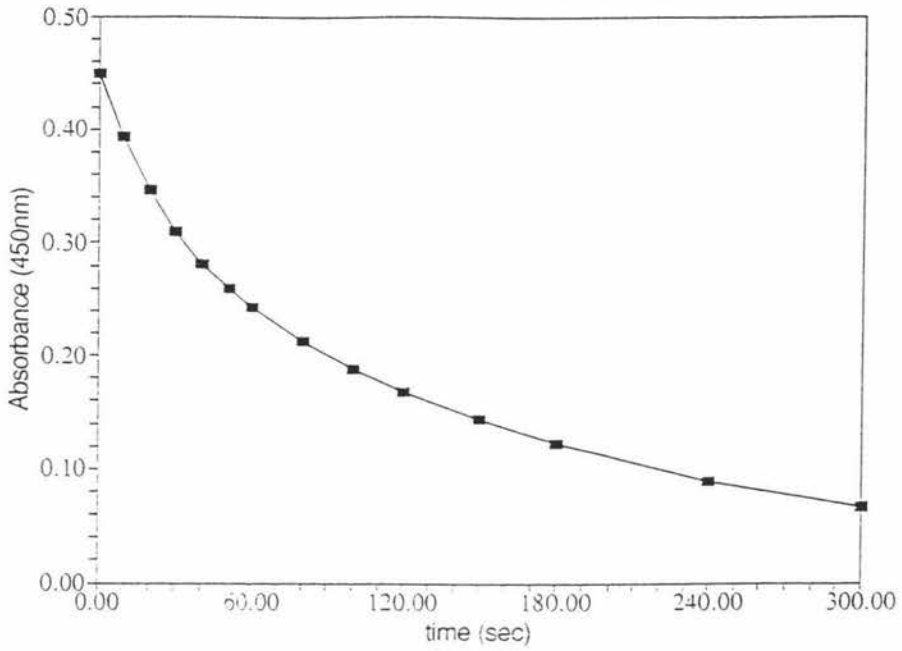

Figure 3.22 *A Five Minute Clearing Curve in Absorbance of a Micrococcus lysodeikticus Suspension by Hen Egg White Lysozyme obtained on the Cecil Spectrophotometer*

The above clearing curve was obtained at a wavelength of 450 nm and at a temperature of 40°C using a substrate concentration of 113 mg L^{-1}, an enzyme concentration of 63 nM and a total reaction mixture volume of 2 mL.

The HEWL clearing curve obtained on the Ovarian Monitor using an enzyme concentration of 24 nM, had a calculated initial absorbance of 0.632 units and an absorbance change in twenty minutes of 0.517 units i.e. there was a decrease from the initial absorbance of approximately 82%. In comparison, the HEWL clearing curve which was obtained on the Cecil spectrophotometer with an enzyme concentration of 63 nM, had an initial absorbance of 0.450 units and an absorbance change in five minutes of 0.38 units, i.e. there was a decrease in absorbance of approximately 85% which was very similar to the value obtained on the Ovarian Monitor data. Thus, from the perspective of an end-point assay these two assay procedures resulted in the generation of similar sets of data.

Furthermore, the two clearing curves obeyed second order kinetics for a similar percentage of their initial absorbance values. More specifically, the clearing curve obtained on the Ovarian Monitor and shown in Figure 3.15 was found to follow second order kinetics until an absorbance value of 71% of the initial absorbance value was

reached, while the HEWL data obtained from the Cecil was found to obey second order kinetics until a value of 62% of the initial absorbance value was reached (see Figure 3.23). Thus, the overall shape of the two clearing curves was similar in absorbance

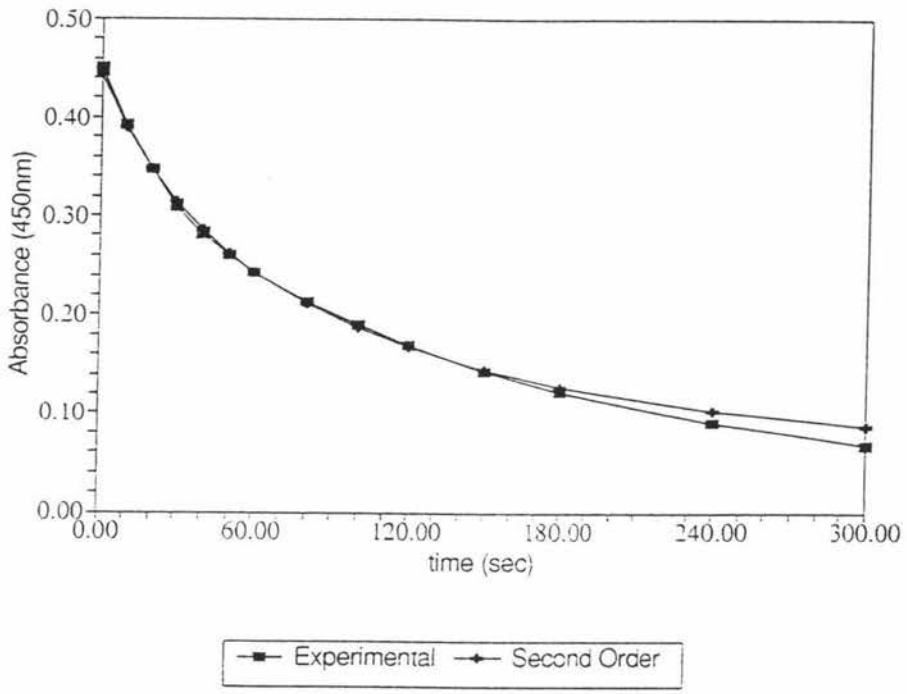

Figure 3.23 *A Five Minute Clearing Curve in Absorbance of a Micrococcus lysodeikticus Suspension by Hen Egg White Lysozyme obtained on the Cecil Spectrophotometer and its fit to a Second Order Rate Equation*

The above clearing curve was obtained at a wavelength of 450 nm and at a temperature of 40°C using a substrate concentration of 113 mg L^{-1}, an enzyme concentration of 63 nM and a total reaction mixture volume of 2 mL.

showing that enzyme concentration, substrate concentration and wavelength did not markedly affect the shape of the clearing curve for HEWL. This method of comparing the second order fits of different clearing curves by expressing the fit as a percentage of the initial absorbance was found to be a useful and simple procedure for the comparison of clearing curves obtained with different parameters or enzymes.

The clearing curves also can be compared on the basis of the number of half lives for which they obeyed second order kinetics. For example, the HEWL clearing curve which was derived from data collected on the Ovarian Monitor had a $t_{1/2}$ of 243 seconds and followed second order kinetics for 2.4 half lives i.e. 720 seconds. This compared

favourably with the HEWL clearing curve obtained on the Cecil spectrophotometer which fitted second order kinetics for 1.76 half lives i.e. 150 seconds ($t_{½}$ = 85 seconds).

The differences observed between the two clearing curves may be the result of there being twice as much substrate in the assays carried out on the Ovarian Monitor. However, in spite of these differences it must be concluded that the general features of the two clearing curves obtained on the different machines were certainly very similar.

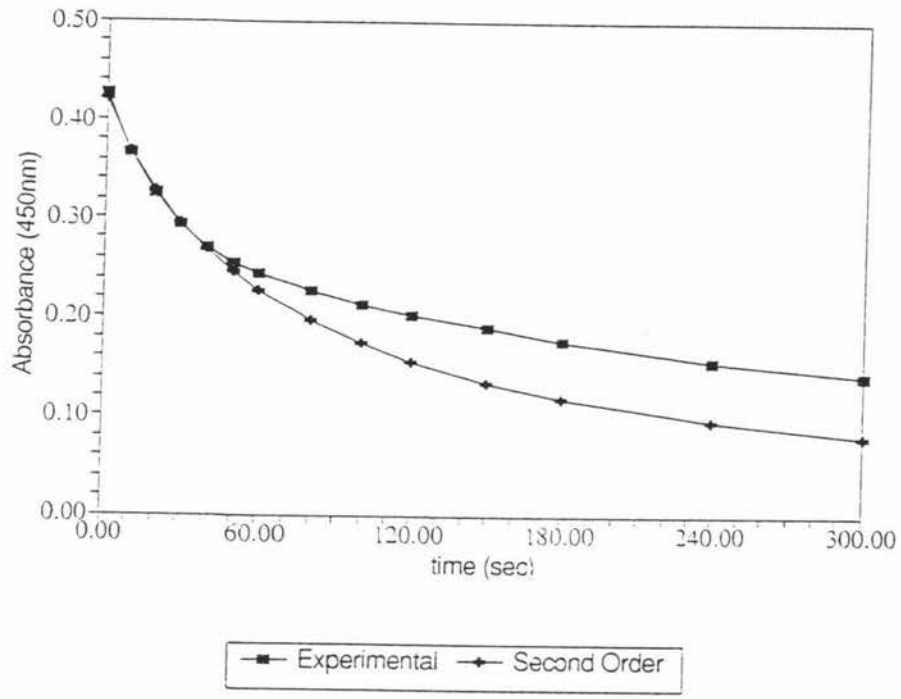

Figure 3.24 *A Five Minute Clearing Curve in Absorbance of a Micrococcus lysodeikticus Suspension by Turkey Egg White Lysozyme obtained in the Cecil Spectrophotometer and its Fit to a Second Order Rate Equation*

The above clearing curve was obtained at a wavelength of 450 nm, and at a temperature of 40°C using a substrate concentration of 113 mg L^{-1}, an enzyme concentration of 63 nM and a total reaction mixture volume of 2 mL.

Figure 3.24 shows that, as found with GEWL, the clearing curve for TEWL was quite biphasic departing from simple second order behaviour after only 40 seconds. The biphasicity of the TEWL affected the clearing curve such that in an end-point assay at the lysozyme concentration of 63 nM, HEWL was clearly superior to TEWL having an absorbance change under these conditions of 0.383 $(5\ min)^{-1}$ compared to TEWL which had an absorbance change of only 0.285 $(5\ min)^{-1}$. Attempts to fit the TEWL clearing

curve obtained on the Cecil to zero order and first order kinetics again failed completely whereas attempts to fit the initial phase of the TEWL clearing curve to a second order rate equation were successful (see Figure 3.24). Under these conditions, TEWL fitted second order kinetics for only 0.57 half lives i.e. 40 seconds ($t_{½}$ = 70 seconds) compared with HEWL which obeyed second order kinetics for 1.76 half lives i.e. 150 seconds ($t_{½}$ = 85 seconds). Thus, on the basis of half lives TEWL was 1.2 times faster than HEWL. However, as found with GEWL an almost perfect fit of the complete TEWL clearing curve was obtained by fitting the two phases of the clearing curve to a second order rate equation (see Figure 3.25). The second phase fitted from 80 seconds to the end of the

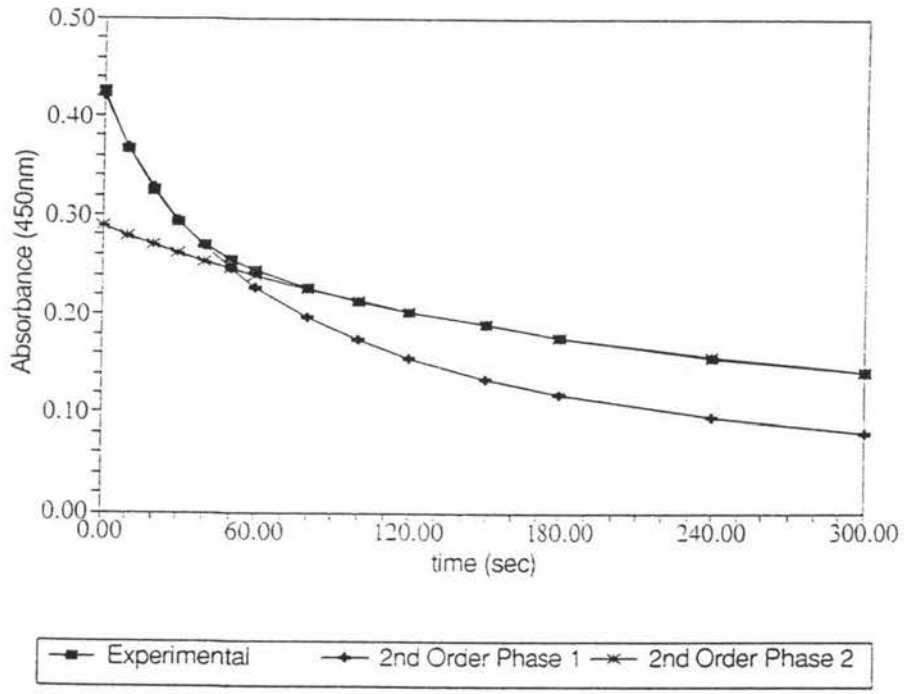

Figure 3.25 *A Five Minute Clearing Curve in Absorbance of a Micrococcus lysodeikticus Suspension by Turkey Egg White Lysozyme obtained in the Cecil Spectrophotometer and its Fit to Two Second Order Rate Equations*

The above clearing curve was obtained at a wavelength of 450 nm, and at a temperature of 40°C using a substrate concentration of 113 mg L^{-1}, an enzyme concentration of 63 nM and a total reaction mixture volume of 2 mL.

full five minute clearing curve and had a $t_{½}$ of 193 seconds, which gives a difference of 2.8 in the relative rates (fast:slow) of the two phases. The change from the first second order process to the second was very abrupt with the change occurring between 40-60 seconds at which time the absorbance was reduced by 38% from the initial value.

Another interesting feature of the fit of the TEWL clearing curve to the second order rate equation compared to HEWL is displayed in Figure 3.26. While the shape of the HEWL clearing curve deviated over time from the second order fit by clearing more quickly than the second order rate equation would predict i.e. HEWL's clearing curve was too linear to be a truly second order reaction, the TEWL clearing curve did the opposite. In other words for TEWL when the absorbance values of the clearing curve began to deviate from the absorbance values predicted by the second order rate equation they did so by changing at a slower rate i.e. the TEWL clearing curve was more biphasic than the second order rate equation predicted.

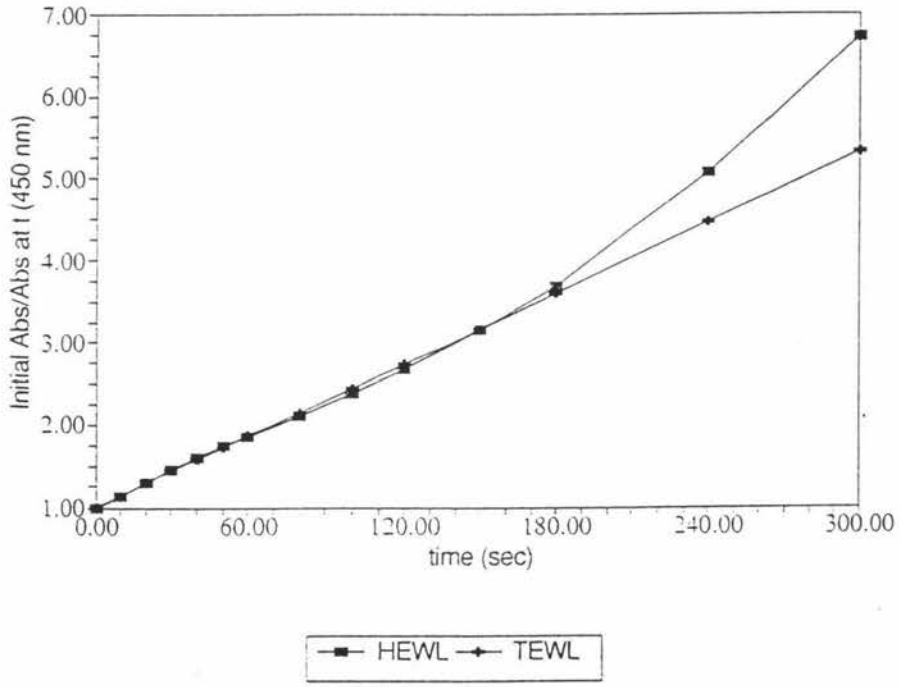

Figure 3.26 *Deviation of Hen Egg White and Turkey Egg White Lysozyme Clearing Curves from Second Order Kinetics*

The clearing curve data with which the above plot was calculated were obtained on a Cecil Spectrophotometer in absorbance at a wavelength of 450 nm at and a temperature of 40°C using a concentration of Micrococcus lysodeikticus of 113 mg L^{-1}, an enzyme concentration of 63 nM and a total reaction mixture volume of 2 mL.

The final comparison of the kinetics of TEWL with HEWL was achieved by an examination of the two enzyme's clearing curves at a range of enzyme concentrations. A summary of these data is given in Figure 3.27 where the second order rate constants are plotted against enzyme concentration for HEWL and TEWL (and HuL). This figure

shows the slope from these two plots to be very similar. Thus, under these assay conditions the inital rates of second order clearing are very similar for the two enzymes and the intrinsic rate constants (or k_{cat} values) for clearing of the initial phase of these two enzymes are essentially identical. However, because the slope of the line for each lysozyme is equal to ($k$cat x [S])/(K_m + [S]) this conclusion is only strictly applicable for this substrate concentration (113 mg L^{-1} of reaction mixture) and the relative rates of clearing of other substrate concentrations requires a knowledge of the K_m values for HEWL and TEWL.

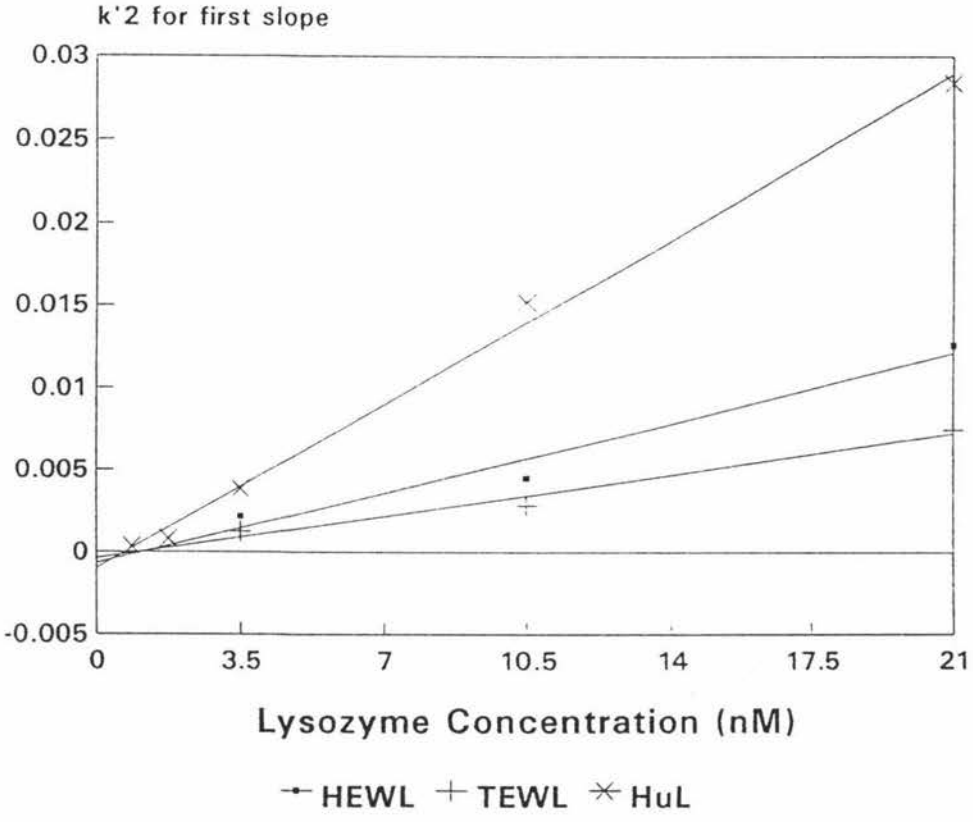

Figure 3.27 *Dependence of the Observed Second Order Rate Constant (k'_2) for Hen Egg White, Turkey Egg White and Human Lysozyme on Enzyme Concentration*

The above rate constants were obtained at a wavelength of 450 nm and at a temperature of 40°C on a Cecil Spectrophotometer using a concentration of Micrococcus lysodeikticus of 113 mg L^{-1} and a total reaction mixture volume of 2 mL.

In conclusion, the results from the above series of experiments on TEWL showed there was no advantage to be gained by substituting TEWL for HEWL in the Ovarian Monitor, and further studies on TEWL were abandoned.

However, the studies on TEWL did help define the two basic criteria required for a potential lysozyme replacement for HEWL in the Ovarian Monitor. Firstly, the prospective enzyme would ideally produce a single phase (i.e. non-biphasic) clearing curve even at relatively high enzyme concentrations. This is necessary so that the range of free lysozyme levels generated by the different urinary concentrations encountered in the assay is clearly defined by changes in the rate of cell lysis. Secondly, for another lysozyme to provide a feasible alternative to HEWL in the Ovarian Monitor, it is also essential for it to possess under standard assay conditions a *k*'cat that is greater than that possessed by HEWL.

3.3.3.4 Human Lysozyme

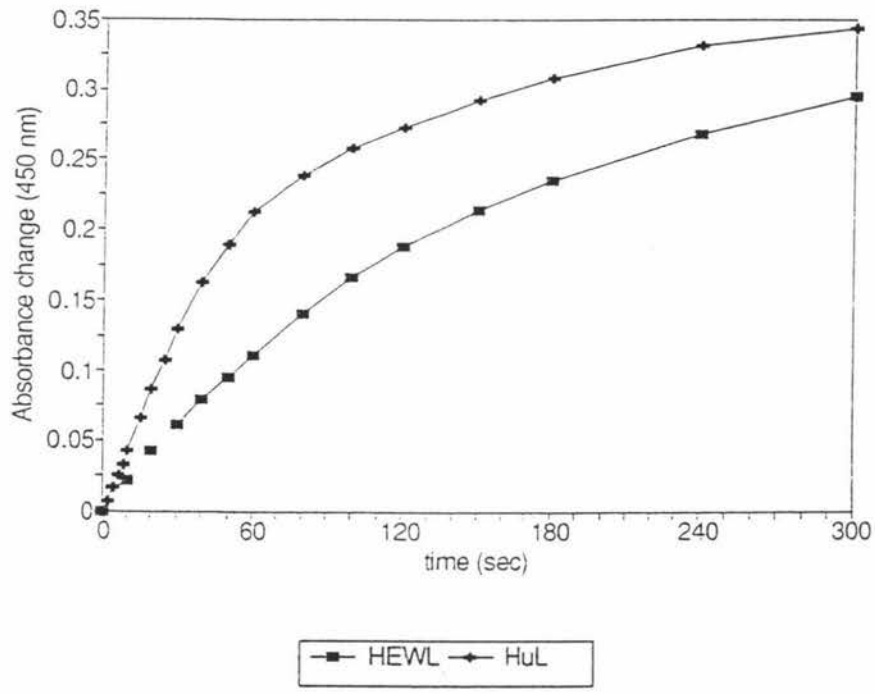

Figure 3.28 *A Five Minute Clearing Curve in Absorbance of a Micrococcus lysodeikticus Suspension by Hen Egg White and Human Lysozyme obtained in the Cecil Spectrophotometer*

The above clearing curve was obtained at a wavelength of 450 nm, and at a temperature of 40°C using a substrate concentration of 113 mg L^{-1}, an enzyme concentration of 21 nM and a total reaction mixture volume of 2 mL.

The human milk lysozyme is reported in the literature (Morsky, 1983) as having an initial clearing rate of 4.4 times faster than that observed for HEWL thus, the clearing

curve for HuL was also examined. All experimental results discussed in this section were obtained using a commercial sample of human milk lysozyme supplied by Sigma. Because the commercial sample gave only one band upon gel electrophoresis when stained with silver nitrate, all kinetic studies were performed directly on the commercial sample i.e. no further purification of the sample was undertaken. Figure 3.28 shows the clearing curve in absorbance at 450 nm obtained with HuL and HEWL over five minutes on the Cecil spectrophotometer using a reaction mixture concentration of *M. lysodeikticus* of 113 mg L^{-1} and enzyme of 21 nM. Clearly, at these concentrations the initial rate of the reaction catalysed by HuL was approximately twice as fast (0.262 ΔAbs min^{-1}) as that observed for HEWL (0.124 ΔAbs min^{-1}). However, it was also unfortunately clearly obvious, as with the other lysozymes examined, that the clearing curve for HuL was biphasic. The HuL clearing curve shown in Figure 3.28 had an initial absorbance of 0.490 units and an absorbance change of 0.344 units in five minutes and thus, had a decrease in absorbance of approximately 70% compared to the value of 66% obtained for HEWL under identical conditions. Thus, although HuL had a faster initial rate than that observed for HEWL at the same enzyme concentration, there was little advantage at the end of five minutes. This means that from the perspective of an end-point assay, compared to HEWL, it is unlikely that the transmission data generated by a HuL-E1G assay would be any more sensitive to differences in urinary hormone concentrations or provide a decrease in assay time.

As was the case with GEWL and TEWL, the most successful duplication of the experimental HuL clearing curve was obtained when each of the two phases were fitted simultaneously to a second order rate equation (see Figure 3.29). The first phase followed second order kinetics for 0.77 half lives i.e. 60 seconds ($t_{½}$ = 77 seconds), while the second phase of the HuL clearing curve followed second order kinetics for x half lives i.e. x seconds ($t_{½}$ = 240 seconds). The degree to which the clearing curve followed second order behaviour can also be expressed in terms of absorbance; the first phase of the HuL clearing curve was found to follow second order kinetics until an absorbance value 57% of the initial absorbance was reached, compared to a value 75% for HEWL and 63% for TEWL. As found for TEWL the deviation of the first phase of the clearing curve from the first second order rate equation was in a negative

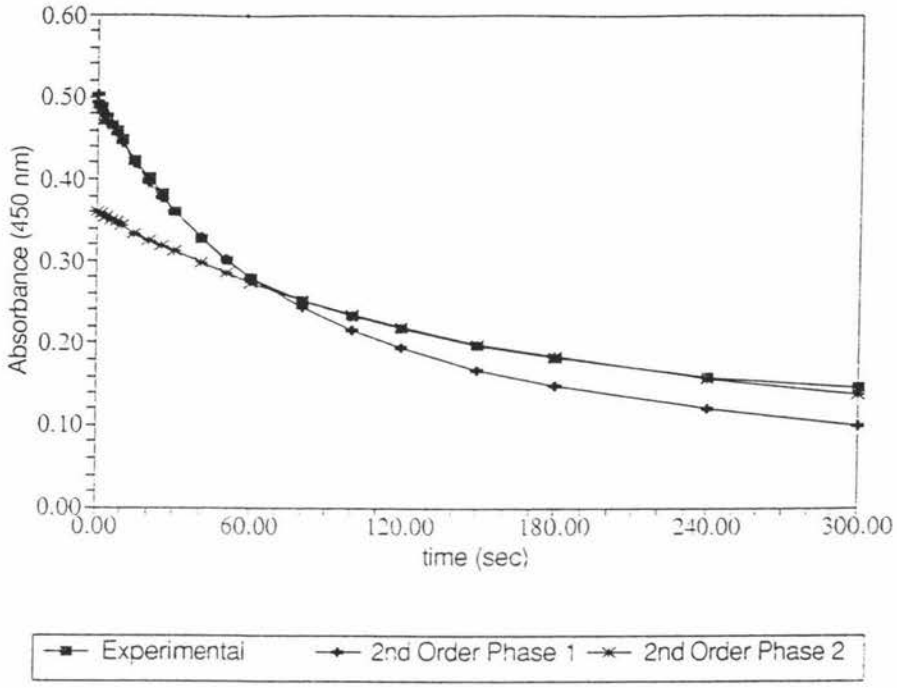

Figure 3.29 *A Five Minute Clearing Curve in Absorbance of a Micrococcus lysodeikticus Suspension by Human Lysozyme obtained in the Cecil Spectrophotometer and its Fit to Two Second Order Rate Equations*

The above clearing curve was obtained at a wavelength of 450 nm, and at a temperature of 40°C using a substrate concentration of 113 mg L^{-1}, an enzyme concentration of 21 nM and a total reaction mixture volume of 2 mL.

direction. In other words when the rate of clearing catalysed by HuL began to deviate from second order kinetics it did so by producing a rate of clearing which was slower than that which would have been found in a truly second order reaction.

The final analysis of the kinetics of the native HuL clearing curve involved a comparison of the *k*'cat values of HuL with HEWL at the substrate concentration of 113 mg L^{-1}. Figure 3.30, a graph of the observed second order rate constants (k'_2) plotted against a range of HuL concentrations, shows that the *k*'cat value (i.e. the slope of the line) began to increase at the higher enzyme concentrations. This was a suprising result, since for a given concentration of substrate the *k*'cat value is expected to be constant.

The *k*'cat value was constant at a value of 0.00140 s^{-1} over the range of 0.3-28 nmoles HuL per litre of reaction mixture, and was 2.3 times higher than the corresponding *k*'cat value of 0.0006 s^{-1} calculated for HEWL and TEWL. This ratio of *k*'cat values is

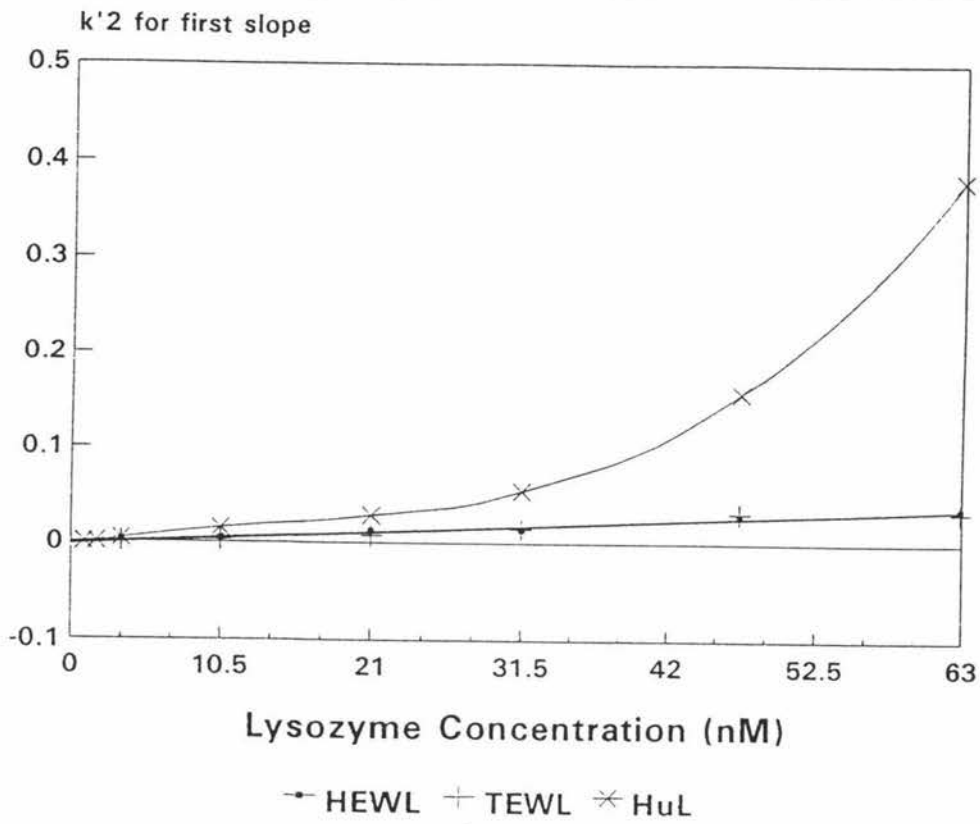

Figure 3.30 *Dependence of the Observed Second Order Rate Constant ($\underline{k}'_2$) for Hen Egg White, Turkey Egg White and Human Lysozyme on Enzyme Concentration*

The above rate constants were obtained at a wavelength of 450 nm and at a temperature of 40°C on a Cecil Spectrophotometer using a concentration of Micrococcus lysodeikticus *of 113 mg L^{-1} and a total reaction mixture volume of 2 mL.*

equivalent to dividing the observed rate constant for a given HuL concentration (within the range of 0.3-28 nM) by the observed rate constant at the same HEWL or TEWL concentration. Thus, because of the difficulty in calculating the *k*'cat value for HuL at the high enzyme concentrations, HuL and HEWL were compared by dividing the observed second order rate constants at high concentrations of HuL by the equivalent observed second order rate constants for HEWL. Using this method the ratios of 3.6, 5.4 and 10.3 were obtained for HuL concentrations of 31.5, 47.2 and 62.9 nM respectively. The explanation for this unusual feature of HuL where the observed second order rate constants do not increase linearly with enzyme concentration is not clear. Such behaviour usually reflects association-dissociation behaviour for multi-subunit enzymes, such as aldehyde dehydrogenase (Blackwell *et al.*, 1987). However, this explanation is not tenable for lysozyme. Although it is well known that HEWL

associates at high concentrations it is difficult to see how this would result in an increased rate of lysis.

Whatever the explanation of this effect it could be utilised to good advantage in a HuL based E1G assay. By electronically equipping the Ovarian Monitor to fit the initial clearing curve to second order kinetics and thus, calculating the observed second order rate constant, a measure of the free enzyme concentration could be obtained. This method has the potential to provide a more sensitve assay than the current HEWL assay because as the free enzyme concentration increases, the observed second order rate constants should increase more rapidly than the enzyme concentration. In terms of the standard curve this means that the portion of the curve covering the high analyte concentrations would become expanded increasing the apparent difference in rates between low and high levels of free enzyme. This would have the effect of allowing greater discrimination between high levels of free E1G thus, making the profile of menstrual cycle data more defined. For these reasons HuL is considered as a possible candidate for substitution into the Ovarian Monitor.

3.3.3.5 T4 Lysozyme

From the perspective of trying to decrease the E1G assay time on the Ovarian Monitor, the studies performed on the kinetics of T4 lysozyme (T4L) were disappointing. Although the usual substrate for T4L is the bacterium *Escherichia coli* (*E. coli*) and not the *M. lysodeikticus* bacterium used for the other lysozymes examined, the kinetics of T4L were examined using *M. lysodeikticus* as a substrate. This was because the bacterium *E. coli* is a potential pathogen and thus, cannot be utilised in any assay designed for home use. Although T4L is reported in the literature (Tsugita *et al.*, 1968) as having an initial rate 250 times greater than HEWL when *E. coli* is utilised as a substrate, when *M. lysodeikticus* is utilised as a substrate, T4L still has a relative initial rate 6.3 times greater than that observed with the same molar amount of HEWL. Thus, on the basis of this reported initial rate for T4L with the substrate *M. lysodeikticus*, T4L was examined as another potential enzyme by which the E1G twenty minute enzyme assay could be reduced.

Unlike the other lysozymes all the kinetic studies on T4L were performed on a Cary

spectrophotometer as opposed to the Cecil. The major factor involved in the transfer of the kinetic studies from the Cecil onto the Cary was based on the Cary's facility for recording and storing the clearing curve data points. This was a real advantage, as it avoided the laborious manual collection of data points which had been necessary with the computer fitting of the clearing curves obtained with the Cecil. Preliminary work on the Cary showed the optics to closely parallel those found in the Ovarian Monitor thus, making the Cary an ideal model by which potential new Ovarian Monitor protocols based on absorbance could be examined. The chief disadvantage found with the Cary was its long delay time (approximately three seconds) from the initiation of the run to the beginning of data collection. This was especially found to be a problem with T4L which had an exceptionally fast and rapidly changing initial rate (see Figure 3.31 for

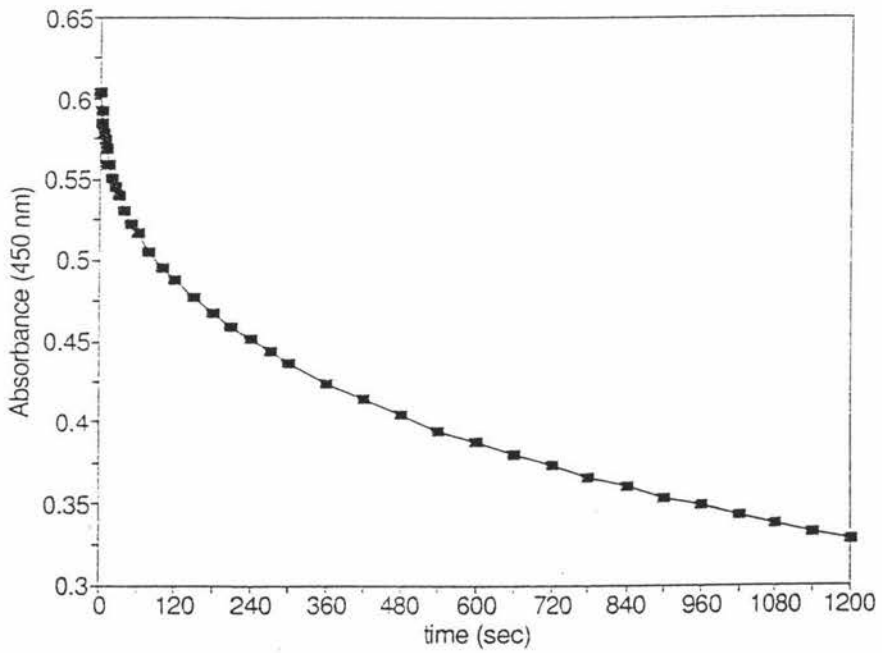

Figure 3.31 *A Twenty Minute Clearing Curve in Absorbance of a Micrococcus lysodeikticus Suspension by T4 Lysozyme obtained in the Cary Spectrophotometer*

The above clearing curve was obtained at a wavelength of 450 nm, and at a temperature of 40°C using a substrate concentration of 113 mg L^{-1}, an enzyme concentration of 7 nM and a total reaction mixture volume of 2 mL.

T4L clearing curve). The multiphasic T4L clearing curve displayed in Figure 3.31 was obtained using a concentration of T4L in the reaction mixture of 7 nM and was associated with an initial rate of 0.190 ΔAbs min^{-1} and a change in absorbance in twenty minutes of 0.275 units. In terms of initial rate T4L was approximately 7 times faster

than the same molar concentration of HEWL which only had an initial rate of 0.0285 ΔAbs units min^{-1} in agreement with the literature (Tsugita, *et al.*, 1968). However, in terms of a twenty minute end-point assay the total absorbance change for T4L of 0.0275 units was very low compared to that observed for HEWL which had an absorbance change in twenty minutes of 0.342 units (see Figure 3.32). Thus, despite the fast initial

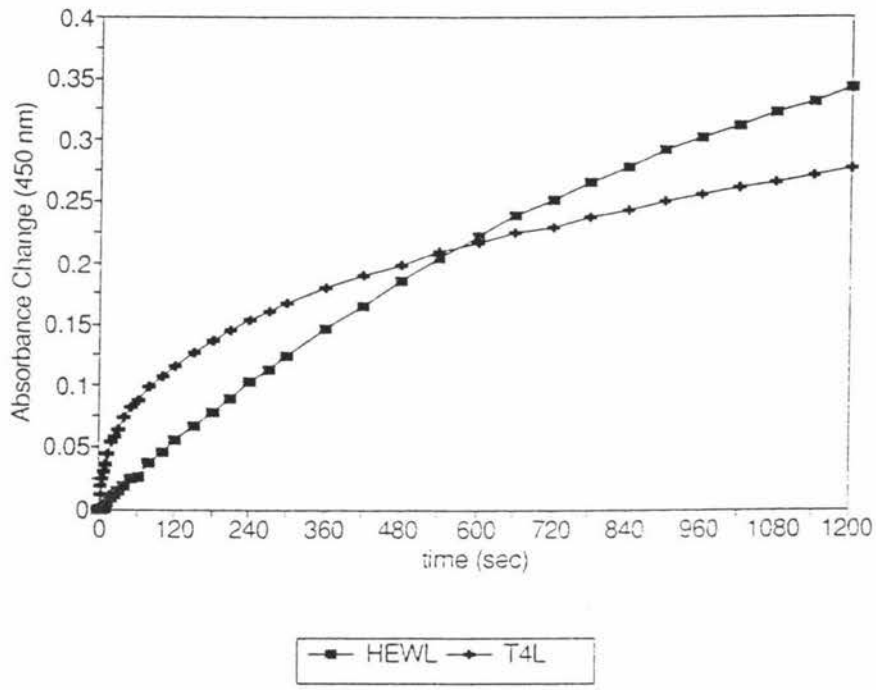

Figure 3.32 *Change in Absorbance in Twenty Minutes of a Micrococcus lysodeikticus Suspension by T4 Lysozyme and Hen Egg White Lysozyme obtained in the Cary Spectrophotometer*

The clearing curve data with which the above plot was calculated was obtained at a wavelength of 450 nm, and at a temperature of 40°C using a substrate concentration of 113 mg L^{-1}, an enzyme concentration of 7 nM and a total reaction mixture volume of 2 mL.

rate, T4L failed to generate an advantage in absorbance in twenty minutes. At five minutes T4L did give a larger absorbance change than TEWL at the same time interval but the value (0.15) was only about 50% of the change caused by HEWL in twenty minutes. Consequently T4L was not a suitable candidate for substitution into the current end-point assay of the Ovarian Monitor. Furthermore, it could not be utilised as an initial rate assay because not only was the initial fast phase very short, but the initial rate never appeared to be constant making any proposed assay method which required a measurement of the initial rate critically dependent upon the time data collection

commenced. The multiphasic nature of the curve also made it difficult to fit to a simple kinetic order, with the clearing curve failing completely to fit to zero, first and second order rate equations. The poor fit of the clearing curve to a second order rate equation is illustrated in Figure 3.33 which shows the graph of the second order rate equation

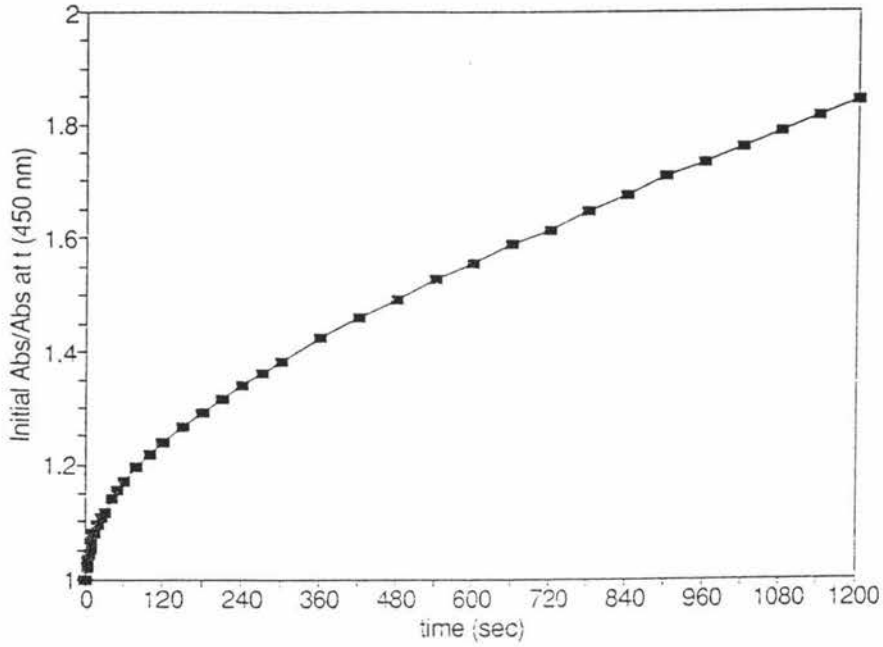

Figure 3.33 Deviation of T4 Lysozyme Clearing Curve from Second Order Kinetics

The clearing curve data with which the above plot was calculated were obtained on a Cary Spectrophotometer in absorbance at a wavelength of 450 nm at and a temperature of 40°C using a concentration of Micrococcus lysodeikticus of 113 mg L^{-1}, an enzyme concentration of 7 nM and a total reaction mixture volume of 2 mL.

plotted against time is never linear i.e. the T4L does not follow a second order rate of clearing for any proportion of the curve. Thus, in the light of these results T4L was not a viable alternative to HEWL for use in the Ovarian Monitor.

3.3.4 MICHAELIS MENTEN PARAMETERS

Because the Michaelis Menten Constant (K_m) is a kinetic parameter which is expressed in terms of substrate concentration (e.g. *M. lysodeikticus* cells in the case of lysozyme) and it has been observed that the sensitivity of the commercial preparations of *M. lysodeikticus* cell walls to lysis has increased over the years (see Section 3.1.2.5), it follows that the values reported for K_m in the literature for any given species of lysozyme will vary depending on the batch of *M. lysodeikticus* used by the researcher.

Furthermore, there are no reports in the literature of the V_{max} and K_m values obtained under the same conditions (i.e. within the one publication) for all the species of lysozyme examined in this thesis. Thus, to enable the different species of lysozyme to be directly compared under the same set of conditions (e.g. substrate with the same sensitivity), it was necessary for their kinetic parameters K_m and V_{max} to be recalculated. Because T4L was found never to obey second order kinetics (see Section 3.3.3.5), the K_m for T4L could not be measured in terms of the the second order fit. Thus, for convenience the Michaelis Menten Constants for the different enzymes were all

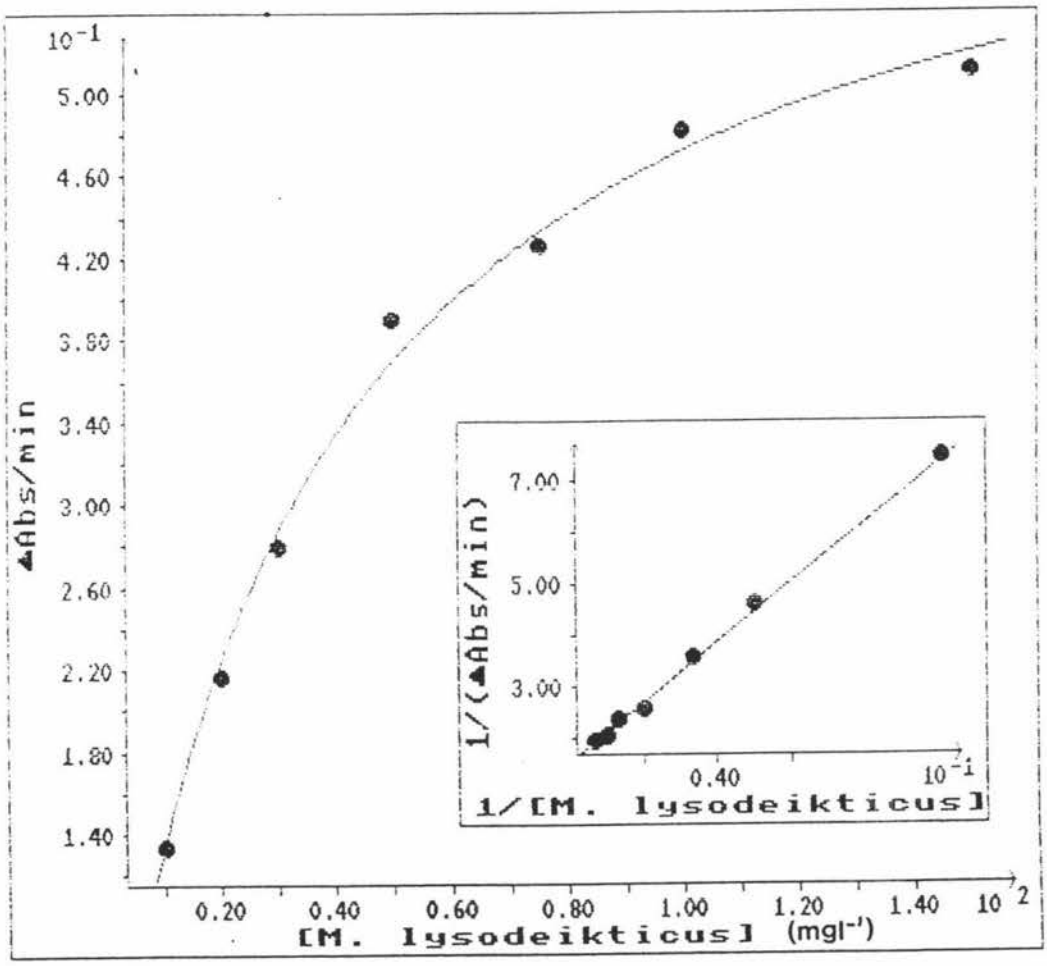

Figure 3.34 *Michaelis Menten Plot for Hen Egg White Lysozyme obtained on the Cary Spectrophotometer using Initial Rate Data*

The initial rate data with which the above plot was calculated were obtained in absorbance at a wavelength of 450 nm and at a temperature of 40°C using an enzyme concentration of 70 nM, a range of concentrations of Micrococcus lysodeikticus of 100-1500 mg L^{-1} and a total reaction mixture volume of 2 mL.

calculated from initial rate data as opposed to the second order kinetic data. An

example of the fitting of the initial rate data to the Michaelis Menten equation (Equation 3.5, Section 3.2.6) is given in Figure 3.34 for HEWL at an enzyme concentration of 70 nM. Figure 3.35 shows an example of how the rate was observed to decrease at the

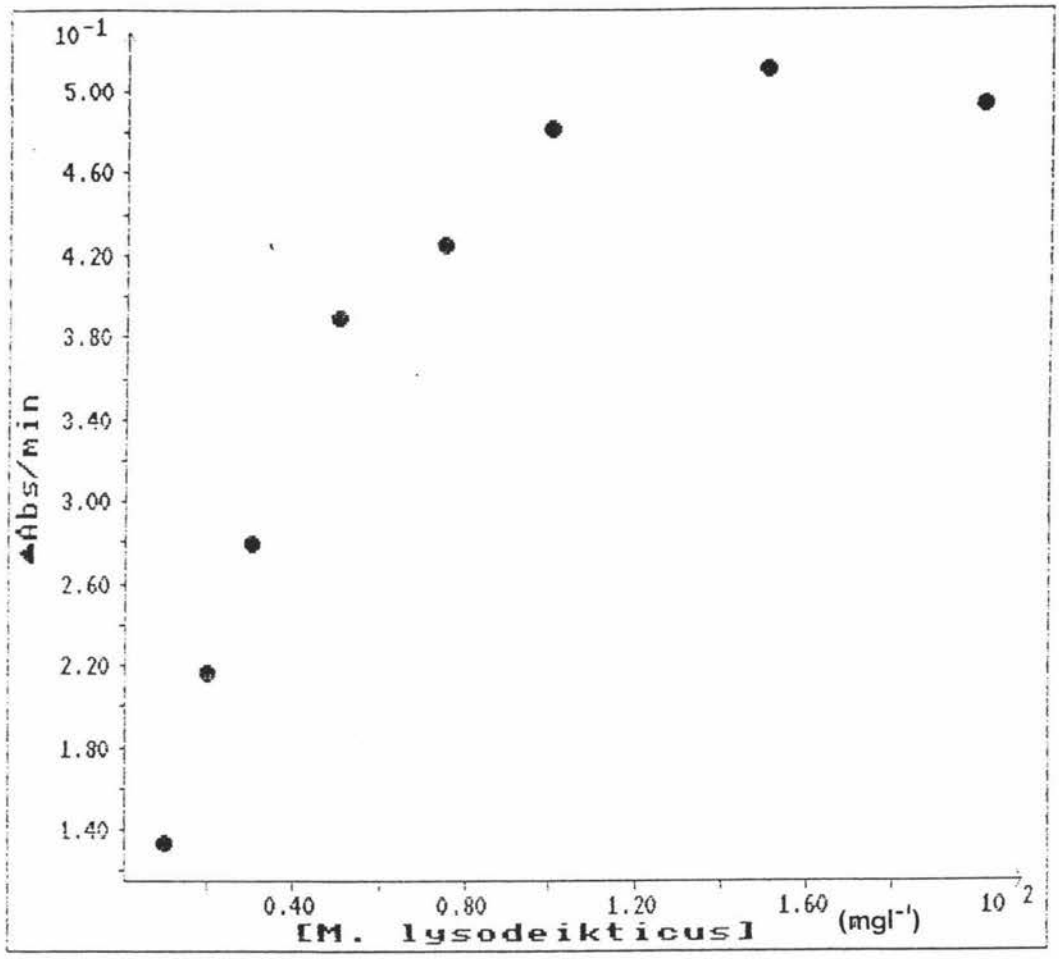

Figure 3.35 *Michaelis Menten Plot for Hen Egg White Lysozyme obtained on the Cary Spectrophotometer using Initial Rate Data showing the Initial Rate to Decrease with Substrate Concentration at Very High Substrate Concentrations*

The initial rate data with which the above plot was calculated were obtained in absorbance at a wavelength of 450 nm and at a temperature of 40°C using an enzyme concentration of 70 nM, a range of concentrations of Micrococcus lysodeikticus of 100-2000 mg L^{-1} and a total reaction mixture volume of 2 mL.

highest substrate concentrations. This effect was observed with all the different lysozymes examined and at all enzyme concentrations examined. Figure 3.34 shows the Michaelis Menten Plot after the removal of the highest substrate concentration value so that the programme ENZFITTER could be used to calculate the K_m and V_{max}, i.e. the Michaelis Menten parameters were calculated only for the range of substrate

concentrations where the initial rate was still observed to be increasing with an increase in substrate concentration.

A summary of the results obtained for the various lysozymes and for HEWL at several enzyme concentrations is shown in Table 3.6.

Table 3.6 *Michaelis Menten Parameters obtained for a Variety of Lysozymes and Several Hen Egg White Lysozyme Concentrations*

Lysozyme	Concentration (nM)	K_m (mg L^{-1})	V_{max} (450 nm) (ΔAbs min^{-1})
TEWL	35	71±12.0	0.59±0.049
HuL	7	39±4.0	0.20±0.090
T4L	7	112±10.1	0.35±0.067
HEWL	7	15±3.3	0.06±0.003
HEWL	35	29±1.6	0.33±0.075
HEWL	70	38±3.4	0.65±0.021
HEWL	105	40±6.9	0.95±0.064

Table 3.6 shows that the range of K_m values (15-112 mg L^{-1}) obtained in this work for a variety of lysozyme species is lower than that obtained by Locquet *et al.* (1968) whom also calculated the K_m for lysoyzme from a variety of sources (range 100-400 mg L^{-1}). Although these two sets of values for K_m are different, the range of values reported in Table 3.6 does encompass the relatively recently obtained K_m value of 67 mg L^{-1} reported by Muraki *et al.* (1987) for HuL (enzyme concentration 69 nM). Because the set of high K_m values were obtained in the late sixties, these results are consistent with the observation that the susceptibility of the commercially obtained *M. lsodeikticus* cells to lysis has increased over the years.

The K_m values for TEWL, HuL and HEWL are the same order of magnitude, hence the

conclusions drawn at a single substrate concentration regarding the relative rates of lysis will remain valid at the higher concentrations used in the Ovarian Monitor. T4L is an exception as the K_m values obtained for T4L and HEWL at equivalent molar concentrations are one order of magnitude different making the relative rates of lysis dependent on the substrate concentration used during the measurements. However, the conclusions drawn from the data obtained on the Cecil spectrophotometer are still valid since the saturation effect will increase the advantage of T4L with respect to the initial rates of lysis. The curvature of the T4L clearing curve still renders this enzyme unsuitable for use in Ovarian Monitor assays.

The K_m values for HEWL are such that at the *M. lysodeikticus* concentration of 214 mg L^{-1} used in the Ovarian Monitor the lysis reaction is proceeding near its V_{max} value. Thus, the assay is not very sensitive to small variations in the initial substrate concentration as sometimes occurs with the assay tubes prepared for home use. That is, the same rate is obtained even if the initial transmission values vary. The same situation is likely to apply for HEWL, but TEWL and T4L would require a much stricter control of the initial substrate concentration if reproducible data were to be achieved in the home assay since the initial lysis rates are on the near linear part of the Michaelis Menten curve. This factor also helps eliminate T4L and TEWL from consideration as possible lysozymes for use in the Ovarian Monitor.

The surprising result from Table 3.6 is that the HEWL data shows that the apparent K_m value increased with increasing enzyme concentration. This is in contradiction to one of the basic tenets of enzyme kinetics; that the K_m value is independent of enzyme concentration. This expectation is of course based on the assumption that the clearing reaction involves a 1:1 enzyme:*M. lysodeikticus* complex. From the point of view of the enzyme and its chemical reaction (e.g. hydrolysis of the NAM-NAG polymer) the basic tenets do apply if each site on the *M. lysodeikticus* cell wall is kinetically equivalent. In this case the hydrolysis kinetics can be represented by Scheme 3.2:

$$E + S \underset{k_{-1}}{\overset{k_1}{\rightleftharpoons}} ES \xrightarrow{k_2} EP \xrightarrow{k_3} E + P$$

Scheme 3.2 *Mechanism for Enzyme Catalysis*

This reaction will show simple saturation kinetics with a unique enzyme concentration independent K_m value. Thus, if the kinetic measurement is the rate of production of reducing sugars no anomalies would be expected.

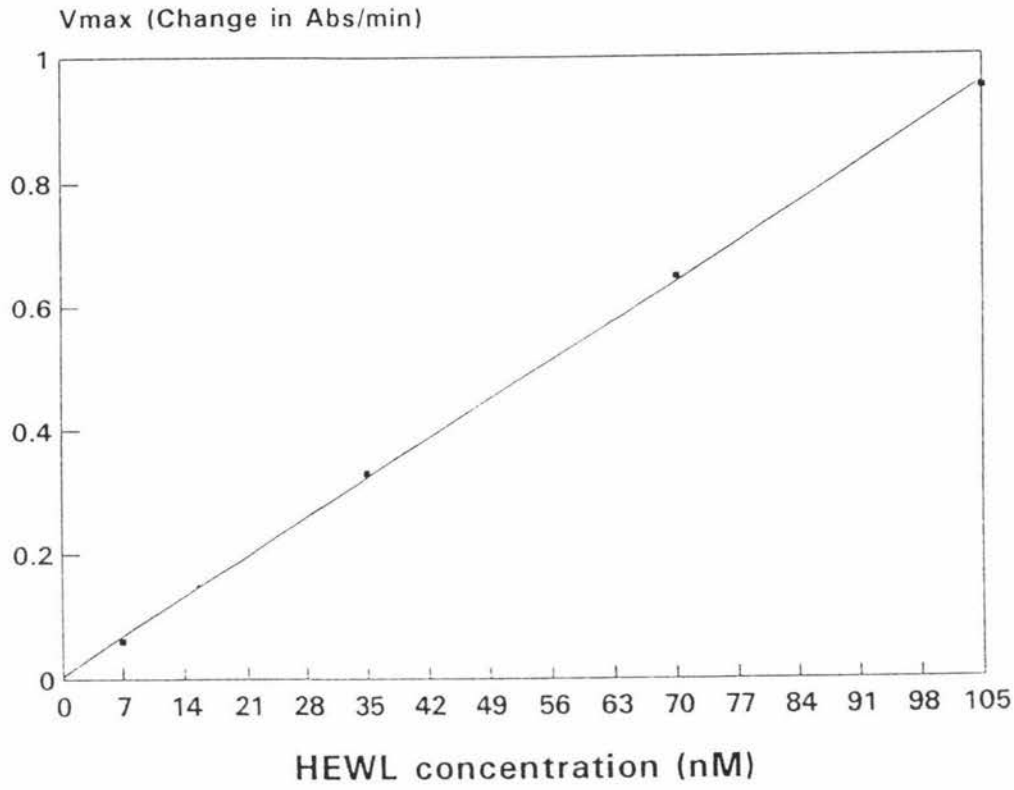

Figure 3.36 The Dependence of V_{max} on HEWL Concentration

The initial rates with which the above data were calculated were obtained in absorbance at a wavelength of 450 nm and at a temperature of 40°C using a range of Micrococcus lysodeikticus concentrations from 100-2000 mg L^{-1} and a total reaction mixture volume of 2 mL.

Despite the behaviour of the K_m values there was a good linear correlation between V_{max} and the enzyme concentration for HEWL (Figure 3.36) even though the data were obtained on different days with different *M. lysodeikticus* suspensions. Although it is clearly the case, it is not immediately obvious on theoretical grounds for the lysozyme - *M. lysodeikticus* system that the relationship should be linear. The substrate molecule possesses a large number of cleavage sites for lysozyme and presumably there is an optimum value for the number of sites which must be cleaved for the maximum rate of lysis. This would be expected to depend on the ratio of the total enzyme concentration

to the total substrate concentration. The situation is complicated further by the fact that lysis may occur as a result of n lysozyme molecules being bound per cell or by one molecule of lysozyme binding n times to the same cell. Also there may be any number of intermediate situations between one and n enzyme molecules bound per cell.

Clearly, the rate of lysis will be faster the larger n is but there may be a limit beyond which any increase in the number of enzyme molecues bound per cell has no further effect on the rate of lysis. This situation would be equivalent to the formation of a dead-end complex in that enzyme molecules would be bound to the cell wall but would not be contributing to the rate of lysis. Addition of extra substrate at this point might further increase the rate since the amount of lytically ineffective lysozyme would be reduced.

The fact that V_{max} was linear with respect to the total enzyme concentration and also that V_{max} was obtained at a higher substrate concentration (S) as the total enzyme concentration (E_o) increased seems to imply that there must be an optimum E_o/S ratio and that V_{max} is obtained when the substrate concentration is sufficiently high that i) all the available enzyme is bound (mass action effect) and ii) the maximum concentration of cells with the optimum number of enzyme molecules per cell is reached. Some support for this suggestion comes from the observation that as the substrate concentration was increased eventually the initial rates began to decline (see Figure 3.35) consistent with the view that n was decreasing. The apparent increase in the K_m value with an increase in the total enzyme concentration probably finds its explanation in the same effect.

The conformity to the Michaelis Menten behaviour may be artefactual in the sense that the apparent hyperbolic relationship is the net result of two essentially oppposite effects. As discussed above an increase in the substrate concentration should increase the total amount of bound enzyme by the mass action effect. However, at the same time there will be a tendency for the number of bound enzyme molecules per cell to decrease as the substrate concentration is increased. Thus, it is entirely reasonable to suggest that a substrate concentration will be reached for each enzyme concentration beyond which further increases are associated with a decrease in the rate of lysis and that this optimum substrate concentration might increase as the enzyme concentration increases. Hence

the apparent K_m value will also increase since this is just the substrate concentration which gives half the maximal rate. In essence this explanation rests on the assumption that under the conditions of V_{max}-K_m determinations there is a substrate concentration region in which some of the enzyme is bound but is ineffective in promoting lysis since the total number of enzyme molecules bound per cell exceeds n.

If this is so then as the substrate concentration increases the concentration of SEn species will increase and so will the rate. However, as the enzyme concentration increases, this will only continue until a higher level of substrate concentration is reached at which point the number of lysozyme molecules per cell becomes less than n and the rate of lysis declines. Whatever the true explanation of these results they have important practical consequences for the lysozyme assay as discussed above and from literature comparisons where the concentration of lysozyme is not controlled.

The different K_m values for the different enzymes can be understood on this basis if the optimum number of enzyme molecules per cell is effectively less for the more active enzymes. This could be a result of more rapid cycling for the more active enzymes at high substrate concentrations hence as the substrate concentration increases further during the K_m determination, the rate of lysis will continue to increase to higher levels of substrate concentrations than for HEWL since less lysozyme molecules per cell are required to give V_{max} and the apparent K_m value will therefore appear to be greater.

3.3.5 ELECTROSTATIC FIELDS AND SECOND ORDER BEHAVIOUR OF CLEARING CURVES

Although the catalytic mechanism for lysozyme outlined in Section 3.1.2.4 is well established, it fails to explain the differences in the clearing curves and initial rates observed with the different enzymes. In particular it fails to explain not only why the initial rate of clearing of a *M. lysodeikticus* suspension varies greatly between the different lysozymes, but also why the lysoyzme species which exhibit the higher relative initial rates were also observed to generate clearing curves with a higher degree of biphasicity. With respect to the clearing curves obtained with the different lysozymes throughout the course of this work this was not a casual observation i.e. the order of increasing relative initial rates of the four different species of lysozyme examined in this

thesis was in strict accordance to the order of the increasing degree of biphasicity observed with the different lysozyme clearing curves. The order was as follows: HEWL, TEWL, HuL, and T4L where T4L was the lysozyme species which exhibited the highest relative initial rate and a higher degree of curvature in the overall shape of its clearing curve. On a more practical level based on the nature of these results it appears highly unlikely that the present twenty minute E1G assay time could be reduced by the simple substitution of the HEWL-E1G conjugate for a different E1G lysozyme conjugate and still measure the rate utilising an end-point assay.

Because the above series of results were all obtained using the same substrate, i.e. lyophilised *M. lysodeikticus* cells, the cause of the differences in the kinetic characteristics of the different lysozyme species must reside in the structure of the lysozyme molecule itself. However, because all evidence on the mechanism of catalysis indicates that the mechanism is the same for all the different species of lysozyme so far investigated (e.g. aspartic and glutamic acid are always the key catalytic residues) it is unlikely that the actual catalytic reaction *per se* is responsible either. Thus, it appears that the underlying cause of the different clearing curves must reside in some more general structural property or characteristic of the different lysozyme species (Jolles & Jolles, 1984).

A more general structural property of lysozyme which is known to vary between the different species is the electrostatic fields associated with the active cleft and the two lobes which the active cleft divides the enzyme molecule into. More specifically the different lysozyme species vary in the magnitude of the electrostatic fields associated with the two sides of the active site cleft and the surrounding two lobes. Since the atomic co-ordinates of the enzymes HEWL, TEWL, HuL and T4L are stored in a protein data bank the calculation of the four enzymes respective electrostatic fields is a relatively simple operation with the aid of a Silicon Graphics System. Figure 3.37 show the electrostatic fields associated with HEWL, TEWL, HuL and T4L respectively obtained from a Silicon Graphics System using the Delphi module. All positive fields are coloured in blue and negative fields in orange. Thus, from these figures it can clearly be seen that all four lysozymes possess a positively and a negatively charged lobe and that a large potential difference exists between the two. Despite the similarity

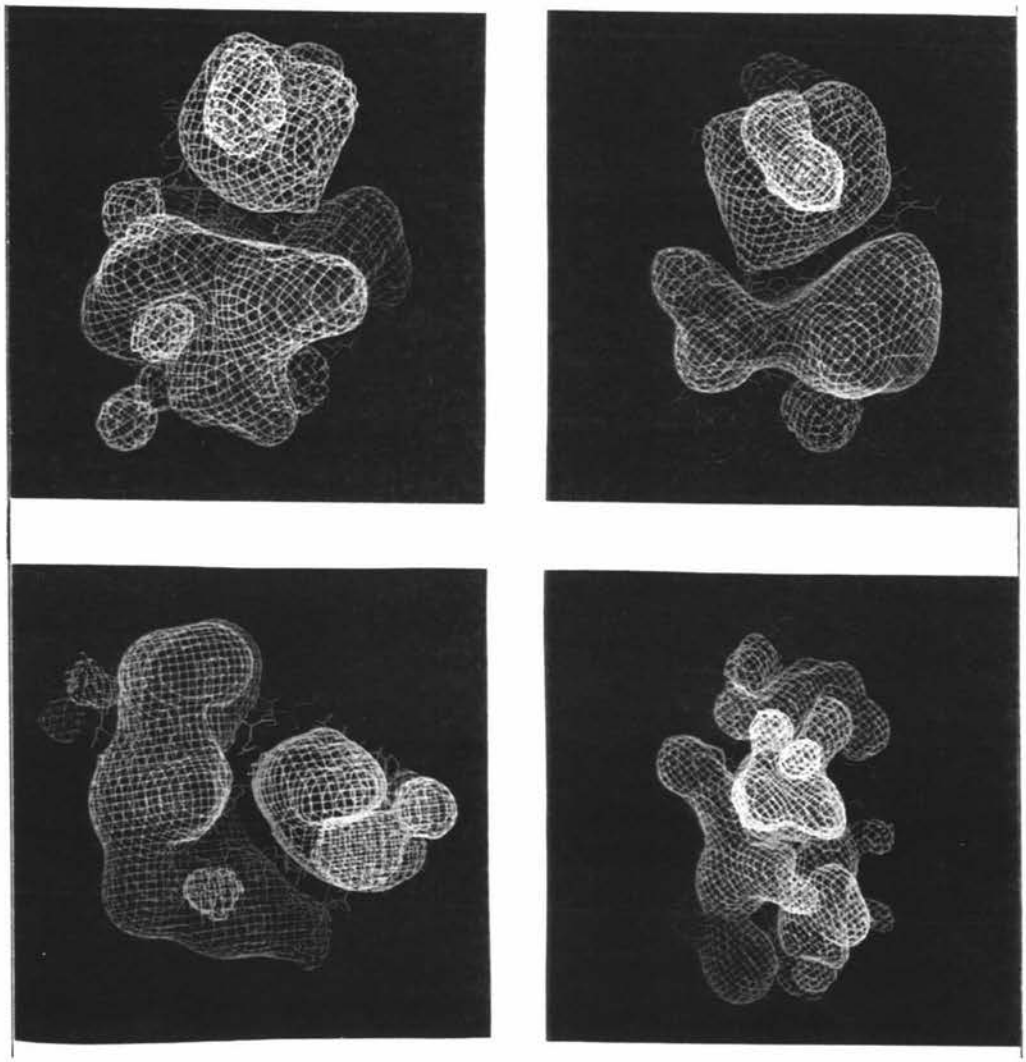

Figure 3.37 *The Electrostatic Potential for a) Hen Egg White Lysozyme (top left), b) Turkey Egg White Lysozyme (top right), c) Human Lysozyme (bottom left) and d) T4 Lysozyme (bottom right) Contoured at +2 kT (blue) and -2 kT (orange) Calculated by the Klapper Algorithm*

Conditions: ionic strength 0.15 M, di-electric constant (ε) = 2. The contours represent equi-potential energy surfaces for a hypothetical test charge. Bound solvent molecules were removed from the models and Glu-35 (or Glu-11 for T4L) was assumed electrically neutral. All other appropriate side chains, including histidine and the N and C termini, were assumed to be fully charged. All lysozyme molecules are arranged so that the active site cleft is on the right hand side.

of the three dimensional structures for HEWL, TEWL and HuL there are marked

differences in the appearances of the electrostatic fields which are sequence dependant.

However, it is not just lysozyme which possesses an electrostatic field as the cell wall of *M. lysodeikticus* has also been shown to be associated with an electrostatic field, except unlike lysozyme, its net charge is negative with the cell having an overall charge of -1.5 μCoulombs cm^{-2} for the pH range 4-8 (Price & Pethig, 1986). Apart from measuring the overall charge of the wall of a *M. lysodeikticus* cell, Price and Pethig have shown by a series of experiments, in which the ionic strength of the reaction mixture was varied, that the rate of clearing of a *M. lysodeikticus* suspension by HEWL is effected by the overall cell wall charge, and have already proposed that an electrostatic attraction between HEWL and the cell wall is an important determinant of lytic activity by HEWL. Although this series of experiments only proved that the lysis rate of *M. lysodeikticus* by HEWL was effected by the ionic strength of the reaction mixture, the results do suggest that the different kinetic characteristics of the clearing curves obtained with the various lysozymes could be due to differences in the various enzymes electrostatic fields.

This has led to the proposal of a tentative model based on electrostatic fields to explain the different kinetic characteristics observed in this work for the various lyosyzme species. For example, it is possible that the positive electrostatic field on lysozyme would attract the negatively charged *M. lysodeikticus* cell wall to the enzyme and may even help align the NAM-NAG polymer into the correct orientation for binding. The proposal that electrostatic fields may help orientate the cell wall for binding is supported by the finding that the site of cleavage is always adjacent to a negative charge on the cell wall (Price and Pethig, 1986). Furthermore the electrostatic fields may enhance the rate of catalysis as well by providing a potential gradient between the two lobes thus, facilitating the mechanism (see Scheme 3.1) whereby the proton of the catalytic glutamic acid residue is donated to the glycosidic oxygen atom on the D ring. Hence, if this proposed mechanism was correct, species of lysozyme which possess a large potential gradient between the two lobes would perform this proton transfer more rapidly and would have a greater intrinsic rate of cleavage than a lysoyzme species associated with a smaller potential gradient across its two lobes. This proposal of the importance of electrostatic fields in determining the rate of lysis is supported by the work of Dao-pin

et al. (1989) who concluded that the electrostatic interactions between lysozyme and the *M. lysodeikticus* cell wall may play a more important role in the enzymatic mechanism than has generally been appreciated and calculated that the rate enhancement due to the electrostatic fields was probably greater than 9 kcal mol^{-1}. More importantly Dao-pin *et al.* measured the potential difference across the two lobes, i.e. across the active site cleft; for HEWL, HuL and T4L and obtained the following results: HuL $3.9x10^{-6}$ Volts cm^{-1}, HEWL $5.4x10^{-6}$ Volts cm^{-1}, and T4L $13.7x10^{-6}$ Volts cm^{-1}. Thus, although the conclusion of Dao-pin *et al.* was that the electrostatic fields of lysozyme did greatly enhance the rate of catalysis, their values calculated for the electrostatic potential across the cleft for the various lysozymes did not correlate with the relative initial rates observed in this work. In other words the order of increasing relative initial rates and potential differences for the different enzymes were not the same suggesting that it was not the potential gradient across the cleft which was the chief determinant of initial rates for lysozyme. However, the initial rates for the different species of lysozyme do increase in the same order as the total charge on the lysozyme molecule as calculated using the Delphi module i.e. the total charge on the lysozyme molecule was in the order T4 > HuL > TEWL > HEWL. If this is also the order of charge on the positive lobe then it may be that it is the electrostatic field on the positive lobe as opposed to the potential difference across the active site cleft which is the most important factor in determining initial rates. If this was in fact true, then it may be that the positive lobe acts to increase the rate of lysis by stabilising the glu-35 residue after it donates the proton as opposed to enhancing the catalytic reaction by facilitating the transfer of the proton itself.

Although a large charge on the positive lobe would aid the binding of the *M. lysodeikticus* cell wall to the active site and thus, aid catalysis by the same process it could also inhibit the turnover number by remaining tightly bound to the positive lobe after cleavage of the glycosidic bond. However, when the substrate concentration is high this effect would probably be fairly limited due to competition by other *M. lysodeikticus* cells weakening the electrostatic attrac ion. Thus, there are two conceivable effects the encounter of an enzyme-cell wall complex with another cell wall would have; either the presence of the second negative field would result in a direct

transfer of the bound lysozyme molecule to the second cell wall or alternatively it may promote the lysozyme molecule to release its current substrate and thus, itself into the bulk solution ready for another round of catalysis. Because the second order rate equation is mathematically derived from a two substrate model this mechanism of binding involving two substrates could account for the second order kinetic behaviour of the clearing curves. This model is very similar to the model proposed by Bernath and Vieth (1972) who examined the effect of non-ionic detergent micelles on HEWL activity and proposed the following model (Scheme 3.3):

$$E + S \rightleftharpoons C_1$$

$$C_1 + S \rightleftharpoons C_2$$

$$C_2 \rightarrow P + E$$

Scheme 3.3 Bernath and Veith Model for Second Order Kinetic Behaviour of Lysozyme

in which a substrate molecule is an "energy furnishing" collision partner to the enzyme substrate complex.

The above mechanism successfully explains why the enzyme species with the most highly charged positive lobe would be associated with the fastest initial rates. This is because the most highly charged lysozyme molecules would not only be most effective in binding lysozyme but in sustaining the rate of catalysis by being displaced at high substrate concentrations by another *M. lysodeikticus* cell wall. However, as the concentration of substrate decreases with the continuing removal of substrate by lysis of the *M. lysodeikticus* cell walls, although the binding of lysozyme to a cell wall would remain as tight as ever, the competition for the bound lysozyme would decrease and thus the rate of release of the bound lysozyme from the lysed cells would become the new rate limiting step as opposed to the rate of catalysis itself. Thus, from this it follows that the lysozyme species with the most highly charged positive lobes would be the ones which are associated with the highest initial rates and greatest degree of curvature in their clearing curves. This is in full accordance with the results presented in this work. Furthermore, because bound lysozyme would always require the presence of a second negatively charged electrostatic field i.e. a *M. lysodeikticus* cell, the second phase of

clearing would also be second order as was observed for GEWL, HuL and TEWL. The poor fit of the T4L data to a kinetic order could also be explained by the above model in that the T4L had by far the greatest total charge and as such the substrate concentration was never high enough for it not to be rate limiting. Not only was the T4L reaction so fast that it was difficult to record the initial rates (especially with the time delay in the Cary), an increase in substrate concentration to a level where it would not be limiting would not have been feasible as it would have made the initial absorbance so high that a change in absorbance could not be easily measured by the spectrophotometer.

The direct correlation between the electrostatic fields and the degree of curvature of the clearing curve is further supported by studies where synthetic substrates, such as p-nitrophenyl-penta-N-acetyl-ß-chitopentoaside, which do not possess an electrostatic field do not generate a clearing curve but rather exhibit a zero order rate of clearing (Nanjo et al., 1988). Whatever the explanation of these results may be, it is clear that electrostatic fields of enzymes play an important role in their function.

3.4 CONCLUSION

From the point of view of decreasing the assay time for the E1G assay these results are disappointing. Any factor which increases the initial rate of lysis also causes the clearing curve to be markedly biphasic, thus rendering other lysozymes unsuitable for an end-point assay. Although it is tempting to think of mutating HEWL (e.g. by replacing trp 62 for tyrosine (Kumagai *et al.*, 1987)) to improve its rate of lysis without affecting the shape of its clearing curve this hope in not borne out by other site-directed mutagenesis studies (Kumagai and Miura, 1989). Thus, there does not seem to be any possibility of using another lysozyme to give a shorter assay time for E1G using an end-point assay. The work described in this chapter suggests that the single amino acid substitutions which have been carried out (see for example, Kumagi *et al.*, 1987) should be examined in terms of the effects on the electrostatic fields. This should prove to be a fertile ground for further study and understanding of the kinetics and mechanism of the lysozyme- *M. lysodeikticus* system.

Despite the fact that a suitable lysozyme could not be found for a direct substitution in

an end-point assay, HuL appears to offer an opportunity for decreasing the assay time. Incorporation of a suitable algorithm into a redesigned Ovarian Monitor to calculate the initial slope (or k_2') would decrease the assay time and may well lead to a more discriminating standard curve, given the increase in rate at high HuL concentrations seen in Figure 3.28. However, this effect would depend on the actual assay conditions and the concentration range for any E1G-HuL conjugate assay system. Before such an analysis can begin to be explored it is first necessary to develop appropriate protein chemistry and protein purification procedures. This is the topic of discussion in Chapter Four.

CHAPTER FOUR

SYNTHESIS OF ESTRONE GLUCURONIDE CONJUGATES OF LYSOZYME

4.1 INTRODUCTION

The work in Chapter Three involved an examination of the kinetics of native lysozymes from various sources with their bacterial substrate *Micrococcus lysodeikticus* (*M. lysodeikticus*). It was concluded that the Ovarian Monitor assay for E1G could not be reduced to a five minute test simply by substituting the HEWL conjugate for a human lysozyme (HuL) conjugate using the current end-point assay (see Section 3.3.4). Instead, the most feasible procedure for reducing the total E1G assay time appeared to be by, either designing a HuL initial rate assay, or a method to linearise the HuL clearing curve by fitting it to a second order rate equation. However, it has been the experience of Melbourne that the shape of the clearing curves obtained for HEWL and HEWL conjugate, although similar, are not identical. Thus, the direct substitution of a different lysozyme in the Ovarian Monitor can not be carried out on the basis of the results obtained from studies on the native lysozymes alone. This means that before the work involved in the substitution of HEWL in the Ovarian Monitor for HuL can be justified, the kinetic characteristics of the human lysozyme-E1G conjugate must be compared with the behaviour found for the native human enzyme in Chapter Three. If, for example, the clearing curve obtained with the human E1G-lysozyme conjugate was less biphasic than that obtained with the native enzyme then despite the negative conclusions from the previous chapter, a direct substitution into the end-point assay could still be possible. This is actually highly probable as a lysozyme-steroid conjugate would have a reduction in its positive electrostatic field relative to the native lysozyme.

Furthermore, examination of the behaviour of the conjugate by wet chemistry, fails to test the effect that freeze drying the conjugate and *M. lysodeikticus* cells onto the walls

of the assay tube has on the shape of the clearing curve. This differentiation between wet and dry chemistry is an important distinction to make, as although in the laboratory it is only practical to examine and optimise the assay conditions using wet chemistry, only dry chemistry may be employed for the use of the Ovarian Monitor in the home.

Before these factors could be examined, and a final decision regarding the substitution of the E1G-HEWL conjugate for an E1G-HuL conjugate could be made, it was necessary first to synthesise estrone glucuronide as no cheap commercial source of this steroid was available. Furthermore, before any human lysozyme conjugations could be attempted on the small amount of enzyme available, the optimum conditions for the conjugation of the steroid glucuronides to HEWL had to be established in our laboratory. This optimisation was a particularly important aspect of the research as the human lysozyme was only readily available through commercial channels at prohibitively expensive rates ($ 4,000 per 50 mg). Thus, two different methods of conjugating E1G to the cheap and readily available HEWL were examined; these were the mixed anhydride method (Erlanger *et al.*, 1959) and the active ester method (Anderson *et al.*, 1964).

The mixed anhydride method is the method used previously by Melbourne for the synthesis of conjugates. However, this method is associated with several practical disadvantages, with the success of the reaction being critically dependent on two variables. Firstly, the reaction must be performed at low temperatures which can be difficult to control, and secondly, the reagents and the starting material must be kept completely dry throughout the synthesis of the mixed anhydride reagent. This means that conjugations by the mixed anhydride method are very demanding in terms of time and other requirements and are easily prone to failure. The active ester method is potentially a much simpler and quicker method of conjugating the steroid to lysozyme demanding less synthetic skill since the reaction can be performed at room temperature and without the strict requirement of the mixed anhydride method for an anhydrous environment. Thus, one major aim of this chapter was to optimise the active ester method of conjugation and then test the feasibility of using this method as a replacement for the mixed anhydride method by comparing the quality and quantity of conjugate obtained by the two different methods under equivalent conditions.

Finally, to produce a sensitive homogeneous enzyme immuno-assay, the assay must be capable of generating high levels of inhibition (i.e. 90% or greater) at baseline urinary hormone levels. The degree of inhibition at the baseline hormone level is a reflection of the relative amounts of free and conjugated lysozyme in the assay. In Melbourne, the separation of the conjugated HEWL from the unreacted HEWL was achieved by running aliquots of the reaction mixture through a CM Sepharose column equilibrated with 10 mM sodium phosphate buffer (pH 6.0) and eluting with an increasing sodium chloride gradient. However, this method of purification has proven to be poorly reproducible and is associated with a variable degree of resolution of the conjugate peaks from each other and from lysozyme. Thus, a particularly important aspect of the ongoing work on the Ovarian Monitor is the establishment of improved chromatographic procedures for the purification of lysozyme conjugates which are suitable for large scale use. These new procedures have to be established with the cheaper HEWL conjugates before any purification of the expensive HuL conjugates can be attempted as the HuL conjugate is too valuable to be expended in the development of a new purification protocol.

Thus, in summary the goals of this project which are addressed in this chapter are:

- to synthesise estrone glucuronide for conjugation with HEWL and HuL;
- to optimise the conjugation of E1G to lysozyme by the mixed anhydride and active ester methods and to assess whether the active ester method can be used as a new standard conjugation procedure;
- to establish new and improved purification procedures for the separation of lysozyme conjugate from free lysozyme using fast protein liquid chromatography (FPLC).

4.2 METHODS

4.2.1 MIXED ANHYDRIDE CONJUGATIONS

4.2.1.1 Activation of Estrone Glucuronide for Conjugation to Hen Egg White Lysozyme

This was carried out according to the procedure shown in Scheme 4.1.

The first step in the conjugation of E1G to HEWL using the mixed anhydride method is the formation of the anion of E1G by reaction with the base tri-n-butylamine (TNB). The E1G is then reacted with isobutylchloroformate (IBC) to form the mixed anhydride reagent necessary to link the E1G molecule to lysozyme.

The nature of the base selected for the activation of the carboxylate group in the previous step is important to prevent the degradation of the mixed anhydride reagent. TNB is a tertiary amine with three bulky n-butyl groups attached to the nitrogen atom thus, preventing it from attacking the carbonyl group of the mixed anhydride reagent for steric reasons. To maintain the integrity of the mixed anhydride reagent, it was not only necessary to use TNB as a base but to perform the reaction in *dry* di-methylformamide (DMF) and under anhydrous conditions as well.

This initial reaction step was performed at 4°C and left for twenty minutes, at the end of which time the reaction mixture was cooled to -10°C. The reaction times and cooling were necessary to prevent the mixed anhydride reagent from disproportionating - i.e. to prevent the mixed anhydride reagent rearranging itself as depicted in Scheme 4.2.

Disproportionation (Vaughan & Osata, 1952) has the disadvantage that for every two mixed anhydride molecules which undergo this reaction one of the original steroid molecules becomes inactivated.

4.2.1.2 Conjugation of Estrone Glucuronide to Hen Egg White Lysozyme

In the conjugation reaction, the E1G becomes linked to HEWL via an amide bond with one of the side chain amino groups of the six lysine residues on the enzyme. Although water destroys the mixed anhydride reagent, the actual conjugation of the E1G mixed anhydride to HEWL must be performed in water as the use of DMF as a solvent results

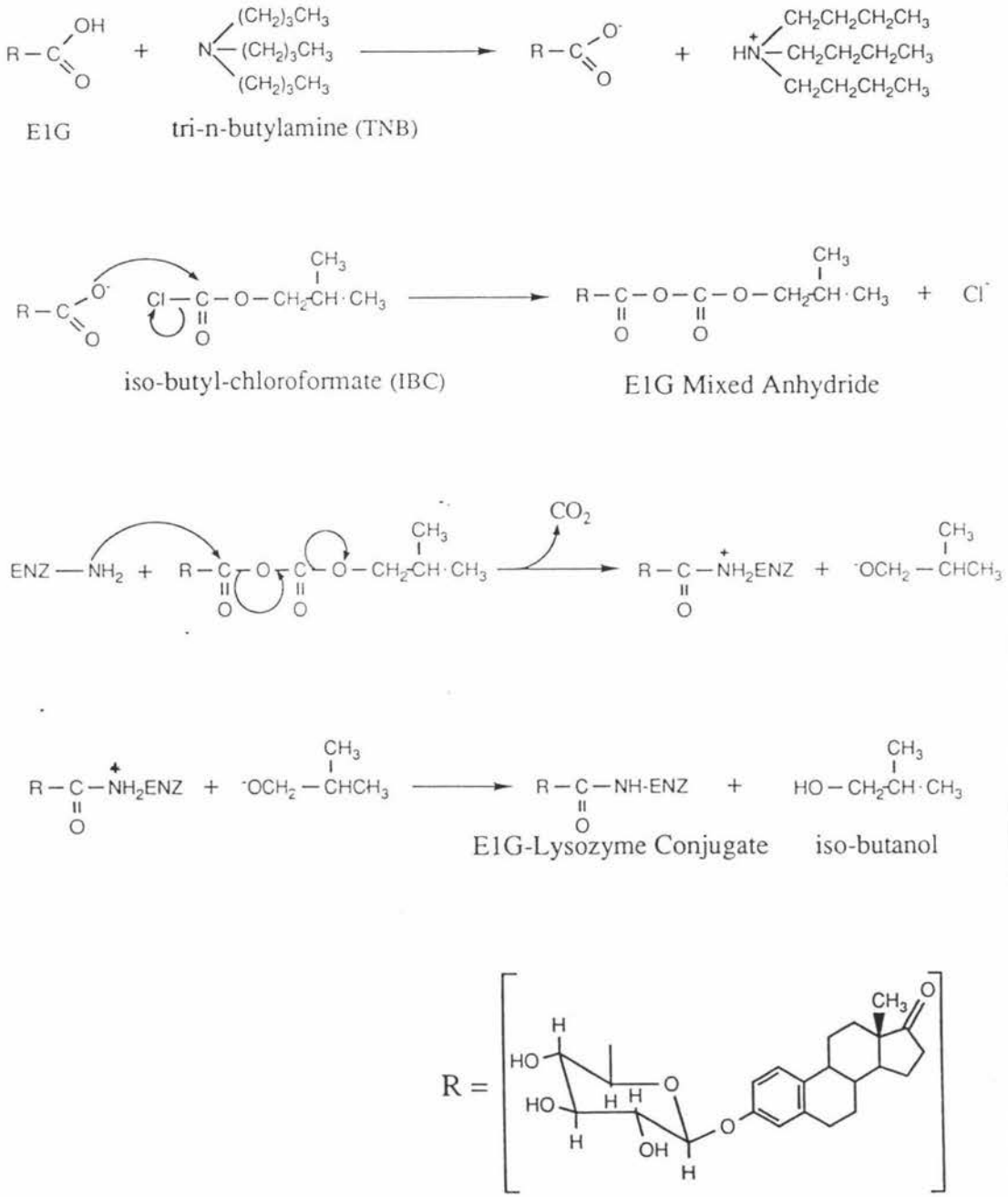

Scheme 4.1 *The Synthesis of Estrone Glucuronide Conjugate by the Mixed Anhydride Method*

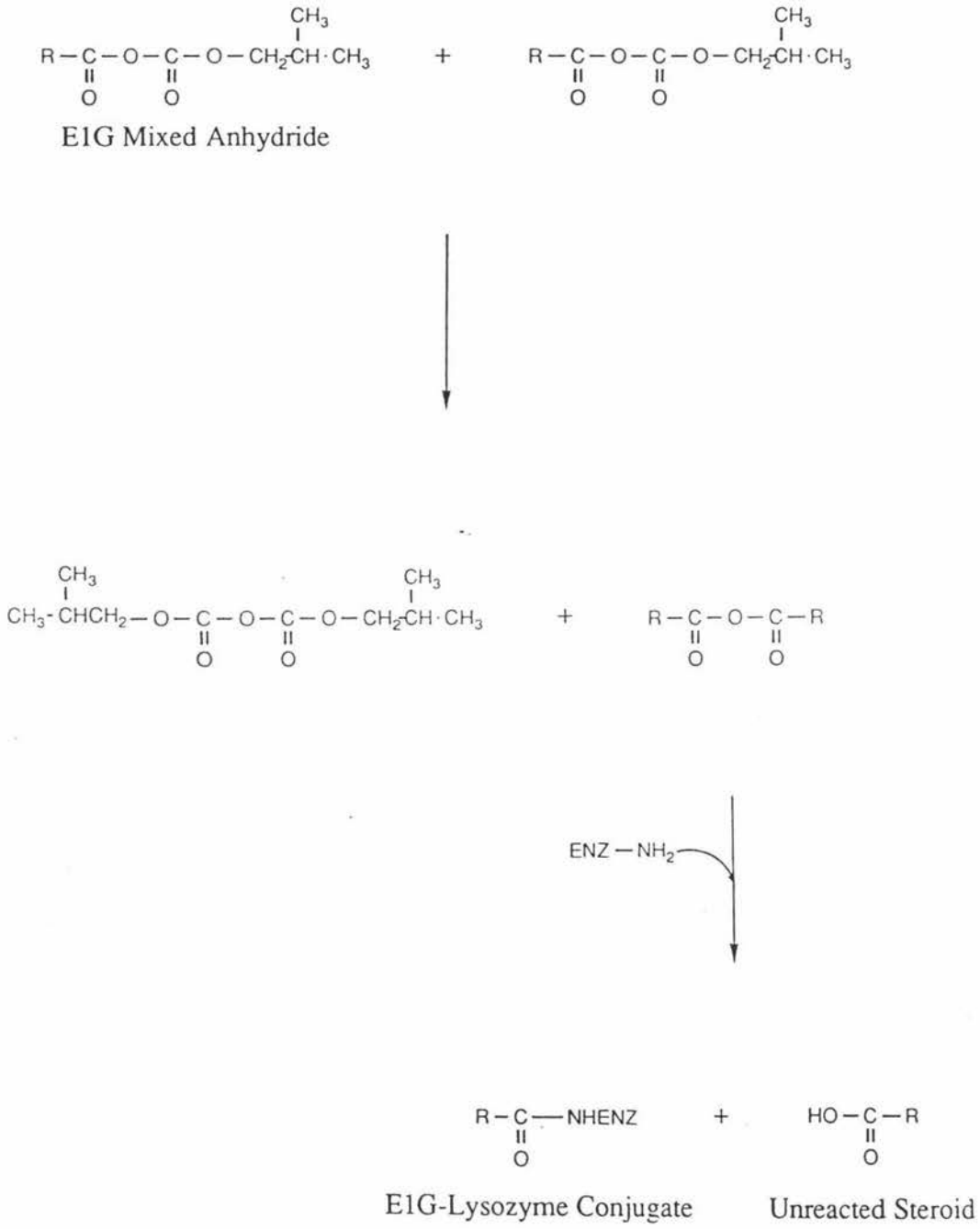

Scheme 4.2 *Disproportionation of the Mixed Anhydride Reagent*

in the denaturation of the lysozyme molecule. However, the performance of the conjugation in water does not pose a threat to the integrity of the mixed anhydride reagent when the concentration of HEWL is very high (close to saturation). This is because the terminal amino groups of the lysine residues from lysozyme have a much higher affinity for the carbonyl carbon on the reagent than the oxygen of a water molecule due to the high nucleophilicity of amino groups relative to water. Thus, at very high lysozyme concentrations the amino group competes very successfully with the water molecules for the mixed anhydride reagent.

Although there are theoretically two carbonyl groups the amino groups from lysozyme could attack on the mixed anhydride reagent, the bulky nature of the isobutyl group ensures that only the carbonyl group directly bonded to the E1G residue is available for attack by the lysozyme. The attack at this position is also favoured, as shown in Scheme 4.1, by the irreversible formation of carbon dioxide and isobutyl alcohol. Thus, the choice of IBC as the substrate in the formation of the mixed anhydride reagent is important in obtaining maximum yields of the chosen conjugate.

The carbon dioxide released from the synthesis of the E1G-HEWL conjugate combines with the water of the reaction medium to form carbonic acid thus, the synthesis of the conjugate is associated with a decrease in pH. Because the conjugation reaction is dependent upon some of the lysine residues of the enzyme molecules having free amino groups available to react with the mixed anhydride, a decrease in pH is also associated with a decrease in the formation of conjugate. Thus, optimal levels of conjugation are only obtained when the pH is carefully monitored throughout the reaction and re-adjusted as necessary back to pH 8.0.

4.2.1.3 General Experimental Details for the Mixed Anhydride Reaction

Because the volumes and quantities of the various reagents for the different conjugations were not standard, these are given in the text of the Results and Discussion Section.

All syringes and the reaction vessel used in the synthesis of the mixed anhydride reagent were dried in advance by washing with acetone, heating in an oven and storing in a desiccator over P_2O_5 until required.

E1G was weighed into a 0.5 ml reaction vessel, dissolved in dry DMF and then cooled to 10°C in a specially designed pre-equilibrated aluminium block equipped with a thermometer. Redistilled TNB, which had been stored over molecular sieves, was then added slowly, and the reaction mixture left for five minutes in the aluminium block at 10°C before cooling slowly to 4°C in a freezer. When the reaction mixture had equilibrated to 4°C, redistilled IBC, which was stored capped with a rubber septum over molecular sieves, was added slowly and the resulting solution left to react at 4°C in a fridge for twenty minutes. The mixed anhydride reagent was stabilised at the end of this time by a slow cooling of the solution to -10°C. This was achieved by the transfer of the aluminium block from the fridge to the bottom of a pre-equilibrated (-10°C) refrigerated centrifuge (Sorvall Superspeed RC2-B) which was used to control the temperature of the reaction. HEWL (Sigma, Prod. No. L-6876) further purified by FPLC (see Section 4.2.4) was weighed into a 10 ml reaction vessel, dissolved in Milli-Q water with stirring, and the pH adjusted to 8.0 with NaOH (0.5 M). Ice was packed round the reaction vessel, which was then placed in the bottom of the refrigerated centrifuge pre-equilibrated to -10°C in preparation for the conjugation. The HEWL solution was protected from freezing by constant mild stirring. The temperature setting of the pH meter was reset at 0°C and the display stabilised at the new pH value of 8.4.

When the mixed anhydride reagent had equilibrated to -10°C, which usually required a period between 30-60 minutes, it was added dropwise to the 0°C HEWL solution over a period of ten minutes with vigorous stirring. This addition was made with a fine tipped pasteur pipette kept dry in a P_2O_5 tube and pre-equilibrated to -10°C in the bottom of the centrifuge. After each addition the pH rapidly fell and was re-adjusted back to aproximately pH 8.4 with 0.5 M NaOH. When the number of moles of NaOH needed to maintain the pH at 8.4 was similar to the number of moles of E1G being added, this was taken as a sign of a successful reaction. Furthermore, an increase in the opacity of the reaction mixture upon the addition of the mixed anhydride reagent to the HEWL solution was used as visual proof of the success of the reaction.

The resulting HEWL-E1G conjugate was stored at 4°C and analysed and purified by FPLC (see Section 4.2.3 & 4.3.3).

4.2.2 ACTIVE ESTER CONJUGATIONS

4.2.2.1 Activation of Estrone Glucuronide for Conjugation to Hen Egg White Lysozyme

HEWL was also conjugated to E1G via the OH of the carboxylic acid group of the sugar residue by activation with dicyclohexylcarbodiimide (DCC) and N-hydroxysuccinimide (NHS) as shown in Scheme 4.3.

4.2.2.2 Conjugation of Estrone Glucuronide to Hen Egg White Lysozyme

Although DCC is a good leaving group, the E1G-DCC complex is insoluble in water and hence, will react only very slowly with HEWL in aqueous solution. Thus, a substitution of the DCC derivative for a more soluble compound which retains the good leaving group properties of DCC, is made before the conjugation of E1G to HEWL. This is achieved by the addition of the compound N-hydroxysuccinimide (NHS) which displaces dicyclohexylurea (DCU) and forms an active E1G-NHS ester. Since DCC is insoluble in water, any unreacted DCC does not react with the protein to generate cross linking between protein molecules as is the case with protein conjugates utilising water soluble carbodiimides.

As with the mixed anhydride reaction, the E1G becomes linked to HEWL via an amide bond with one of the side chain amino groups of the six lysine residues on the enzyme.

4.2.2.3 General Experimental Details for the Active Ester Reaction

Again, because the volumes and quantities of the various reagents for the different active ester conjugations were not standard, these are given in the text of the Results and Discussion Section.

Dry E1G was weighed into a small glass vial, dissolved in dry DMF and kept in a dessicator until required. Stock solutions of DCC and NHS were prepared in dry DMF such that 20-30 μl aliquots provided the requisite amount of reagent. The required aliquots of the DCC and NHS solutions were then added to the E1G solution. The volume of DMF in which the E1G sample was dissolved, was such that upon the addition of the DCC and NHS solutions the active ester reaction mixture had a total volume of approximately 150-250 μl. The resulting reaction mixture was mixed by

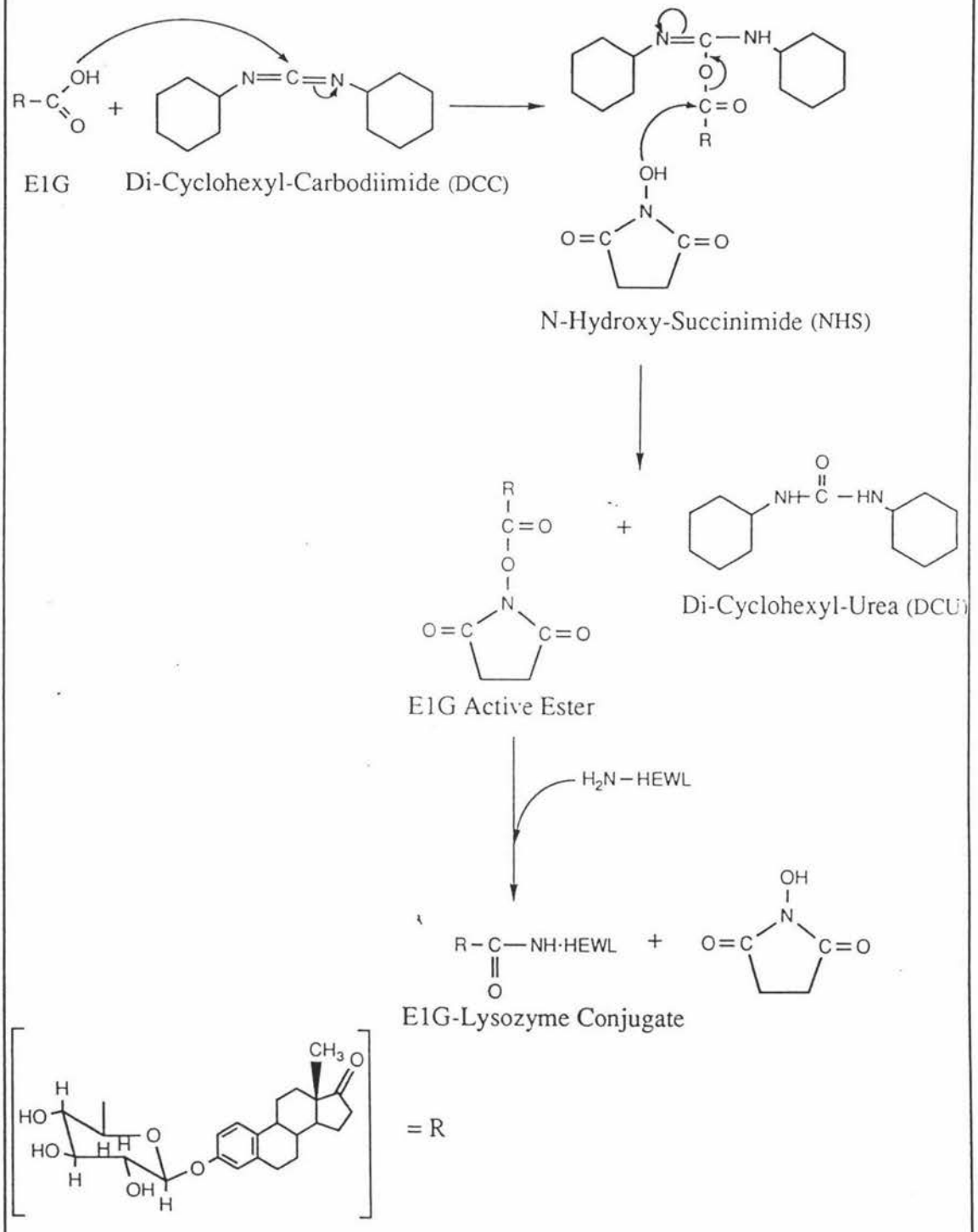

Scheme 4.3 *The Synthesis of Estrone Glucuronide Conjugate by the Active Ester Method*

inversion and left to equilibrate at room temperature for one hour in a dessicator.

HEWL was dissolved with stirring in 1% $NaHCO_3$ and then left to equilibrate to 4°C in preparation for the conjugation.

The conjugation was performed at 4°C with constant stirring by the dropwise addition of the active ester reaction mixture to the lysozyme solution using a dry pasteur pipette and was associated with the formation of a white precipitate. Upon the complete addition of the active ester reagent, the reaction mixture was left for an hour at 4°C after which period of time the reaction had gone to completion as shown by the FPLC traces obtained after running the sample through a Mono-S column using 7 M urea buffers.

In preparation for analysis and purification by FPLC, the conjugation mixture was then dialysed against Milli-Q water (3 changes x 2 litres) for 48 hours to remove the sodium bicarbonate.

4.2.3 FAST PROTEIN LIQUID CHROMATOGRAPHY PURIFICATION AND ANALYSIS

All FPLC work was performed on a Pharmacia FPLC system connected to a Pharmacia flow cell single path 280 nm ultra violet (UV) monitor. All buffers prepared for use on the FPLC system as well as samples prepared for analysis and purification by FPLC, were pre-filtered through 0.2 μm filters before loading.

All analytical work performed on the FPLC system was carried out on a Mono-S cation exchange column (5 x 0.5 cm I.D.). Purifications of conjugate and lysozyme were performed using various combinations of the following FPLC columns; a CM Sepharose fast flow cation exchange column (50 x 1.6 cm I.D.), an Alkyl Superose hydrophobic interaction column (5 x 0.5 cm I.D.) and a Mono-S cation exchange column (5 x 0.5 cm I.D.).

Conjugates synthesised by both the mixed anhydride and active ester methods were analysed on a Mono-S column. The following buffers were used with the Mono-S cation exchange column in the analysis of the HEWL and conjugate samples for purity.

Buffer A - 50 mM $NaH_2PO_4.2H_20$ in 7 M urea (pH 6.0).
Buffer B - 50 mM $NaH_2PO_4.2H_20$ in 7 M urea + 1.0 M NaCl (pH 6.0)

The Mono-S column was also used for analysis of conjugate fractions after further purification steps using Alkyl Superose, CM Sepharose, and CM Sepharose fast flow column chromatography.

The following non-urea buffers were used with the Alkyl Superose, CM Sepharose and CM Sepharose fast flow columns in the purification of HEWL-E1G conjugate:

Buffer A - 10 mM $NaH_2PO_4.2H_2O$ (pH 6.0).

Buffer B - 10 mM $NaH_2PO_4.2H_2O$ + 1.0 M NaCl (pH 6.0).

All chromatographic conditions for the individual traces are recorded on the figure legends.

Large scale purifications which resulted in the A_{280} readings going off scale during column elution had their A_{280} profiles obtained manually. These A_{280} profiles were obtained by the measurement of the absorbance of the individual fractions at appropriate dilutions using a Shimadzu spectrophotometer and a matched set of quartz cuvettes.

All reagents were reagent grade or higher, and all buffers and samples were prepared with Milli-Q water.

4.2.4 PURIFICATION OF HEN EGG WHITE LYSOZYME

Before conjugation experiments could be carried out it was necessary to purify the HEWL to remove an impurity in the commercial sample.

The following buffers were used with the CM Sepharose fast flow column in the purification of HEWL.

Buffer A - 10 mM $NaH_2PO_4.2H_2O$ (pH 6.0)

Buffer B - 10 mM $NaH_2PO_4.2H_2O$ + 0.6 M NaCl (pH 6.0)

A CM Sepharose fast flow column was washed with buffer A at a flow rate of 2 ml min^{-1} for one hour and the column was then washed with 15% buffer B (i.e. 0.09 M NaCl) until equilibrated. HEWL (3.032 g, 0.209 mmoles) was dissolved in

buffer A (20 mls) and loaded onto the pre-equilibrated column with a peristaltic pump at a flow rate of 4 ml min^{-1}. Elution was undertaken using a 15-100% salt gradient (i.e. 0.09-0.60 M NaCl) at a flow rate of 1 ml min^{-1}. Fractions were collected every 7.5 mls (i.e. every 7.5 minutes). The fractions containing the main peak were then pooled (165 mls), and dialysed against Milli-Q water over 72 hours (4 changes x 5 litres) before freeze drying overnight to give purified HEWL (1.93 mg, 0.133 mmol). Purified HEWL (6 mg, 0.413 μmol) and urea (4.2 g) were made up to volume in a 10 ml volumetric flask with Milli-Q water to make a 7 M urea solution. A 50 μl sample of the purified HEWL solution (0.03 mg, 2.07 nmol) was then injected manually onto the Mono-S column pre-equilibrated with 7 M urea buffer (see Section 4.2.3 for urea buffers) and eluted off as a single peak using a gradient of 0-40% buffer B (i.e. 0-0.40 M NaCl) in 30 minutes.

4.2.5 INHIBITION STUDIES

The quality of the conjugate purified by FPLC was assessed by measuring its percentage inhibition in a standard assay mixture containing monoclonal antiserum on the Ovarian Monitor. The control assay (i.e. the non-antiserum assay) was carried out essentially as described in Section 3.2.1.3 except that the concentration of *M. lysodeikticus* stock solution was reduced to 12 mg 2 ml^{-1}. The inhibition assay was performed essentially as for the control assay except for the order of addition of the reagents and samples and it was performed in the presence of antiserum. The monoclonal antiserum utilised in these assays was specific to E1G and was donated by Dr. Keith Henderson, Wallaceville Animal Research Centre where it was raised in sheep against E1G coupled to an albumin protein carrier.

Inhibition Assay

Conjugate	x μl
Antiserum	10 μl (dil 1/100)
Tris Maleate Buffer (40 mM)	80 μl
Vortex	
Tris Maleate Buffer (40 mM)	240 μl
M. lysodeikticus Suspension (12 mg 2 ml^{-1})	10 μl

Both the control and inhibition assays were initiated with the addition of the *M. lysodeikticus* suspension. The conjugate was diluted so that it gave a transmission change of less than 350 in twenty minutes in the control assay, and the same concentration of conjugate was used for the inhibition assays. All assays were twenty minute end-point assays.

4.3 RESULTS AND DISCUSSION

4.3.1 SYNTHESIS OF 17-OXOESTRA-1,3,5(10)-TRIENE-3-YL-ß-D-GLUCO-PYRANOSIDURONIC ACID

17-Oxoestra-1,3,5(10)-triene-3-yl-ß-D-glucopyranosiduronic acid, which will be referred to in the text as E1G, was synthesised essentially according to Conrow and Bernstein

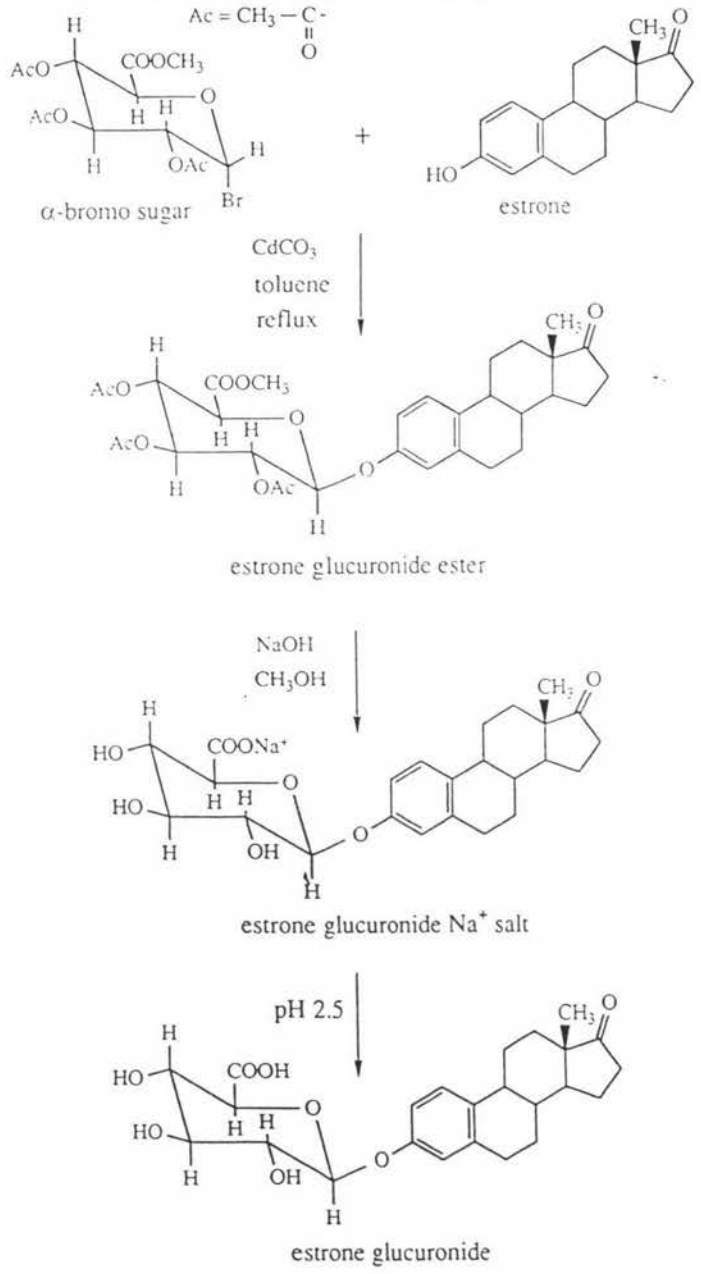

Scheme 4.4 *The Synthesis of Estrone Glucuronide*

(1971), as shown in Scheme 4.4.

4.3.1.1 Coupling of the Bromosugar to Estrone

3-Hydroxy-estra-1,3,5(10)-triene-17-one (Sigma, Prod. No. E 9750) henceforth referred to by its trivial name estrone, was coupled to the bromosugar, methyl-1-bromo-1-deoxy-2,3,4-tri-O-acetyl-α-D-glucopyranuronate (synthesised and supplied by Mr Y. Wu) using cadmium carbonate ($CdCO_3$) (BDH) as a catalyst. $CdCO_3$ catalyses the reaction by activating the bromosugar in a one to one molar ratio to form an ortho-ester intermediate (Banoub & Bundle, 1978) which reacts with estrone. This coupling occurs in a stereospecific manner (Scheme 4.5) as a result of neighbouring group participation by the 2-acetoxy group to give the α-orthoester. In the product forming step the alcohol partner (estrone in this case) can most easily attack from the ß-face giving the required isomer (ß-glucuronide). The reaction was driven in the forward direction by using an excess of the bromosugar, which ensured most of the steriod was reacted and hence simplified the purification procedure for the steroid-sugar derivative. The overall molar

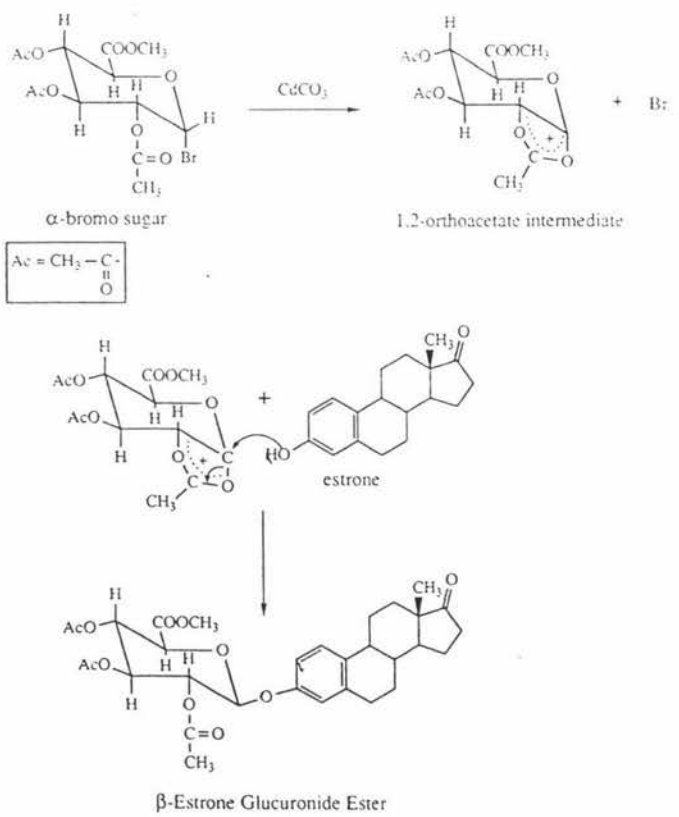

Scheme 4.5 *Mechanism of the Koenigs-Knorr Coupling of the Bromosugar to Estrone*

ratio of estrone:bromosugar:$CdCO_3$ used in the synthesis was 1:3:3.

All toluene used in the preparation was pre-dried over molecular sieves. The bromosugar (873 mg, 2.2 mmoles) was weighed into a dry 25 ml stoppered conical flask, to which toluene (approximately 20 mls) was then added, and kept in the dark until required. Estrone (198 mg, 0.73 mmoles) and cadmium carbonate (380 mg, 2.2 mmoles) were weighed into a dry 50 ml two necked flask to which dried toluene (approximately 30 mls) was then added. The solution was then heated with stirring in a hot oil bath, and the toluene allowed to distil until the total volume was reduced to approximately two-thirds of the original. This volume was then kept constant by additions of the previously prepared bromosugar toluene solution via a dry syringe through a rubber septum. After all the bromosugar had been added, the volume of the toluene solution was kept constant by the continuous additions of further aliquots of dry toluene from washings of the bromosugar flask until approximately another 20 mls of toluene had been added. After the second addition of toluene was complete, the flask was removed from the oil bath and left at room temperature overnight. A successful reaction was indicated by the formation of a pink precipitate (cadmium carbonate) and verified by running a thin layer chromatography plate (TLC) of a sample of the reaction mixture against standard estrone ester dissolved in acetone. The TLC was run in a 1:1 mixture of hexane:ethyl acetate, stained with Kober Reagent (90% ethanol + 10% concentrated sulphuric acid) by immersion and developed for ten minutes at 120°C.

The cadmium carbonate was removed by filtration after gentle heating of the toluene to redissolve any product which had crystallised out. The filtration step was repeated four to five times using the toluene from the distillation step in conjunction with intermittent warmings to wash the flask. This step was repeated until a total volume of approximately 10 mls of toluene had been used, and no visible residue was left adhering to the sides of the flask. The toluene was removed by rotary evaporation until a brown oil was obtained, and the methyl-[17-oxoestra-1,3,5(10)-triene-3-yl-2',3',4'-tri-*O*-acetyl-ß-D-glucopyranosid] uronate, (estrone glucuronide ester) was redissolved with heating in acetone (10 mls). Water (30 mls) was then added to the flask to precipitate out the crude product leaving the unreacted bromosugar dissolved in solution.

The crude methyl-[17-oxoestra-1,3,5(10)-triene-3-yl-2',3',4'-tri-*O*-acetyl-ß-D-glucopyranosid] uronate product was then recrystallised twice from a 1:1 mixture of

dichloroethane:ethanol (approximately 3 mls). After washing with ethanol, the first crop of crystals were filtered and dried on a vacuum line to give 68 mg of the pure product.

The mother liquors from the above crystallisations were rotary evaporated to dryness and the resulting solid dried on the vacuum line for two hours. The residue was then redissolved in the minimal quantity of dichloromethane and the sample loaded onto an Aluminum Oxide-S standardised column (30 x 2 cm I.D.) pre-equilibrated with a 1:1 ratio of hexane:ethylacetate. The sample was eluted using the same 1:1 mixture of hexane:ethylacetate and collected as forty successive fractions (approximately 3 mls each). The fractions which showed significant quantities of product by TLC were pooled, rotary evaporated and the product then redissolved in a 1:1 dichloromethane:ethanol solvent mixture and left to crystallise as before to give a further crop of white shiny crystals (81.4 mg). The combined yield of crystals was 138 mg (0.235 mmol) of methyl-[17-oxoestra-1,3,5(10)-triene-3-yl-2',3',4'-tri-*O*-acetyl-ß-D-glucopyranosid] uronate (32% yield).

The crystals appeared to be pure as they gave a single spot on TLC and a melting point of 229-231°C was obtained on a Bausch and Lomb melting point apparatus. This compares favourably with the literature value of 222-230°C (Conrow & Bernstein, 1971).

The structure of the product was confirmed by nuclear magnetic resonance spectroscopy (NMR) in deuterated chloroform on a JEOL GX-270 spectrometer. The ^1H spectrum was performed at an operating frequency of 270 MHz and referenced relative to the internal standard tetramethylsilane (δ = 0.0 ppm). The resulting NMR spectrum is shown in Figure 4.1. and generated the following spectral data: ^1H NMR (270 MHz; $CDCl_3$): δ 0.91 (s, 3H, 18-CH_3), 2.04 (s, 3H, $COCH_3$), 2.05 (s, 3H, $COCH_3$), 2.06 (s, 3H, $COCH_3$), 3.74 (s, 3H, OCH_3), 4.15 (m, 1H, J = 9.51 Hz, H-5'), 5.09 (d, 1H, J = 7.33 Hz, H-1'), 6.73 (d, 1H, J = 2.19 Hz, H-4), 6.77 (dd, 1H, J = 8.43, 2.77 Hz, H-1), 7.20 (d, 1H, J = 8.43 Hz, H-2)

The large coupling constants for the anomeric proton and the C5' proton are consistent with a trans configuration of the C1' and C2' protons, and the C4' and C5' protons of the sugar ring. This shows that the sugar ring is in the chair configuration, and more

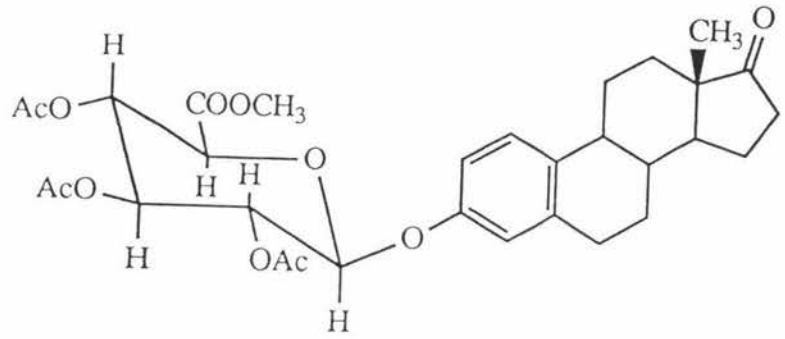

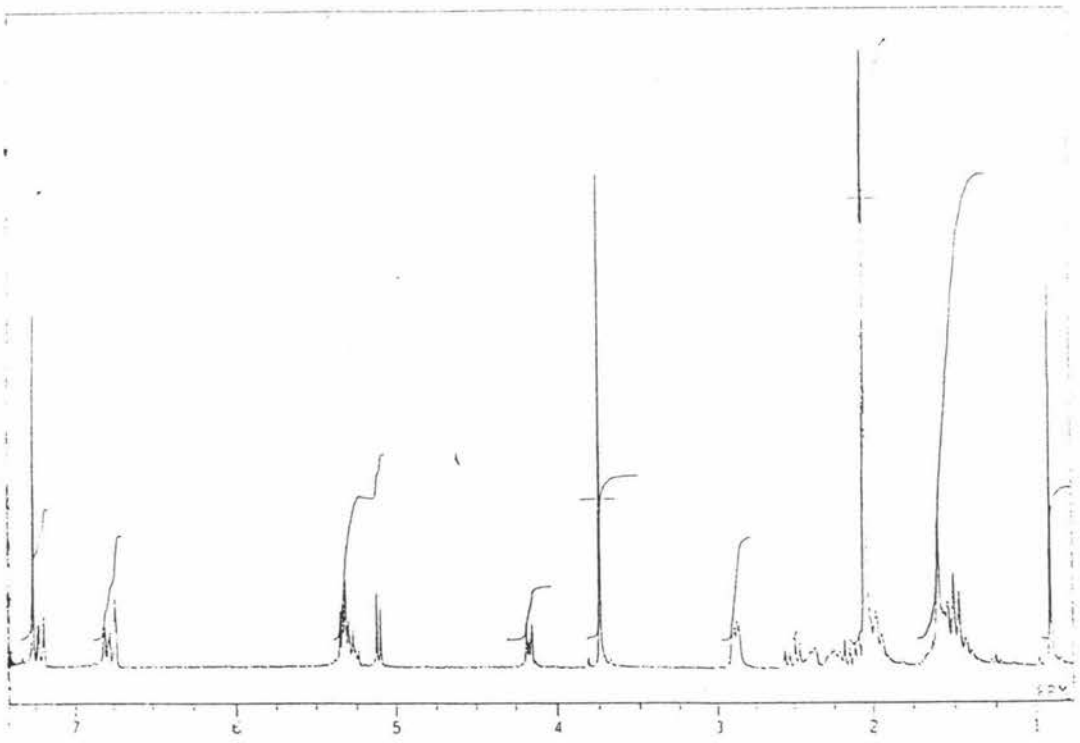

Figure 4.1 *^1H NMR Spectrum of Methyl-[17-oxoestra-1,3,5(10)-triene-3-yl-2',3',4'-tri-O-acetyl-β-D-glucopyranosid] Uronate*

importantly that the steroid group is attached in the ß position as required. The NMR

spectrum also shows that the sugar ring is completely acetylated with the integrals being consistent with a molecule which contains one steroid group for each sugar residue.

4.3.1.2 Preparation of 17-oxoestra-1,3,5(10)-triene-3-yl-ß-D-glucopyranosiduronic acid

In the next step in the synthesis, the acetate groups were removed from the ester by hydrolysis. In order to ensure an excess of NaOH in the hydrolysis, a molar ratio of 1:5 ester:NaOH was used. To 138 mg of estrone glucuronide ester, 0.6 mls of NaOH (2 M) was added very slowly with stirring and the mixture left to stir at room temperature overnight. When the hydrolysis reaction was complete as indicated by TLC, the pH was adjusted from 13 to 7.25 with glacial acetic acid and the solution then rotary evaporated to dryness. The sample was then redissolved in a small volume of methanol:water 3:2. Crystals of sodium-[17-oxoestra-1,3,5(10)-triene-3-yl-ß-D-glucopyranosid] uronate, i.e. the sodium salt of estrone glucuronide (E1G-(Na)), were collected by filtration 48 hours later and washed with methanol.

The final step in the preparation of E1G was the removal of the sodium ions from the sugar group to yield the acid form of estrone glucuronide (E1G-(H)). This was achieved by titration to pH 2.3 with HCl. A successful titration with a high concentration of product was indicated by the formation of a white precipitate. The E1G-(H) was purified using XAD-2 chromatography (20 x 2 cm I.D.). The column was prepared by sequential washing with 200 mls of water, methanol:water 50:50, methanol, methanol:water 50:50, and water again. The sample was then dissolved in a 1:9 mixture of methanol:water (total volume 44 mls) and loaded onto the column. After loading, the column was thoroughly washed with water (500 mls) to remove salts, before eluting with a 75:25 mixture of methanol:water (200 mls). The column was then regenerated with 100% methanol (200 mls). The sample in the 75% methanol wash was concentrated by rotary evaporation and freeze dried to remove the water. The solid product was then dried on a vacuum line to give a final yield of 45.3 mg (43%, 0.102 mmol) of 17-oxoestra-1,3,5(10)-triene-3-yl-ß-D-glucopyranosiduronic acid, melting point 165-168°C.

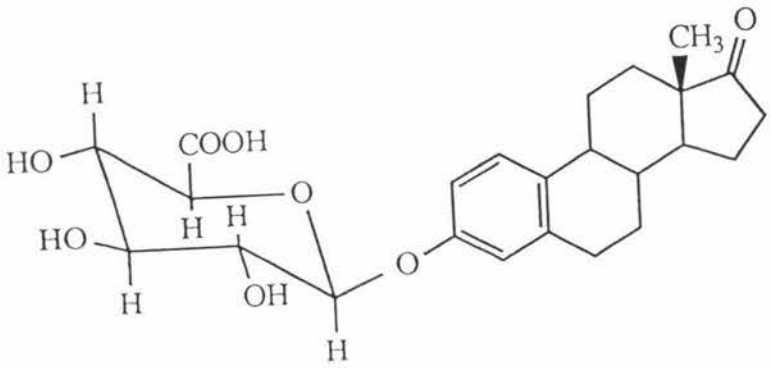

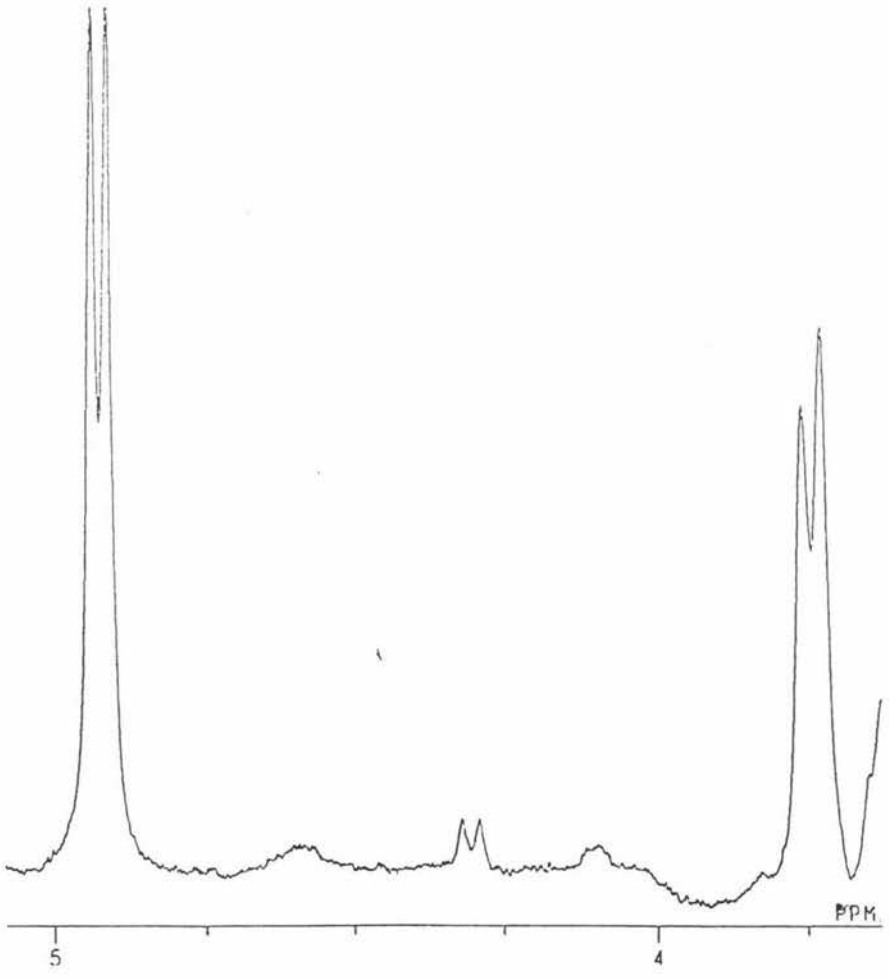

Figure 4.2 *^{1}H NMR Spectrum of 17-oxoestra-1,3,5(10)-triene-3-yl-β-D-glucopyranosiduronic Acid*

The structure of the E1G-(H) product was confirmed as for the E1G ester (see

Section 4.3.1) by NMR spectroscopy using dimethylsulphoxide (DMSO) as a solvent in which the compound was readily soluble. The key features of the NMR spectrum are summarised below.

^{1}H NMR (270 MHz; DMSO-d_6): δ 0.82 (s, 3H, 18-CH_3), 3.72 (d, 1H, J = 8.79 Hz, H-5'), 4.91 (d, 1H, J = 7.96 Hz, H-1' anomeric proton), 6.71 (s, 1H, H-4), 6.77 (d, 1H, J = 8.43 Hz, H-1), 7.17 (d, 1H, J = 8.43 Hz, H-2)

Due to the interference from the DMSO solvent in the NMR spectrum, only the part of the NMR spectrum which displayed the anomeric proton and the C5' proton of the glucuronide ring is shown (see Figure 4.2). Thus, the presence of the sugar ring in the correct conformation and the ß orientation of the glucuronide ring were confirmed by the large coupling constants for both protons (7-9 Hz) indicating a trans configuration at these two positions. This was an important feature of the NMR spectrum as it confirmed that no racemisation of the sugar ring had taken place during the exposure of the E1G-sodium salt to high acid conditions during the formation of E1G-(H).

4.3.2 CATION EXCHANGE CHROMATOGRAPHY ON THE THE MONO-S COLUMN WITH SEVEN MOLAR UREA

Lysozyme is a very basic protein with an iso-electric point (IEP) of 10.5 (Verhamme *et al.*, 1988). This very high IEP is partly due to the six lysine residues on its external surface, one of which is the N terminal residue. Although other linkages are possible using the mixed anhydride and active ester methods, stable linkages of a steroid molecule to lysozyme are only formed through the lysine residues. Thus, there are a total of seven theoretical sites at which a steroid molecule can become permanently linked via an amide bond to lysozyme; this includes the α amino group of the N terminal lysine residue and the ε amino groups of all six lysine residues. Because the formation of an amide bond is associated with the removal of a positive charge, a successful conjugation reaction is associated with a net decrease in the overall charge on the enzyme. Thus, the theoretical minimum charge for an individual lysozyme conjugate molecule would occur when each of the seven sites were bound to a steroid molecule.

The Mono-S column is a cation exchange column and thus, is expected to be ideally

suited for the separation of lysozyme and the different families of conjugates from each other. This is because a cation exchange column separates the components of the reaction mixture according to charge with the most highly charged molecules binding most tightly and hence eluting last. Thus, the order of elution would be expected to be from the most highly substituted lysozyme conjugate which has nearly all of its positive charges due to lysine groups neutralised, to lysozyme itself which retains all seven of its lysine derived positive charges, being eluted last.

Evidence that lysozyme conjugate purified on a cation exchange column using 7 M urea, does in fact elute in order of the number of free lysine residues on each lysozyme molecule, comes from two studies performed in Melbourne. In one experiment, fractions of acetylated lysozyme, purified from a CM Sepharose cation exchange column, were titrated for lysine residues and the average number of free lysine residues per lysozyme molecule in each fraction was determined. This experiment showed that the order of elution of the fractions and the level of conjugation, as indicated by the number of free lysine residues, were related, with the earlier eluting fractions having the higher levels of conjugation (fewer free lysines). Furthermore, in a separate experiment, the analysis of the different fractions eluted from a CM Sepharose column for tritium labelled PdG from a PdG lysozyme conjugation, again showed that it was the earlier eluting peaks which were associated with the higher degrees of acylation and higher levels of radioactivity (unpublished results). Thus, it appears that when cation exchange chromatography is used in conjunction with 7 M urea buffers, the order of elution of the different conjugate families is determined by the overall degree of charge neutralisation of the lysine groups i.e. the number of conjugated steroid groups per lysozyme molecule irrespective of the nature of the acyl group.

Because the experiment with radioactive PdG conjugate showed the PdG conjugates to elute from an ion exchange column in order of decreasing substitution (i.e. increasing charge), and the relative retention times of the various PdG and E1G conjugate peaks from the Mono-S column are identical in 7 M urea (see Figure 4.3 (a) and (b) for E1G and PdG elution profiles respectively), then it seems reasonable to conclude that the E1G conjugate peaks will also separate on a Mono-S column in order of increasing charge.

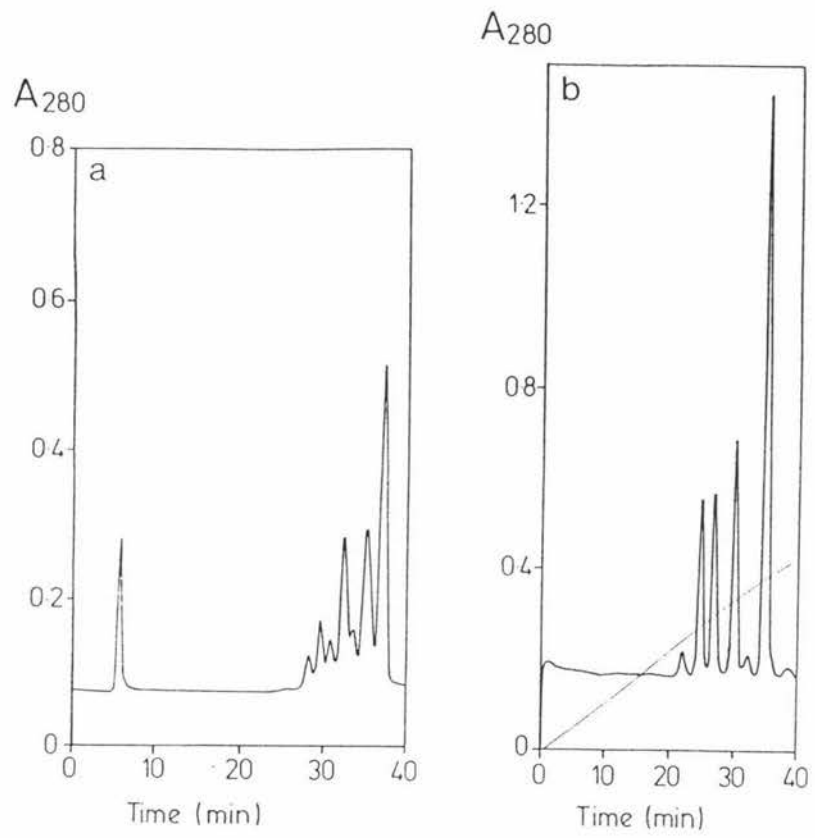

Figure 4.3 *FPLC Profile for an E1G and PdG Conjugation Reaction Mixture on a Mono-S Column using 7 M Urea Buffers*

(a) E1G:HEWL 3:1 Active Ester Conjugation; Figure 4.3 (b) PdG:E1G 1.5:1 Mixed Anhydride Conjugation. Conditions: sample preparation - 50 µl of reaction mixture in 300 µl of buffer A; volume injected - 100 µl; flow rate - 0.5 ml min^{-1}; gradient (a) - 0% buffer B 0-5 minutes, 0-40% buffer B 5-35 minutes; gradient (b) - 0-17% buffer B 0-30 minutes, 17-30% buffer B 30-60 minutes.

However, although the same elution behaviour i.e. retention times was observed for the different peaks with the different steroid acylating agents, for both the 7 M urea CM Sepharose columns and 7 M urea Mono-S columns, the peak ratios do vary with the method of acylation and acylating agent. Thus, each conjugation method is associated with its own order as to the ease of acylation of the different lysine residues. For example, with acetylation of lysozyme with acetic anhydride, the order of decreasing reactivity of the lysine residues in lysozyme was Lys-116, Lys-1 (α-NH_2), Lys-33, Lys-96, with Lys-13 and Lys-1 (ε-NH_2) being approximately last equal (Lee *et al.*, 1975). However, to date no data have been published on the order of reactivity of these lysine

residues for acylation with the active esters of steroid glucuronide groups.

For the present project, it was found that when the Mono-S column was used in conjunction with the 7 M urea buffers, it gave consistently good resolution between the conjugate and lysozyme peaks, and was highly reproducible. This made it an invaluable tool, not only for evaluating the success and range of conjugates formed from a given conjugation reaction, but for the rapid evaluation of the success of other column chromatography work in the development of a separation procedure for the conjugate families from each other as well as from lysozyme.

Unfortunately, this analytical procedure was not completely suitable for the purification of conjugate as it has been the experience of Melbourne that the exposure of conjugate fractions to 7 M urea results in a lowering of their inhibitions (unpublished data). Furthermore, due to the small capacity of the Mono-S column it was not suitable for large scale purifications of conjugate (i.e. greater than 1 mg of protein).

Using the 7 M urea buffers, the last peak to elute from the Mono-S column was always presumed to be lysozyme. This presumption was confirmed by running a sample of pure lysozyme (see Section 4.2.4) under identical chromatographic conditions. For the E1G conjugations, the different conjugate peaks were classified according to their retention times relative to the lysozyme peak starting with E1 which eluted closest to the lysozyme peak (see Figure 4.3 (a)). This labelling of the conjugate peaks usually could be achieved by a simple visual inspection of the Mono-S elution profile.

Although a chromatographic peak may represent conjugate with a certain number of steroid substitutents, the different conjugate molecules within a particular peak may not necessarily be equivalent, as the steroid groups may be attached to different lysine residues. Furthermore, although it is possible that a conjugate peak does consist of a discrete conjugate species, this can not be assumed to be the case until conjugate from the peaks is isolated and subjected to amino acid sequencing. Thus, until the peaks have been properly characterised, it is more correct for them to be considered as made up of conjugate families instead. This characterisation work is currently being performed by other members of the Ovarian Monitor research group at Massey.

4.3.3 SYNTHESIS AND PURIFICATION OF HEN EGG WHITE LYSOZYME ESTRONE GLUCURONIDE CONJUGATES

The first step in the purification of HEWL-E1G conjugates from a conjugate reaction mixture is the separation of conjugate from the free lysozyme fraction. However, because in solutions of high lysozyme concentrations such as the conjugation reaction mixture, lysozyme has a tendency to undergo self association to form dimers and other higher self assemblies, the free lysozyme component of the reaction mixture consists of several chromatographically distinct lysozyme fractions (Jolles & Jolles, 1984). In fact there is evidence of this in the present study which suggests that lysozyme may complex with lysozyme conjugates as well. Hence, the separation of conjugate from free lysozyme is not a simple task, especially considering that the self assemblies of lysozyme have a tendency to co-elute with the conjugate fractions. Thus, the isolation of pure, highly inhibitable E1G-lysozyme conjugate is a particularly important, and at the time of the commencement of this project, unsolved aspect of research on the continuing development of the Ovarian Monitor.

The following sections describe, analyse and discuss the results of a series of experiments performed during the development of a purification scheme for E1G-lysozyme conjugates.

4.3.3.1 Conjugation of Hen Egg White Lysozyme using the Estrone Glucuronide Mixed Anhydride

The first successful conjugation of HEWL to E1G was carried out according to the mixed anhydride protocol as described in Section 4.2.1.3 using a molar ratio of E1G to HEWL of 2:1. The conjugation was performed using the following quantities: 200 mg HEWL (14 μmol) purified as in Section 4.2.4 and dissolved in 5 mls of Milli-Q water, 12.4 mg E1G-(H) (28 μmol), 200 μl DMF, 6.6 μl TNB (27.8 μmol), and 3.6 μl IBC (27.9 μmol).

The addition of the mixed anhydride reagent to the HEWL solution was associated with the formation of a white precipitate indicating a successful reaction. To confirm this,

a sample was prepared for analysis on the Mono-S column using 7 M urea buffers (see Section 4.2.3) by diluting a 50 µl aliquot of the reaction mixture into 300 µl of the starting buffer. A 50 µl sample of the resulting solution was then injected directly onto the Mono-S column pre-equilibrated with 100% buffer A i.e. 0 M NaCl. The sample was then eluted using an increasing salt gradient of 0-40% (i.e. 0-0.40 M) in 30 minutes at a flow rate of 0.5 ml min^{-1}, to give the elution profile seen in Figure 4.4.

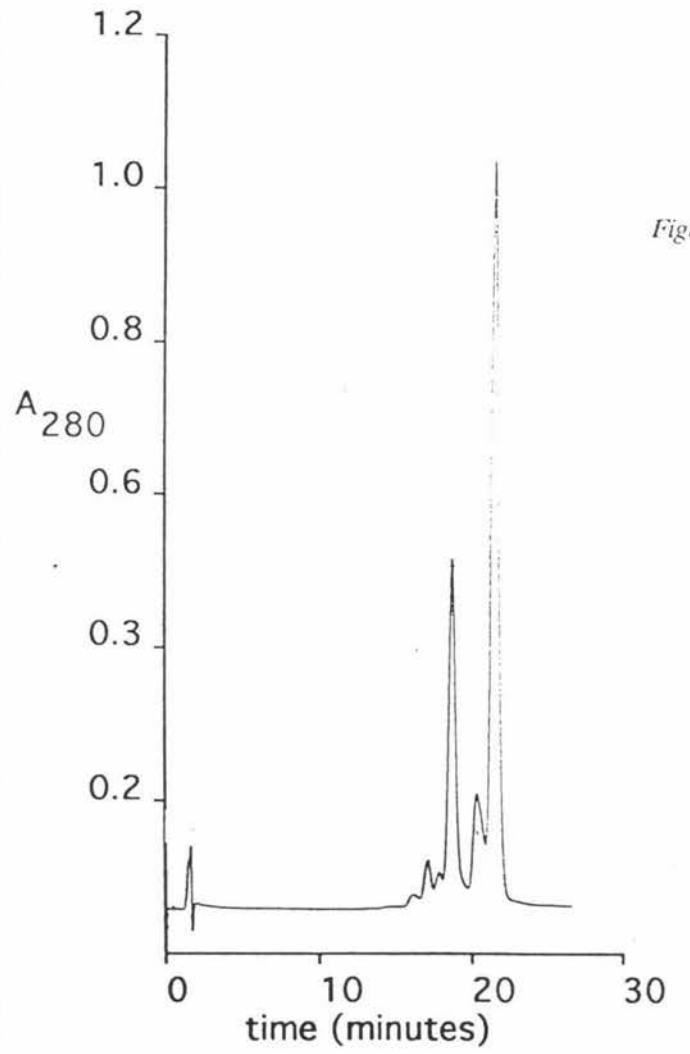

Figure 4.4 *FPLC Profile for the Reaction Mixture of a HEWL - E1G Conjugation Synthesised by the Mixed Anhydride Method using a Molar Ratio of E1G:HEWL of 2:1 on a Mono-S Column using 7 M Urea Buffers*

Conditions: sample preparation - 50 µl of reaction mixture in 300 µl of buffer A; volume injected - 50 µl; flow rate - 0.5 ml min^{-1}; gradient - 0% buffer B 0-5 minutes, 0-40% buffer B 5-35 minutes.

Figure 4.4 shows that on the basis of relative peak heights 43% of the original lysozyme was successfully conjugated to E1G. Of the conjugated lysozyme the predominant conjugate family was E3 which represented 63% of the total, but there were also significant quantities of E1 (20%) with the remaining 17% being made up of small amounts from the E4, E5 and E6 conjugate families. This conjugate pattern was similar

to a sample of E1G-lysozyme conjugate provided by Professor J. Brown (Melbourne).

On the evidence of the analytical Mono-S trace, an attempt was made to purify the main body of conjugate from the reaction mixture in a single run on a CM Sepharose fast flow column using non-urea buffers (see Section 4.2.3). The sample was prepared for loading by diluting it in a 1:1 ratio of sample to 30% buffer B to get the ionic strength of the sample the same as the starting gradient. This resulted in the formation of a precipitate which was partly removed by spinning the sample for five minutes at speed 5 on a bench centrifuge (Gallenkamp Junior). The sample was then loaded, along with

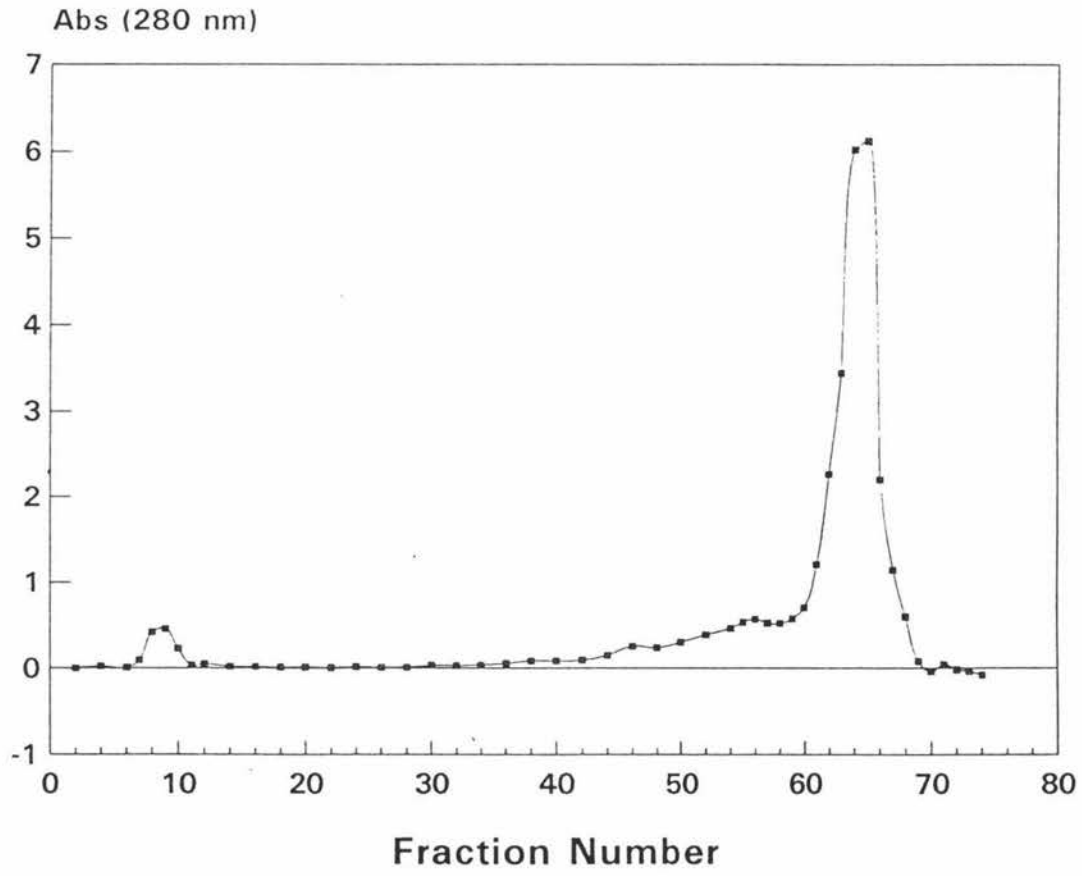

Figure 4.5 *A_{280} Profile for the Reaction Mixture of a HEWL-E1G Conjugation Synthesised by the Mixed Anhydride Method using a Molar Ratio of E1G:HEWL of 2:1 on a CM Sepharose Fast Flow Cation Exchange Column using Non-urea Buffers*

Conditions: sample preparation - 1:1 mix of total volume of reaction mixture (4.4 mls) with 30% buffer B; volume loaded - 8.8 mls; flow rate - 1 ml min^{-1}; gradient 15-30% buffer B in 500 minutes, 30-40% buffer B in 50 minutes, held at 40% buffer B for 210 minutes; fraction collection - 10 ml 10 min^{-1}.

all of the remaining precipitate, onto the column pre-equilibrated with 15% buffer B

(0.15 M NaCl) where a narrow precipitation band could be seen on the column. Elution of the conjugate was then undertaken using an increasing salt gradient and a flow rate of 1 ml min^{-1}. A gradient of 15-30% buffer B (0.15-0.30 M NaCl) in 500 minutes followed by a 30-40% (0.30-0.40 M NaCl) gradient in 50 minutes, and holding at 40% buffer B (0.40 M NaCl) for a further 210 minutes, was used to elute the sample.

The resulting elution profile consisted of one large peak which was immediately preceded by a small peak only partly resolved from the main peak (see Figure 4.5). The amount of conjugate in the small peak, and the distribution of conjugate across the main peak was analysed using inhibition studies of the various fractions (see Section 4.2.5 for protocol). Inhibition studies represent a particularly important analytical procedure by providing the ultimate test for pure conjugate. In this test, a pure conjugate fraction is defined as one which can generate a high level of inhibition (i.e. greater than 90%), while a lower level of inhibition is used as a positive marker for the presence of lysozyme.

The results obtained from the inhibition studies performed on the above mentioned fractions showed the amount of conjugate to increase across the main peak with most of the conjugate concentrated in the peaks trailing edge (see Table 4.1).

Table 4.1 *Percentage Inhibition of Fractions resulting from a Mixed Anhydride 2:1 E1G:HEWL Conjugation after Purification on a CM Sepharose Fast Flow (Non-urea) Column*

Fraction	% Inhibition
peak tube of small peak	23
leading edge of main peak	1
peak fraction of main peak	41
trailing edge of main peak	63

This distribution of the conjugate was unexpected as it meant that the elution profile could not be explained solely on the basis of separation according to charge as discussed

in Section 4.3.2. A separation on the basis of charge would have resulted in the conjugate being eluted first and therefore concentrated in the leading edge of the main peak, not the trailing edge as the inhibition studies confirmed. Thus, it is apparent that in the absence of 7 M urea the separation obtained on a cation exchange column is determined by other factors in addition to the charge considerations.

4.3.3.2 Conjugation of Hen Egg White Lysozyme with the Estrone Glucuronide Active Ester

The first successful conjugation of HEWL to E1G by the active ester method was essentially carried out as described in Section 4.2.2.3 except that the HEWL was dissolved in water (as in the mixed anhydride reaction) as opposed to a 1% solution of sodium bicarbonate and the NHS and DCC were weighed out directly. This conjugation was performed using a ratio of E1G to HEWL of 3:1 and the following quantities of reagents: 108 mg HEWL (7.6 μmol) purified as in Section 4.2.4 and dissolved in 3 mls of Milli-Q water, 10.2 mg E1G-(H) (23 μmol), 200 μl DMF, 2.6 mg NHS (23 μmol), and 4.6 mg DCC (22 μmol). Approximately one hour after the active ester reagent was first synthesised crystals had formed in the solution. A heavy precipitate was also formed upon the addition of the active ester reagent to the HEWL solution. After twenty minutes the pH had decreased to 6.0 and was re-adjusted back to pH 7.7 using 0.5 M NaOH (500 μl). The large volume of 0.5 M NaOH required to restore the pH suggested that all future active ester conjugations should be performed in 1% sodium bicarbonate as reported in the literature (Anderson *et al.*, 1964).

A sample of the reaction mixture was analysed on the Mono-S column using conditions identical to those used to analysis the mixed anhydride conjugate (see Section 4.3.3.1) except that 100 μl was injected onto the column instead of the previous 50 μl. The resulting elution profile is shown in Figure 4.3 (a).

The Mono-S profile is markedly different from that obtained from the mixed anhydride reaction mixture (Figure 4.4) and showed that the active ester conjugation gave a particularly high yield of product, with 65% of the original lysozyme conjugated. Compared to the mixed anhydride conjugation, this active ester conjugation gave a much more uniform distribution of conjugates across the different conjugate families with a significant decrease in the percentage contribution of the E3 conjugate family to the total

conjugate yield. In this conjugation, there were approximately equal quantities of the E1 and E3 peaks which accounted for 30% and 29% of the conjugate yield respectively. The rest of the conjugate yield was distributed almost equally between E2 (11%), E4 (10%), E5 (13%), and E6 (7%). Thus, the level of very highly substituted conjugates was increased with the E4, E5 and E6 conjugate families now accounting for 30% of the conjugate yield as opposed to the 17% yield which was encountered with the mixed anhydride reaction. This higher percentage of total conjugates and the increased percentage of highly substituted conjugates for the active ester conjugation, is probably a reflection of the higher 3:1 conjugation ratio of E1G to HEWL compared to the mixed anhydride ratio of only 2:1.

The conjugate in the active ester reaction mixture was purified on the CM Sepharose fast flow column (no urea) using conditions identical to those used previously on the mixed anhydride reaction mixture (see Section 4.3.3.1). As before a precipitate was formed upon addition of the sample to the loading buffer. Hence, it was spun for a longer period of time (40 minutes) and at a higher speed (6,000 G) on a Sorvall Superspeed RC2-B centrifuge. However, this procedure also failed to remove all the precipitate thus, once again all of the remaining turbid sample was loaded on to the cation exchange column. The elution profile was identical to that obtained with the mixed anhydride reaction mixture, and as before, various fractions from across the elution profile were analysed for conjugate by percentage inhibitions. The results of the inhibition studies are given in Table 4.2 below.

Table 4.2 *Percentage Inhibition of Fractions resulting from an Active Ester 3:1 E1G:HEWL Conjugation after Purification on a CM Sepharose Fast Flow (Non-urea) Column*

Fraction	% Inhibition
peak fraction of small peak	27
leading edge of main peak	32
peak fraction of main peak	85
trailing edge of main peak	82

Thus, the conjugate was once again found to be distributed across the peaks with the proportion of conjugate increasing towards the trailing edge of the main peak i.e. the conjugate had a tendency to be eluted last despite the fact that it would have had less overall positive charge than the unreacted lysozyme. Hence, it appears the attachment of the non-polar steroid molecules to lysozyme is affecting the elution behaviour of the conjugate and its separation from lysozyme. Furthermore, although it is theoretically possible to separate material with a reasonable degree of inhibition from the trailing edge of the main peak and rechromatograph it, this is clearly not satisfactory as a purification procedure.

4.3.3.3 Purification of Combined Hen Egg White Lysozyme Estrone Glucuronide Conjugates by CM Sepharose Chromatography in Seven Molar Urea

Due to the very poor separation of conjugate from lysozyme obtained on CM Sepharose fast flow columns using pH 6.0 buffers, it was decided to combine the protein fractions from both conjugations together, as indicated by the A_{280} values, and investigate their behaviour in 7 M urea. The combined fractions were concentrated to a volume of approximately 30 mls using a 350 ml capacity diaflow apparatus fitted with a 10,000 molecular weight cut-off filter and then dialysed against Milli-Q water to remove the buffer salts. Because the precipitate is soluble in urea and the conjugates separate in order of their net charges in urea buffers, their utilisation for the purification of conjugate was expected to result in a much higher resolution of the conjugate and lysozyme peaks from each other than was obtained using procedures which utilised the non-urea buffers. Furthermore, although urea does cause denaturation of the protein, the conjugates will renature upon removal of the urea by dialysis (Parente & Wetlaufer, 1984; Goldberg *et al.*, 1991). Thus, although the use of urea buffers meant that conjugate enzymic activity i.e. percentage inhibition could potentially be adversely affected, the percentage inhibitions were sacrificed at this stage in the purification in favour of the greater requirement to obtain a separation of conjugate from unreacted lysozyme.

After concentration and dialysis, the combined protein fractions had a final volume of 30 mls and the concentrated conjugate solution was purified on a CM Sepharose fast

flow column using the following urea buffers:

Buffer A - 10 mM $NaH_2PO_4.2H_20$ in 7 M urea (pH 6.0).

Buffer B - 10 mM $NaH_2PO_4.2H_20$ in 7 M urea + 1 M NaCl (pH 6.0)

i.e. these are the same buffers as used in the previous purification on a CM Sepharose fast flow column except with 7 M urea added.

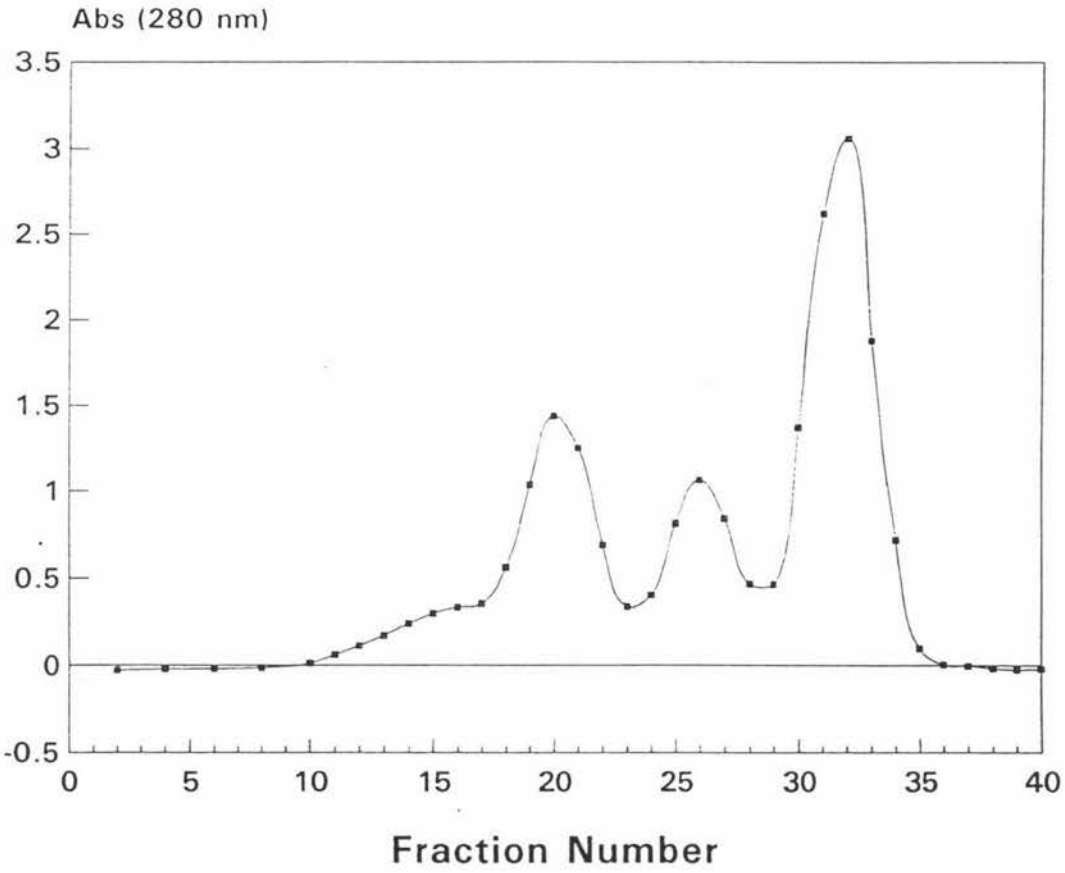

Figure 4.6 *A_{280} profile for the Purification of the Combined Fractions of a Mixed Anhydride (2:1 Molar Ratio of E1G:HEWL) and Active Ester Conjugation (3:1 Molar Ratio of E1G:HEWL) on a CM Sepharose Fast Flow Cation Exchange Column using 7 M Urea Buffers*

Conditions: sample preparation - equilibrated with 15% buffer B by addition of buffer components and making up to volume with Milli-Q water; volume loaded - 60 mls; flow rate - 1 ml min^{-1}; gradient 15-30% buffer B in 500 minutes, 30-40% buffer B in 50 minutes, held at 40% buffer B for 210 minutes; fraction collection 10 ml 10 min^{-1}.

The 30 ml sample was prepared for loading by the addition of the correct quantities of

the buffer components and Milli-Q water to make a final volume of 60 mls which was equivalent to the sample being equilibrated in 15% buffer B (0.15 M NaCl). The sample was then loaded onto the column pre-equilibrated with 15% buffer B (0.15 M NaCl) and elution was undertaken using an increasing salt gradient and a flow rate of 1 ml min^{-1}. A gradient of 15-30% buffer B (i.e. 0.15-0.30 M NaCl) in 500 minutes

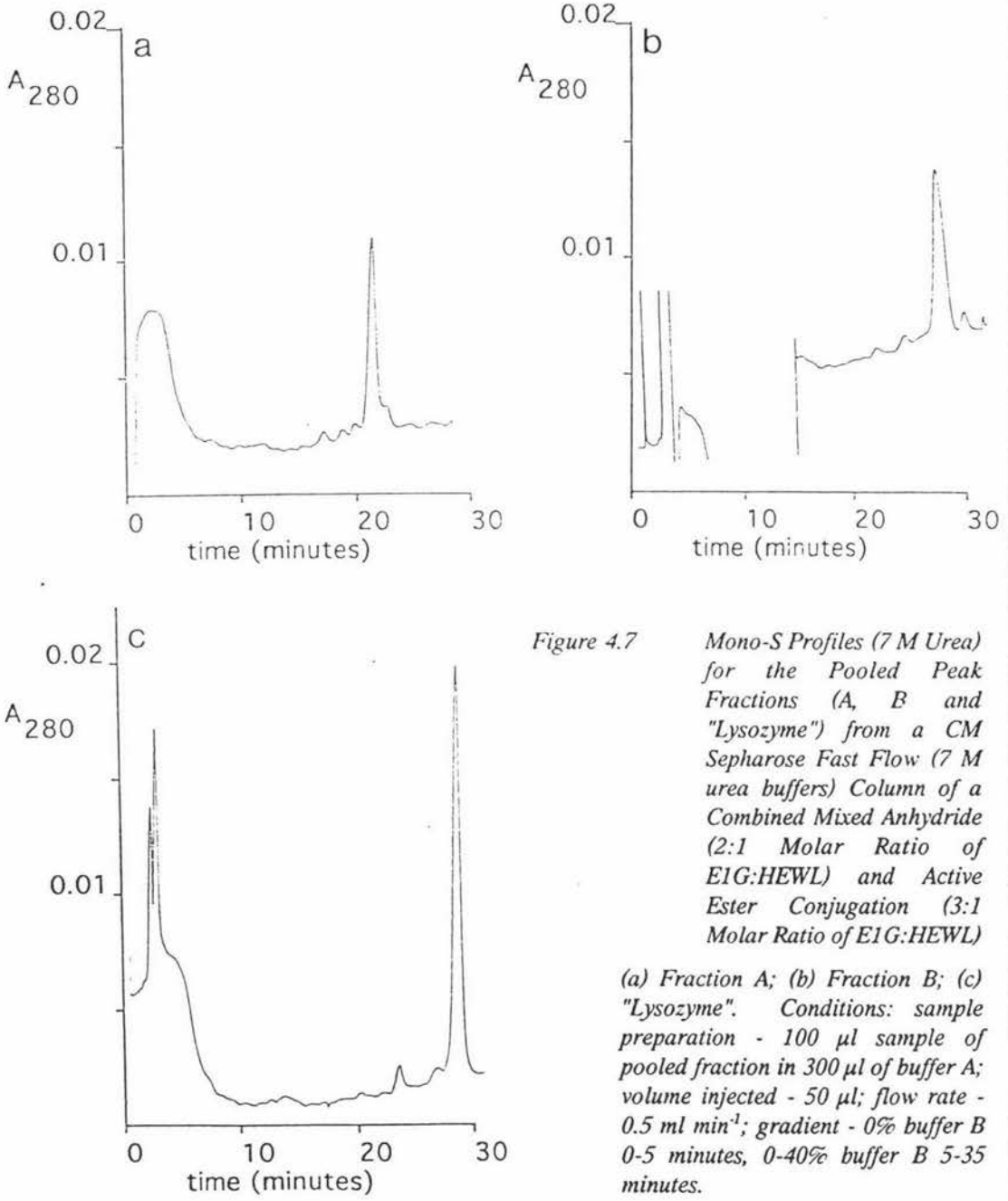

Figure 4.7 *Mono-S Profiles (7 M Urea) for the Pooled Peak Fractions (A, B and "Lysozyme") from a CM Sepharose Fast Flow (7 M urea buffers) Column of a Combined Mixed Anhydride (2:1 Molar Ratio of E1G:HEWL) and Active Ester Conjugation (3:1 Molar Ratio of E1G:HEWL)*

(a) Fraction A; (b) Fraction B; (c) "Lysozyme". Conditions: sample preparation - 100 µl sample of pooled fraction in 300 µl of buffer A; volume injected - 50 µl; flow rate - 0.5 ml min^{-1}; gradient - 0% buffer B 0-5 minutes, 0-40% buffer B 5-35 minutes.

followed by a 30-40% gradient (0.30-0.40 M NaCl) in 50 minutes, and isocratic elution at 40% buffer B (0.40 M NaCl) for a further 210 minutes, was used to elute the sample

i.e. the same gradient was used as for the previous purification with non-urea buffers.

Figure 4.6 shows the elution profile to consist of three peaks which have been labelled A, B and "lysozyme" in order of elution. The pooled fractions for each of these peaks were analysed for the different conjugate families and lysozyme by running samples through the analytical Mono-S column in 7 M urea (see Figures 4.7 (a), (b) and (c) for elution profiles and column conditions). However, because of the dilute nature of the conjugate after the CM Sepharose fast flow chromatography, when the conjugate samples from the 7 M urea column were analysed on the Mono-S column, they gave very poor quality Mono-S traces with the attenuator of the UV monitor having to be set at, or near, maximum sensitivity. Thus, very small aliquots of the peak fractions were also saved for later analysis on the newly installed Pharmacia SMART system which was capable of producing high resolution hydrophobic interaction chromatography profiles on very small sample volumes (5-20 μl).

Despite the poor quality of the Mono-S elution profiles they did show that conjugate peak A from the CM Sepharose fast flow column (7 M urea) consisted mostly of the E3 conjugate family with only trace amounts of free lysozyme present (see Figure 4.7 (a)), while the Mono-S profile of the conjugate peak B (Figure 4.7 (b)) consisted mostly of the E1 conjugate family although once again there were still trace amounts of lysozyme present. The Mono-S trace of the last peak labelled "lysozyme" showed it to clearly contain the vast majority of the free lysozyme (see Figure 4 (c)). Thus, the utilisation of the CM Sepharose column in conjunction with 7 M urea buffers appears to be an effective method for separating the different conjugate families from lysozyme and from each other as long as the structural integrity of the lysozyme is not a paramount consideration.

One feature of these Mono-S traces which became apparent upon their comparison with the Mono-S traces obtained from the original reaction mixtures was the conspicuous absence of the early eluting more highly substituted conjugate families, E4, E5, and E6. There are two possible explanations for this disappearance of half the different conjugate families. Either they were removed during centrifugation of the reaction mixtures, or they precipitated out onto the first CM Sepharose fast flow column in the absence of 7 M urea at the high salt concentrations necessary for elution. This precipitation effect

is probably the result of the more highly substituted conjugates being more non-polar because of the strongly hydrophobic nature of their attached steroid groups. Thus, under conditions of high salt concentrations and in the absence of urea, the most highly substituted conjugates become salted out. These precipitated conjugates would then be removed either by centrifugation or by their failure to be eluted off the non-urea columns. It is likely in the above attempts at purification that the two effects acted in concert to remove the E4, E5 and E6 conjugate families. Interestingly, this explanation does require there to be some hydrophobic interaction effects between the CM Sepharose fast flow column and lysozyme.

After the Mono-S elution profiles confirmed the success of the 7 M urea CM Sepharose fast flow column in the purification of HEWL-E1G conjugate, the peak fractions of the conjugate peaks A and B were tested for percentage inhibitions with E1G antibodies using standard procedures (see Section 4.2.5). The results were lower than expected given that neither fraction A nor B, contained significant amounts of lysozyme, with the peak fraction of the conjugate A peak having an inhibition of 71% and the conjugate B peak fraction having an inhibition of only 53%. The reason for this is not clear but may relate to the conjugate folding incorrectly on dialysis from the 7 M urea solution (Goldberg *et al.*, 1991) or possibly from carbamylation of lysozyme itself. This latter factor would give rise to a lysozyme which has two units less positive charge than native lysozyme since a lysine residue is converted from an amino group to a carbamic acid group. Such a species would co-elute with a di-substituted E1G-lysozyme conjugate but would not be inhibited by the E1G antibody. Clearly a second chromatographic step may increase the percentage inhibition if the second possibility occurs or alternatively the cyanate content of the urea could be reduced by standard procedures (e.g. holding at low pH or passing through a mixed bed resin) thus, avoiding the problem. Regardless, of the cause of this phenomenon, the 7 M urea column did satisfactorily achieve the goal of removing the unreacted lysozyme.

4.3.3.4 Effect of Varying Ratios of Estrone Glucuronide Active Ester to Hen Egg White Lysozyme

Although, the active ester method was the preferred method due to the relative ease with which it could be performed compared with the mixed anhydride method, further

conjugations using both methods were carried out in an attempt to optimise the conditions for both procedures. The optimum conditions were defined as those which maintained the production of high levels of conjugate relative to free lysozyme, and still ensured the formation of only minimal levels of the highly substituted conjugates. This requirement for conjugates with only low levels of substitution is based on the experience in Melbourne that the highly substituted conjugates do not normally provide the best conjugate for the Ovarian Monitor assay. This is because more antibody is required to neutralise the lysozyme activity of the more highly substituted lysozyme conjugates compared to the conjugate species with only low levels of substitution. Because high levels of antibody result in the shifting of the standard curve towards higher hormone concentrations, the assay becomes less sensitive to changes in urinary hormone concentrations. Thus, for the assay to be maintained under optimum conditions, ideally only low substituted conjugates should be utilised (i.e one E1G per lysozyme molecule).

In an attempt to reduce the level of highly substituted conjugates which was experienced when a ratio of E1G:HEWL of 3:1 was used in the previous active ester conjugation, another active ester conjugation was performed where the ratio of E1G to HEWL was reduced to 1.5:1. Because of the good separation obtained previously on the 7 M urea CM Sepharose fast flow column of conjugates from lysozyme, this conjugation, and all future conjugations were processed directly using urea buffers on the CM Sepharose fast flow column as a first purification step.

This conjugation was carried out essentially as described in Section 4.2.2.3 using the following quantities of reagents: 113.4 mg HEWL (7.9 μmol) purified as in Section 4.2.4 and dissolved in 4 mls of 1% sodium bicarbonate solution, 5.3 mg E1G-(H) (12 μmol) dissolved in 100 μl DMF, 21 μl NHS dissolved in DMF (70 mg ml^{-1}, 12 μmol), and 21 μl DCC dissolved in DMF (130 mg ml^{-1}, 13 μmol). The active ester reagent was added slowly to the HEWL solution with stirring approximately one hour after its formation. The addition of the active ester reagent to the HEWL solution was again associated with the immediate formation of a slight precipitate. Throughout the conjugation the pH remained relatively stable at around pH 8.55.

The reaction mixture was analysed again under standard conditions on the Mono-S

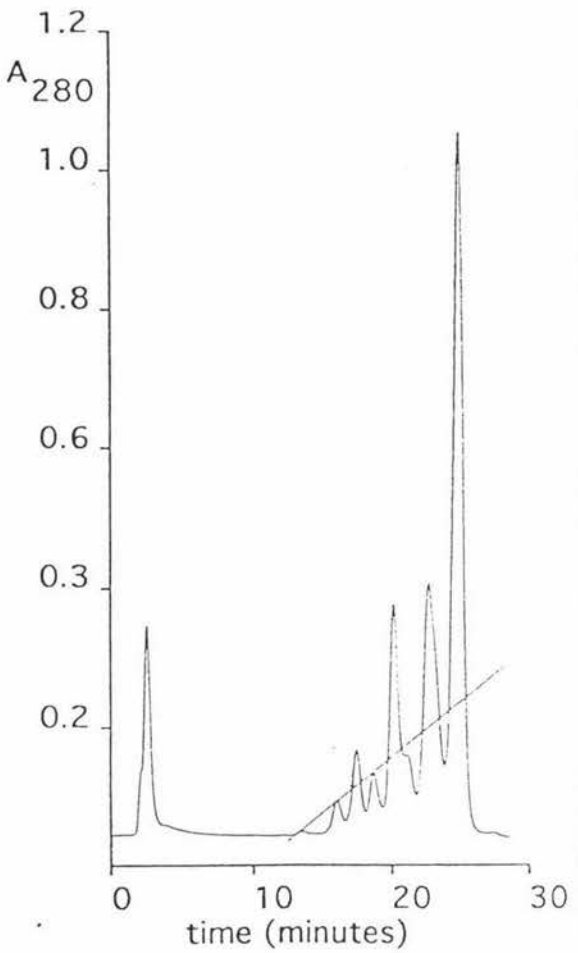

Figure 4.8 *7 M Urea Mono-S Profile for the Reaction Mixture of a HEWL-E1G Conjugation Synthesised by the Active Ester Method using a Molar Ratio of E1G:HEWL of 1.5:1*

Conditions: sample preparation - 50 µl of reaction mixture in 300 µl of buffer A; volume injected - 50 µl; flow rate - 0.5 ml min^{-1}; gradient - 0% buffer B 0-5 minutes, 0-30% buffer B in 5-35 minutes.

column to give the elution profile shown in Figure 4.8 (see figure legend for column conditions). Figure 4.8 shows the conjugation to have been successful, with 53% of the original lysozyme conjugated based on relative peak heights compared to 65% for the previous active ester conjugation (3:1 molar ratio of E1G:HEWL). Of the conjugated lysozyme, the E1 and E3 conjugate families predominated accounting for 37% and 30% of the conjugate yield respectively. Compared to the previous active ester conjugation, this conjugation was also associated with slightly lower levels of the highly substituted conjugates with the E4, E5 and E6 conjugate families now accounting for only 23% of the total conjugate yield as opposed to the 30% yield experienced previously. Thus, overall it appears that a decrease in the level of highly substituted conjugates can not be achieved without decreasing the total amount of lysozyme conjugated, and does not markedly reduce the levels of the highly substituted conjugates.

After analysis of the active ester conjugation reaction mixture (1.5:1 E1G:HEWL) on the Mono-S column the sample was dialysed to remove the sodium bicarbonate in preparation for loading onto the CM Sepharose fast flow column (7 M urea). The

column conditions are recorded in the figure legend of the resulting elution profile (Figure 4.9) and were essentially the same as those used for purifying conjugate from

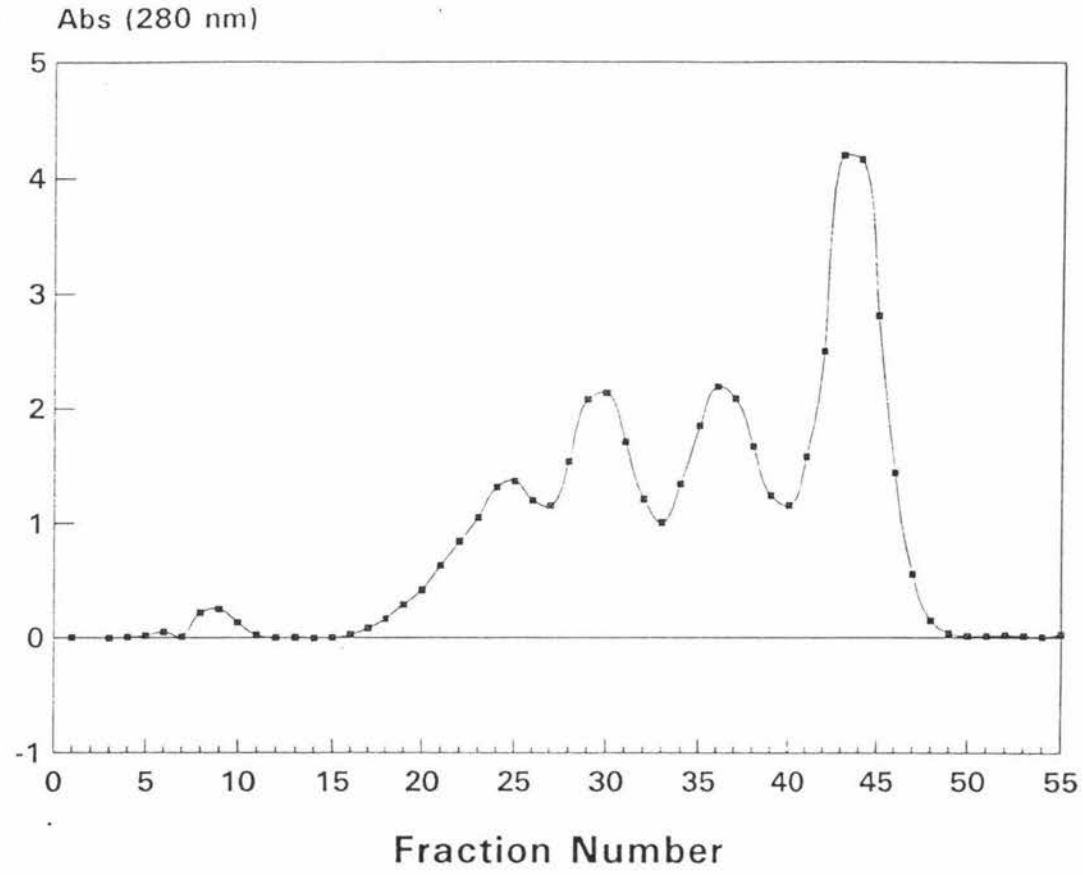

Figure 4.9 *A_{280} Profile for the Purification of the Reaction Mixture of an Active Ester Conjugation (Molar Ratio E1G:HEWL 1.5:1) on a CM Sepharose Fast Flow Cation Exchange Column using 7 M Urea Buffers*

Conditions: sample preparation - equilibrated with 15% buffer B by addition of buffer components and making up to volume with Milli-Q water; volume loaded - 8 mls; flow rate - 1 ml min^{-1}; gradient 15-27% buffer B in 400 minutes; fraction collection - 5 ml 5 min^{-1}.

the combined mixed anhydride/active ester conjugations (see Section 4.3.3.3) except for the gradient which was substantially shortened by running from 15 to 27% buffer B (0.15-0.27 M NaCl) in 400 minutes. The elution profile differed from that obtained previously with the combined mixed anhydride/active ester conjugate purification only in that it now contained an extra broad peak which eluted just before the conjugate A peak. This peak was in the same position as the gradient leading up to the conjugate A peak in the combined mixed anhydride/active ester conjugate purification (see Figure 4.6). As previously, fractions were saved from the peak tubes for analysis on the

SMART system and inhibition studies. The results of the inhibition studies are shown in Table 4.3

Table 4.3 *Percentage Inhibition of Fractions resulting from an Active Ester 1.5:1 E1G:HEWL Conjugation after Purification on a CM Sepharose Fast Flow 7 Molar Urea Column*

Fraction	% Inhibition
"Early eluting" fraction	86
"Conjugate A" peak fraction	79
"Conjugate B" peak fraction	55
"Lysozyme" peak fraction	0

All four peaks (i.e. the extra peak, the conjugate A and B peaks, and the "lysozyme peak") were analysed on the Mono-S column (7 M urea). The elution profiles for the conjugate A, B and lysozyme peaks were essentially identical to the equivalent profiles previously obtained from the combined mixed anhydride/active ester conjugation purification. As previously, the conjugate A and B peaks consisted almost exclusively of conjugate from the E3 and E1 families respectively and the "lysozyme" peak consisted almost exclusively of lysozyme. The extra "early eluting" peak, as would be expected if separation was on the basis of charge, consisted predominantly of the E4, E5 and E6 conjugate families and smaller amounts of E3 and lysozyme. As would be expected the degree of inhibition was reduced as the tubes were taken nearer the lysozyme peak.

Thus, the Mono-S trace of this "early eluting" peak supported the proposal that 7 M urea was necessary for the isolation of the highly substituted conjugate families with the CM Sepharose fast flow column and in its absence the highly substituted conjugate families were removed by precipitation on the column with the increasing NaCl gradient (compare Figure 4.6 with Figure 4.9). This effect is a serious disadvantage for purification schemes not involving 7 M urea when high degrees of substitution by the

steroid groups are encountered.

4.3.3.5 Further Optimisation of both the Mixed Anhydride and Active Ester Methods

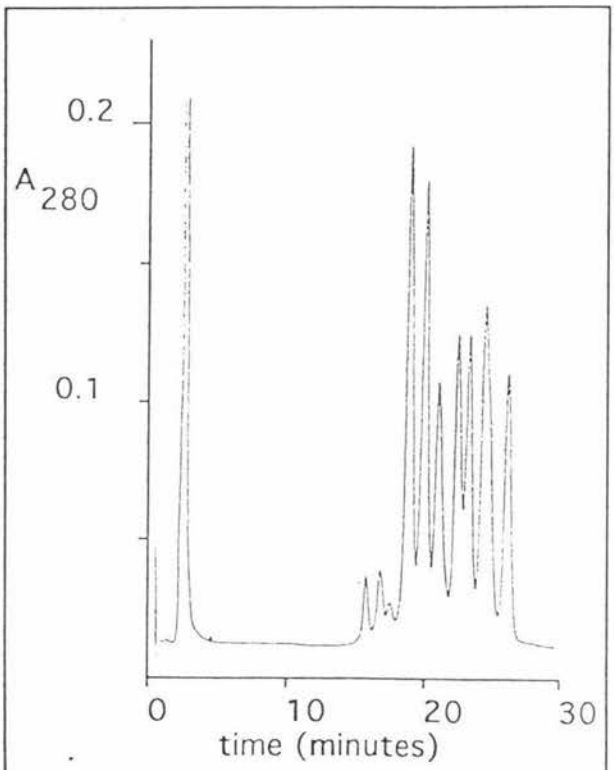

Figure 4.10 *7 M Urea Mono-S Profile for a 3:1 E1G:HEWL Active Ester Conjugation Performed in the Presence of a 50% Excess of Coupling Reagents*

Conditions: sample preparation - 50 µl sample in 300 µl of buffer A; volume injected - 50 µl; flow rate - 0.5 ml min^{-1}; gradient - 0% buffer B 0-5 minutes, 0-40% buffer B 5-45 minutes.

Figure 4.10 shows the Mono-S profile (7 M urea) of a 3:1 E1G:HEWL active ester reaction mixture. This active ester conjugation was carried out essentially as for the previous 3:1 active ester conjugation (see Section 4.3.3.2) except that a 50% excess of DCC and NHS was used i.e. the moles of DCC and NHS were both 1.5 times higher than the moles of E1G. The Mono-S elution profile for the conjugation performed with an excess of coupling reagents showed the conjugation to have been more successful in terms of the total percentage of lysozyme conjugated having a conjugation rate of 89% compared to the previous yield of 65% i.e. only 11% of the lysozyme in the original reaction mixture was not conjugated. However, as seems to be the common trend with an increase in the percentage conjugate yield, there was also a drastic increase in the number and percentage of highly substituted conjugates with the E1, E2 and E3 conjugates only accounting for 39% of the total conjugate yield in this conjugation as opposed to the previous percentage yield of 70%.

One feature of particular interest of this conjugation's Mono-S profile compared to the Mono-S profile obtained with the 3:1 E1G:HEWL ratio and no excess of reagents (see

Figure 4.3 (a) to compare) was that there was now three extra very early eluting conjugate peaks appearing on the trace which had not been seen on the Mono-S traces for any of the previous conjugations. This showed that the supposition of one peak for each level of steroid substitution must be incorrect as there is only a total of seven potential steroid binding sites on each lysozyme molecule, and there was now a total of nine conjugate peaks.

Thus, in summary the above conjugation proved that a 50% excess of DCC and NHS was effective in increasing the efficiency of the reaction i.e. the level of conjugation for a given ratio of E1G:HEWL. It was because of this, in conjunction with the fact that the 3:1 conjugation was now associated with an even higher percentage of highly substituted conjugates (E4 or higher), that it was decided to examine the effect a 50% excess in the amount of coupling reagents would have on the level of lysozyme conjugation when a lower ratio of E1G to HEWL was employed. The ratio selected was 1.5:1 (E1G:HEWL) which was the same ratio which had up to this stage resulted in the best conjugation as evidenced by the Mono-S trace (see Figure 4.8) in terms of the total percentage of lysozyme converted into low substitution conjugates.

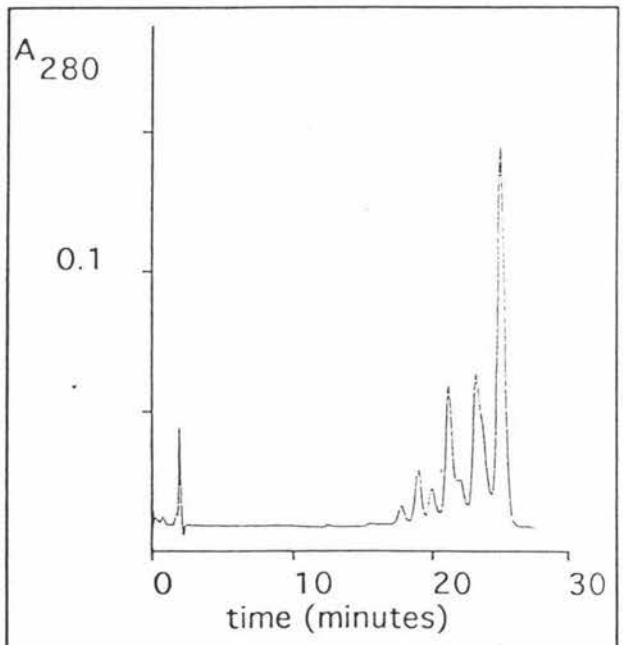

Figure 4.11 *7 M Urea Mono-S Profile for a 1.5:1 E1G:HEWL Active Ester Conjugation Performed in the Presence of a 50% Excess of Coupling Reagents*

Conditions: sample preparation - 50 µl sample in 300 µl of buffer A; volume injected - 50 µl; flow rate - 0.5 ml min^{-1}; gradient - 0% buffer B 0-5 minutes, 0-40% buffer B 5-45 minutes.

However, when the Mono-S traces of the two 1.5:1 conjugation ratios were compared, the 7 M urea Mono-S profiles were remarkedly similar (see Figure 4.11 for the trace of the conjugation performed with an excess of reagents). Thus, this indicated that the utilisation of an excess of DCC and NHS relative to the quantity of E1G was not

effective in increasing the percentage conjugate yield at a ratio of E1G:HEWL of 1.5:1. However, for the conjugation in which the active ester reagent was made up in the absence of an excess of reagents, the active ester reagent was also made in a much lower total volume of DMF (i.e. only 140 µl as opposed to 220 µl). Thus, it may be that the efficiency of the reaction is increased by two factors; firstly by using an excess of DCC and NHS relative to the moles of E1G, and secondly by synthesising the active ester reagent in a small total volume i.e. there is also a concentration effect. Hence, in conclusion it appears that the same level of conjugation can be achieved using a lower ratio of E1G:HEWL by using an excess of DCC and NHS, and by using a smaller reaction volume for the synthesis of the active ester reagent. This means that the amount of active ester required for any given E1G:HEWL conjugation ratio can be reduced, which is a particularly significant finding as it is the E1G which is expensive to make in terms of time and starting material.

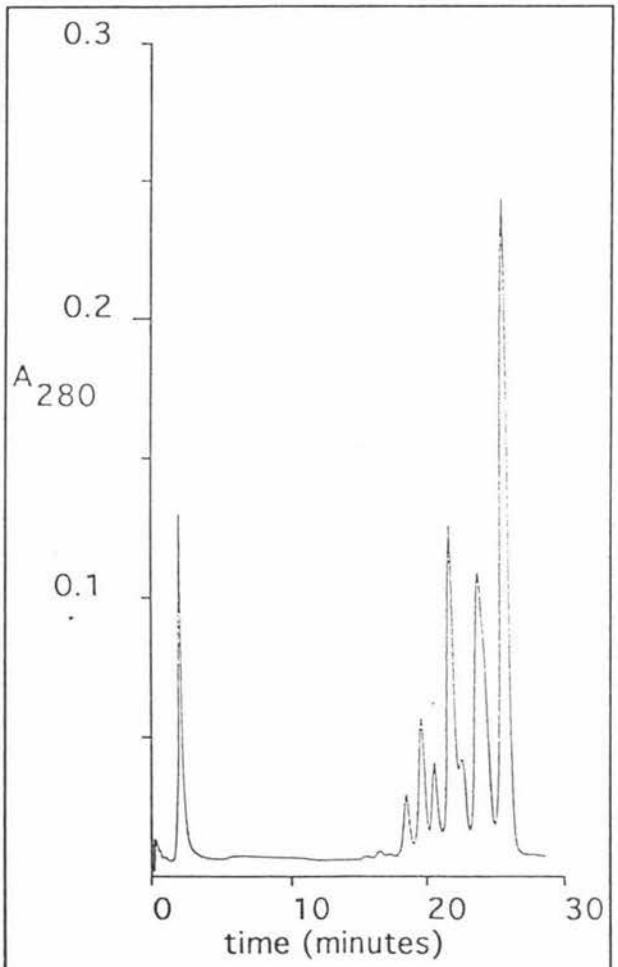

Figure 4.12 *7 M Urea Mono-S Profile for an E1G:HEWL Active Ester Conjugation by Titration Performed in the Presence of a 50% Excess of Coupling Reagents*

Conditions: sample preparation - 50 µl sample in 300 µl of buffer A; volume injected - 50 µl; flow rate - 0.5 ml min^{-1}; gradient - 0% buffer B 0-5 minutes, 0-40% buffer B 5-45 minutes.

A further active ester conjugation was also performed in order to determine if the precipitation was, as presumed, highly substituted conjugate. The active ester reagent was synthesised essentially as in the first 3:1 active ester conjugation (see Section 4.3.3.2.) except it used a 50% excess of DCC and NHS relative to the amount of

E1G. This active ester reagent was then used to titrate a 1% sodium bicarbonate HEWL solution (4 mls, 100 mg) until the formation of the first precipitate. From the volume of active ester reagent added it was calculated that a total amount of 6.9 μmoles of E1G was utilised in the conjugation. This corresponds to a ratio of E1G:HEWL of 1.1:1 and gave the following Mono-S trace in 7 M urea (see Figure 4.12). Thus, it appears for the active ester reaction even with a 1.1:1 ratio of E1G:HEWL and with titration to the first

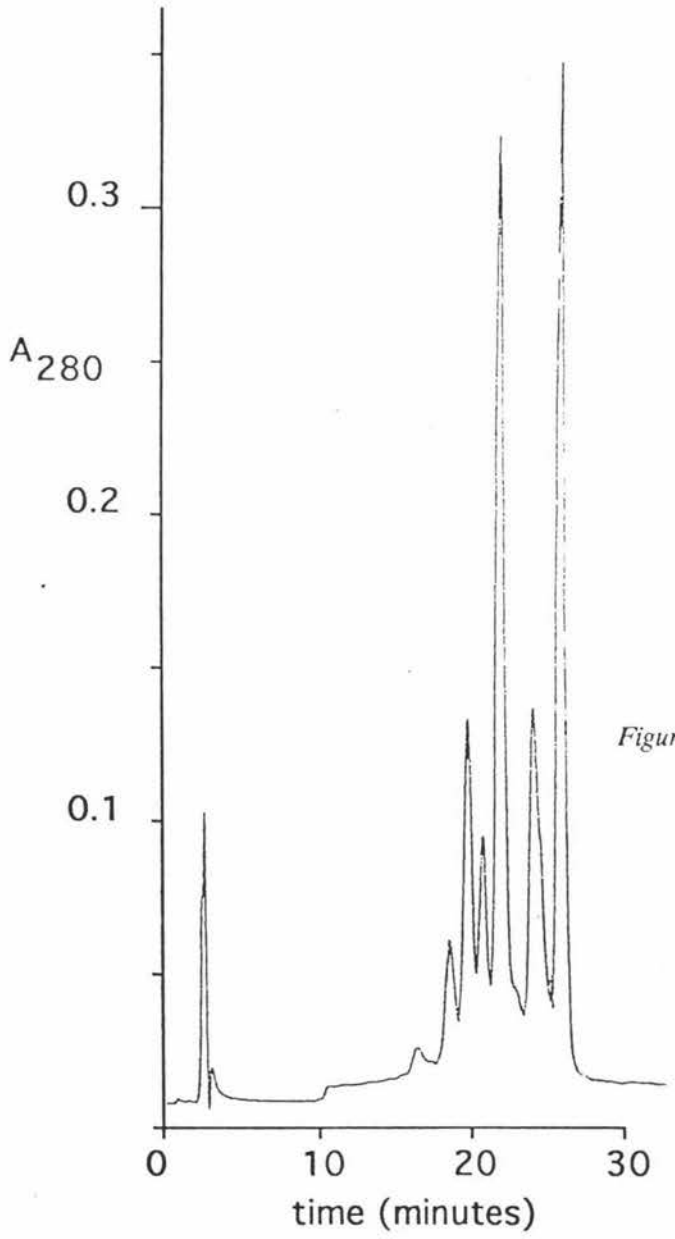

Figure 4.13 *7 M Urea Mono-S Profile for a 3:1 E1G:HEWL Mixed Anhydride Conjugation Performed in the Presence of a 50% Excess of Coupling Reagents*

Conditions: sample preparation - 50 μl sample in 300 μl of buffer A; volume injected - 50 μl; flow rate - 0.5 ml min^{-1}; gradient - 0% buffer B 0-5 minutes, 0-40% buffer B 5-45 minutes.

appearance of precipitate, there are still substantial quantities of the highly substituted

conjugates formed with the conjugate families of E4 and higher contributing over 30% of the total conjugate yield.

A mixed anhydride conjugation using an E1G:HEWL ratio of 3:1 was also performed according to the protocol outlined in Section 4.2.1.3. The conjugation was performed using the following quantities: 100 mg HEWL (7 μmol) purified as in Section 4.2.4 and dissolved in 4 mls of Milli-Q water, 10 mg E1G-(H) (22.6 μmol), 220 μl DMF, 5.3 μl TNB (23.3 μmol), and 3.0 μl IBC (23.3 μmol). These conditions were comparable to the earlier 3:1 active ester conjugation which was performed using a 50% excess of DCC and NHS because they used the same volume of DMF, the same ratio of E1G:HEWL, the same number of moles of E1G and HEWL, and the HEWL was dissolved in the same total volume. Thus, by comparing the 7 M urea Mono-S traces obtained with the two different reaction mixtures, a direct comparison could be made between the two different methods in terms of the total conjugate yield and the distribution of this yield between the high and low substituted conjugates. Figure 4.13 shows the 7 M urea Mono-S profile obtained with mixed anhydride conjugation while Figure 4.10 shows the 7 M urea Mono-S profile obtained with the active ester conjugation. By comparing these two Mono-S traces, it becomes apparent that under equivalent conditions conjugations performed using the mixed anhydride method are associated with a lower total conjugate yield (i.e. 69% versus 90% for the active ester method). The mixed anhydride conjugate fraction was also associated with less of the highly substituted conjugates with the mixed anhydride conjugation having 36% of its conjugate belonging to the E4 conjugate family or higher as opposed to over 60% for the active ester conjugation.

The reason for the different discrimination of the two reagents for the available lysine sites on lysozyme is not clear but it is a significant finding. Despite the fact that the active ester conjugation reaction is more convenient, the quality of the conjugate produced by the mixed anhydride method may be superior (i.e. more discrete populations of lower substituted conjugates) when the immunoassay results are considered. However, this does not effect the discussions relating to the subsequent purification of HEWL-E1G conjugate.

4.3.3.6 Attempted Removal of Hen Egg White Lysozyme by Precipitation with Sodium Chloride

A further active ester conjugation was performed in order to investigate the possibility that the predisposition of the highly substituted conjugates to precipitate out at high salt concentrations which was disadvantageous during cation exchange chromatography nevertheless could be utilised as a method for separating lysozyme from the conjugates. Furthermore, the differential solubility of the conjugates might also fractionate them into low and highly substituted fractions.

This conjugation was carried out essentially as described in Section 4.2.2.3 and used a ratio of E1G:HEWL of approximately 1.6:1. The following quantities of reagents: 110 mg HEWL (7.7 μmol) purified as in Section 4.2.4 and dissolved in 4 mls of 1% sodium bicarbonate solution, 5.3 mg E1G-(H) (12 μmol) dissolved in 200 μl DMF, 20 μl NHS dissolved in DMF (70 mg ml^{-1}, 12 μmol), and 20 μl DCC dissolved in DMF (130 mg ml^{-1}, 13 μmol). The active ester reagent was added to the HEWL solution approximately one hour after synthesis. The addition of the active ester reagent to the HEWL solution was associated with the immediate formation of a slight precipitate which increased with time.

The precipitation experiment was performed on a small aliquot (1 ml) removed from the conjugation reaction mixture. The rest of the conjugate from the remaining reaction mixture was dialysed to remove the sodium bicarbonate and then prepared, loaded, and eluted from a CM Sepharose fast flow column using 7 M urea buffers according to the same protocol used for purifying conjugate from the combined mixed anhydride/active ester conjugations (see Section 4.3.3.3). The elution profile was very similar to the one obtained previously under the same conditions (see Figure 4.6) and as previously, fractions were saved from the peak tubes for analysis on the SMART system.

For this experiment, a conjugate fraction was precipitated out of the 1 ml aliquot from the reaction mixture by dialysis against 1 M NaCl (100 mls x 3 changes). The precipitate was then spun down by centrifugation for 15 minutes (Gallenkamp bench centrifuge, speed 5) and the resulting supernatant carefully removed using a pasteur pipette. The remaining precipitate was washed with 1 M NaCl solution (1 ml) and recentrifuged (15 minutes, speed 5) and the resulting supernatant combined with the

supernatant from the first centrifugation (conjugate fraction 1). The combined precipitate fraction was then redissolved in Milli-Q water (2 mls) and redialysed against 1 M NaCl solution (100 mls x 2 changes). After dialysis the sample was centrifuged (15 minutes, speed 5) as before to remove the precipitate. The resulting supernatant (conjugate fraction 2) was decanted, and the precipitate was redissolved in 1 ml Milli-Q

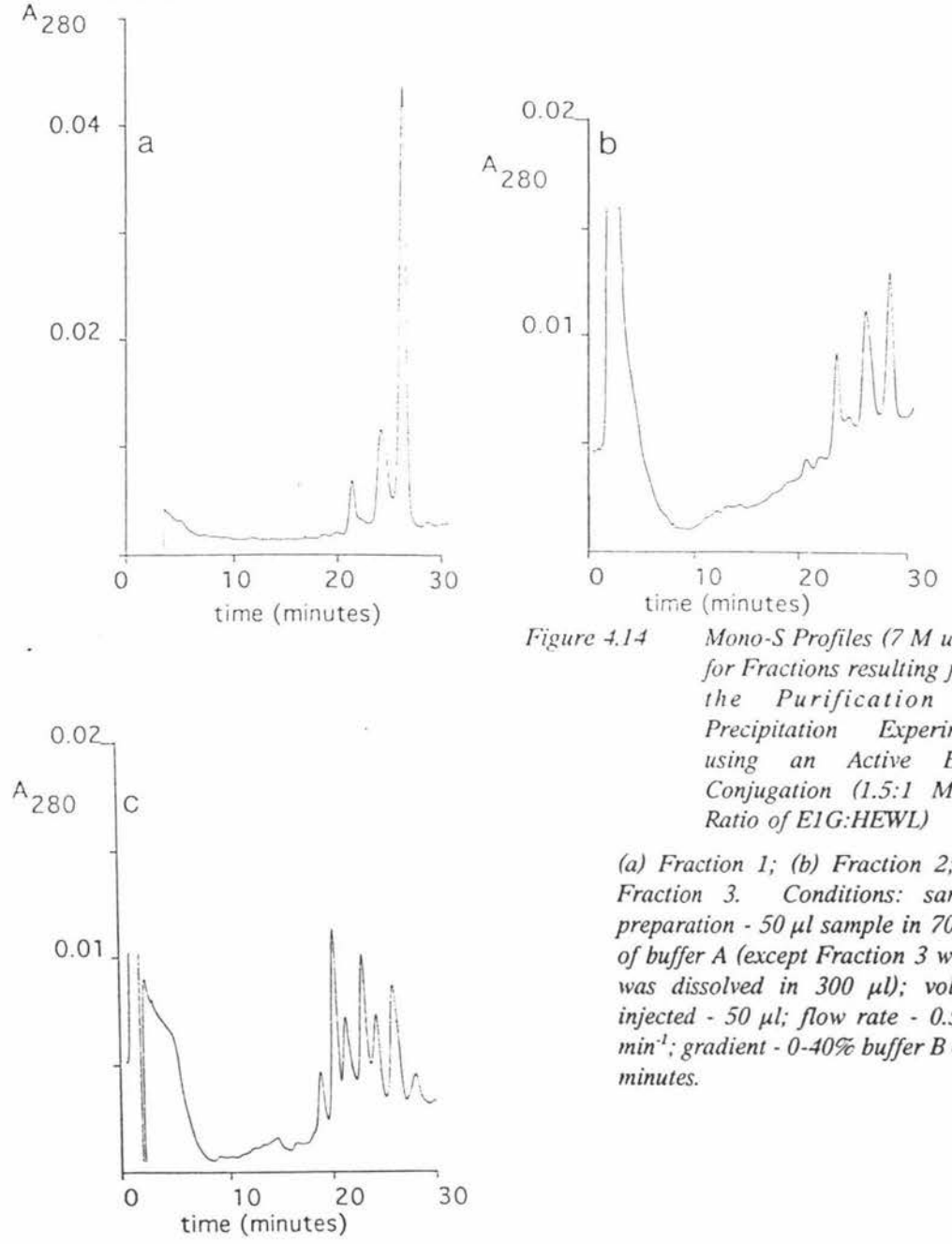

Figure 4.14 *Mono-S Profiles (7 M urea) for Fractions resulting from the Purification by Precipitation Experiment using an Active Ester Conjugation (1.5:1 Molar Ratio of E1G:HEWL)*

(a) Fraction 1; (b) Fraction 2; (c) Fraction 3. Conditions: sample preparation - 50 µl sample in 700 µl of buffer A (except Fraction 3 which was dissolved in 300 µl); volume injected - 50 µl; flow rate - 0.5 ml min^{-1}; gradient - 0-40% buffer B 0-40 minutes.

water (conjugate fraction 3). The three conjugate fractions were then analysed on the Mono-S column using 7 M urea buffers for differences in the distribution of the

different conjugate families. The Mono-S profiles are shown in Figure 4.14 (see figure legends for details of the column conditions).

If this purification by precipitation procedure had been successful, it would be expected that the combined supernatant fraction (i.e. fraction 1) would consist predominantly of the most soluble, lowly substituted conjugates and have a large free lysozyme component. Furthermore, fraction 2 would be expected to consist predominantly of the next most soluble components, and fraction 3 would have a very high proportion of the least soluble, very highly substituted conjugates and very little lysozyme.

The Mono-S traces were found to correlate roughly with these predictions with fraction 1 (Figure 14 (a)) consisting predominantly of lysozyme and small amounts of the low substituted conjugates. Fraction 2 (Figure 14 (b)) was found to consist of roughly equal amounts of free lysozyme, and E1 and E3 conjugate families, while fraction 3 (Figure 14 (c)), in contrast, showed significant quantities of free lysozyme and all six different conjugate families. Thus, each of the three fractions generated from the above procedure were found to have their own distinctive range of predominant conjugate families but all were associated with varying levels of lysozyme. In summary, the method was quite effective in separating the highly substituted conjugates from a significant proportion of the lowly substituted conjugates. However, because it failed to separate the desired conjugate families from lysozyme, the method could not be adopted as a step in a standard conjugate purification procedure.

4.3.3.7 Analysis of Hen Egg White Lysozyme Estrone Glucuronide Conjugates with the SMART System; Evidence for Important Hydrophobic Effects

The Pharmacia SMART micro-chromatographic system was not available at the time any of the previously mentioned conjugations and associated column chromatography were performed. However, when it became available for departmental reasearch, it was used to analyse the fractions saved from the peaks obtained on the CM Sepharose fast flow column (7 M urea). These fractions were all analysed under identical conditions on a Pharmacia reverse phase μRPC C2/C18 P3.2/3 hydrophobicity column using the following eluents.

Eluent A - 0.05% formic acid + 1% NaCl in water/acetonitrile	1:9
Eluent B - 0.05% formic acid + 1% NaCl in water/acetonitrile	2:3

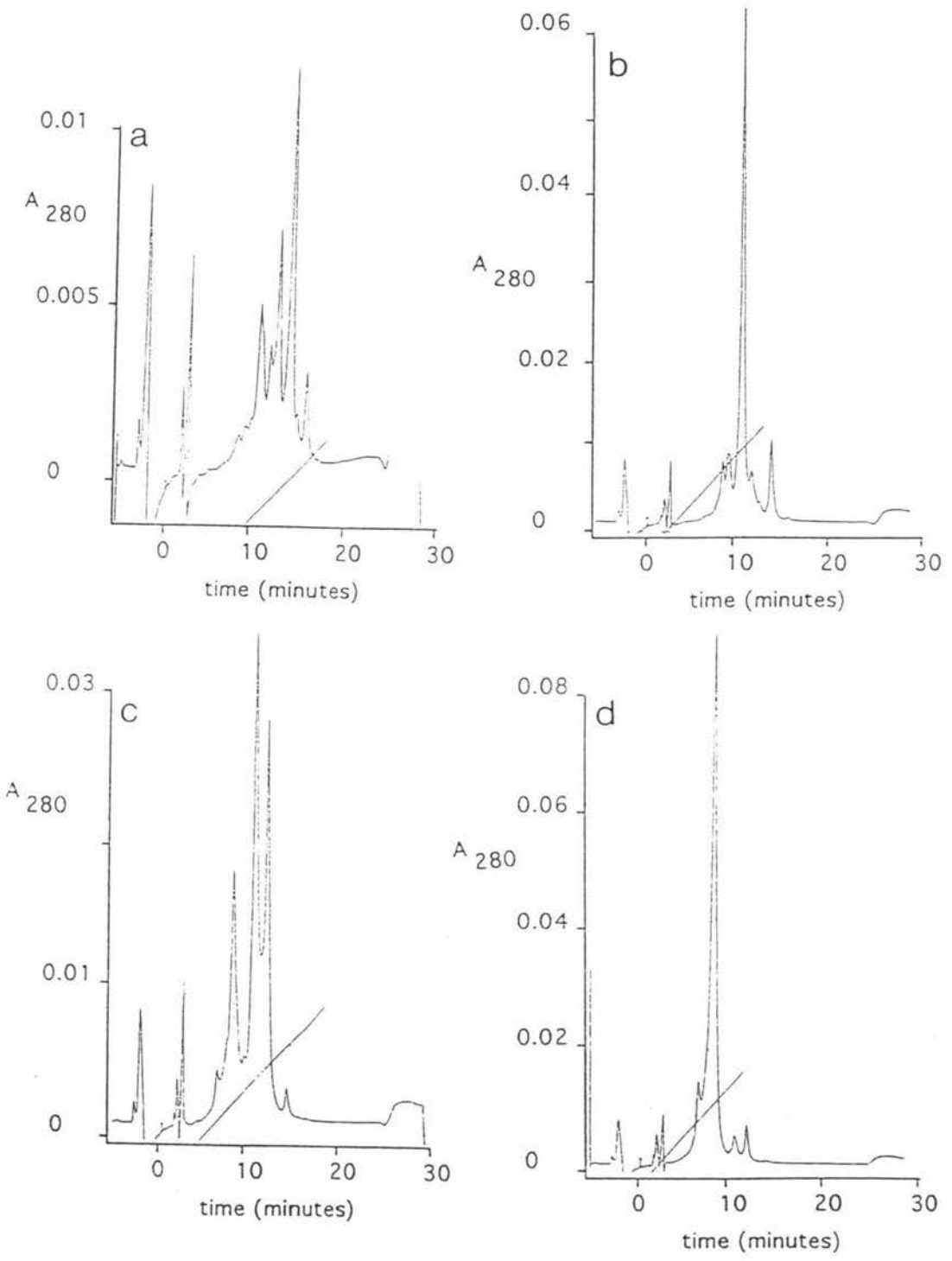

Figure 4.15 *SMART Profile obtained on a Reverse Phase Hydrophobicity Column for Fractions resulting from a CM Sepharose Column on a 1.5:1 E1G:HEWL Active Ester Conjugation*

(a) "early eluting" fraction; (b) conjugate A; (c) conjugate B; (d) "lysozyme" fraction. Conditions: as stated in the text.

Elution was undertaken using a gradient of 50-70% eluent B (i.e. 75-69% acetonitrile) in 20 minutes.

Figure 4.15 show the resulting elution profiles from the SMART system of the four different fractions, obtained from the active ester conjugation which used a molar ratio of E1G:HEWL of 1.5:1, after purification on the CM Sepharose fast flow column (7 M urea) (see Figure 4.9).

Figure 4.15 (d) shows the chromatographic behaviour of the major component of the "lysozyme" fraction which had a retention time of 8.6 minutes. This peak was found in all the other elution profiles and in a position where it preceded almost exclusively all other peaks. This indicates that free lysozyme is one of the least hydrophobic components of the conjugation mixture, which would be expected as it is not conjugated to any hydrophobic steroid groups. Because the addition of a hydrophobic steroid group is associated with the removal of a positive charge, and the Mono-S column separates the components of a sample on the basis of charge, this result was also consistent with the 7 M urea Mono-S elution profiles which showed lysozyme to elute last relative to the different conjugates. Thus, the Mono-S and SMART elution profiles were consistent with respect to the elution of free lysozyme. Furthermore, the SMART reverse phase column profile (see Figure 4.15 (a)) for the "early eluting" fraction from the CM Sepharose fast flow column (7 M urea) showed many peaks with a longer retention time relative to the retention times of the other peak fractions on the reverse phase column. This result was also consistent with the equivalent Mono-S elution profile which showed the components of this "early eluting" fraction from the CM Sepharose fast flow column to have the shortest retention times. In other words, the fraction from the CM Sepharose fast flow column which the Mono-S profiles indicated as containing the lysozyme conjugates with the lowest charges was the same peak as the SMART reverse phase column elution profiles indicated as having the most hydrophobic groups. Thus, once again the elution profiles from the Mono-S cation exchange column and the hydrophobic reverse phase column of the SMART system were consistent.

Another interesting feature of the SMART elution profile of this "early eluting" fraction was that, excluding the lysozyme peak, eight separate peaks and shoulders could be counted on the profile. This value is higher than the number of sites on a lysozyme

molecule available for conjugation to a steroid molecule. One possible interpretation of this observation is that the reverse phase column on the SMART system is distinguishing between lysozyme conjugates with the same total number of steroid substituents, but in which the steroid molecules are conjugated to a different set of lysine residues.

The interpretation of the elution profiles of the conjugate A and B fractions on the reverse phase column was less straight forward (see Figures 4.15 (b) and (c) respectively). The elution profile of the conjugate A fraction showed one major peak, while the elution profile of the conjugate B fraction showed two major peaks, one of which eluted in the same position as the major peak observed in the conjugate A profile. This result is inconsistent with the equivalent Mono-S traces as these traces showed only one major peak for both the fraction A and fraction B elution profiles (see Figures 4.7 (b) and (c)), of which the major peak of the fraction A profile had the shorter retention time. Thus, the two different columns appear to be separating the conjugates into different groups of conjugate species. The best explanation for the above series of results is that although charge and hydrophobicity are in general inversely related, the site of conjugation of the steroid to the enzyme must also be important. If this was the case, this would mean the site of conjugation would be an important determinant of the binding and elution patterns for a given conjugate species on the different columns.

On the evidence of the elution profiles obtained on the SMART system it was concluded that the composition of the conjugate A and B fractions obtained off the various CM Sepharose fast flow columns (7 M urea) were identical for the different conjugations. Thus, on the basis of these elution profiles, the pooled conjugate A and B fractions obtained from the different conjugations were combined to yield a single conjugate A and a single conjugate B fraction. The combined fractions were then concentrated to a volume of approximately 10 mls each using a 50 ml capacity diaflow apparatus fitted with a 10,000 molecular weight cut-off filter.

Although the Mono-S cation exchange and the reverse phase hydrophobic columns both indicated the levels of free lysozyme in both the peak A and B fractions for the different conjugations to be very low, all the A and B fractions were still associated with very low percentage inhibitions. Thus, although the conjugate obtained by purification on the

CM Sepharose fast flow column (7 M urea) appeared to be devoid of free lysozyme it was not yet in a form suitable for use in the Ovarian Monitor assay.

4.3.3.8 Alkyl Superose Chromatography as a Second Step in the Purification of Hen Egg White Lysozyme Estrone Glucuronide Conjugates

In order to address the problem of poor quality conjugate, it was decided to investigate an Alkyl Superose chromatographic step. This attempt at improving the percentage inhibition of conjugate was first investigated using the conjugate from the pooled peak A fraction as it was this fraction which had consistently shown the highest inhibitions from the purifications of the different conjugations. Furthermore, because purification of conjugate using 7 M urea on a cation exchange column (i.e. a CM Sepharose fast flow column) always resulted in conjugate with suprisingly low inhibitions it was felt that the second chromatographic step should avoid the use of both urea and cation exchange columns. Since, the analytical reverse phase column was a hydrophobic interaction column and had been found to be very successful in discriminating between the different conjugate species and lysozyme it was decided to attempt the further purification of the conjugate A peak on a hydrophobicity column. Thus, the conjugate from the combined conjugate A fraction was purified further on a small scale on a hydrophobic Alkyl Superose FPLC 5/5 column using the following ammonium sulphate buffers.

Buffer A - 50 mM $NaH_2PO_4.2H_2O$ + 1.7 M $(NH_4)_2SO_4$ (pH 6.6)
Buffer B - 50 mM $NaH_2PO_4.2H_2O$ (pH 6.6)

The combined conjugate A sample was prepared for loading by dissolving it in a 1:1 ratio of sample to buffer A at two times the normal concentration. The sample was then injected (50 µl) onto the column pre-equilibrated with 100% buffer A and elution was undertaken using an decreasing ammonium sulphate gradient and a flow rate of 0.5 ml min^{-1}. A gradient of 0-100% buffer B (i.e. 1.7-0.0 M ammonium sulphate) in 40 minutes, followed by holding buffer B at 100% for a further 30 minutes was used to elute the sample.

Figure 4.16 shows the elution profile to consist of one major peak followed by several smaller peaks. The major peak was collected and analysed for the presence of conjugate

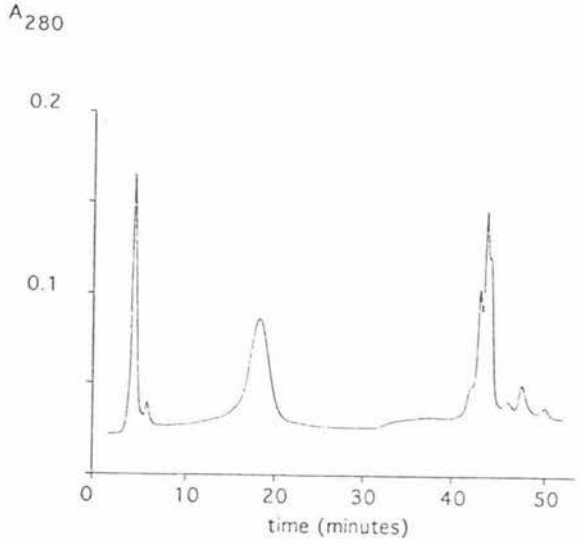

Figure 4.16 *Alkyl Superose Profile for the Purification of the Combined Conjugate A Peak*

Conditions: as stated in the text.

by inhibition assays. The assays showed the major peak to consist of high quality conjugate having a percentage inhibition of 91% which was much higher than that of any conjugate which had been obtained previously throughout the project.

This increase in the percentage inhibitions was much greater than the amount of lysozyme which the Mono-S trace could account for. There are two possible explanations for this phenomenom. Firstly, it may be due to the removal of carbamylated lysozyme or secondly, it could be due to the enzyme renaturing on the hydrophobic column. Regardless of the reason for this increase in activity, the fact that it was reproducible and did provide good quality conjugate, meant that conjugate could from this point on be purified, at least on a small scale, in a simple two step procedure. Thus, the first step in the isolation of good quality conjugate would involve the removal of most of the unreacted lysozyme using cation exchange chromatography in 7 M urea buffers. The conjugate obtained from such a step could then be further purified and the activity restored by running it through an Alkyl Superose column using non-urea buffers. The amount of conjugate purified in this way could not exceed about 1 mg per column run but this was sufficient to allow testing of the conjugate in immunoassays.

Because of the high purity of the conjugate and percentage inhibitions obtained when the Alkyl Superose column was utilised, its potential to be utilised as single chromatographic step for the purification of the conjugate reaction mixture was also investigated. This was examined by passing an aliquot of the 3:1 E1G:HEWL mixed anhydride reaction mixture through an Alkyl Superose column (see Figure 4.17) and examining the different fractions for lysozyme content by analysis on the Mono-S

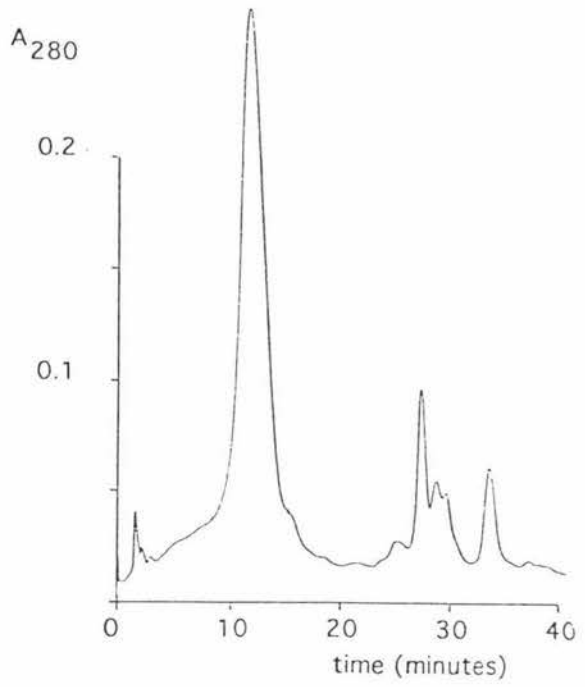

Figure 4.17 *Alkyl Superose Profile for a 3:1 E1G:HEWL Mixed Anhydride Reaction Mixture*

Conditions: as for 4.16 except injection volume was 100 µl.

column (7 M urea) as usual. The resulting Alkyl Superose elution profile was similar to the one obtained previously (see Figure 4.16) which was known to contain only very low amounts of lysozyme. However, when the fractions were examined on the Mono-S column they were all shown to contain significant amounts of lysozyme with the proportion of lysozyme increasing across the main peak in order of elution. Furthermore, although the initial Mono-S trace of the reaction mixture did show it to consist of over 30% lysozyme, no lysozyme peak was seen at 1.4 M ammonium sulphate (i.e. 0% buffer B) where controls with pure lysozyme have shown it to elute. This indicates that lysozyme must be forming complexes with the conjugate. Thus, in conclusion it is apparent that conjugate can not be purified in a single step on the Alkyl Superose column.

4.3.3.9 Dependence of Elution Profiles from Cation Exchange Columns on pH

Before coming to a final decision as to the best purification procedure it was decided to optimise the conditions under which cation-exchange chromatography was performed given the hydrophobic effects recognised in this work on the cation exchange columns. Although the Alkyl Superose column step appeared to restore immune reactivity it is clearly advisable to avoid denaturing conditions if possible.

Because the addition of every steroid group onto a lysozyme molecule is associated with the removal of one positive charge, the poor separation of conjugate from lysozyme

experienced on cation exchange columns in the presence of non-urea buffers, was unexpected. This poor separation could not be explained by simple charge effects thus, further investigation into the separation of conjugate from lysozyme on cation exchange columns was carried out. Since the small Mono-S column could be efficiently utilised with relatively short programme times, this series of experiments was performed on the Mono-S cation exchange column as opposed to the large CM Sepharose fast flow column.

Four different non-urea buffer systems each titrated to a different pH value were compared for their ability to separate conjugate and lysozyme. The four different pH values examined were 4.3, 6.0, 7.6, and 9.5. The buffering agent used for each buffer system was sodium di-hydrogen phosphate (10 mM), except for the pH 9.5 buffer where glycine (50 mM) had to be used as the buffering agent instead. All buffers were titrated to their various pH values with either 0.5 M NaOH or HCl, except for the pH 4.3 buffer where pH 4.3 was the pH of a 10 mM sodium di-hydrogen phosphate solution. Buffer B of each buffer system was identical to buffer A in each case except it contained 1 M NaCl in addition to the buffering agent. Thus, buffer A and B of the pH 6.0 buffering system were both identical to the previous buffers used to purify conjugate on the CM Sepharose fast flow columns (no urea).

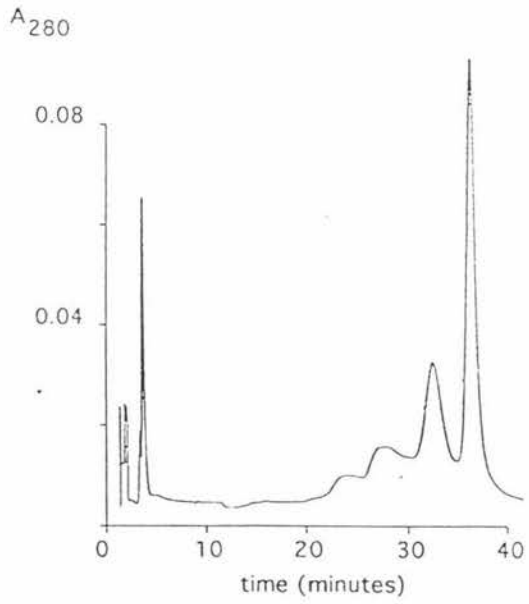

Figure 4.18 *Mono-S Profile for a 1.1:1 E1G:HEWL Active Ester Reaction Mixture utilising pH 9.5 Non-urea Buffers*

Conditions: sample preparation - 100 µl sample in 600 µl of buffer A; volume injected - 300 µl; flow rate - 0.5 ml min^{-1}; gradient - 0% buffer B 0-5 minutes, 0-10% buffer B 5-10 minutes, 10% buffer B 10-15 minutes, 12% buffer B 15-25 minutes, 12-25% Buffer B 25-45 minutes.

This series of experiments was performed on aliquots of an active ester conjugation reaction mixture which was made

using a ratio of E1G:HEWL of 1.1:1 (see Section 4.2.2.3) because this conjugation was associated with a low level of highly substituted conjugates. Thus, precipitations of conjugates on the column at high salt concentrations would be minimised. The four Mono-S elution profiles shown on the following pages (Figures 4.18-4.21) were obtained after optimisation of the gradient for each buffer system, with the gradients for each buffer system being reported in the figure legends. Inhibition studies on fractions obtained using the pH 9.5 buffer system showed the early eluting peaks (Figure 4.18) to be associated with approximately 60% inhibition while the last peak gave no inhibition. Thus, at pH 9.5 all the conjugate was associated with the early eluting peaks and lysozyme was eluted last. This result was in marked contrast to the findings at pH 4.3 (Figure 4.19) where inhibition studies showed the first peak to be associated with

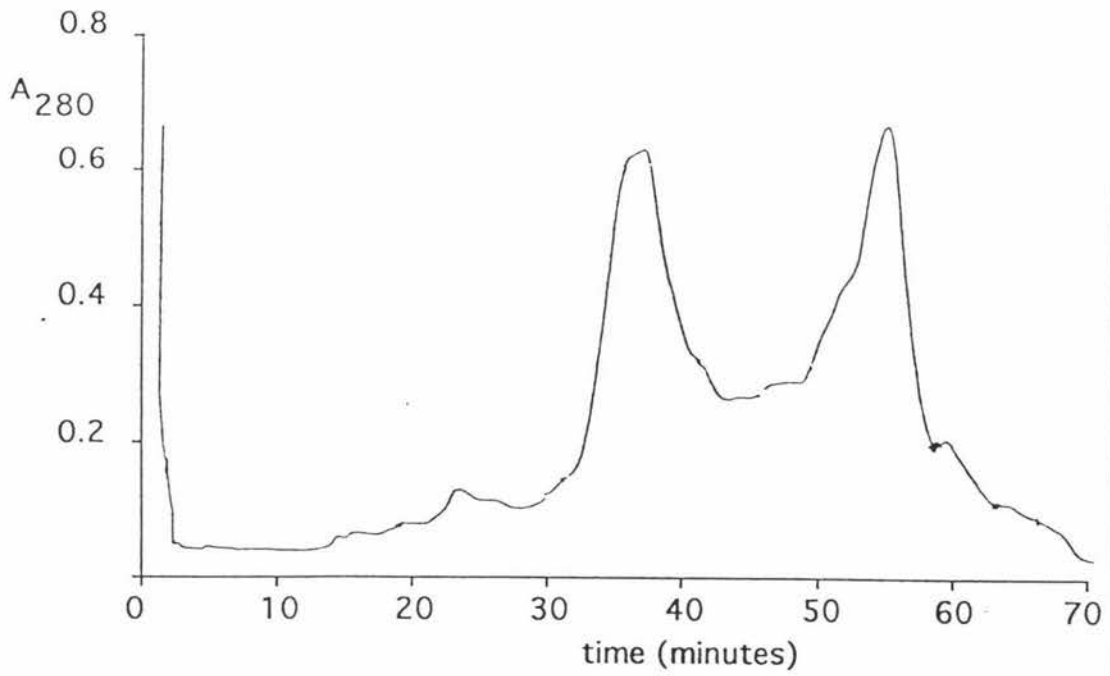

Figure 4.19 *Mono-S Profile for a 1.1:1 E1G:HEWL Active Ester Reaction Mixture utilising pH 4.3 Non-urea Buffers*

Conditions: volume injected - 75 µl; flow rate - 0.5 ml min^{-1}; gradient - 0-35% buffer B 0-5 minutes, 35% buffer B 5-40 minutes, 35-37% buffer B 40-42 minutes, 37% buffer B 42-45 minutes, 37-40% buffer B 45-46 minutes, 40-45% buffer B 46-50 minutes, 45-75% buffer B 50-52 minutes, 75% buffer B 52-60 minutes, 75-100% buffer B 60-61 minutes, 100% buffer B 61-65 minutes, 100-0% buffer B 65-66 minutes, 0% buffer B 66-80 minutes.

0% inhibition (lysozyme) and the last peak to be associated with 70% inhibition. The result at pH 6.0 was intermediate between these two extremes and had a profile which

very closely resembled the profile obtained with the same buffers on the CM Sepharose fast flow column (see Figure 4.20). Inhibition studies on this elution profile showed the

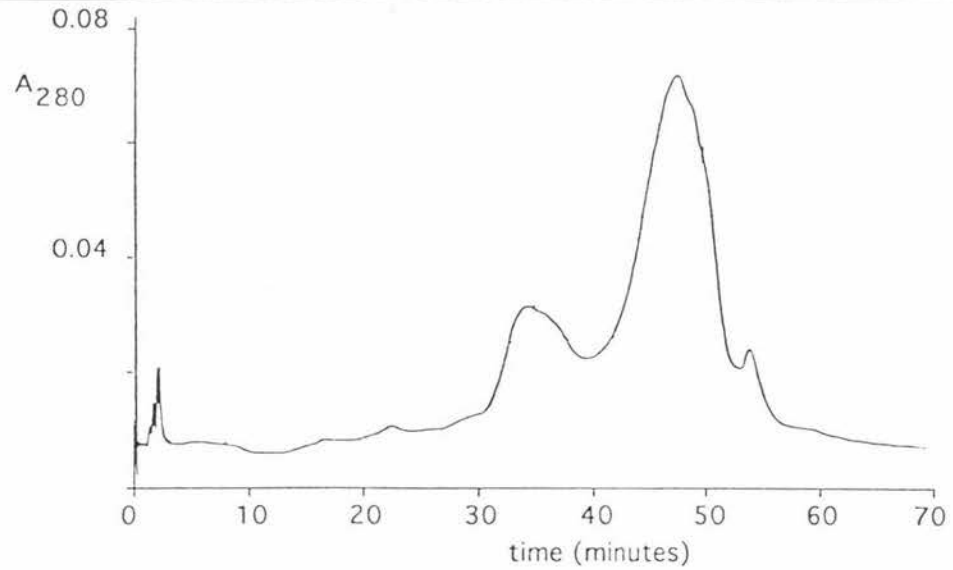

Figure 4.20 *Mono-S Profile for a 1.1:1 EIG:HEWL Active Ester Reaction Mixture utilising pH 6.0 Non-urea Buffers*

Conditions: sample preparation - 50 µl sample in 450 µl of buffer A; volume injected - 100 µl; flow rate - 0.5 ml min^{-1}; gradient - 0% buffer B 0-5 minutes, 0-20% buffer B 5-10 minutes, 20% buffer B 10-45 minutes, 20-40% buffer B 45-50 minutes, 40% buffer B 50-75 minutes.

small peak and the main peak to both contain conjugate. In the main peak the distribution of conjugate was such that the level of inhibition increased towards its trailing edge as observed previously (see Table 4.4). The elution profile at pH 7.6 (Figure 4.21) was similar to the profile obtained at pH 9.5 except that the peaks were not quite as well resolved. Thus, the elution pattern was highly dependent on the buffer pH, and this effect was such that as the pH of the buffer increased from 4.3 to 9.5, the order of elution of conjugate and lysozyme reversed so that the conjugate was eluted last. Thus, the conjugate and lysozyme only eluted in the order expected if elution was dependent exclusively on charge (i.e. in order of increasing charge), when high pH buffers were utilised for the purification procedure. The explanation for these results lies in the different salt concentrations required to elute the conjugates and lysozymes at the different pH values. As shown in Table 4.4 the concentration of salt required to cause elution of the conjugates and lysozyme increased as the pH decreased.

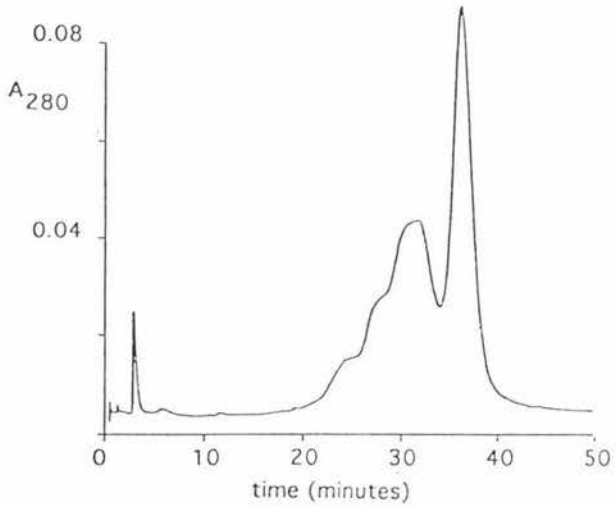

Figure 4.21 *Mono-S Profile for a 1.1:1 E1G:HEWL Active Ester Reaction Mixture utilising pH 7.6 Non-urea Buffers*

Conditions: sample preparation - 50 µl sample in 450 µl of buffer A: volume injected - 100 µl; flow rate - 0.5 ml min^{-1}; gradient - 0-10% buffer B 0-5 minutes, 10-20% buffer B in 5-50 minutes.

This is understandable in general terms on the basis of charge on the protein since as the pH moves further away from lysozymes IEP of 10.5 (Verhamme et al., 1988) the net charge on the protein increases and thus, the higher the salt concentration required for its elution. However, this cannot be the only effect of the increase in salt concentration because at pH 4.3 the conjugate requires a higher salt concentration for elution than the lysozyme.

The elution profile obtained with the pH 4.3 buffers on the Mono-S column would be expected if the order of elution was determined by hydrophobic interactions as well. If this was true then hydrophobic interactions would be promoted by the high salt concentrations required to neutralise the electrostatic attraction between the cationic lysozyme derivatives and the column. Thus, the steroid-lysozyme conjugates would require a higher ionic strength relative to lysozyme for elution in order to overcome their higher binding energy due to the increased hydrophobic contribution from their steroid groups i.e. they would elute later. As the pH of the columns is increased the salt concentration required to neutralise the electrostatic attractions is reduced and so is the hydrophobic effect. Thus, above pH 6.0 the order of elution is as expected i.e. the lysozyme conjugates eluted from the column before lysozyme. However, the resolution is poor compared to that obtained using 7 M urea buffers under identical conditions. It could be that a retarding effect of the now much weaker hydrophobic interaction is sufficient to cause this loss in resolution. The hydrophobic effect is clearly a function

of the three dimensional structure of the proteins since its importance is much reduced under denaturing conditions.

Table 4.4 *Concentration of Sodium Chloride required for Elution of Lysozyme and Conjugate at Four Different Buffer pH Values*

Buffer pH and fraction	NaCl concentation required for elution (M)
4.3	
Lysozyme	0.35
Conjugate	0.75
6.0	
Conjugate (small peak)	0.20
Lysozyme/Conjugate	0.25
7.6	
Conjugate (mean)	0.16
Lysozyme	0.17
9.5	
Conjugate	0.15
Lysozyme	0.17

Thus, in conclusion, any purification scheme for the separation of steroid-lysozyme conjugates from lysozyme must take into account salt gradients, buffer pH, hydrophobic interactions and charge considerations as all these factors are inter-related. Furthermore, the use of pH 4.3 phosphate buffers on a Mono-S column appears promising as the first chromatographic step in the purification of conjugate directly from a conjugate reaction mixture. This method has the advantage that it provides a purification procedure to

remove most of the unreacted lysozyme without requiring the utilisation of denaturing urea buffers unlike with the purification procedures which utilised the CM Sepharose fast flow column (see Section 4.3.3.3). Unfortunately, this method has the disadvantage that it can only be performed on a small scale. The surprising result obtained with conjugate purified by the Mono-S column (pH 4.3) was that its percentage inhibition still remained unacceptable at 78%. This inhibition of the conjugate fraction was lower than expected considering the small percentage of free lysozyme (4%) found in the conjugate fraction after analysis using 7 M urea buffers on the Mono-S column. In fact this level of 78% was similar to the level experienced using the conjugate purified with the CM Sepharose fast flow column (7 M urea). Furthermore, the conjugate fractions resulting from the two different purification methods both had their conjugate activities restored to 90% inhibition or higher after purification on an Alkyl Superose column using non-urea buffers. This result suggests that the Alkyl Superose column cannot be restoring activity to the conjugate which has been exposed to urea by removing carbamylated lysozyme or the enzyme renaturing on the column. Alternatively, it may be that the Alkyl Superose column was necessary for the renaturation of conjugate after exposure to pH 4.3 for conjugate purified by the Mono-S column as well as for the renaturation of conjugate after exposure to urea for the conjugate fraction which was purified on the CM Sepharose fast flow column.

In conclusion, the Mono-S column using pH 4.3 non-urea buffers followed by the Alkyl Superose column was considered preferable as the purification scheme for a HuL conjugation so as to avoid the exposure of the human lysozyme to urea.

4.4 FUTURE DIRECTIONS

The work presented in this chapter suggests the best method of attaining pure, good quality lysozyme conjugates is an active ester conjugation using a 50% excess of coupling reagents and a high concentration of steroid to reagent, followed by purification utilising the scheme outlined above. If this was successful for human lysozyme, this would enable the HuL conjugate to be very quickly prepared and its suitability for reducing the Ovarian Monitor assay time examined.

Although the scheme outlined above is the most effective method for the separation of

steroid lysozyme conjugate from lysozyme found to date, because the Mono-S and Alkyl Superose columns are both small columns, the method is not suitable for the large scale purification of conjugate and needs to be adapted in the future. More specifically, on the basis of this work, this requires replacing the small Mono-S column of the above purification scheme with the much larger S Sepharose fast flow column, and the small Alkyl Superose column with the much larger Butyl Superose column. When this work is completed the way will be clear for further optimisation and development of the Ovarian Monitor. There is no doubt that the availability of a five minute Estrone Glucuronide assay will be a major advance in do-it-yourself fertility control.

REFERENCES

Acros M, Gurpide E, Vande Wiele R L and Lieberman S: Precursors of Urinary Pregnanediol and their Influence on the Determination of the Secretory Rate of Progesterone. *J. Clin. Endocrinol. Metab.*, **24,** 237-245, (1964).

Adlercreutz H, Brown J, Collins W, Gobelsman U, Kellie A, Campbell H, Spieler J and Braissand G: The Measurement of Urinary Steroid Glucuronides as Indices of the Fertile Period in Women. World Health Organisation, Task Force on Methods for the Determination of the Fertile Period, Special Programme of Research, Development and Research Training in Human Reproduction. *J. Steroid Biochem.*, **17,** 695-702, (1982).

Anderson S W, Zimmerman J E and Callahan F M: The Use of Esters of N-hydroxysuccinimide in Peptide Synthesis. *J. Am. Chem. Soc.*, **86,** 1839-1842 (1964).

Austin C R: Sperm Fertility, Viability and Persistence in the Female Tract. *J. Reprod. Fertil.*, **suppl. 22,** 75-89, (1975).

Badwe R A, Gregory W M, Chaudary M A, Richards M A, Bentley A E, Rubens R D and Fentiman I S: Timing of Surgery during Menstrual Cycle and Survival of Premenopausal Women with Operable Breast Cancer. *Lancet,* **337,** 1261-1264 (1991).

Baird D T, (1977). *Synthesis and Secretion of Steroid Hormones*. Academic Press, New York. p. 305.

Baird D T: A Model for Follicular Selection and Ovulation: Lessons from Superovulation. *J. Steroid. Biochem.*, **27,** 15-23, (1987).

Baird D T and Fraser I S: Blood Production and Ovarian Secretion Rates of Estradiol-17β and Estrone in Women throughout the Menstrual Cycle. *J. Clin. Endocrin. Metab.*, **38,** 1009-1017, (1974).

Baird D T, Horton R, Longcope C and Tait J F: Steroid Dynamics under Steady State Conditions. *Recent Prog. Horm. Res.* **25,** 611-644, (1969).

Banoub J and Bundle D R: 1,2-Orthoacetate Intermediates in Silver Trifluoromethanesulphonate Promoted Koenigs-Knorr Synthesis of Disaccharide Glycosides. *Can. J. Chem.*, **57,** 2091-2097 (1978).

Barrett S A and Brown J B: An Evaluation of the Method of Cox for the Rapid Analysis of Pregnanediol in Urine by Gas Liquid Chromatography. *J. Endocrinol.*, **47**, 471-480, (1970).

Batty M: Monitoring an Exponential Smoothing Forecasting System. *Oper. Res. Quart.*, **20**, 319-325, (1969).

Benagiano G and Bastianelli C: Clinical Trials of the Ovulation Method. *Int. J. Gynecol. Obstet.*, **suppl 1**, 91-98, (1989).

Bernath F R and Vieth W R: Lysozyme Activity in the Presence of Non-ionic Detergent Micelles. *Biotech. Bioeng.*, **XIV**, 737-752 (1972).

Billings E L, (1992). *Teaching the Billings Ovulation Method.* The Ovulation Method Research and Reference Centre of Australia, 12.

Billings E L, Billings J J, Brown J B and Burger H G: Symptoms and Hormonal Changes accompanying Ovulation. *Lancet.*, **1**, 232-234, (1972).

Billings E L and Westmore A, (1980). *The Billings Method.* Anne O'Donovan Pty Ltd, Victoria. pp. 29-49.

Blackwell L F and Brown J B: Application of Time-series Analysis for the Recognition of Increases in Urinary Estrogens as Markers for the Beginning of the Potentially Fertile Period. *Steroids,* **57**, 554-562, (1992).

Blackwell L F, Motion R L, MacGibbon A K H, Hardman M J and Buckley P D: Evidence that the Slow Conformation Change Controlling NADH Release from the Enzyme is Rate-Limiting during the Oxidation of Propionaldehyde by Aldehyde Dehydrogenase. *Biochem. J.*, **242**, 803-808 (1987).

Bolt H M, (1979). *Metabolism of Estrogens - Natural and Synthetic*. Pharmaceutical Therapeutics, Pergamon Press, Great Britain. **4**, p. 19.

Brown J B: Urinary Excretion of Estrogens during the Menstrual Cycle. *Lancet,* **1**, 320-323, (1955).

Brown J B: Pituitary Control of Ovarian Function - Concepts Derived from Gonadotrophin Therapy. *Aust. N. Z. J. Obstet. Gynaec.*, **18**, 47-54, (1978).

Brown J B and Blackwell L F, (1989). *Ovarian Monitor Instruction Manual.* Ovulation Method Research and Reference Centre of Australia, Victoria, 3.

Brown J B, Blackwell L F, Cox R I, Holmes R M and Smith M A: Chemical and Homogeneous Enzyme Immunoassay Methods for the Measurement of Estrogens and Pregnanediol and their Glucuronides in Urine. *Prog. Clin. Biol. Res.,* **285,** 119-138, (1988).

Brown J B, Blackwell L F, Holmes J and Smyth K: New Assays for Identifying the Fertile Period. *Int. J. Gynecol. Obstet.,* **suppl. 1,** 111-122, (1989).

Brown J B and Gronow M, (1985). Endocrinology of Ovulation Prediction in *Clinical Reproductive Endocrinology.* R.P. Shearman (Ed.). Churchill Livingstone, Edinburgh. pp. 165-184.

Brown J B, Holmes J and Baker G: Use of the Home Ovarian Monitor in Pregnancy Avoidance. *Am. J. Obstet. Gynecol.,* **165,** 2008-2011 (1991).

Brown J B, MacLeod S C, McNaughton C, Smith M A and Smyth B: A Rapid Method for Estimating Estrogens in Urine using a Semi-automatic Extractor. *J. Endocrinol.,* **42,** 5-15, (1968).

Burger H G: Estradiol: The Physiological Basis of the Fertile Period. *Int. J. Gynecol. Obstet.,* **suppl. 1,** 5-9, (1989).

Canfield R E and McMurray S: Purification and Characterisation of a Lysozyme from Goose Egg White. *Biochem. Biophys. Res. Comm.,* **26,** 38-42 (1967).

Cekan S Z, Beksac M S, Wang E, Shi S, Masironi B, Landgren B M and Diczfalusy E: The Prediction and/or Detection of Ovulation by Means of Urinary Steroid Assays. *Contraception,* **33,** 327-345, (1986).

Cembrowski G S, Westgard J O, Eggert A A and Toren E C: Trend Detection in Control Data: Optimisation and Interpretation of Trigg's Technique for Trend Analysis. *Clin. Chem.,* **21 (10),** 1396-1405, (1975).

Collins W P: Biochemical Indices of Potential Fertility. *Int. J. Gynecol. Obstet.,* **Suppl. 1,** 35-43, (1989).

Colobert L and Lenior J: Mechanism of the Lysis of *P. coccus* (sp. Sarcina flava) by Lysozyme. *Ann. Inst. Pasteur,* **92,** 74-88, (1957).

Conrow R B and Bernstein S: Steroid Conjugates. VI. An Improved Koenigs-Knorr Synthesis of Aryl Glucuronides Using Cadmium Carbonate, a New and Effective Catalyst. *J. Org. Chem.,* **36,** 863-870, (1971).

Conway B: *Assessment of a Home Test for Urinary Pregnanediol Glucuronide.* B. Med. Sci. Thesis. University of Melbourne (1986).

Cormack D H, (1984). *Introduction to Histology,* J. B. Lippincott Company, Philadelphia. pp. 386-389.

Dao-pin S, Der-Ing L and Remmington S J: Electrostatic Fields in the Active Sites of Lysozymes. *Proc. Natl. Acad. Sci. USA,* **86,** 5361-5365, (1989).

Erlanger B F, Borek F, Beiser S M and Lieberman S: Steroid-Protein Conjugates II: Preparation and Characterisation of Conjugates of Bovine Serum Albumin and Progesterone Deoxycorticosterone and Estrone. *J. Biol. Chem.*, **234,** 1090-1094 (1959).

Flynn A and Brooks M, (1984). *A Manual of Natural Family Planning.* George Allen Unwin, London. p. 122.

Gadum H: Lognormal Distributions. *Nature,* **156,** 463-466, (1945).

Ganong W F, (1987). *Review of Medical Physiology.* Appleton and Lange, California. p. 367.

Goldberg M E, Rudolph R and Jaenicke R: A Kinetics Study of the Competition between Renaturation and Aggregation during the Refolding of Denatured-Reduced Egg White Lysozyme. *Biochemistry,* **30,** 2790-2797 (1991).

Gorin G, Wang S F and Papapavlou L: Assay of Lysozyme by its Lytic Action on *Micrococcus lysodeikticus* Cells. *Anal. Biochem.,* **39,** 113-127, (1971).

Gross B A: Clinical Indicators of the Fertile Period. *Int. J. Gynecol. Obstet.,* **suppl. 1,** 45-51, (1989).

Grutter M G, Weaver L H and Matthews B W: Goose Lysozyme Structure: An Evolutionary Link Between Hen and Bacteriophage Lysozymes. *Nature*, **303**, 828-304, (1983).

France J T: The Detection of Ovulation for Fertility and Infertility. *Rec. Adv. Obstet. Gynaecol.*, **14**, 215-239.

Hobrick P and Nilsen M: Early Urinary Conjugated Metabolites of Intravenously Injected (6.7-^{3}H)-estradiol-17ß in the Human Subject. *J. Steroid Biochem.* **5**, 15-20, (1974).

Hoff J D, Quigley M E and Yen S S C: Hormonal Dynamics at Midcycle: A Re-evaluation. *J. Clin. Endocrinol. Metab.*, **57**, 792-796, (1983).

Ireland J J: Control of Follicular Growth and Development. *J. Reprod. Fert.*, **suppl. 34**, 39-54, (1987).

Jolles P: Lysozymes from Rabbits Spleen and Dog Spleen. *Methods Enzymol.*, **5**, 137-140, (1962).

Jolles P and Jolles J: What's New in Lysozyme Research? *Mol. Cell. Biochem.*, **63**, 165-189, (1984).

Karsch F J: Central Actions of Ovarian Steroids in the Feedback Regulation of Pulsatile Secretion of Luteinising Hormone. *Ann. Rev. Physiol.*, **49**, 365-382, (1987).

Kirby A J: Mechanism and Stereoelectronic Effects in the Lysozyme Reaction. *Crit. Rev. Biochem.*, **22**, 283-315, (1987).

Kumagai I, Kojima S, Tamaka E and Miura K: Conversion of Trp 62 of Hen Egg White Lysozyme to Tyr by Site-Directed Mutagenesis. *J. Biochem.*, **102**, 733-740, (1987).

Kumagai I and Miura K: Enhanced Bacteriolytic Activity of Hen Egg White Lysozyme Due to Conversion of Trp 62 to other Aromatic Amino Acid Residues. *J. Biochem.*, **105**, 946-948, (1989).

La Rue J N and Speck J C: Turkey Egg White Lysozyme: Preparation of the Crystalline Enzyme and Investigation of the Amino Acid Sequence. *J. Biol. Chem.*, **245,** 1985-1991 (1970).

Lee C L, Atassi M Z and Habeeb A F S A: Enzyme and Immunochemical Properties of Lysozyme. *Biochim. Biophys. Acta,* **400,** 423-432 (1975).

Leute R K, Ulman E F, Goldstein A and Herzenberg L A: Spin Immunoassay Technique for Determination of Morphine. *Nature New Biology,* **236,** 93-94, (1972).

Lewis C D: Statistical Monitoring Techniques. *Med. & Biol. Engng.,* **9,** 315-323, (1971).

Liu J H and Yen S S C: Induction of Midcycle Gonadotropin Surge by Ovarian Steroids in Women: A Critical Evaluation. *J. Clin. Endocrinol. Metab.,* **57,** 797-802, (1983).

Locquet J P, Saint-Blancard J and Jolles P: Apparent Affinity Constants of Lysozymes from Different Origins for *Micrococcus lysodeikticus*. *Biochim. Biophys. Acta*, **167,** 150-153 (1968).

Malcom B A, Rosenberg S, Corey M J, Allen J S, De Baetselier A and Kirsch J F: Site-directed Mutagenesis of the Catalytic Residues Asp-52 and Glu-35 of Chicken Egg White Lysozyme. *Proc. Natl. Acad. Sci. USA,* **86,** 133-137 (1989).

Marshall F H A, (1984). *Physiology of Reproduction.* Churchill Livingstone, Melbourne. p. 729.

McKenzie H A and White F H: Determination of Lysozyme Activity at Low Levels with Emphasis on the Milk Enzyme. *Anal. Biochem.,* **157,** 367-374 (1986).

Moghissi K S: Prediction and Detection of Ovulation. *Fertil. Steril.,* **34,** 89-98, (1980).

Morsky P: Turbidimetric Determination of Lysozyme with *Micrococcus lysodeikticus* Cells: Re-examination of Reaction Conditions. *Anal. Biochem.,* **128,** 77-85, (1983).

Muraki M, Morikawa M, Jigami Y and Tanaka H: The Role of Conserved Aromatic Amino Acid Residues in the Active Site of Human Lysozyme: A Site Specific Mutagenesis Study. *Biochim. Biophys. Acta*, **916,** 66-75 (1987).

Musey P I, Green R N and Hobkirk R: The Role of an Enterohepatic System in the Metabolism of 17ß-E2-17G in the Human Female. *J. Clin. Endocrin. Metab.*, **35,** 448-457, (1972).

Nanjo F, Sakai K and Usui T: p-Nitrophenyl Penta-N-Acetyl-ß-Chitopentoasoside as a Novel Synthetic Substrate for the Colourmetric Assay of Lysozyme. *J. Biochem.*, **104,** 255-258 (1988).

Ogino K: Ovulationstermin und Konzephonstermin [Ovulation Period and Conception Period]. *Zentralblatt fur Gynaek.*, **54,** 464-479, (1930).

Parente E S and Wetlaufer D B: Influence of Urea on the High-Performance Cation-Exchange Chromatography of Hen Egg White Lysozyme. *Journal of Chromatography*, **288,** 389-398 (1984).

Parkes A S: Historical Note. *J. Biosc. Sci.*, **3,** 331-337, (1971).

Phillips D C: The Three-Dimensional Structure of an Enzyme Molecule. *Sci. Amer.*, **215(5),** 78-90, (1966).

Poteete A R, Dao-Pin S, Nicholson H and Matthews B W: Second-Site Revertants of an Inactive T4 Lysozyme Mutant Restore Activity by Restructuring the Active Site Cleft. *Biochem.*, **30,** 1425-1432, (1991).

Price J and Pethig R: Surface Charge Measurements of *Micrococcus lysodeikticus* and the Catalytic Implications for Lysozyme. *Biochim. Biophys. Acta*, **889,** 128-135 (1986).

Rossman M G and Argos P: Exploring Structural Homology of Proteins. *J. Mol. Biol.*, **105,** 75-95, (1976).

Royston J P: Basal Body Temperature, Ovulation and the Risk of Conception with Special Reference to the Lifetimes of Sperm and Egg. *Biometrics,* **38,** 397-406, (1982).

Rubenstein K E, Schneider R S and Ullman E F: "Homogenous" Enzyme Immunoassay. A New Immunological Technique. *Biochem. Biophys. Res. Comm.*, **47,** 846-851, (1972).

Sambrook J, Fritsch E F and Maniatis T, (1989). *Molecular Cloning: A Laboratory Manual.* Cold Spring Harbor, Laboratory Press, New York.

Schiphorst L E M, Collins W P and Royston J P: An Estrogen Test to Determine the Times of Potential Fertility in Women. *Fertil. Steril.*, **44,** 328-334, (1985).

Serra G B (Ed), (1983). *Comprehensive Endocrinology - The Ovary.* Raven Press, New York. p. 432.

Shugar D: Ultra-violet Inactivation of Lysozyme. *Biochim. Biophys. Acta.*, **8,** 302-310, (1952).

Siiteri K and MacDonald P C, (1973). Extraglandular Conversion of Androgens. Female Reproduct. Syst. Vol 2 pt.1 Sect.7 Endocr. Hbk. Physiol. Greep, R.O., and Astwood, E.B., (Eds) American Physiological Society Washington DC pp. 615-630.

Stanczyk F Z, Miyakawa I and Goebelsmann U: Direct Radio-immunoassay of Urinary Estrogen and Pregnanediol Glucuronides during the Menstrual Cycle. *Am. J. Obstet. Gynecol.*, **137,** 443-450, (1980).

Stryer L, (1981). *Biochemistry.* W.H. Freeman, New York. pp. 135-148.

Thornton S J, Pepperell R J and Brown J B: Home Monitoring of Gonadotrophin Ovulation Induction using the Ovarian Monitor. *Fertil. Steril.*, **54,** 1076-1082 (1990).

Trigg D W: Monitoring a Forecast System. *Oper. Res. Quart.*, **15,** 271-274, (1964).

Tsugita A, Inouye M, Terzaghi E and Streisinger G: Purification of Bacteriophage T4 Lysozyme. *J. Biol. Chem.*, **243,** 391-397, (1968).

Vaughan J R and Osata R L: The Preparation of Peptides using Mixed Carbonic Carboxylic Acid Anhydrides. *J. Amer. Chem. Soc.*, **74,** 676-678, (1952).

Verhamme I M A, Van Dedem W K and Lauwers A R: Ionic Strength Dependent Substrate Inhibition of the Lysis of *Micrococcus luteus* by Hen Egg White Lysozyme. *Eur. J. Biochem.*, **172,** 615-620, (1988).

World Health Organisation (WHO), Special programme of research development and research training in human reproduction, ninth annual report. *WHO* December (1980).